*Max-Planck Institut für molekulare Physiologie*

*Technische Universität Dortmund*

# Design, Synthesis and Biological Evaluation of a Pseudo Natural Product Compound Collection

## Dissertation

For the achievement of the academic degree of the

**Doctor in Natural Science**

(Dr. rer. Nat.)

Submitted to

The Faculty of Chemistry and Chemical Biology

Technical University of Dortmund

By

M.Sc. Okan Yildirim

from Dortmund, Germany

Dortmund 2021

1. Gutachter: Prof. Dr. Dr. h.c. Herbert Waldmann

2. Gutachter: Prof. Dr. Andrey P. Antonchick

The present dissertation was written in the period from March 2018 to June 2021 under the supervision and guidance of Prof. Dr. Dr. h.c. Herbert Waldmann at Faculty of Chemistry and Chemical Biology at the Technical University of Dortmund and the Max-Planck-Institute for Molecular Physiology in Dortmund.

*Results presented in this thesis contributed to the following publication:*

O. Yildirim, M. Grigalunas, L. Brieger, C. Strohmann, A. P. Antonchick, H. Waldmann. "Dynamic Catalytic Highly Enantioselective 1,3-Dipolar Cycloadditions". *Angew. Chem. Int. Ed.*, **2021**, *60*, 20012-20020.

# Table of Contents

Abstract ..... I
Kurzzusammenfassung ..... III
1 Introduction ..... 1
1.1 Natural Products ..... 2
1.2 Biology-Oriented Synthesis (BIOS) ..... 3
1.3 Pseudo Natural Products ..... 6
1.4 1,3-Dipolar Cycloadditions ..... 11
1.4.1 1,3 Dipolar Cycloadditions and Frontier MolecularOrbital (FMO) Theory ..... 12
1.4.2 Asymmetric 1,3 Dipolar Cycloadditions ..... 16
1.5 Dynamic Covalent Chemistry (DCC) ..... 19
1.5.1 Dynamic Combinatorial Libraries (DCL) ..... 20
1.5.2 Selection Strategies for the Selective Design of Dynamic Combinatorial Library (DCL) ..... 21
1.6 Stereodivergent Synthesis ..... 23
2 Aim of the Thesis ..... 27
3 Dynamic Catalytic 1,3-dipolar Cycloaddition ..... 28
3.1 Introduction ..... 28
3.2 Initial results and optimization ..... 30
3.3 Development of the asymmetric double 1,3-dipolar CA and reaction scope ..... 32
3.4 Development of the mixed asymmetric double 1,3-dipolar CA ..... 37
3.5 Mechanistical studies of the stereochemical course of the double cycloaddition ..... 40
3.5.1 Mechanistical studies on the first step of the reaction sequence ..... 40
3.5.2 Mechanistical studies on the second step of the reaction sequence ..... 45
3.5.3 Summary of the mechanistical study ..... 54
3.6 Selective synthesis of the *endo, exo*-stereoisomer ..... 55
3.7 Biological evaluation of the tricyclic double cycloaddition products ..... 58
3.8 Conclusion ..... 60
4 Sequential 1,3-dipolar cycloaddition and dearomatization of indoles ..... 61
4.1 Introduction ..... 61
4.2 Aim of the project ..... 62
4.3 Results and discussion ..... 63
4.4 Conclusion ..... 66
5 Summary of the Thesis ..... 67
6 Experimental section ..... 69
6.1 General Information ..... 69
6.2 Synthesis of iminoesters ..... 71
6.3 Synthesis of cyclic enone ..... 75
6.4 Synthesis of double cycloaddition *endo, endo*-products ..... 78

6.5 Synthesis of mono cycloaddition products ..... 104
6.6 Synthesis of mixed double cycloaddition *endo, endo*-products ..... 108
6.7 Synthesis of double cycloaddition *endo, exo*-products ..... 125
6.8 Synthesis of pyrrolidine fused indoles ..... 133
6.8.1 Synthesis of indole precursor ..... 133
6.8.2 Synthesis of indole and pyrrolidine fused polycyclic compound ..... 135
6.9 Synthesis of polycyclic pyrroloindoline by dearomatization ..... 140
6.10 Crystal Data ..... 146
6.10.1 X-Ray analysis ..... 146
6.11 Experimental studies on the double cycloaddition ..... 152
6.11.1 Experimental studies on the stepwise addition ..... 152
6.11.2 Experimental studies on the mono cycloaddition ..... 154
6.11.3 Experimental studies on the second cycloaddition ..... 160
6.11.4 Experimental studies on the racemic mono adduct ..... 163
7 References ..... 165
8 Appendix ..... 170
8.1 List of abbreviations ..... 170
8.2 Acknowledgement ..... 173
8.3 Curriculum Vitae ..... 174
8.4 Eidesstattliche Versicherung (Affidativ) ..... 175

## Abstract

Natural product (NP) scaffolds are valuable starting points for the design and synthesis of novel bioactive compounds as employed in biology-oriented synthesis (BIOS). However, the exploration of chemical and biological space by this method is limited by the guiding NPs. Combining NP fragments in an unprecedented not accessible by current biosynthetic pathways could enable the discovery of novel chemical and biological space. Compound classes obtained by the de novo combination of unrelated NP-derived fragments are called pseudo natural products (pseudo NPs).

Based on the concept of synthesis of pseudo NP compound libraries, an enantioselective double 1,3-dipolar cycloaddition was applied to cyclopentadienones to combine two pyrrolidine fragments in an unprecedented manner (Chapter 3). Highly complex tricyclic molecules with up to eight stereocenters were obtained, including a quaternary center. Detailed mechanistic studies revealed that the double cycloaddition proceeds via an enantioselective dynamic covalent process. In dynamic covalent chemistry (DCC) the reaction follows a thermodynamically controlled pathway in an equilibrium process, allowing the interconversion of products. Time-dependent analysis showed kinetically controlled and thermodynamically favored product formation and an enantioselective interconversion of stereoisomers. Conditions for the selective synthesis of thermodynamically and kinetically controlled structurally complex double cycloadducts with high stereoselectivity from a common set of reagents were developed.

Furthermore, a pseudo NP compound library was designed by combining the pyrrolidine scaffold with pyrroloindoline, generating a highly complex polycyclic compound class (Chapter 4). A synthetic strategy was designed employing an asymmetric 1,3-dipolar cycloaddition, indole formation and dearomatization. Excellent diastereoselectivity was achieved through a substrate controlled cyclization process.

***Chapter 3***

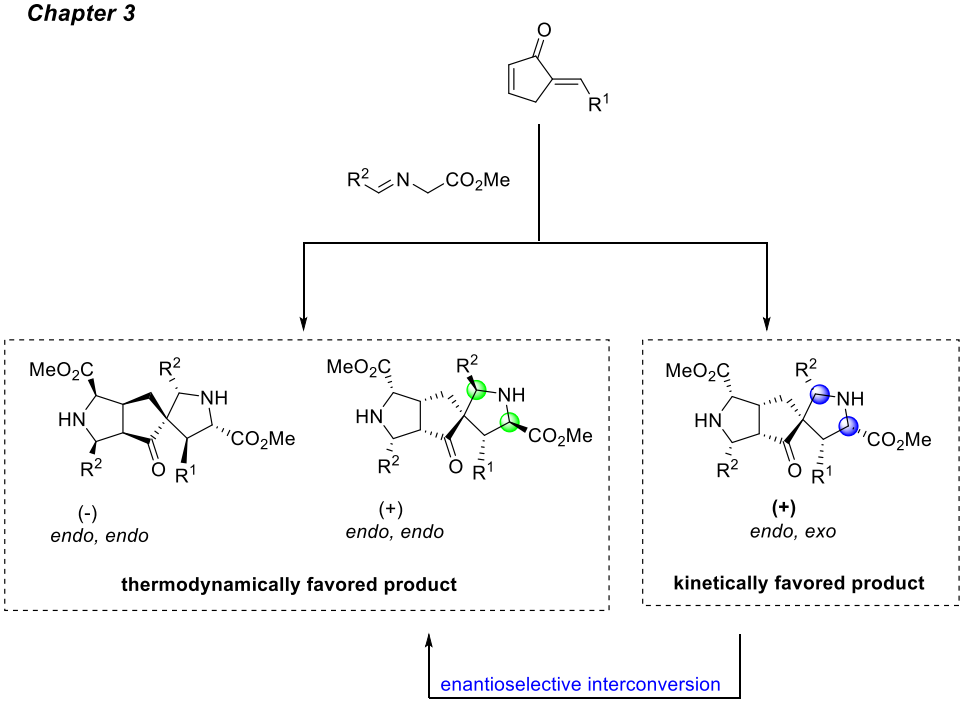


***Chapter 4***

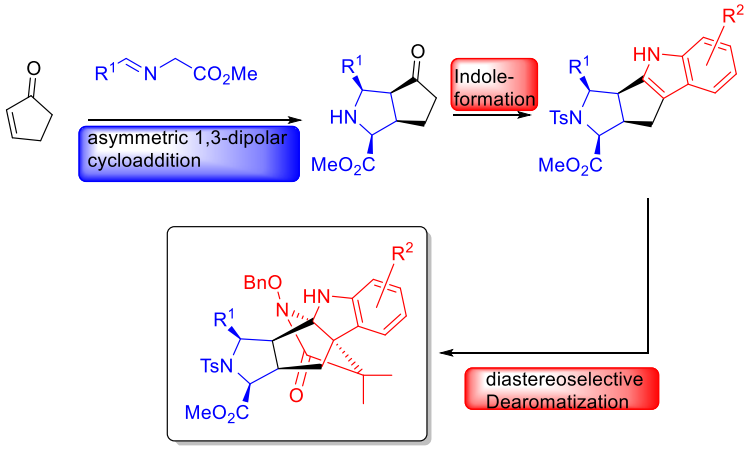

## Kurzzusammenfassung

Naturstoff-Grundgerüste sind wertvolle Ausgangspunkte für das Strukturdesign und die Synthese von neuen bioaktiven Verbindungen, wie bereits in der Biologie orientierten Synthese (BIOS) durchgeführt. Die Untersuchung des chemischen und des biologischen Raums ist jedoch von der Wahl des Naturstoffes eingeschränkt. Die Kombination von Naturstofffragmenten in neuartiger Weise, welche über biosynthetische Wege unzugänglich ist, könnte die Entdeckung von neuen chemischen und biologischen Räumen ermöglichen. Verbindungsklassen, welche durch Kombination von nicht miteinander verwandten Naturstofffragment erhalten werden, werden als Pseudo-Naturstoffe bezeichnet.

Für die  der Synthese von Bibliotheken von Pseudo-Naturstoffen wurde eine enantioselektive doppelte Cycloaddition an Cyclopentadienon durchgeführt, welche eine neuartige Kombination von Pyrrolidin-Fragmenten ermöglichte (Kapitel 3). Hochkomplexe trizyklische Moleküle mit bis zu acht Stereozentren wurden erhalten, wobei eines der Stereozentren ein quaternäres Zentrum ist. Intensive mechanistische Untersuchungen zeigten, dass die doppelte Cycloaddition durch einen dynamischen kovalenten Prozess abläuft. In der dynamischen kovalenten Chemie folgt die Reaktion einem thermodynamisch kontrollierten Reaktionsverlauf in einem Gleichgewichtsprozess, in welcher die Produkte umgewandelt werden. Eine zeitabhängige Analyse zeigte die Bildung von kinetisch und thermodynamisch kontrollierten Reaktionsprodukten und eine enantioselektive Umwandlung der jeweiligen Stereoisomere. Des Weiteren wurden Reaktionsbedingungen für die selektive Synthese von sowohl kinetisch als auch thermodynamisch kontrollierten hochkomplexen Cycloadditions-Produkten mit hoher Stereoselektivität unter Anwendung von gleichen Reagenzien entwickelt.

Des Weiteren wurde eine weitere Pseudo-Naturstoff-Substanzbibliothek durch Kombination von Pyrrolidin-Grundgerüsten mit Pyrroloindolin entwickelt, bei der polyzyklische Verbindungen erhalten wurden. Eine Synthesestrategie aus 1,3-dipolarer Cycloaddition, Indol-Bildung und anschließender Dearomatisierung wurde angewendet. Exzellente Diastereoselektivität wurde durch eine substrat-kontrollierte Zyklisierung erzielt.

***Kapitel 3***

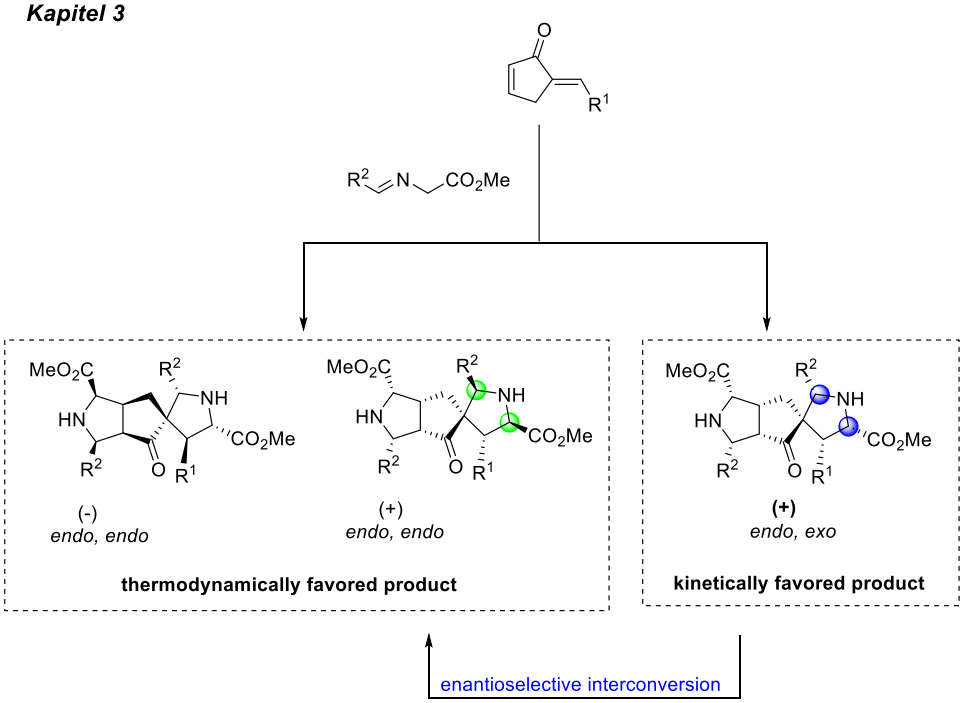


***Kapitel 4***

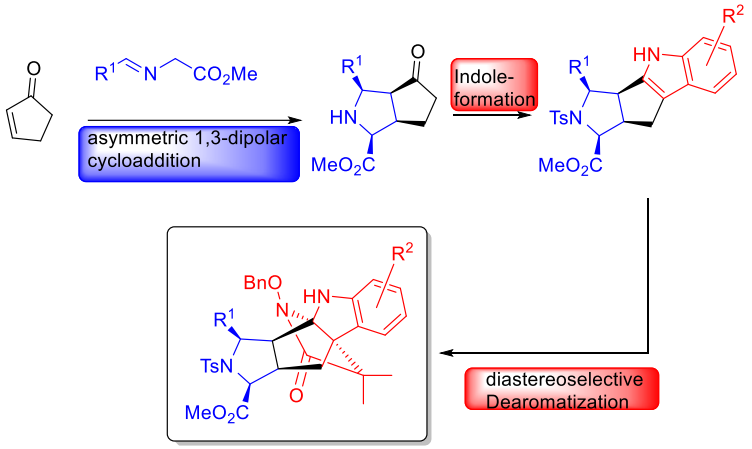

# 1 Introduction

The design of bioactive small molecules is of high importance in chemical biology. Natural product (NP) scaffolds are fundamentally inspiring starting points for the design and research of molecules endowed with biological relevance.[1] The privileged scaffolds of NPs cover a wide range of chemical and biological space which is not fully explored yet. In order to explore novel chemical and biological space which are not covered by guiding NPs, promising strategies have been employed such as biology-oriented synthesis (BIOS)[2] and the synthesis of pseudo NPs.[3-4] As BIOS is confronted with chemical and biological limitations the design principle of pseudo NPs, combining NP scaffolds in an unprecedented manner, enables the opportunity to explore novel chemical and biological space which are not covered by NPs.[4]

Highly important NP scaffolds are heterocycles such as pyrrolidines. A very powerful method to generate pyrrolidines and to combine them with various NP scaffolds is the 1,3-dipolar cycloaddition.[5] It is a very efficient method to synthesize five membered heterocycles in an highly stereospecific fashion.[5] With respect to the origin of homochirality and the importance of getting access to enantiopure compounds, stereodivergent synthesis in 1,3-dipolar cycloadditions have gained particular interest allowing the selective formation of desired stereoisomers under certain conditions.[5]

Although the 1,3-dipolar cycloaddition leads to the formation of stable cyclized products, it has been observed that retro cycloadditions can occur which lead to interconversion of products, thus resulting in change in equilibrium of a reaction.[6] Those highly complicated dynamic processes[7] can be employed for the construction of a stereodivergent synthesis of chiral molecular frameworks to obtain kinetically and thermodynamically favoured products.

## 1.1 Natural Products

New molecular discovery programs for the identification of bioactive molecules is at the heart of chemical biology, medicinal chemistry and the pharmaceutical industry. The discovery of selective probes for bioactivity is of high value in the course of drug discovery as modulation of biological processes can have a great impact on the understanding of diseases and thus afford new therapeutic opportunities.[8-9] Natural Products (NPs) have served as rich source for the design, development and research of bioactive molecules and have historically made a great contribution for the treatment of cancer as well as infectious diseases as well as played a vital role in other therapeutic areas.[10-12] One of the greatest examples demonstrating the power of NPs is the discovery of penicillin from mold in 1928 and its effect on infectious disease.[13] A recent analysis of new medicines approved by the US Food and Drug Administration (FDA) revealed that 34% of those drugs are either NPs or derived from NPs.[14] This impressive contribution to drug discovery is related to the notable ability of NPs to provide significantly improved hit rates, even against the more difficult screening targets such as the protein-protein interactions.[15] NPs offer enhanced properties over conventional synthetic molecules as they are optimized by nature over the years by evolution.[16] They exhibit a higher degree of complexity, stereochemistry and greater molecular rigidity than purely synthetic compounds, enabling them to cover a wider range of chemical space.[12] The NP pool is enriched with bioactive compounds and therefore can be regarded as privileged for molecular interactions with respective targets.[2] Despite the fact that NPs and their structural analogues are predestined for drug discovery and are used as inspiration for bioactive compounds, pharmaceutical companies have reduced the application of NPs for novel drug candidates. This diminution is due to challenges related to technical barriers such as screening, isolation and optimization as well as complex multistep synthetic and supply problems.[15, 17-19] In order to overcome these limitations, novel approaches have been designed that NP-inspired including biology-oriented synthesis and pseudo natural products.

## 1.2 Biology-Oriented Synthesis (BIOS)

The analysis of biological systems using small molecules is a fundamental aspect in chemical biology. Bioactive small molecules are predestined tools for the interrogation of highly complicated biological network as their mode of action compared to most genetic approaches can be rapid, tuneable, conditional, and reversible.[20] The development of selective small molecule modulators of all proteins encoded by the human genome is a priority target in chemical biology research.[2] However, a key challenge that arises is the identification of biologically relevant chemical space as the possible number of small molecules populating druglike chemical space exceeds $10^{60}$, which is unfeasible to study all possibilities.[21] Nevertheless, in nature, evolutionary conservation of molecular architectures leads to a limited number of possible small molecule binding sites. Furthermore, NPs have come from function-driven evolution of biosynthetic pathways and their scaffolds are highly conserved in nature.[22] By considering this phenomena, Waldmann *et al* introduced the concept of biology-oriented synthesis (BIOS) which builds on structural conservatism in the evolution of proteins and NPs.[2, 23] BIOS is a design principal strategy taking inspiration from NP structures leading to synthesis of biologically relevant compound collections.[24-25] The strategy uses NPs as prevalidated starting points by simplification the structure to a core scaffold with retained bioactivity and further modifications to obtain new compound classes (Figure 1).[24] Based on structural simplification, a synthetic route is designed to get rapid access to a NP-inspired compound classes for biological evaluation.

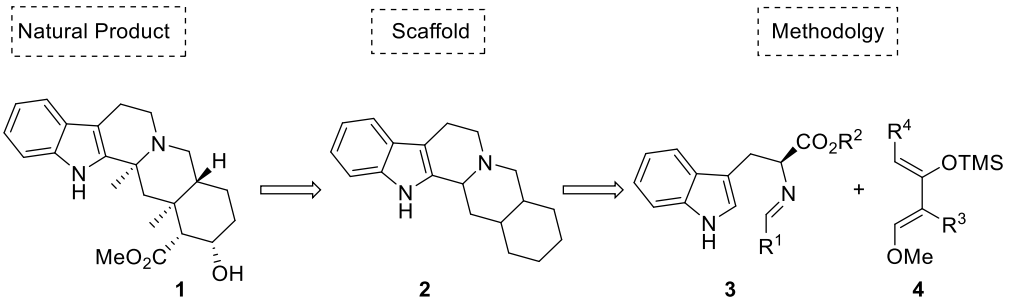


**Figure 1**: Design principles for biology-oriented synthesis (BIOS)

The gaps in chemical space which are not exploited by NPs can be covered by BIOS enabling novel bioactivity. The initial development of BIOS strategy employing a hierarchical classification of NP scaffolds required cheminformatic analysis of NPs and their scaffold structures.[26] A visual representation of scaffold relationships in a scaffold tree developed a

structural classification of NPs (SCONP) as organizing principle for charting the known chemical space explored by nature (Figure 2). In the scaffold tree highly complex scaffolds are located on the outside and become simpler by moving to the centre. It can be used as guiding tool for the efficient development of NP-derived compound collections and assures retention of bioactivity by moving from complex structures to simpler scaffolds along the branches of trees.[26]

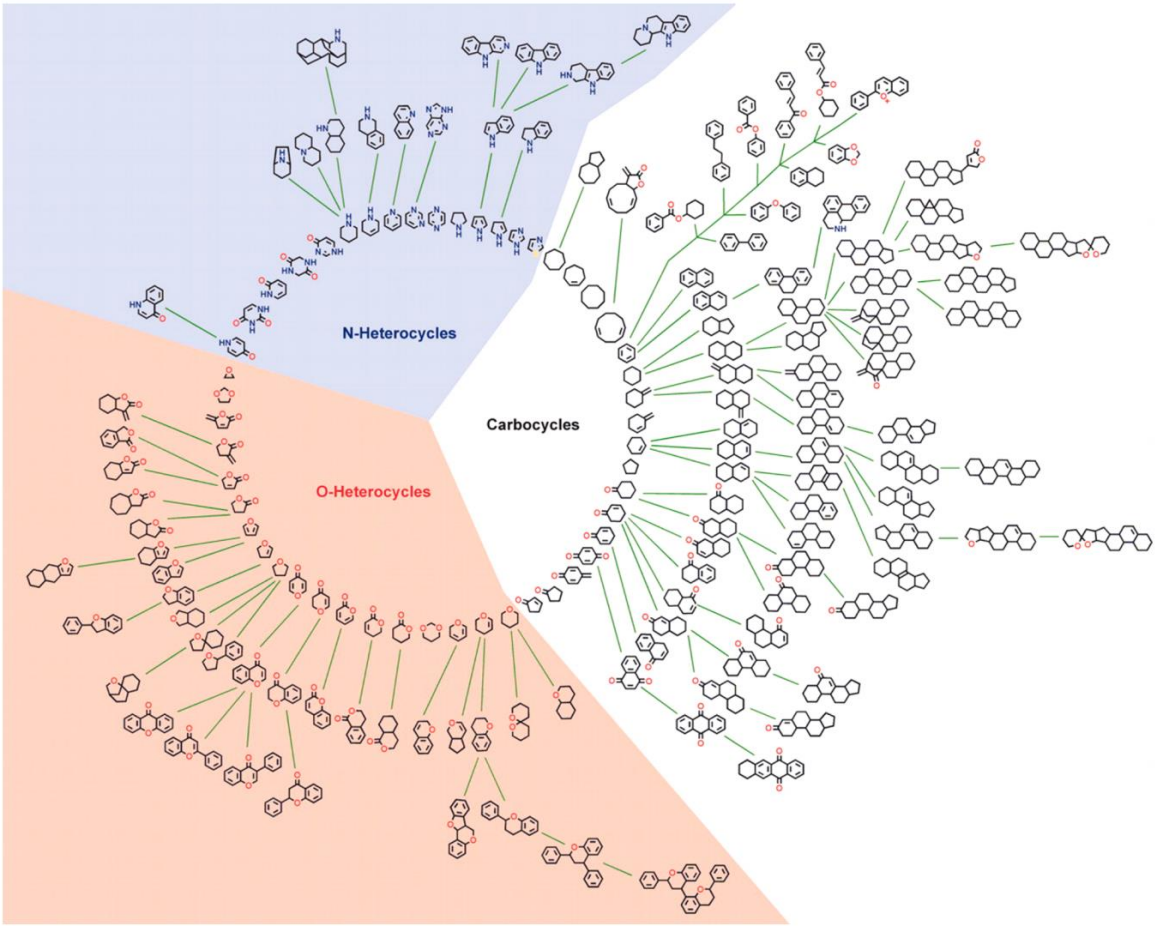


**Figure 2**: Graphical star-like representation of the NP scaffold tree. For clarity of the graphic illustration, only scaffolds are shown that represent cumulatively at least 0.2% of the NP population in the DNP. [26]Reprinted from ref. 20, Copyright (2005) National Academy of Sciences.

The SCONP scaffold tree enables a systematic design for the rapid synthesis of potentially bioactive compound libraries that can provide hit rates.[27-28] A strategical approach for the structure simplification of a complex NP based on SCONP and corresponding aid for library design is illustrated in Figure 3.[26, 29]

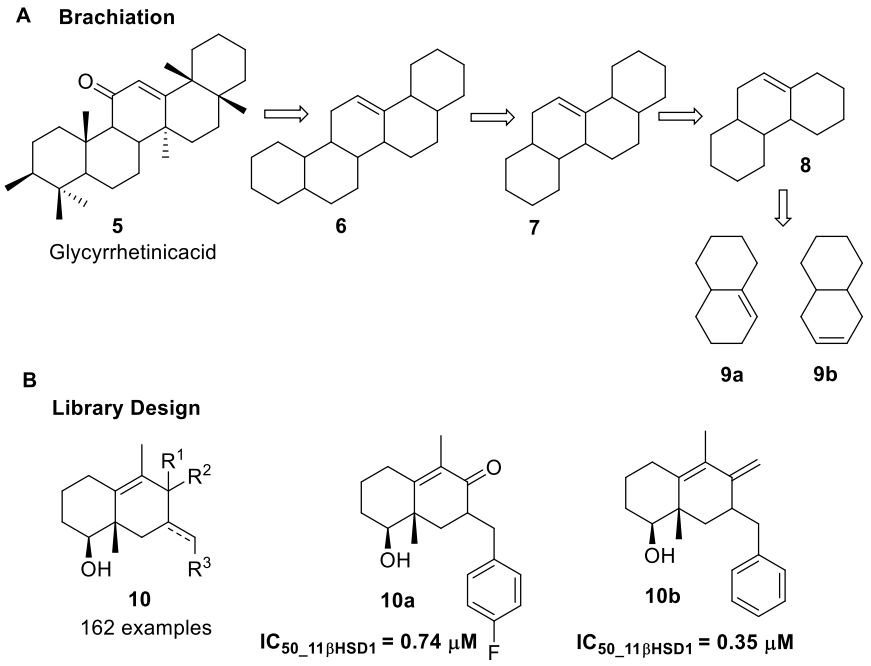


**Figure 3:** (**A**) SCONP Brachiation of Glycyrrethinicacid to a simplified core scaffold. (**B**) Library synthesis of 11βHSD1 inhibtors.

The BIOS strategy for the development of optimized structures regarding the bioactivity has been applied in several examples. By simplification the highly complex structure of the NP rychnophylline (**11**) to its *spiro*-core scaffold and diversification afforded five active compounds in the neurite growth assays (Figure 4).[30] In a similar approach, reducing the structural complexity of NP sominone (**14**) to the dehydro-δ-lactone scaffold **15** enabled the synthesis of potent inhibitors of the Hedgehog signaling pathway (Figure 4).[31]

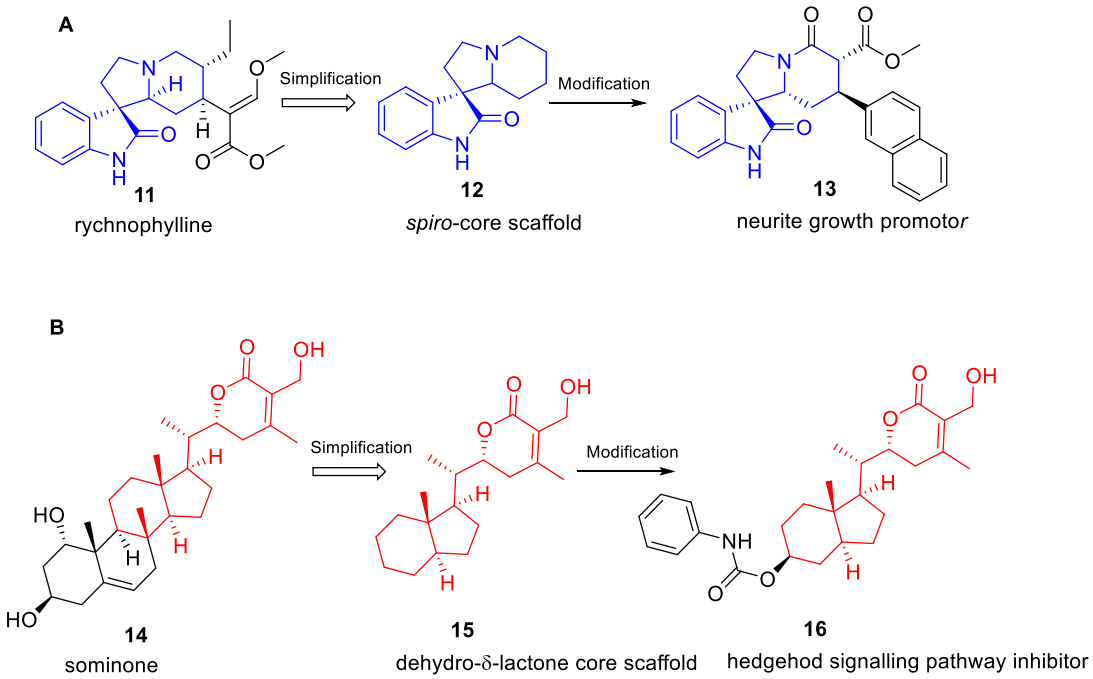


**Figure 4**: BIOS application on (**A**) rychnophylline **11** and (**B**) sominone **14** resulted in synthesis of compounds with enhanced bioactivity.

Even though the BIOS strategy promotes the discovery of chemical space which is not covered by NPs, this strategy is confronted with limitations. NPs occupy only a limited amount of existing chemical space and the NP-like chemical space is remarkably larger than existing NP-scaffolds.[32-33] Regarding this aspect compounds derived from application of BIOS show a chemical limitation and result in compound collections with retained and similar bioactivities to the structurally related NPs, thus also limiting the analysis and investigation of biological space.

## 1.3 Pseudo Natural Products

To overcome the limitation of BIOS regarding the chemical and biological space due to partial retention of guiding NP scaffolds and taking advantage of the biological relevance of NPs the design of novel scaffolds in the course of a program of pseudo natural products (pseudo NPs) was developed.[3-4, 34] The design principle in pseudo NPs is based on the combination of unrelated NP fragments in a unprecedent way and novel arrangements which is not accessible through existing biosynthetic pathways (Figure 5).[4] This combination concept provide access to novel compound classes endowed with characteristics of NPs and with unprecedented or unexpected bioactivities due to covering novel chemical and biological space. The design principle of pseudo NPs is inspired by combining strategies that take advantage from nature

and includes principles that cover a broad spectrum of chemical space such as fragment-based compound design. Inspiration for efficient *de novo* combination of unrelated fragments was achieved by cheminformatic analysis by simplifying a vast number of NPs to approximately 2000 NP-based fragments in which the key properties of the related NPs were preserved.[35] Pseudo NP compound classes should consist of diverse bioactive fragments including high content of stereogenic centres which is relevant for the three-dimensional character, as chirality has a great impact on bioactivity.[36-37] To provide distinct structural features and high order of diversity, heteroatoms should be incorporated in the fragments. Following those design criteria, it is hypothesized that the obtained scaffolds significantly differ from NP compound classes and show unexpected and novel bioactivity.

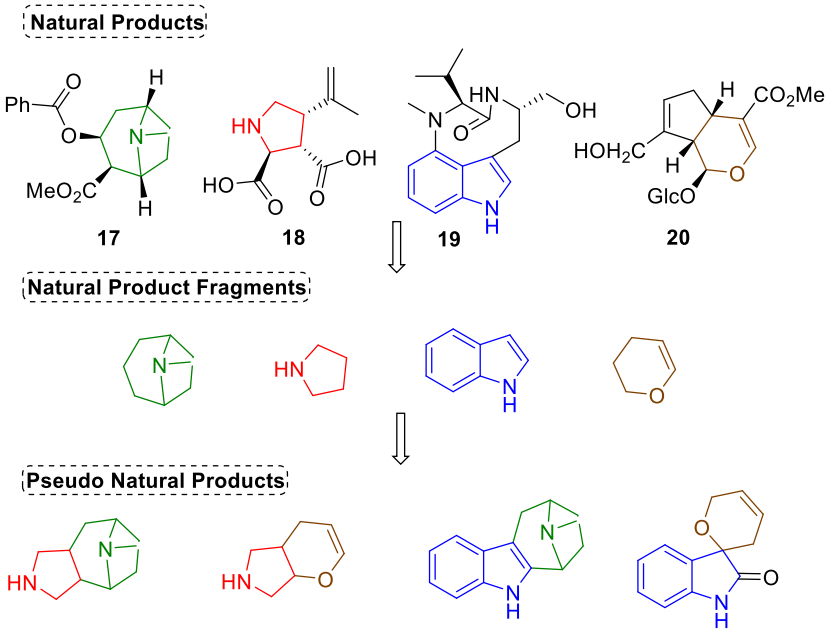


**Figure 5**: General concept of Pseudo Natural Products. Natural Product fragments are identified and recombined.

The combination of fragments obtained from different biosynthetic pathways would further extend the biological and chemical space and would dramatically increase the novelty of scaffolds with unpredicted, diverse and unrelated features regarding the bioactivity. Many connectivity patterns are possible for the combination NP scaffolds for the design of pseudo NPs. Here, NP scaffolds can be connected in certain arrangements which cannot be found in nature or they can be connected in a fashion which incorporates specific structural patterns faced in NPs. By consideration the design principle of pseudo NPs such as high content of stereogenic center for the three dimensional character or complexity and diversity of scaffolds NP fragments can be combined through different connectivity patterns to generate

novel and various pseudo NPs (Figure 6).[4] In order to connect two fragments a monopodal connection type can be used, which represents a simple type of connection, is also found in NPs (Figure 6). Connection of fragments through one common atom would lead to the formation of a *spiro* cycle. In this case a quaternary centre could be generated which is of high interest and value in chemical synthesis. The *spiro* fusion would increase the complexity of the resulting scaffold (Figure 6). Another type of connection for fragments is the edge fusion, resulting in an arrangement by sharing two common atoms. A bridged bicyclic scaffold can be obtained by sharing three or more common atoms inducing a higher content in the three-dimensional structure. In a bridged bipodal connection fashion the fragments may not share any common atoms and may be linked through intervening connection points resulting in a bridged scaffold incorporating a third fragment. The eligibility of the connection types for the corresponding fragment needs to considered with respect to the synthetic feasibility.

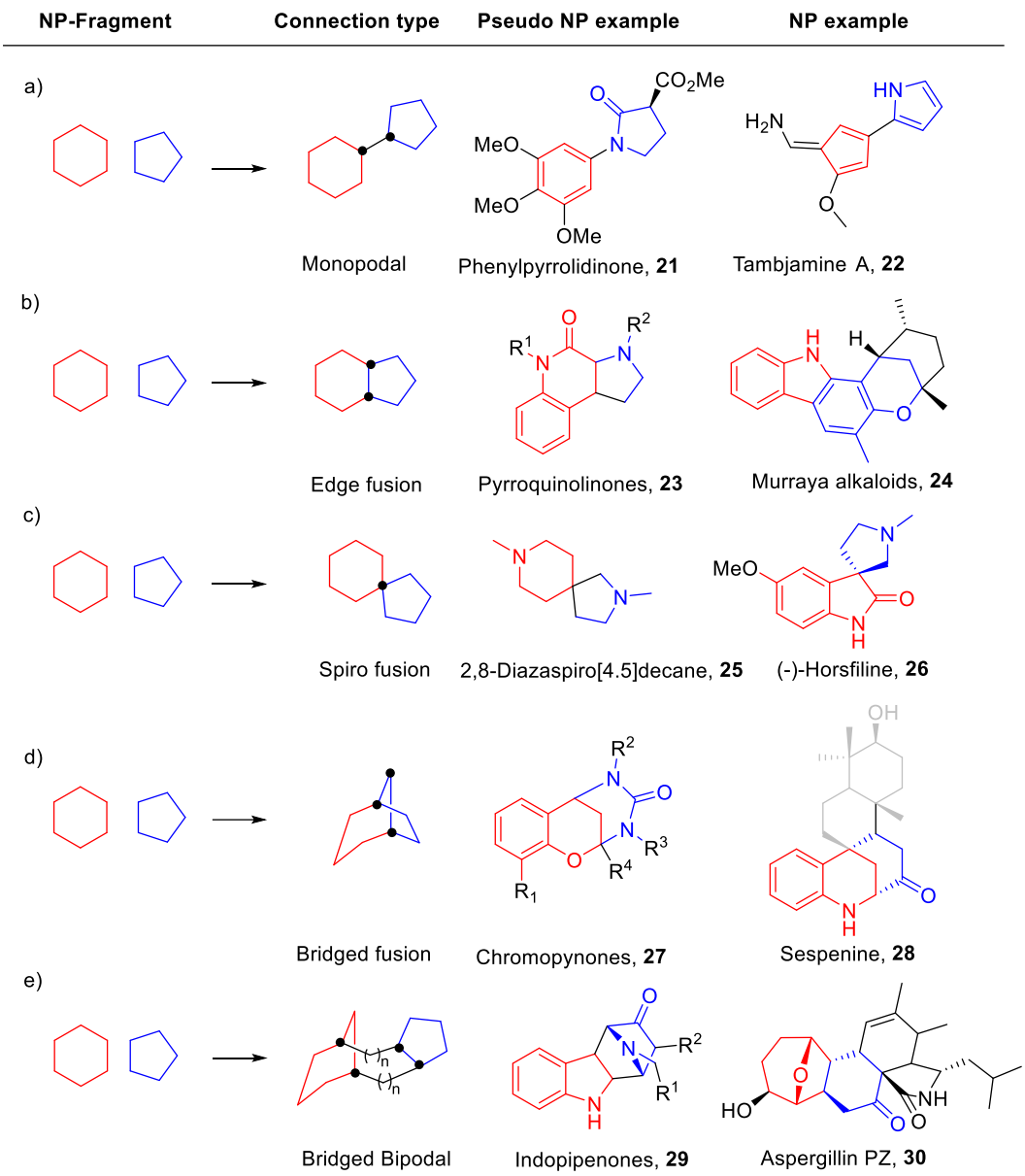


**Figure 6**: Illustration of possible connevtivities of NP scaffolds for the design of pseudo NPs.

The first illustrative example for the design of a pseudo NP was provided by executing the synthesis of chromopynones **27** through the unprecedented combination of chromane and a tetrahydropyrimidone (THPM) fragment by a bridged fusion connection (Figure 7).[3] The synthesis of the chromopynone pseudo NP compound class **27** was proceeded in a telescoped process via a Biginelli reaction followed by multistep cascade reactions. Biological evaluation revealed that the chromopynone **27** define novel, structurally unprecedented glucose uptake restriction chemotype targeting glucose transporters GLUT-1 and -3 including inhibition of cancer cells.[3] The novel biological effect of the chromopynones **27** is neither observed in chromane containing NPs nor in THPM containing NPs. The covering of novel chemical and biological space of the chromopynones **27** were explored by cheminformatic analysis

displaying that their scaffolds occupy different chemical space than NPs. This analysis reveals the non-accessibility of chromopynones **27** via a biosynthetic pathway. Furthermore, an additional pseudo NP compound collection utilized an asymmetric copper-catalyzed 3+2 cycloaddition to effectively combine indole and tropane NP fragments.[38] This method enabled the formation of multiple stereocenters and provided a stereogenically complex library of indotropanes **39**, which were identified as selective inhibitors of MLCK1 (Figure 7).[39]

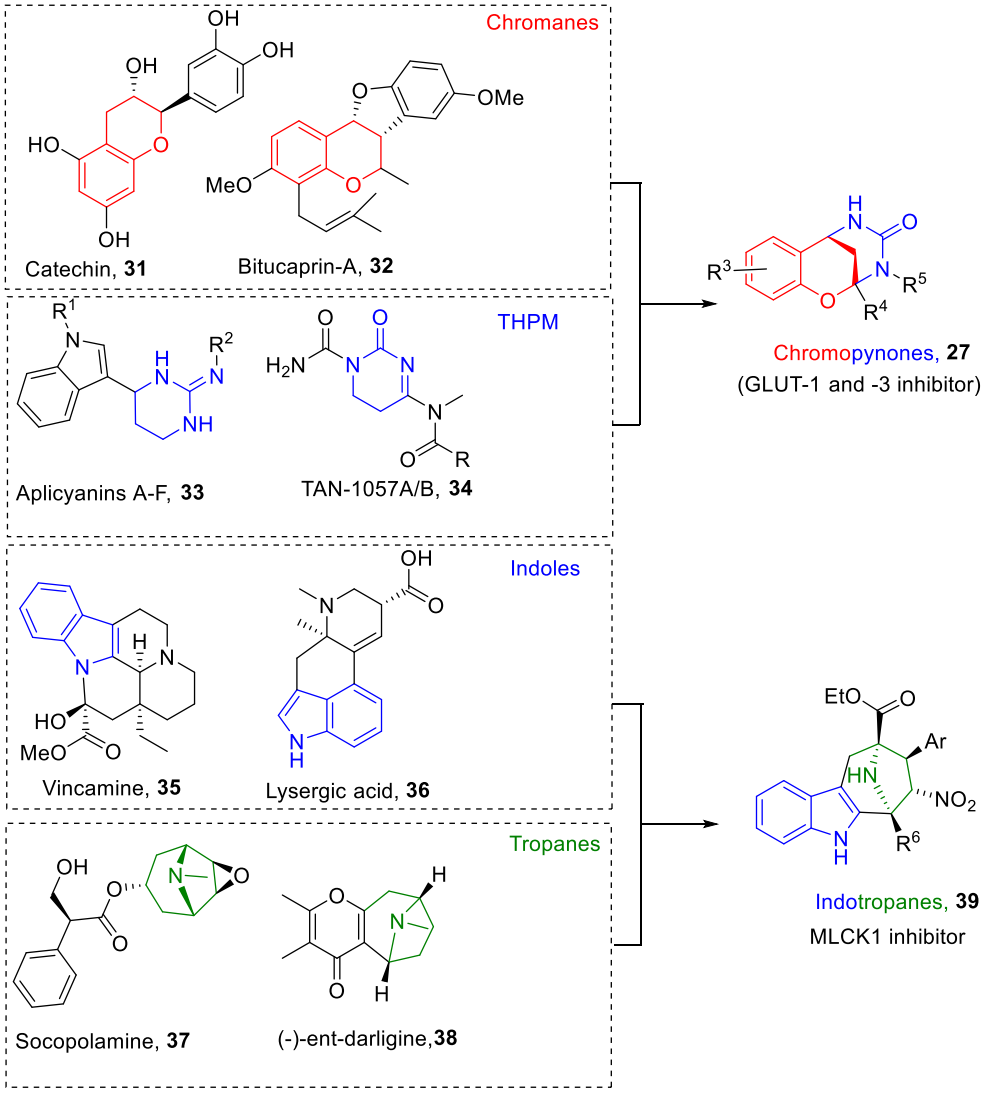


**Figure 7**: Design of a pseudo NP library for chromopynones **27** and indotropanes **39**.

The design principle of pseudo NPs shows the development of novel compound classes with unique areas of chemical and biological space being previously unoccupied by NPs and BIOS libraries.[4, 40] In general, multiple combinations of NP fragments are possible and need to be analyzed in a systematic manner. For greatly facilitating the *de novo* combination of NP

fragments, creative synthetic methods need be developed and applied that will enable rapid access to expanded libraries of pseudo NPs.

As pseudo NPs display novel and unpredicted bioactivities, profiling in unbiased phenotypic screening platforms needs to be applied to facilitate their full analysis regarding their biological targets.[4] The application of the cell painting assay in combination with powerful target identification methods may facilitate the analysis of pseudo NPs with respect to the discovery of new bioactivities.[4, 40]

Very common and important NP frameworks are heterocycles which can be applied for the design and synthesis of a pseudo NP compound library to combine them with various different NP scaffolds. A very convenient method allowing the construction of fused polycyclic compounds containing complex NP scaffolds are cycloaddition reactions such as the 1,3-dipolar cycloaddition.

## 1.4 1,3-Dipolar Cycloadditions

Five membered heterocycles are widely found in NP and bioactive compounds and their synthesis are high in demand.[41-43] The 1,3 dipolar cycloaddition (CA) represents a powerful synthetic method for the preparation of heterocycles and is among the most prominent reactions in organic synthesis.[5, 43] The utility of this fundamental reaction is extended in many fields of chemistry, from natural product synthesis, material science and chemical biology. The attractive feature and extensive application of 1,3 dipolar CA is based on the intrinsic efficiency, atom economy, and the control of the desired product regarding regio- and stereoselectivity.[5, 44] The first 1,3 dipolar CA was reported by E. Buchner in 1888 by describing the reaction between methyl diazoacetate **40** with dimethyl fumaric acid ester **41** leading to the formation of cycloaddition product pyrazole **42** (Scheme 1)**.**[45]

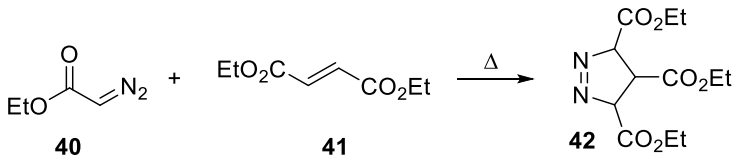


**Scheme 1**: First 1,3 dipolar cycloaddition.

For the establishment of a general concept for the 1,3-dipolar CA, in 1960, Rofl Huisgen provided a basic idea indicating the reaction proceeding through a concerted process after systematic studies.[46-47] A fundamental understanding of the concerted reaction mechanism was further achieved through development of the concept of orbital symmetry by Woodward and

Hoffmann.[48-49] Their work made a great contribution for mechanistical explanations regarding the selectivity of cycloadditions including the 1,3 dipolar CA on an orbital level.

### 1.4.1 1,3 Dipolar Cycloadditions and Frontier MolecularOrbital (FMO) Theory

In a 1,3 dipolar CA, a 1,3 dipole molecule, a 4π system, undergoes a cycloaddition with a 2π electron delivering dipolarophile to generate a five membered ring and formation of two new σ-bonds. The 1,3-dipole is defined as a-b-c species **43** and represented with a zwitterionic sextet and octet mesomeric structure (Figure 8). In the electron sextet structure the atom *a* is bearing a positive charge and the negatively charged centre atom *c* has an unpaired electron (Figure 8). In a concerted reaction four electrons of the dipolar compound **43** which are located in the parallel orientated *p*-orbitals overlaps with the two electrons in the p orbital of the dipolarophile d-e **44** to generate the desired CA product **45**.[44]

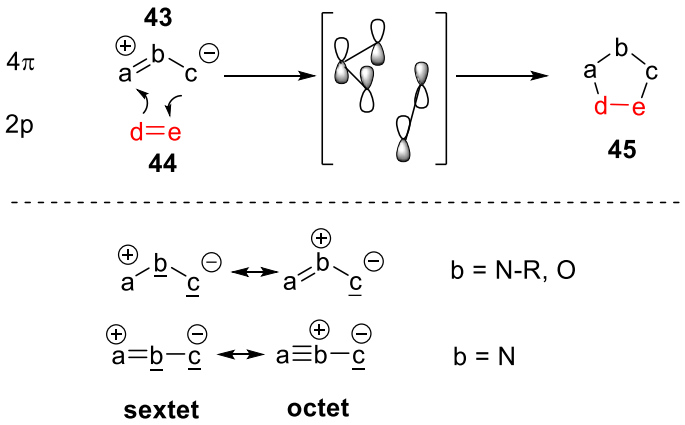


**Figure 8**: General basic illustration of the 1,3-dipola cycloaddition.

The 1,3-dipolar CA usually proceeds through a thermally allowed concerted reaction mechanism with results in a stereo and regio specific manner.[44] The stereospecific outcome can be explained with the FMO theory based transition state and is due to the suprafacial combination of the three $p_z$ orbitals of the 1,3 dipole and the two $p_z$ orbitals of the dipolarophile. Therefore, the concerted mechanism can be described with $[_{\pi}4_s + _{\pi}2_s]$ as a pericyclic shift in accordance with the Woodward-Hoffmann rules.[49] The prerequisite for the reaction to occur is a certain similarity in orbital energy to enable the interaction of the highest occupied molecular orbital (HOMO) and the lowest uncopied molecular orbital (LUMO).[50-51] The dominating interaction of the 1,3-dipole and the dipolarophile is highly dependent on the relative energy of the orbitals which is vastly affected by substituent effects. Electron deficient dipolarphiles favor an $HOMO_{dipol}$-$LUMO_{dipolarphile}$ interaction wherein an inverse interaction is

observed for electronrich dipolarophiles ($LUMO_{dipol}$-$HOMO_{dipolarphile}$) as for the latter case the energy of the $HOMO_{dipolarphile}$ increases and lowers the gap to the $LUMO_{dipol}$. Figure 9 illustrates the HOMO and LUMO dominating interaction of the 1,3-dipolar cycloaddition.[44]

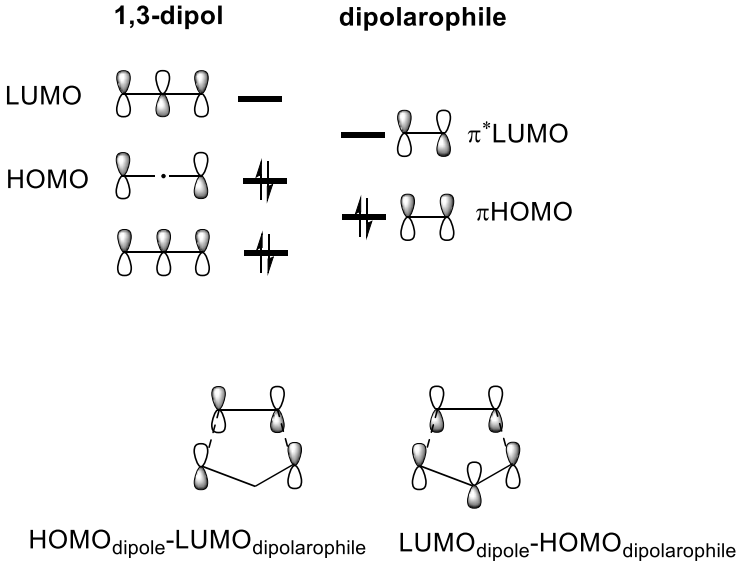


**Figure 9**: The HOMO-LUMO interaction in 1,3-dipolar CA.

With respect to the relative FMO energies of the 1,3-dipole and the dipolarophile the 1,3-dipolar CA can be divided into three types (Figure 10).[44, 52-53] In type I, the dominant interaction of the FMO is that of the $HOMO_{dipol}$ with the $LUMO_{dipolarophile}$ which are observed for reaction azomethine ylides. In type II, the energy gap between the FMO are very low and can be considered as equal implying that both interactions, HOMO as well as LUMO are of high priority and prevailing. An inverse dominating interaction is observed for type III in which the $LUMO_{dipol}$ is overlapping with the $HOMO_{dipolarophile}$ due to higher energy level of the $HOMO_{dipolarophile}$.

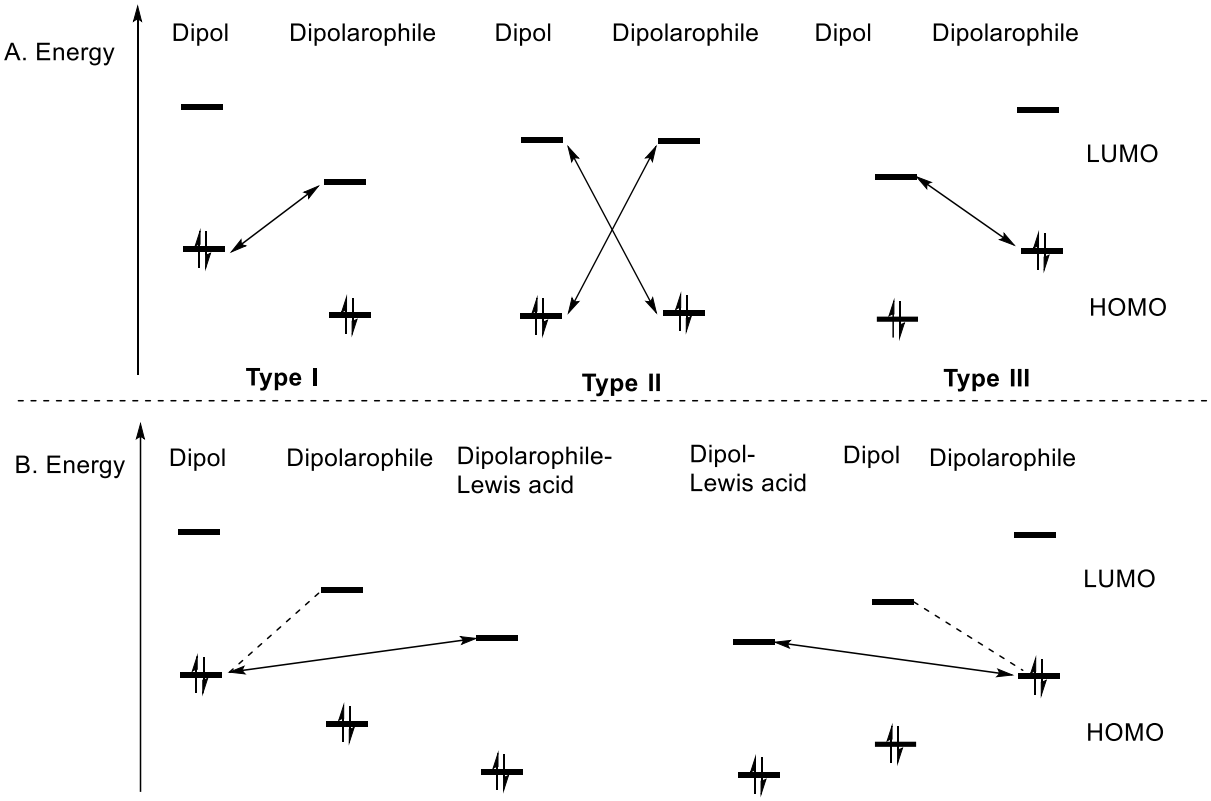


**Figure 10**: A. Classification of the 1,3-dipolar cycloaddition on basis of the FMO. B. Change in relative energy of the FMO in presence of a Lewis acid.

Lewis acids play a vital role in 1,3-dipolar cycloadditions regarding the FMO energy and possess the ability to accelerate the reaction.[44] The coordination of Lewis acids to the corresponding dipole/dipolarophile alters the energy of the FMO. Upon coordination, the energy of the FMO are decreased relative to the non-coordinated species and thus decreasing the energy gap between the HOMO and the LUMO of the reacting species. This phenomenon changes the reaction rate and allows a faster interaction of the orbitals. The utilization of a Lewis acid is also a fundamental aspect in a asymmetric fashion of the 1,3-dipolar cycloaddition for inducing enantioselectivity in combination with a chiral ligand.[44]

The 1,3-dipolar CA might create up to four stereocenters in the final product and therefore also the control of diastereoselectivity is of high importance as *endo* and *exo* products can be formed. The *endo/exo* selectivity are primarily controlled by the structure of the substrates and by the catalyst.[44, 54] It should be noted that analogues to Diels-Alder (DA) reaction, the *endo* transition state it stabilized by secondary orbital interactions of the *p* orbitals over the *exo* transition state (Figure 11).

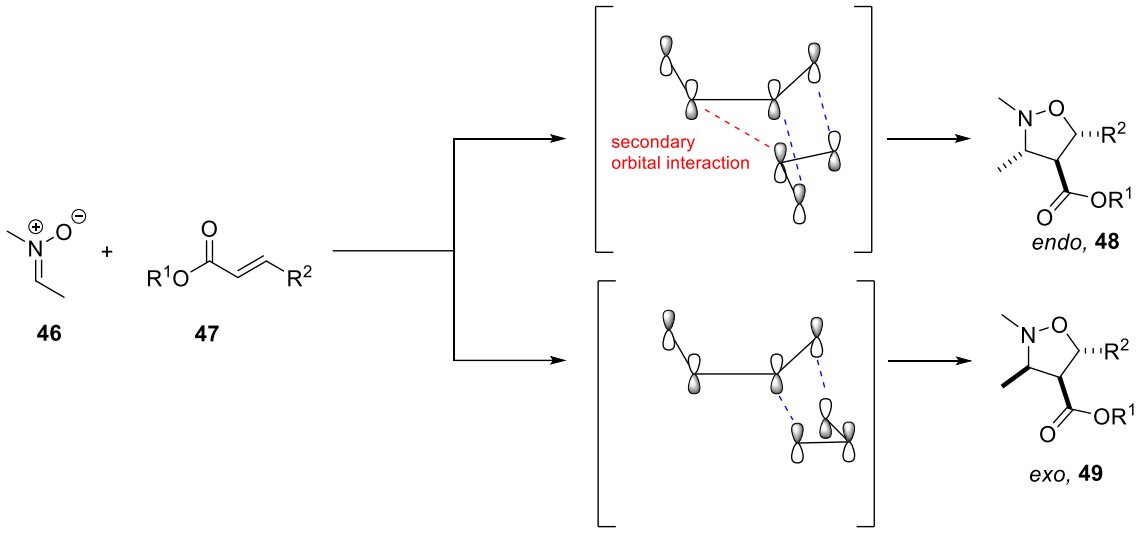


**Figure 11**: Endo/Exo transition states for 1,3 dipolar cycloaddition of **46** and **47.** Primary orbital interactions are highlighted in blue, secondary orbital interactions are highlighted in red.

Based on the FMO theory, the 1,3-dipolar CA is a thermally allowed reaction but photochemically forbidden.[49] In order to proceed the reaction, the *p* orbitals with same face need to overlap. In case of a photochemically reaction the HOMO in excited state of one reactant and the LUMO in ground state of another reactant need to be considered. This would lead to an interaction of *p* orbitals with opposite face and thus resulting in an antibonding process and no product formation (Figure 12).

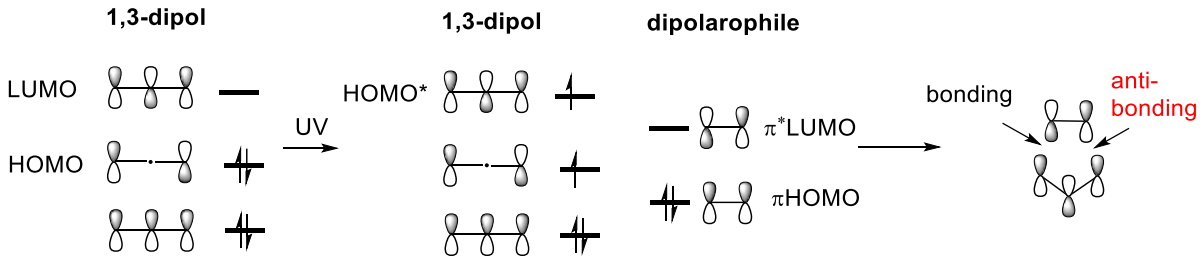


**Figure 12**: Illustration of FMO in a photochemical fashion of 1,3-dipolar CA.

The concerted mechanism in 1,3-dipolar CA assures the stereospecificity in the product, however a stepwise mechanism is also possible, which can lead to mixture of stereoisomers. A stepwise mechanism might be related to steric hinderance and rotation of the formed intermediate results in loss of stereoselectivity.[55]

### 1.4.2 Asymmetric 1,3 Dipolar Cycloadditions

Five membered nitrogen heterocycles, especially highly substituted pyrrolidines, are present in important pharmaceuticals, natural alkaloids and building blocks in organic synthesis.[5, 56-57] In this context, the asymmetric version of the 1,3-dipolar CA plays a fundamental role for the preparation of highly enantioselective five membered heterocycles.[5] Here, the 1,3-dipolar CA of azomethine ylides derived from α-iminoesters with activated alkenes established a powerful and convergent method for the synthesis of substituted chiral pyrrolidines.[5, 43] In the catalytic asymmetric 1,3-dipolar CA of azomethine ylides, the α-iminoester **50** acts as a dipole precursor. Upon coordination to a chiral metal complex through nitrogen and oxygen, a five membered metallocycle **A** is formed which increases the acidity of the corresponding α-proton of the α-iminoester. Deprotonation of the α-proton generates the azomethine ylide dipole which has nucleophilic character and can react with activated olefin **51** through a concerted/stepwise mechanism to afford substituted enantioenriched pyrrolidine **52** (Figure 13).

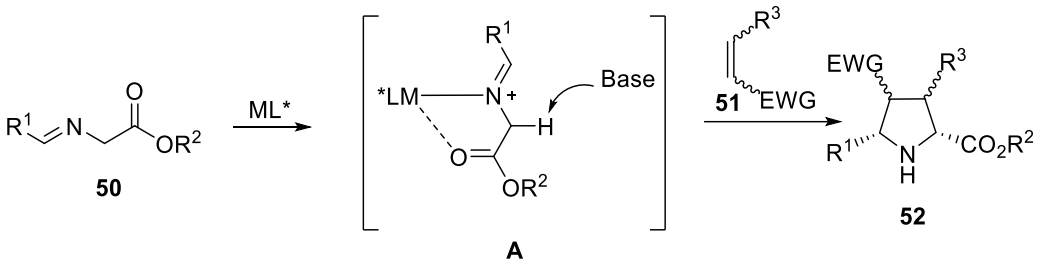


**Figure 13**: Catalytic asymmetric 1,3-dipolar CA of iminoesters **50** with activated olefins **51**.

The first asymmetric catalytic 1,3-dipolar CA of azomethine ylides with activated olefines were reported in independent work by Zhang and Jorgensen (Figure 14).[58-59] Zhang and co-workers employed a AgOAc/xylyl-FAP chiral catalyst system for the 1,3-dipolar CA of α-iminoester **50** with dimethyl maleate **53** affording *endo*-selective CA products **55** with good enantioselectivity. A Zn-catalyzed CA was applied by Jorgensen's group yielding enantioselective *endo*-cycloadducts **58** from α-iminoester **50** and acrylates **56.** Since the development of the first asymmetric 1,3-dipolar CA, much attention has been paid to developing enantioselective variants over the past decade due to its widespread application. Thus, the development of ferrocene based P,S ligands possessing planar chirality, such as (*R*)-Fesulphos ligand **60**, results in a highly reactive catalyst system displaying great enantioselectivity and a wide range of scope in the asymmetric 1,3-dipolar CA of azomethine ylides.[60-61] The first example of employing (*R*)-Fesulphos **60** as a chiral inducing ligand in 1,3-dipolar CAs was described by Carretero and co-workers in a Cu(I)-mediated reaction between

α-iminoester **50** and maleinimide **59** affording *endo*-selective CA product **61** with excellent enantioselectivity (Figure 14).[61]

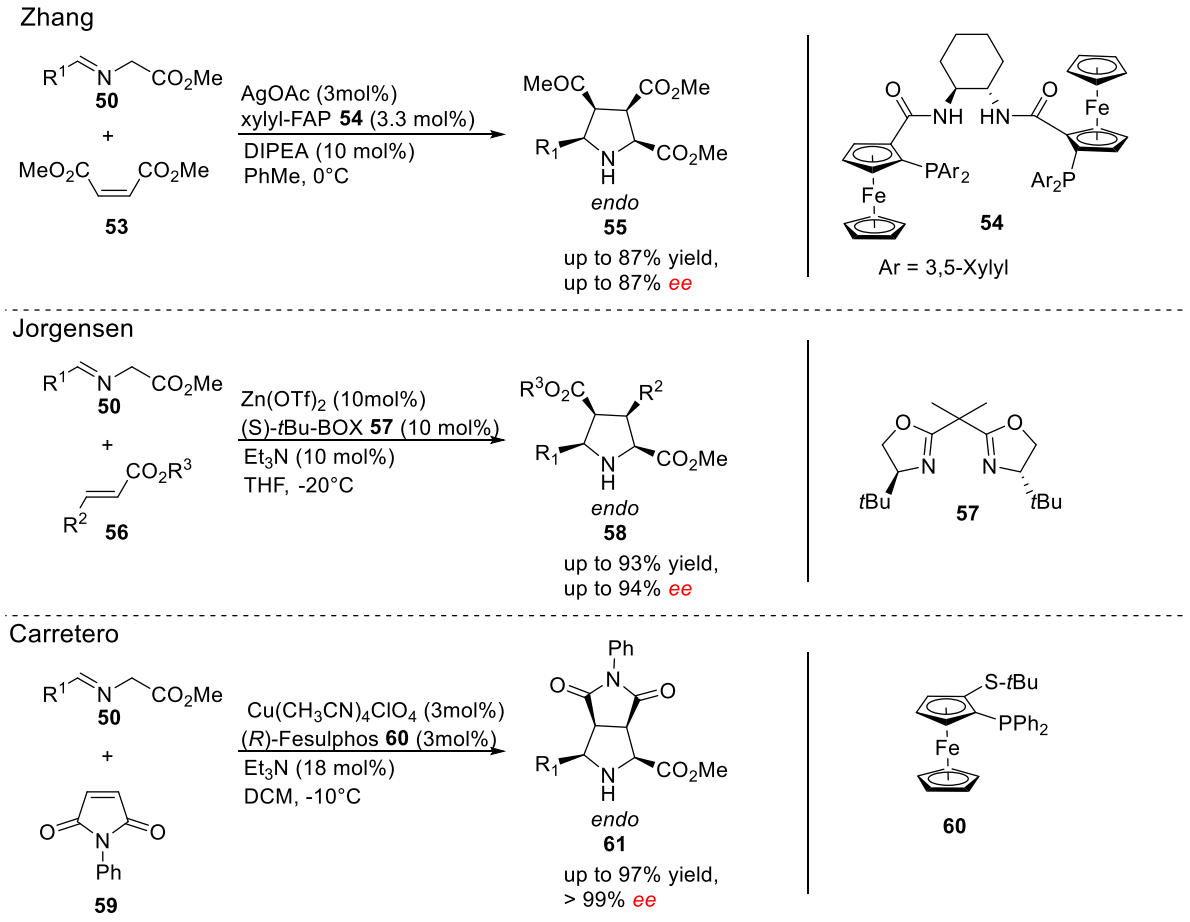


**Figure 14**: Asymmetric 1,3-dipolar CA of α-iminoester **50** with different activated alkenes under different chiral conditions.

Recent advances have shown that the asymmetric fashion of the 1,3-dipolar CA is one of the most efficient stereocontrolled methods to access molecules with multiple stereocenters. The group of Herbert Waldmann has applied this reaction type to numerous experiments in the course of BIOS and pseudo NP programs to obtain bioactive compound libraries.[57] The power of the asymmetric 1,3-dipolar CA was exploited for advanced synthetic applications such as the synthesis of complex molecules with quaternary spirocenters leading to bioactive compounds.[62] Based on this, the first asymmetric synthesis of 3,3'-pyrrolidinyl spirooxindoles **64** through a 1,3-dipolar cycloaddition of an azomethine ylides to a 3-arylidene- or alkylidene oxindole **62** was developed by Waldmann and co-workers (Figure 15).[62] In this context, one of the highly impressive applications was the generation of products with up to 8 stereocenters in a single step by two consecutive additions of azomethine ylides p-benzoquinone **65** (Figure

15).[63] In presence of catalytic amounts of Cu(I) and (*R*)-Fesulphos as ligand the reaction proceed with enantio-, diastereo- and regioselectivity. As the chirality is introduced in the first step of the reaction sequence of double CA, both enantiomers could be selectively obtained using the same set of reagents by changing the order of the iminoester addition.[63] Furthermore, Antonchick, Waldmann and co-workers harnessed the power of the 1,3-dipolar CA reaction method by combining it with higher order of cycloadditions (6+3) (Figure 15).[64]

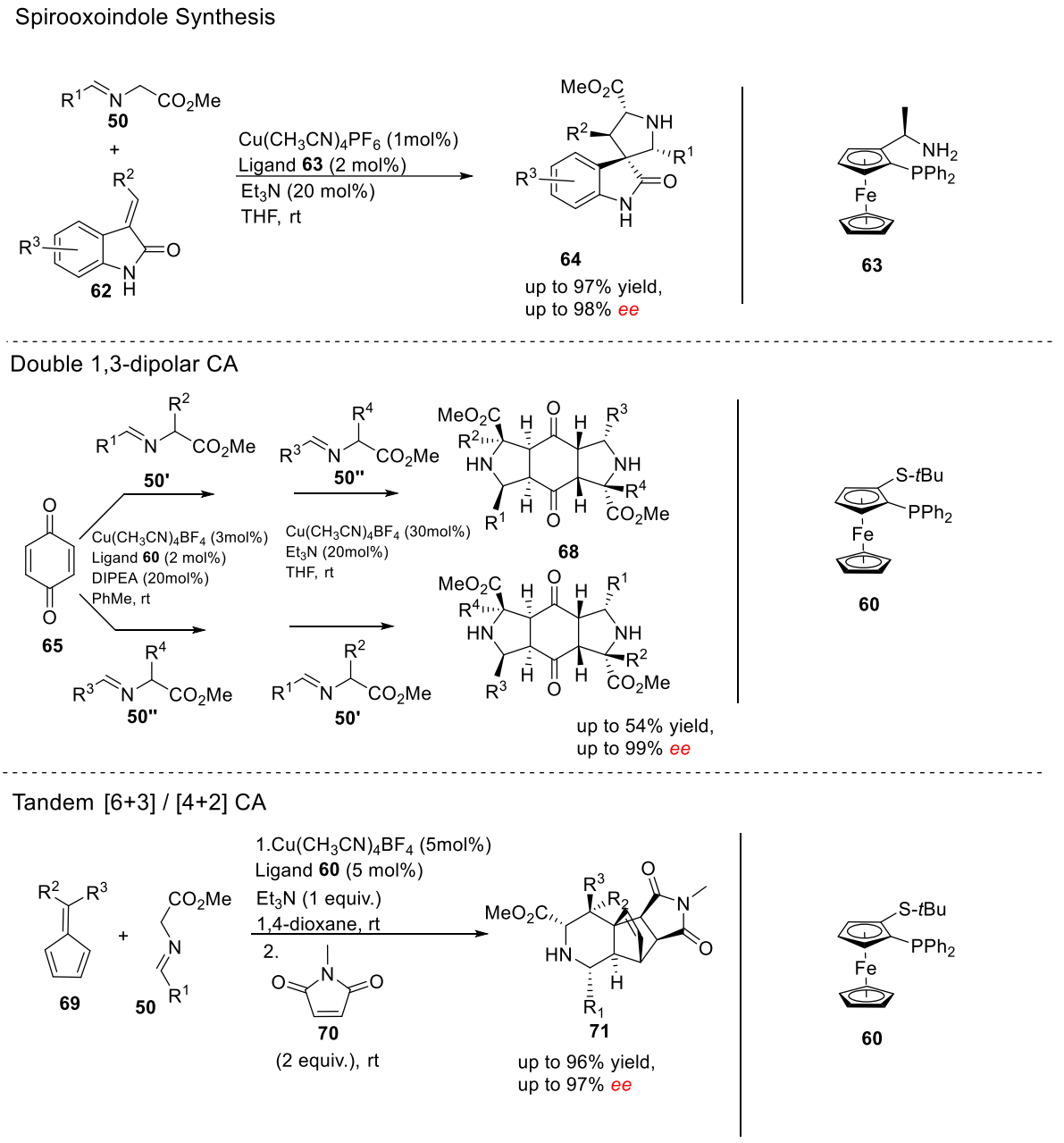


**Figure 15**: Selected examples of asymmetric 1,3-dipolar CA for the synthesis of highly complex bioactive molecules with multiple stereoenters by the group of Herbert Waldmann.

Although the 1,3-dipolar cycloaddition leads to the formation of very stable stable [3+2]-cycloadducts in stereospecific manner, it has been observed that a retro-1,3-dipolar CA can also proceed leading to interconversion of stereosisomers in terms of covalent bond breaking and reforming.[6] Aly and co-workers reported the interconversion of *endo*-adduct to *exo*-adduct in a reversible 1,3-dipolar CA.[6] This dynamic mode has a great influence on the equilibrium process of a reaction as well as on the product distribution under certain conditions. This complicated procedure is a dynamic covalent process.

## 1.5 Dynamic Covalent Chemistry (DCC)

The molecular synthesis of organic compounds leading to a product distribution of an irreversible reaction is usually dominated by kinetically controlled reactions.[7, 65] The irreversible nature of the reaction guarantees that, once the particular product is formed, it is stable and not possible to be reformed or be converted into another product. The product distribution in an irreversible fashion is highly dependent to the relative difference between the initial state and the transition state Gibbs energies ($\Delta G^{\ddagger}$) (Figure16).[66] However, covalent bonds have the ability to be formed and broken reversibly under fast equilibrium by exposing them to external stimuli leading to product formation under thermodynamic control.[7, 67] Product distribution in reversible systems reflects the relative Gibbs energies of the products, thus shifting the equilibrium to the formation of products with the relatively lowest energy ($\Delta G$) (Figure 16).[68-70]

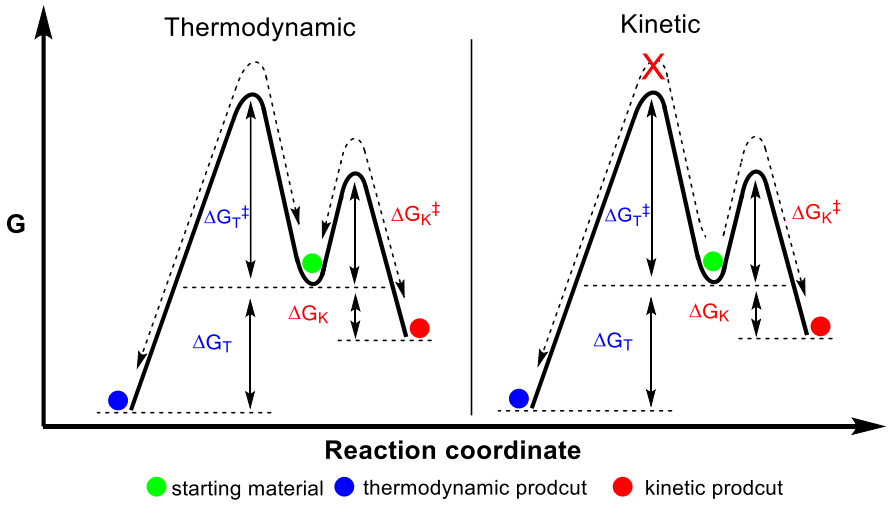


**Figure 16**: Free energy profile illustrating thermodynamically and kinetically controlled reactions.

In the context of reversible bond formation thermodynamic equilibrium control, Rowan et al. introduced the concept of dynamic covalent chemistry (DCC).[7] DCC is a dynamic process that allows exchange and interconversion of molecular components under conditions of equilibrium control providing a thermodynamically based system. The concept of DCC was mainly proposed in the context of supramolecular chemistry regarding the self-assembly of building blocks into highly complicated systems.[68] Here, the reversible nature of reactions permits ‘‘error checking“ and “proof reading“ for interconverting components to access the thermodynamically most stable adduct based on non-covalent interactions.[68] While in supramolecular chemistry weak noncovalent interactions dominate, for DCC more robust covalent bonds are relevant with slower kinetics of bond cleavage and formation. Some selected examples of dynamic covalent reactions are shown in Figure 17.[71]

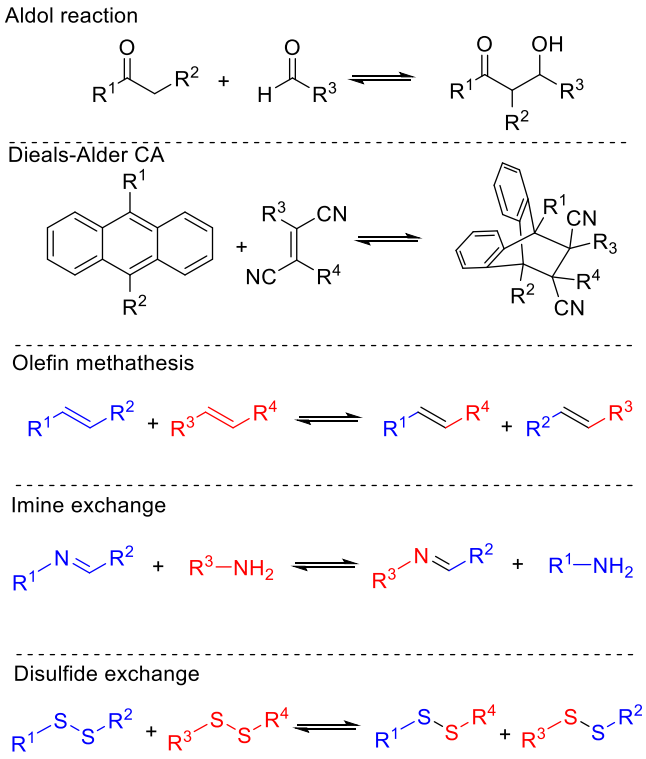


**Figure 17**: Selected examples dynamic covalent reactions.

### 1.5.1 Dynamic Combinatorial Library (DCL)

In DCC, the chemistry of complex processes under thermodynamically driven control establishes the basis for the design of dynamic combinatorial libraries (DCL). A DCL is thermodynamic controlled mixture of interconverting building blocks through a reversible

process generating a complex mixture of products that can respond to various external stimuli.[70] Thus, as a dynamic system the library can reorganize in order to minimize the total free energy of the system. A selective library design can be achieved by consideration of stabilization effects such inter/intra molecular interactions, the use of a template, for a template directed amplification of specific library members or the use of a host/guest system to enable specific interactions with a certain library member.[69] A selective shift in equilibrium of a DCL can be induced by exposing the DCL to external stimuli employing a thermodynamic trap (Figure 18).[70] However, since DCLs strive for the lowest overall Gibbs energy, in some cases the interconversion of library members will not proceed smoothly due to intramolecular interactions of library members acting as a kinetic trap and blocking the system to achieve the thermodynamically controlled equilibrium.

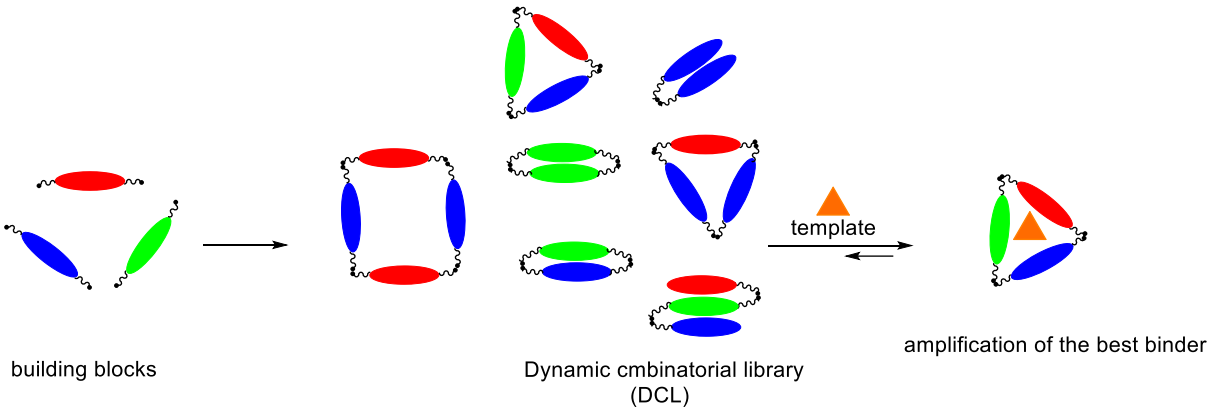


**Figure 18**: Schematic representation of a dynamic combinatorial library and amplification of one specific library in presence of a template.

### 1.5.2 Selection Strategies for the Selective Design of Dynamic Combinatorial Libraries (DCL)

The reversibility of dynamic covalent reactions and their feasibility of constructing a dynamic combinatorial library (DCL) was demonstrated and applied in several examples. Ramström and co-workers developed a dynamic covalent system in combination with an enzyme mediated asymmetric resolution.[72] A reversible nitro aldol (Henry) reaction was employed in which various arylaldehydes **72-76** were reacted with 2-nitropropane **77** to afford corresponding nitroalcohols **78-82** in a stereo-unspecific manner. Thus, a DCL with ten nitroalcohols **78-82** (*R* and *S* isomers) was obtained. Upon treatment of the library with lipase PS:C I, a kinetic

resolution proceeded shifting the equilibrium of the generated library towards formation of selective one library member (Figure 19):

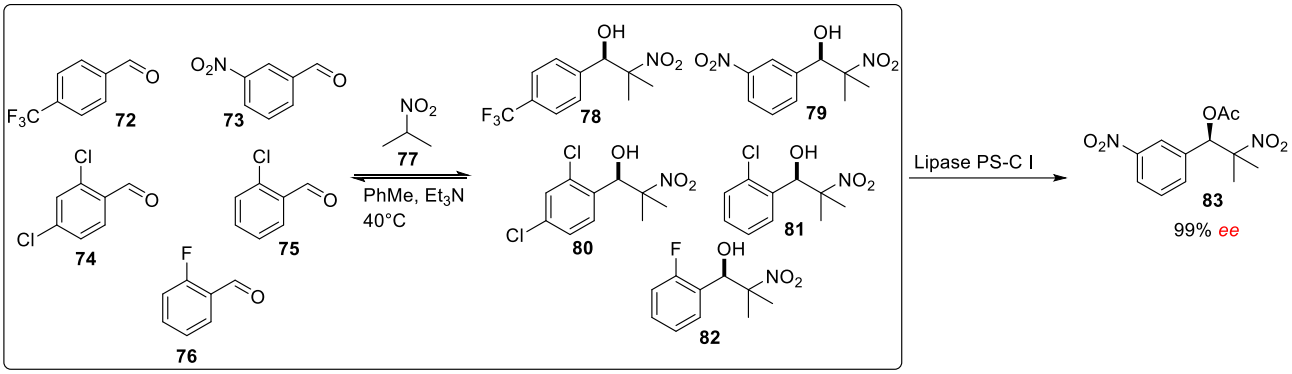


**Figure 19**: DCL of nitroaldol and Lipase-mediated dynamic kinetic resolution.

Another impressive strategy which is observed in DCLs enabling amplification of one library member is the autocatalytic amplification. The DCL is coupled to self-replication of a library member, that is stabilized through duplex formation via intermolecular interactions creating selectively a self-replicating library. In 2008 Xu and Giuseponne reported a DCL employing aldehydes **84-86** and amines **87-88** as building blocks.[73] A reversible imine formation takes place generating a library in which only one library member (**89**) is stabilized by formation of a duplex with itself. This stabilizing effect over other libraries results in an autocatalytic self-replicating process shifting the equilibrium of the DCL (Figure 20).[73]

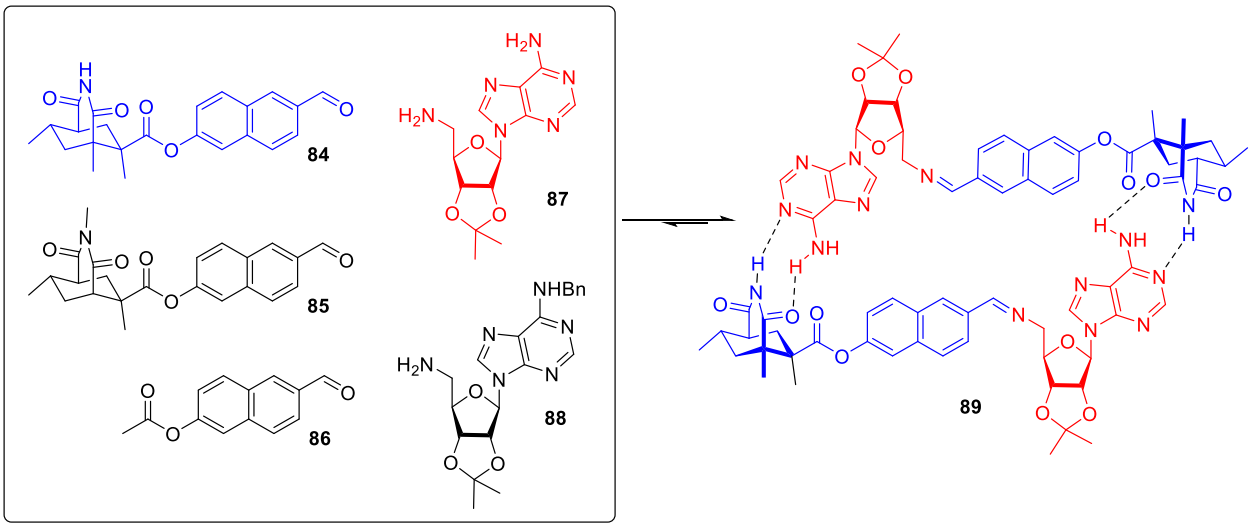


**Figure 20**: Representation of a self-replicated autocatalytic controlled DCL by mixing aldehydes **84-86** and amines **87-88**.

An enzyme-catalyzed DCL was designed by Turner and co-workers in a reversible aldol reaction using a thermodynamic trap.[74] A DCL of sialic acid analogues **91** was generated

through a NANA-Aldolase-catalyzed aldol reaction. The addition of wheat germ agglutinin (WGA), a well-studied binder for sialic acid, lead to exceed formation of one library member and acting as molecular trap. It should be noted that the preparation of sialic acids through traditional synthetic methods is very challenging, but the application of enzyme catalysis facilitates the preparation and allows rapid access to a library. In the absence of a molecular trap, a 1:1 mixture of libraries was obtained, wherein the utilization of a binder enabled the selective formation of one library member (Figure 21).

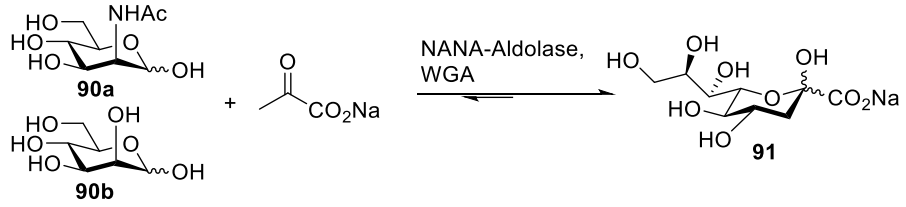


**Figure 21**: NANA-Aldolase-catalyzed DCL generation in presence of a thermodynamic trap WGA.

DCC enables an equilibrium shift through reversible reactions. It offers the opportunity to control the equilibrium in a stereospecific manner allowing the formation of products with the desired stereochemistry. It is a powerful method to design conditions for highly complex systems to achieve product formation in a stereospecific manner, thus enabling a stereodivergent synthesis which is in high demand and often very challenging. The selective preparation of stereoisomers plays a fundamental role in asymmetric synthesis.

## 1.6 Stereodivergent Synthesis

Chiral molecules in living organisms exist almost exclusively as single enantiomers which is fundamental for molecular recognition and replication processes and establishes the origin of life.[75-76] The homochirality of biological molecules including amino acids and sugars, which serve as building blocks for homochiral polymers such as proteins, DNA and RNA is one of the most important phenomena to understand the origin of life.[75] Thus, the synthesis of enantiomerically pure compounds and access to both enantiomers of a chiral molecule is one of the greatest challenges and high in demand in asymmetric synthesis. The concept of stereodivergent synthesis addresses and considers the selective preparation of stereoisomers starting from the same substrate and controlling multiple stereocenters.[77] The stereochemical outcome is highly dependent on chiral parameters as the structure of the applied chiral ligand is crucial. Furthermore, non-chiral parameters including solvent effects or additives can tune the stereochemical course of a reaction by affecting the transition state.[78-79]

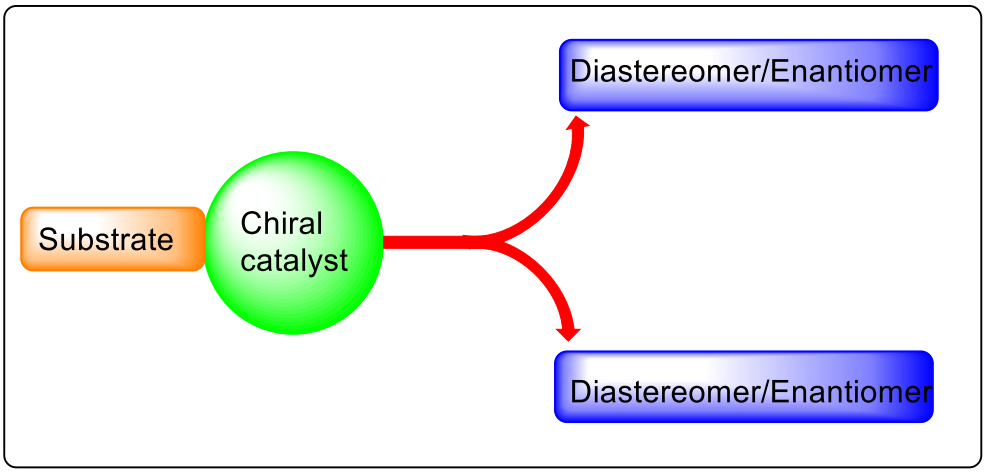


**Figure 22**: Schematic representation of the possible stereochemical outcome for a stereodivergent synthesis.

Over the years, fully stereodivergent strategies to control the stereochemical outcome in an enantio- and diastereodivergent fashion were developed. Carreira et al applied a dual chiral catalyst system to achieve a stereodivergent synthesis in α-allylation of aldehydes (Figure 23).[80] A coupling of amine and Ir-catalysis through chiral enamine and allyl metal intermediate species formed a stereodivergent dual catalytic system in which two different and highly face-selective catalytic cycles are combined and provide access to all possible stereoisomers in highly stereoselective form.

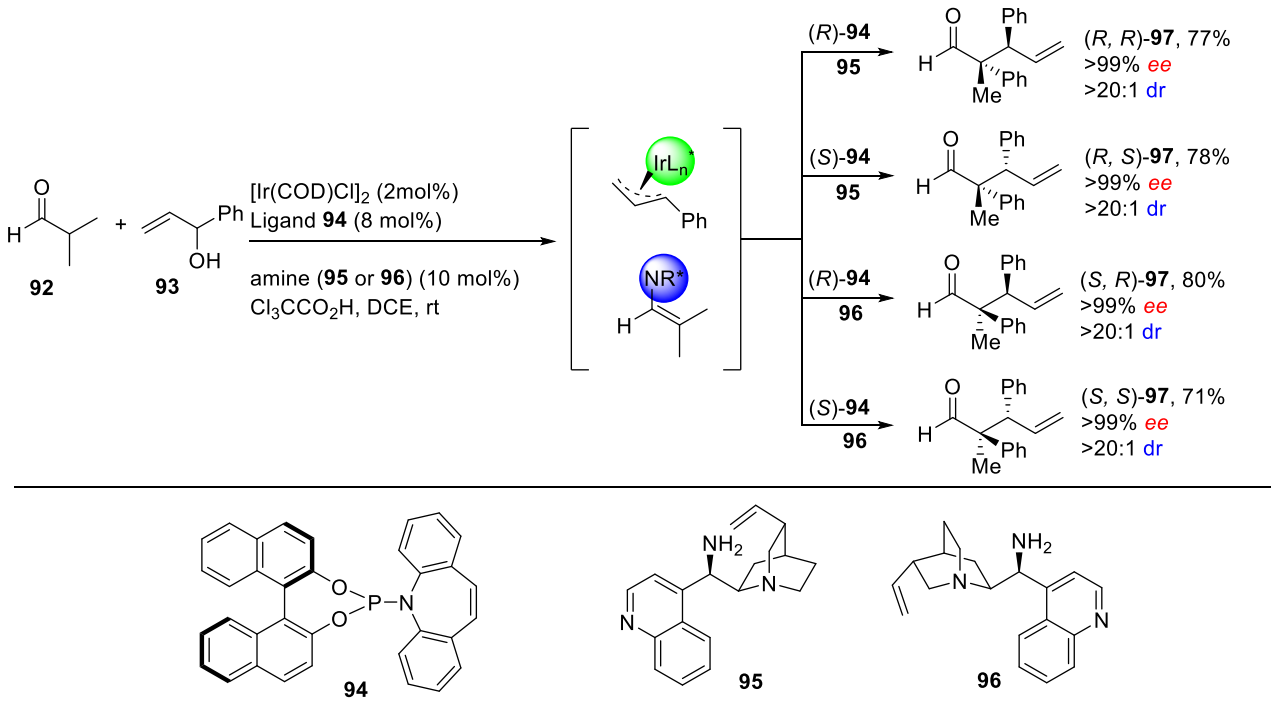


**Figure 23**: Stereodivergent allylic alkylation of aldehydes via a dual chiral catalyst system.

A well-established method for an enantiodivergent synthesis is kinetic resolution (KR).[81-82] This method takes advantage of an enhanced selective reactivity of one enantiomer of a pair of enantiomer towards the chiral catalyst. One enantiomer matches with the chiral environment of the chiral catalyst and therefore is transformed to the desired product wherein the other enantiomer remains unreacted affording both substrates in enantioenriched form.[82] Waldmann, Antonchick and co-workers observed the phenomenon of kinetic resolution by preparing an iridoid inspired compound library **99** via a asymmetric Cu(I)/(*R*)-Fesulphos catalyzed 1,3-dipolar CA of α-iminoesters **50** with racemic 2*H*-pyran-3(6*H*)-ones **98** (Figure 24).[83] The stereochemical course of the kinetic resolution is due to sterically unfavourable interactions of one enantiomer of the racemic 2*H*-pyran-3(6*H*)-ones **98** in the corresponding transition state. The reaction enabled the synthesis of enantiomerically enriched bioactive compounds inhibiting the Hedgehog pathway.

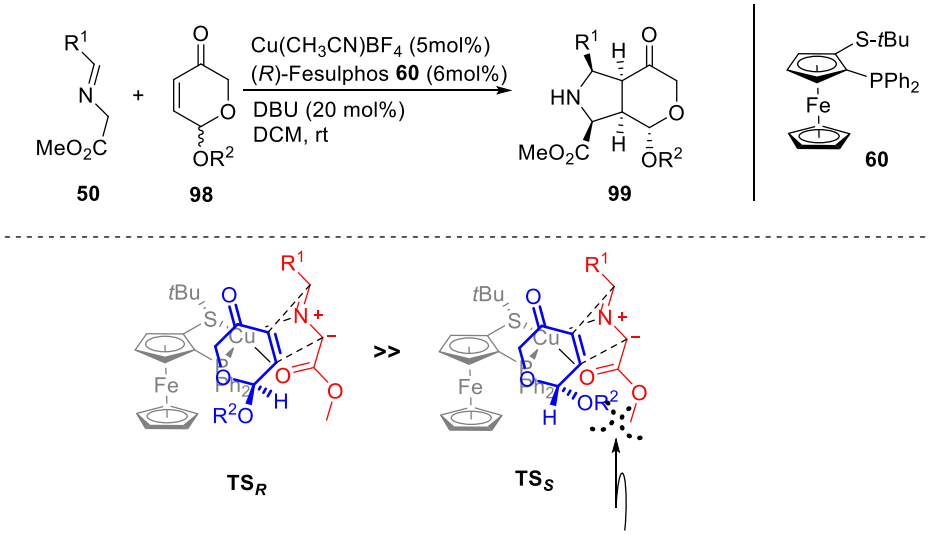


**Figure 24**: Kinetic resolution in 1,3-dipolar CA of α-Iminoesters **50**.

Alternatively, reaction time can also act as a fundamental parameter controlling the stereochemical outcome of a reaction. The stereochemical course of a reaction can change over time allowing a time-dependent stereodivergent synthesis. In this context, You and co-workers reported a time-dependent enantiodivergent synthesis in an Ir-catalyzed allylic substitution reaction enabling the selective preparation of both enantiomers at different time points (Figure 25).[84] Both enantiomers could be obtained using the same set of reagents by only varying the reaction time, which provides an alternative method, for the preparation of both enantiomers of a chiral molecule. Mechanistical studies revealed that a sequential kinetic resolution occurs.

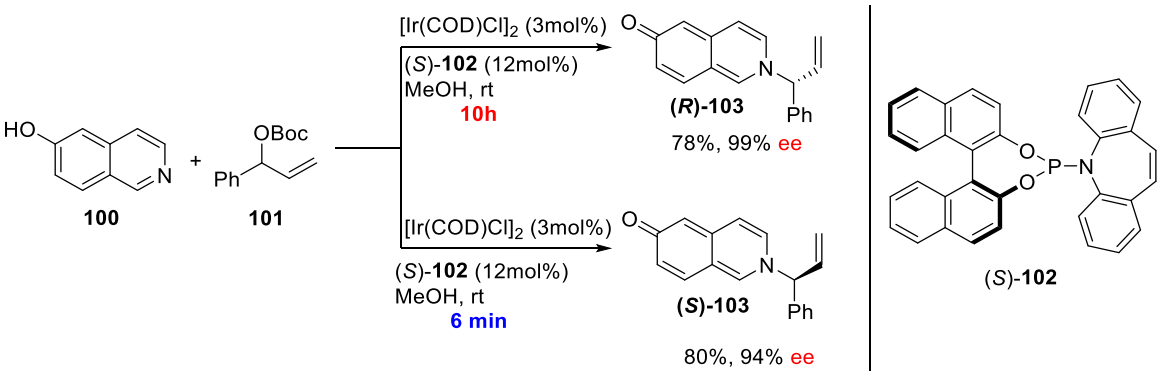


**Figure 25**: Time dependent enantiodivergent synthesis.

Stereodivergent synthesis is a powerful strategy to access enantiopure compounds. However, it is a highly complicated process and small changes of reaction parameters can have a great impact on the stereochemical outcome.

# 2 Aim of the Thesis

NPs define the prevalidated regions of chemical space, and they are used as starting points for BIOS. Compound collections derived from BIOS are enriched in bioactivity and enable to explore chemical space which are not covered by NPs.[2] However, the BIOS strategy is confronted with biological and chemical limitations. In order to overcome these limitations, the concept of pseudo NPs was introduced, which is the de novo combination of biologically unrelated NP fragments to generate compounds that may explore novel biological and chemical space.[4]

With regard to the program of pseudo NPs, the aim of this thesis is the development, optimization and establishment of a double asymmetric 1,3-dipolar CA for the synthesis of a pyrrolidine-based polycyclic pseudo NP compound library with different connection types. Thus, starting from simple α-iminoesters **50** a double asymmetric 1,3-dipolar CA will be employed to various α-alkylidene-2-cyclopentenones **104**, affording tricyclic compounds **105** with 8 stereocenters generated, including one quaternary centre due to a spirocyclic formation. Based on the generation of multiple stereocenters, conditions for a stereodivergent synthesis will be optimized to access the desired products in highly enantiomerically pure form and the stereochemical course of the double 1,3-dipolar CA reaction will be analyzed. Method development for a stereodivergent synthesis will be based on utilizing the same set of reagents. Furthermore, the 1,3-dipolar CA reaction will be explored with regard to reversibility in the context of DCC. In addition, the synthesized pseudo NP compound library which might cover novel areas of biological space will be investigated for potential bioactivity evaluation.

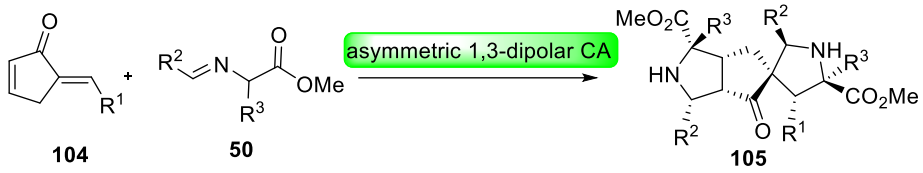


**Figure 26**: Double 1,3-dipolar CA to α-alkylidene-2-cyclopentenones **104** to provide a pyrrolidine-based tricyclic pseudo NP compound library.

# 3 Dynamic Catalytic 1,3-dipolar Cycloadditions

## 3.1 Introduction

The pyrrolidine fragment is an important motif in NPs, pharmaceuticals and in biological probes and is accessible by a 1,3-dipolar CA of azomethine ylides and dipolarophiles.[57] By performing a 1,3-dipolar CA to cyclic dipolarophiles, polycylic compounds with considerable complexity can be obtained, thus allowing the combination of the pyrrolidine fragment with different unrelated NP fragments in a fused fashion. Our group has reported a double 1,3 -dipolar CA of azomethine ylides to cyclic dipolarophiles generating fused polycyclic compounds with multiple stereocenters.[63] Here the combination of the pyrrolidine fragment with different NP fragments was achieved. The 1,3-dipolar CA of α-iminoesters **50** with p-benzoquinone **65** enabled the synthesis of 5,6,5-tricyclic compounds **68** by an edge fusion of two pyrrolidine moieties to a p-benzoquinone moiety (Figure 27).[63] Another example for a double 1,3-dipolar CA affording fused polycyclic compounds reported by our group is the reaction between α-iminoesters **50** cyclopentandiene **106**.[85] A copper and oxygen mediated *in situ* oxidation of cyclopentadiene **106** to the corresponding activated dipolarophile **107** and subsequent double 1,3-dipolar CA yielded the 5,5,5-tricyclic compound **108**. Here, two pyrrolidine motifs are connected to a cyclopentanone moiety again via an edge fusion, and 8 stereocenters are created in one pot.

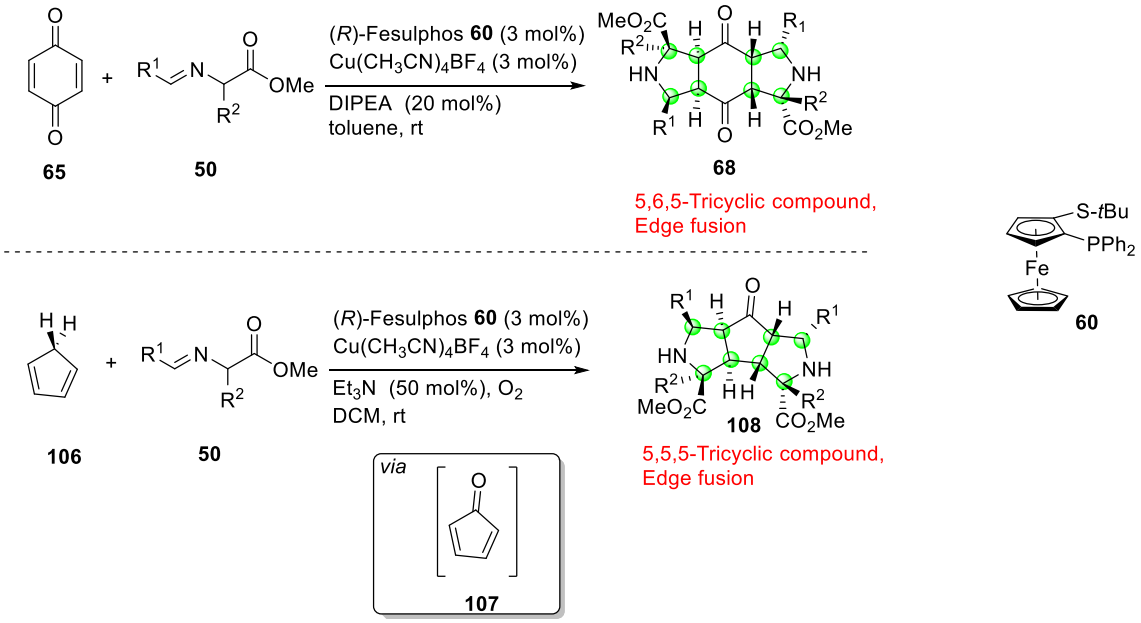


**Figure 27**: Asymmetric double 1,3-dipolar CA for generation of fused tricyclic compound.

The tricyclic compounds **68** and **108** are both symmetrical compounds and are generated through double 1,3-dipolar CA by two equivalent endocyclic double bonds. As the double bonds of the dipolarohiles **65**/**106** are equivalent and endocyclic, a double 1,3-dipolar CA can only provide a symmetrical edge fused tricyclic compound. However, it was proposed to design a non-symmetrical tricyclic pseudo NP compound class through a double 1,3-dipolar CA enabling the introduction of pyrrolidine moieties in different connection types and in an unprecedented manner. In order to realize this design strategy, the double cycloaddition needs to react with a cyclic dipolarophile that consists of two non-equivalent double bonds bearing different reactivities. In addition, one of the double bonds needs to be excocyclic to enable a different connection rather than an edge-type fusion. By considering these relevant aspects, α-alkylidene-2-cyclopentenones **104** were envisioned as dipolarophile for double 1,3-dipolar CAs endowed with the key properties (Figure 28). The [2+3] double CA on α-alkylidene-2-cyclopentenones **104** with azomethine ylides generated *in situ* allows the introduction of one pyrrolidine moiety in an edge-type fusion by reaction with the endocyclic conjugated double bond as well as the embedding in a spirotype fusion due to the exocyclic activated double bond. Thus, the generation of a non-symmetrical tricyclic compound **105** containing a spiro cycle can be achieved. The highly complex, non-symmetrical tricyclic compound **105** contains NP fragments such as pyrrolidine and cyclopentanone.

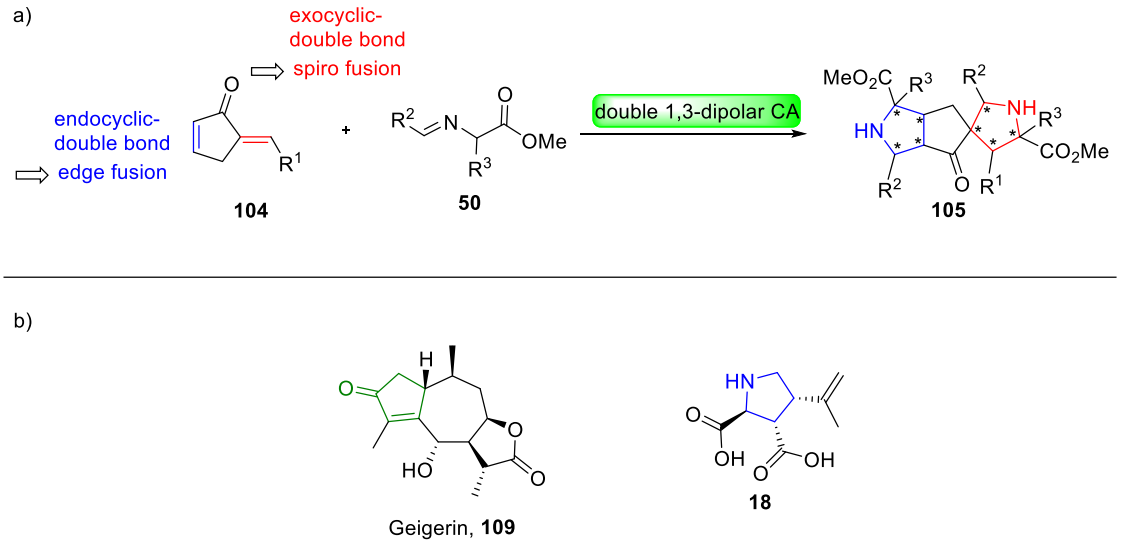


**Figure 28**: a) Proposal for the synthesis of the non-symmetrical tricyclic pseudo NP compound **105**; b) Pyrrolidine and cyclopentanone fragment containing NPs.

## 3.2 Initial results and optimization

To establish a reaction sequence for the double 1,3-dipolar CA, initial screening studies were conducted with α-alkylidene-2-cyclopentenone **104a** and α-iminoester **50a**, which were selected as model substrates. The attention was first focussed on the preparation of a racemic version of the double 1,3-dipolar CA and different reaction parameters such as nonchiral ligands, solvents, bases as well as various metal catalysts (Table 3.1). A copper-catalyzed reaction using $PPh_3$ as non-chiral ligand, in the presence of $Et_3N$ in DCM afforded the desired double cycloaddition product with low yield but with high diastereoselectivity (entry 1). In the absence of any ligand the yield drops further as it has a great impact on the electronic properties of the metal catalyst (entry 2). However, changing the solvent from DCM to THF or changing the base to an inorganic base, only traces of the desired product were observed for a copper-catalyzed reaction (entry 3-4). As the screening of different conditions with a copper mediated reaction did not provide satisfying results, silver was employed as metal source. Due to its insolubility in DCM also only traces of product were observed in absence of any coordinating ligand for a silver-catalyzed reaction (entry 6). AgOAc forms a soluble complex by coordination with $PPh_3$ thus in the presence of $PPh_3$ as ligand the double CA can be efficiently catalyzed with AgOAc to yield cycloadduct **105a-rac** with 82% yield and excellent diastereoselectivity (*d.r.* >20:1) (entry 7). It is noteworthy that only a single diastereomer was obtained as 8 stereocenters are created in the double 1,3-dipolar CA.

**Table 3.1** Representative conditions for the optimization of the double 1,3-dipolar CA on a selected example*.

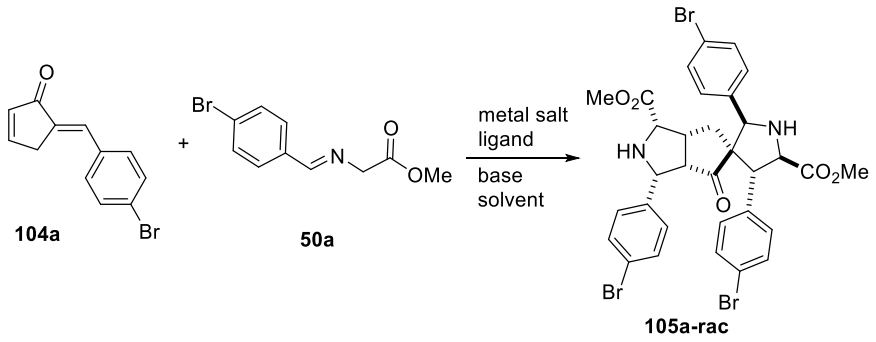


| Entry | Catalyst | Catalyst (mol%) | Ligand | Ligand (mol%) | Base (40 mol%) | Solvent | Time (h) | d.r. † | Yield‡ (%) |
|---|---|---|---|---|---|---|---|---|---|
| 1 | $Cu(CH_3CN)_4PF_6$ | 6 | $PPh_3$ | 6.5 | $Et_3N$ | DCM | 24 | >20:1 | 25 |
| 2 | $Cu(CH_3CN)_4PF_6$ | 6 | - | 6.5 | $Et_3N$ | DCM | 24 | >20:1 | 20 |
| 3 | $Cu(CH_3CN)_4PF_6$ | 6 | $PPh_3$ | 6.5 | $Et_3N$ | THF | 48 | n.d. | trace |
| 4 | $Cu(CH_3CN)_4PF_6$ | 6 | $PPh_3$ | 6.5 | $Cs_2CO_3$ | DCM | 24 | n.d. | trace |

**Continuation of Table 3.1**

| | | | | | | | | | |
|---|---|---|---|---|---|---|---|---|---|
| 5 | $Cu(CH_3CN)_4PF_6$ | 6 | $PPh_3$ | 6.5 | $Et_3N$ | PhMe | 24 | >20:1 | 17 |
| 6 | AgOAc | 6 | - | 6.5 | $Cs_2CO_3$ | DCM | 24 | n.d. | trace |
| **7** | **AgOAc** | **6** | **$PPh_3$** | **6.5** | **$Cs_2CO_3$** | **DCM** | **24** | **>20:1** | **81** |
| 8 | AgOAc | 6 | $PPh_3$ | 6.5 | $K_2CO_3$ | DCM | 24 | n.d. | trace |
| 9 | $Cu(CH_3CN)_4BF_4$ | 6 | $PPh_3$ | 6.5 | $Cs_2CO_3$ | DCM | 24 | >20:1 | 15 |
| 10 | AgOTf | 6 | $PPh_3$ | 6.5 | $Cs_2CO_3$ | DCM | 48 | n.d. | n.d. |
| 11 | AgOAc | 6 | BINAP | 6.5 | $Cs_2CO_3$ | $Et_2O$ | 24 | >20:1 | 30 |
| 12 | $AgSbPF_6$ | 6 | $PPh_3$ | 6.5 | $Cs_2CO_3$ | $Et_2O$ | 24 | n.d. | n.d. |

*Reaction conditions: ligand $PPh_3$, catalyst, base (40 mol%, 0.048 mmol), iminoester **50a** (2.2 equiv., 0.26 mmol) and cyclic enone **104a** (1 equiv., 0.12 mmol), ambient temperature. †Determined by $^1$H NMR spectroscopy. ‡Isolated yields of **105a-rac** after column chromatography. †d.r. – diastereomer ratio determined by $^1$H-NMR spectroscopy, n.d. – not determined.

After establishment of reaction conditions for the double cycloaddition, the regioselectivity of the first cycloaddition was investigated. The α-alkylidene-2-cyclopentenone **104a** bears two non-equivalent conjugated double bonds. This leads to the fundamental question, whether the cycloaddition occurs preferentially on the endocyclic double bond to generate the monoadduct **110a** or proceeds on the exocyclic double bond to afford the spirocycle **111a**. Another possibility is that both conjugated double bonds do not show any large difference in terms of reactivity and thus the cycloaddition takes place on both sides simultaneously. Thus, in order to figure out the regioselectivity of the reaction, cyclic enone **104a** was treated with 1.1 equivalent of iminoester **50a** under the optimized conditions which resulted in the regioselective formation of mono adduct ***rac*-110a** with high diastereoselectivity. (*d.r.* >20:1) (Figure 29). The first cycloaddition occurs selectively on the endocyclic conjugated double bond, although the exocyclic double bond of enone **104a** is more activated from an electronic point of view. It is additionally attached to a $sp^2$-hybridized carbon (aryl), which decreases the electron density of the related double bond and thus enhancing the reactivity towards a dipole. Despite the fact that the exocyclic double bond is more activated towards a reaction with a dipole, it needs to be considered that the exocyclic double bond leads to the formation of a spirocycle, which is sterically hindered. However, the regioslectivity of the monoaddition can be tuned by varying the electronic and steric properties of the endocyclic double bond of enone **104a**. A change in regioselectivity was observed when a methyl substituent was introduced at the endocyclic double bond of the dipolarophile (R=$CH_3$). Mono cycloaddition of cyclic enone **112a** and the ylide derived from glycine methyl ester imine **50a** resulted in formation of spirocycle ***rac*-111a**

in 57% yield and with good diastereoselectivity (10:1) (Figure 29). The introduction of a methyl group at the endocyclic double bond affects the reactivity in two fundamental aspects regarding electronic and steric reasons: The methyl group increases the electron density of the double bond and thus lowers the relative activity towards a dipole. Furthermore, it adds steric bulkiness by slightly shielding the double bond. Thus, the decreased reactivity of the endocyclic double bond results in selective formation of the spirocycle ***rac*-111a**.

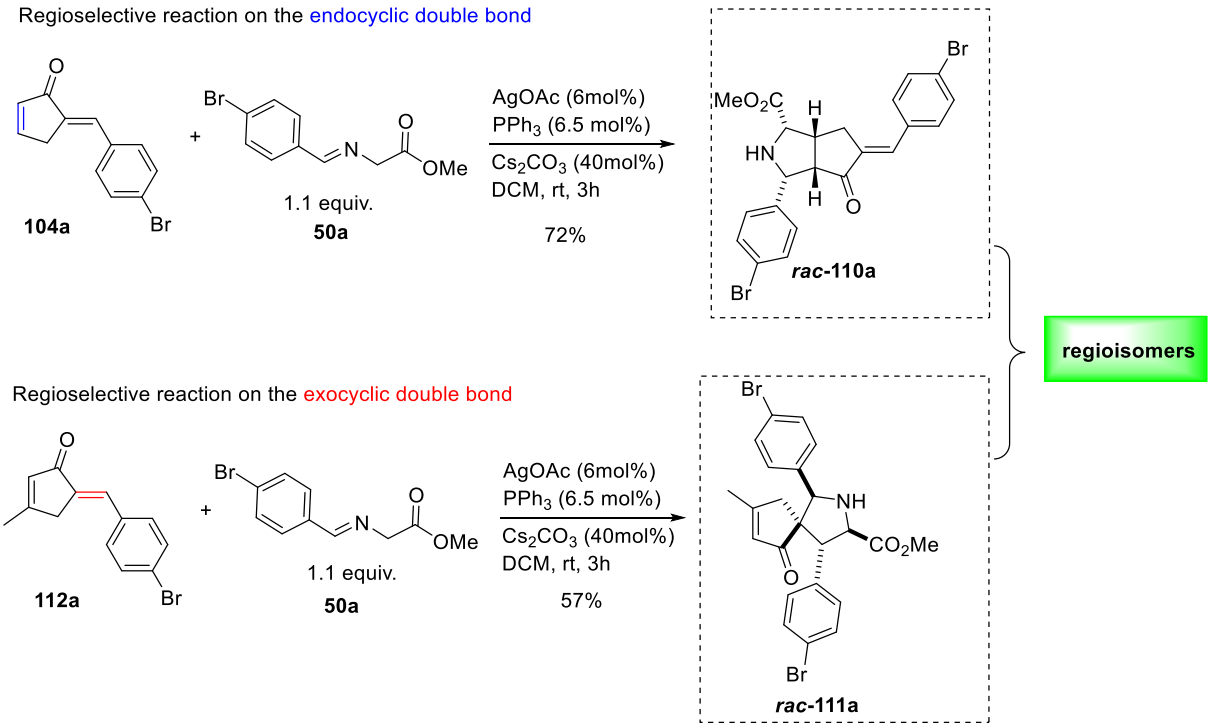


**Figure 29**: Outline of the regioselectivity for the monoaddition.

## 3.3 Development of the asymmetric double 1,3-dipolar CA and reaction scope

To extend the studies of the double 1,3-dipolar CA to an asymmetric transformation, screening studies were conducted to explore the enantioselective synthesis of enone **104a** and imine **50a** as model substrates by employing different chiral catalysts, Lewis acids, bases and solvents (Table 3.2). Copper salts in presence of planar chiral ligands and axial chiral ligands yield the desired product only with low to moderate enantioselectivity regardless of the solvent with $Et_3N$ as base (entry 1-4). The highest ee with copper as Lewis acid was obtained in combination with the planar chiral *S,P*-ferrocenyl ligand (*R*)-Fesulphos **60**, with high diatstereoselectivity but low yield. (entry 5). By switching from copper based Lewis acids to silver catalyst, experimental results indicated the best result could be obtained using AgOAc (6 mol%) as a Lewis acid in

combination with the *S,P*-ferrocenyl ligand (*R*)-Fesulphos **60** in dichloromethane using cesium carbonate ($Cs_2CO_3$; 40 mol%) as a base at room temperature after 24 h (entry 7). Under these conditions, tricyclic compound **105a** was obtained in 81% yield with high diastereoselectivity (*d.r.* > 20:1) and excellent enantioselectivity (99% *e.e.*). By changing the solvent from dichloromethane to other organic solvents like toluene or tetrahydrofuran, a dramatic drop in enantioselectivity and yield was observed (entries 13-15).

**Table 3.2**: Optimization of the reaction conditions for the enantioselective 1,3-dipolar cycloaddition of enone **104a** with imine **50a**.*

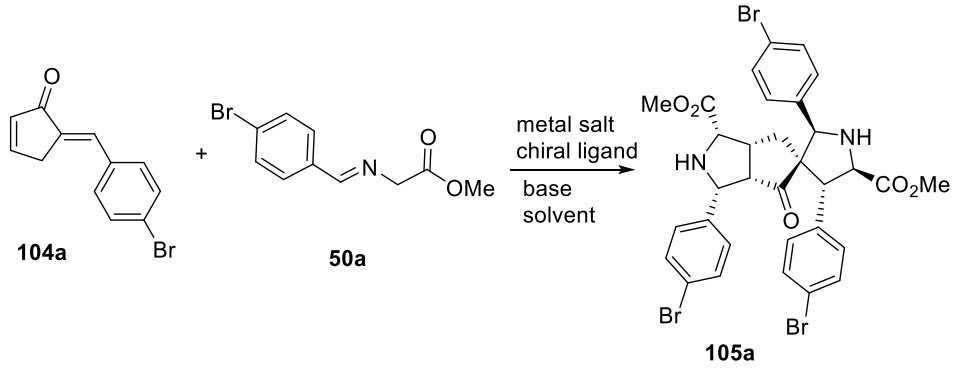


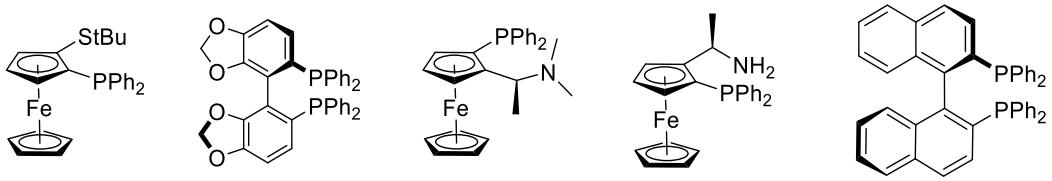


| Entry | Catalyst | Ligand | Base (40 mol%) | Solvent | d.r. † | Yield‡ (%) | e.e.§ |
|---|---|---|---|---|---|---|---|
| 1 | $Cu(CH_3CN)_4PF_6$ | **66** | $Et_3N$ | DCM | >20:1 | 25 | 30 |
| 2 | $Cu(CH_3CN)_4PF_6$ | **67** | $Et_3N$ | DCM | >20:1 | 20 | 55 |
| 3 | $Cu(CH_3CN)_4PF_6$ | **63** | $Et_3N$ | DCM | n.d. | trace | n.d. |
| 4 | $Cu(CH_3CN)_4PF_6$ | **113** | $Et_3N$ | DCM | >20:1 | 40 | 70 |
| 5 | $Cu(CH_3CN)_4PF_6$ | **60** | $Et_3N$ | DCM | >20:1 | 33 | 81 |
| 6 | AgOAc | **60** | $Et_3N$ | DCM | >20:1 | 27 | 65 |
| **7** | **AgOAc** | **60** | **$Cs_2CO_3$** | **DCM** | **>20:1** | **81** | **99** |
| 8 | AgOAc | **60** | $K_2CO_3$ | DCM | n.d. | trace | n.d. |
| 9 | $Cu(CH_3CN)_4BF_4$ | **60** | $Cs_2CO_3$ | DCM | >20:1 | 15 | 7 |
| 10 | AgOTf | **60** | $Cs_2CO_3$ | DCM | n.d. | trace | n.d. |

**Continuation of Table 3.2**

| | | | | | | | |
|---|---|---|---|---|---|---|---|
| 11 | $Cu(CH_3CN)_4PF_6$ | **60** | $Cs_2CO_3$ | DCM | >20:1 | 27 | 20 |
| 12 | $AgSbPF_6$ | **60** | $Cs_2CO_3$ | DCM | n.d. | trace | n.d. |
| 13 | AgOAc | **60** | $Cs_2CO_3$ | THF | >20:1 | 30 | 80 |
| 14 | AgOAc | **60** | $Cs_2CO_3$ | $Et_2O$ | >20:1 | 37 | 11 |
| 15 | AgOAc | **60** | $Cs_2CO_3$ | PhMe | >20:1 | 20 | 9 |

*Reaction conditions: ligand (6.5 mol%), catalyst (6 mol%), base (40 mol%, 0.048 mmol), iminoester **50a** (2.2 equiv., 0.26 mmol) and cyclic enone **104a** (1 equiv., 0.12 mmol), ambient temperature. †Determined by $^1$H NMR spectroscopy. ‡Isolated yields of **105a** after column chromatography. §Determined by HPLC analysis on chiral phase. †d.r. – diastereomer ratio determined by $^1$H-NMR spectroscopy, n.d. –not determined.

Notably this reaction created eight stereocenters including one quaternary center in a one-pot transformation in a highly stereoselective manner. The planar chiral ligand (*R*)-Fesulphos **60** enables the control of enantio- and diastereoselectivity for the reaction. The absolute configuration of product **3a** was determined by crystal structure analysis (**Supplementary Information, Crystal Data**), which revealed that product **105a** is formed by double *endo*-selective cycloaddition. The stereochemical outcome of the reaction can be explained with respective to the transition state based on the face selective approach of enone **104** to azomethine ylide **50** controlled by the chiral environment of the chiral ligand **60** (Figure 30). The chiral ligand (*R*)-Fesulphos **60** and the iminoester **50** form a tetrahedral complex **A** with silver.[86] Based on computational studies only one orientation out of two possible orientations of the iminoester with respect to (*R*)-Fesulphos **60** is possible, thus avoiding unfavored steric interactions between the phenyl moieties of the dipehnylphosphine and the imine.[86] The approach of the enone **104** proceeds from the *re*-face with respect to the dipole in an endoselective fashion, as the *si*-face is blocked by the bulkiness of the *t*-Butyl group of the ligand **60**. In this step the stereocenter of the mono addition product **110** is set. The formed mono adduct **110** acts as dipolarophile in the second cycloaddition step. A *re*-face selective attack to complex **A** in diastereoselective manner takes place to yield the double *endo*-selective product **105**.

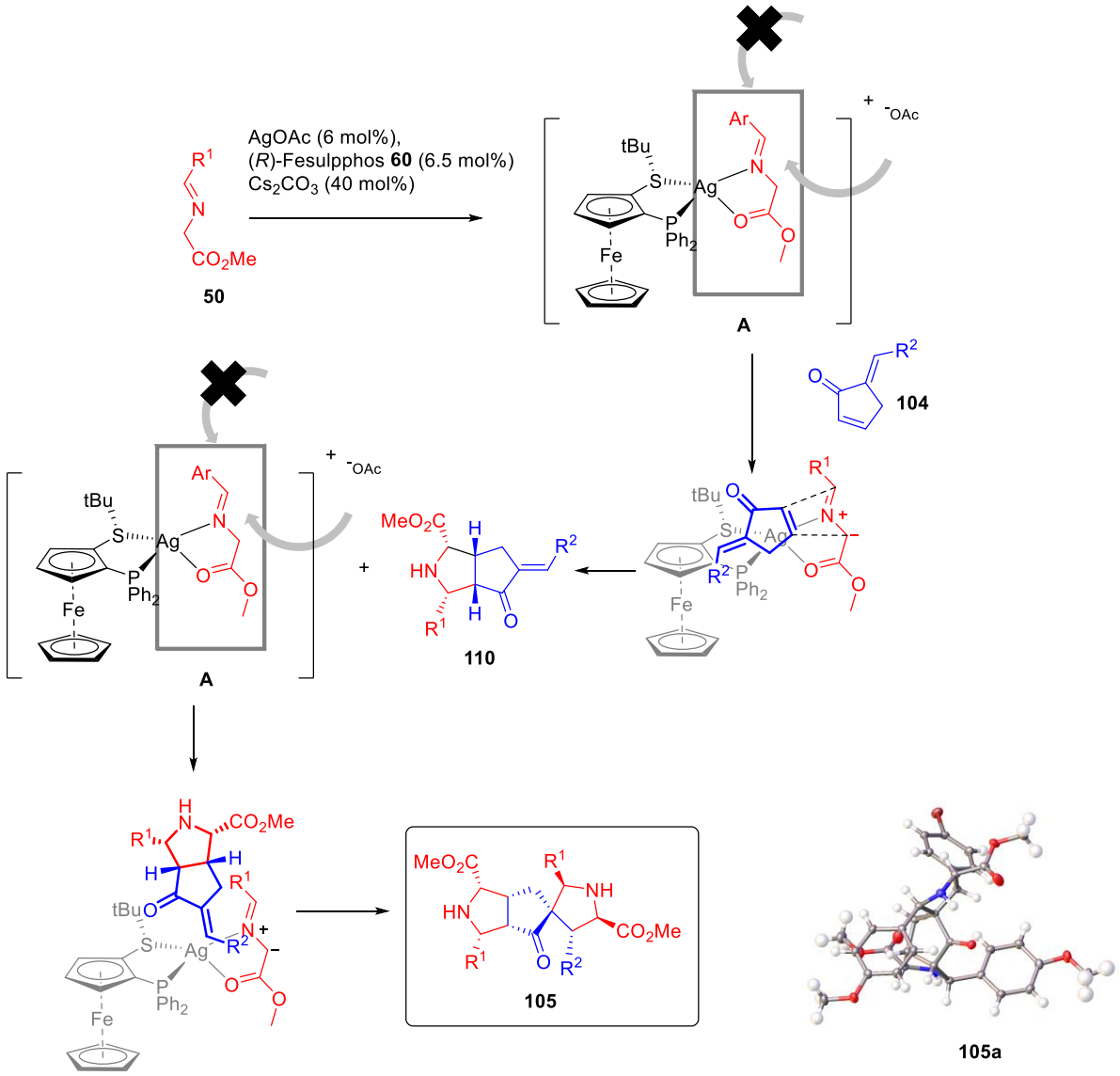


**Figure 30**: Proposed intermediates and transition states for the asymmetric double endo-selective cycloaddition.

With the optimized conditions in hand, the scope of the tandem asymmetric double 1,3-dipolar CA was studied. Various substituted α-iminoeters **50** from corresponding aldehydes as well as different cyclic enones **104** obtained by a titanium mediated aldol-condensation were prepared.[87] The scope of the tandem reaction is wide. Regardless of the substitution pattern of the aromatic ring in the cyclic enone **104** as well as the imine **50**, the double cycloaddition product is obtained with excellent diastereo- (>20:1) and enantioselectivity (91-99% *e.e.*) and with moderate to good yields (**105a-105y** in Table 3.3). Both, electron-withdrawing and electron-donating substituents were well tolerated, wherein in presence of electron-donating groups such as methyl or methoxy, the yield was reduced to 60-63% (**105e** and **105g**, respectively). In case of electron-neutral or withdrawing substituents such as bromine or

fluorine (**105a** and **105f**) afforded the product with relatively higher yields (75-81%). The scope was expanded to heterocyclic containing azomethine ylides which reacted to provide the products (**105i** and **105j**) with moderate yields and with very high enantioselectivity. Overall, the enantioselectivity remained unaffected regardless of the substitution pattern. By introducing a sterically hindered moiety on the exocyclic double bond such as a *tert-butly* substituent, the double cycloaddition proceeded with 21% yield (**105v**) but still with very high enantioselectivity and excellent diastereoselectivity (>20:1). Furthermore, employing of a methyl substituent to the endocyclic double bond of the enone yielded **105x** with two quaternary centers with high enantioselectivity (93% *e.e.*). A more hindered α-phenyl substituted ylide, afforded product **105k** in 21% yield but with high enantioselectivity (91% *e.e.*), thereby inducing formation of three quaternary centers. For all of examples, the products were formed as single diastereomers (*d.r.* > 20:1) after 24h (Table 3.3).

**Table 3.3 l Results of the enantioselective synthesis of the chiral compounds 105[a]**

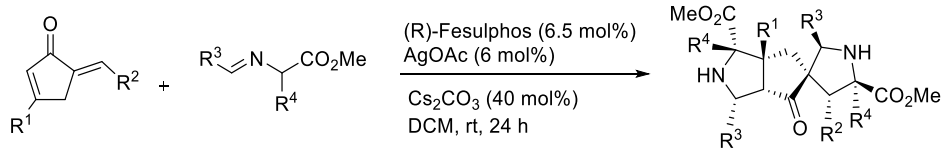


104 50 105

| Product | $R^1$ | $R^2$ | $R^3$ | $R^4$ | Yield (%)[b] | *e.e.*[c] |
|---|---|---|---|---|---|---|
| **105a** | H | 4-Br-$C_6H_4$ | 4-Br-$C_6H_4$ | H | 81 | 99 |
| **105b** | H | 4-Br-$C_6H_4$ | 3-Br-$C_6H_4$ | H | 72 | 91 |
| **105c** | H | 4-Br-$C_6H_4$ | 2-Br-$C_6H_4$ | H | 65 | 96 |
| **105d** | H | 4-Br-$C_6H_4$ | 4-Cl-$C_6H_4$ | H | 81 | 98 |
| **105e** | H | 4-Br-$C_6H_4$ | 4-MeO-$C_6H_4$ | H | 60 | 98 |
| **105f** | H | 4-Br-$C_6H_4$ | 4-F-$C_6H_4$ | H | 75 | 98 |
| **105g** | H | 4-Br-$C_6H_4$ | 4-Me-$C_6H_4$ | H | 63 | 93 |
| **105h** | H | 4-Br-$C_6H_4$ | 2-naphtyl | H | 66 | 97 |
| **105i** | H | 4-Br-$C_6H_4$ | 3-furyl | H | 40 | 95 |
| **105j** | H | 4-Br-$C_6H_4$ | 2-furyl | H | 45 | 95 |
| **105k** | H | 4-Br-$C_6H_4$ | 4-Br-$C_6H_4$ | Ph | 21 | 91 |
| **105l** | H | 4-$NO_2$-$C_6H_4$ | 4-F-$C_6H_4$ | H | 80 | 95 |
| **105m** | H | 4-$NO_2$-$C_6H_4$ | 3-Br-$C_6H_4$ | H | 72 | 91 |
| **105n** | H | 4-MeO-$C_6H_4$ | 4-F-$C_6H_4$ | H | 65 | 98 |
| **105o** | H | 4-Me-$C_6H_4$ | 4-F-$C_6H_4$ | H | 60 | 98 |

**Continuation of Table 3.3**

| | | | | | | |
|---|---|---|---|---|---|---|
| **105p** | H | 2-naphtyl | 4-F-$C_6H_4$ | H | 65 | 95 |
| **105q** | H | 3-Br-$C_6H_4$ | 4-Br-$C_6H_4$ | H | 81 | 91 |
| **105r** | H | 3-Br-$C_6H_4$ | 2-Br-$C_6H_4$ | H | 60 | 91 |
| **105s** | H | 2-Br-$C_6H_4$ | 4-Br-$C_6H_4$ | H | 80 | 95 |
| **105t** | H | 3-Br-$C_6H_4$ | 4-MeO-$C_6H_4$ | H | 55 | 91 |
| **105u** | H | 4-Cl-$C_6H_4$ | 4-Cl-$C_6H_4$ | H | 80 | 95 |
| **105v** | H | $^t$Butyl | 4-Br-$C_6H_4$ | H | 21 | 93 |
| **105w** | H | 3-Br-$C_6H_4$ | 4-F-$C_6H_4$ | H | 75 | 95 |
| **105x** | Me | 4-Br-$C_6H_4$ | 4-Br-$C_6H_4$ | H | 40 | 93 |
| **105y** | H | 4-Br-$C_6H_4$ | [Fe($\eta^5$-$C_5H_5$)($\eta^5$-$C_5H_4$)] | H | 48 | 94 |

[a]For General Procedure, see experimental part. [b]Isolated yields of the pure major enantiomer after column chromatography. Diastereomeric ratio for all products is >20:1. [c]Determined by HPLC analysis using a chiral stationary phase. Me, methyl; Ph, phenyl.

## 3.4 Development of the mixed asymmetric double 1,3-dipolar CA

To stress the utility of this reaction by expanding the chemical space accessible via the double cycloaddition, we examined whether a sequential multicomponent transformation could give access to cycloadducts formed from two different imines. As the cyclic enones **104** consist of two different activated double bonds which differ in reactivity as outlined in the regioselective transformation (see chapter 3.2), a sequence was established in which cyclic enones **104** were treated with 1.1 equiv. of an iminoester **50** in the presence of (*R*)-Fesulphos (**60**, 6.5 mol%), AgOAc (6 mol%) and $Cs_2CO_3$ (40 mol%) in dichloromethane for 3 h followed by treatment with a second, different iminoester **50´** for 24 h. The first cycloaddition proceeds selectively on the endocyclic double bond and the second cycloaddition occurs on the exocyclic double bond enabling the generation of mixed double cycloaddition products **114** by means of a sequential one-pot, three-component reaction (**115a**–**115o** in **Table 3.4**). The scope of the mixed double cycloaddition products **115** is wide, tolerating various substituents. Although the mixed double cycloaddition products were obtained with excellent diatstereoselectivity (>20:1), however, unexpectedly they were obtained with lower enantioselectivity (82-91% *e.e.*) relative to the two-component double-cycloaddition products **105,** for which the products were formed with up to 99% *e.e.*

**Table 3.4 l Results of the enantioselective synthesis of the tandem cycloadditions with two different imines[a]**

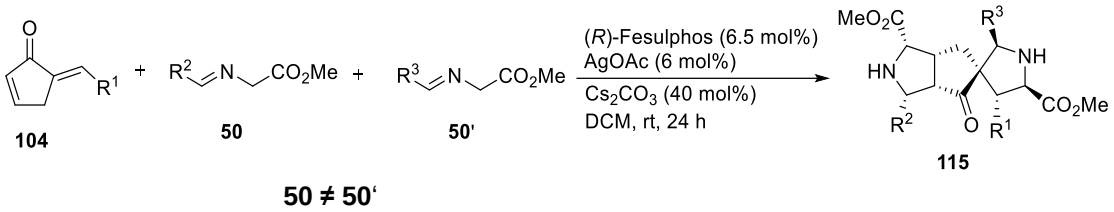


**50 ≠ 50'**

| Product | $R^1$ | $R^2$ | $R^3$ | Yield (%)[b] | e.e.[c] |
|---|---|---|---|---|---|
| **115a** | 4-Cl-$C_6H_4$ | 4-Cl-$C_6H_4$ | 4-Br-$C_6H_4$ | 77 | 85 |
| **115b** | 4-Cl-$C_6H_4$ | 4-Cl-$C_6H_4$ | 4-Me-$C_6H_4$ | 65 | 82 |
| **115c** | 4-Cl-$C_6H_4$ | 4-Cl-$C_6H_4$ | 4-MeO-$C_6H_4$ | 56 | 84 |
| **115d** | 4-Br-$C_6H_4$ | 4-Me-$C_6H_4$ | 2-naphtyl | 75 | 89 |
| **115e** | 4-Cl-$C_6H_4$ | 4-Me-$C_6H_4$ | 4-MeO-$C_6H_4$ | 70 | 85 |
| **115f** | 4-Cl-$C_6H_4$ | 4-Me-$C_6H_4$ | 4-Br-$C_6H_4$ | 65 | 90 |
| **115g** | 4-Br-$C_6H_4$ | 4-Me-$C_6H_4$ | 2-Br-$C_6H_4$ | 56 | 90 |
| **115h** | 4-Br-$C_6H_4$ | 4-Me-$C_6H_4$ | 4-MeO-$C_6H_4$ | 69 | 89 |
| **115i** | 4-Br-$C_6H_4$ | 4-Me-$C_6H_4$ | 4-F-$C_6H_4$ | 78 | 90 |
| **115j** | 4-Br-$C_6H_4$ | 4-Me-$C_6H_4$ | 4-Br-$C_6H_4$ | 72 | 87 |
| **115k** | 4-Br-$C_6H_4$ | 4-Br-$C_6H_4$ | 3-Br-$C_6H_4$ | 69 | 89 |
| **115l** | 4-Br-$C_6H_4$ | 4-Br-$C_6H_4$ | 4-F-$C_6H_4$ | 72 | 90 |
| **115m** | 4-Br-$C_6H_4$ | 4-MeO-$C_6H_4$ | 4-Br-$C_6H_4$ | 61 | 90 |
| **115n** | 4-Br-$C_6H_4$ | 4-F-$C_6H_4$ | 4-Br-$C_6H_4$ | 70 | 91 |
| **115o** | 4-Br-$C_6H_4$ | 4-F-$C_6H_4$ | 3-Br-$C_6H_4$ | 75 | 87 |

[a]General procedure can be found in experimental part. [b]Isolated yields of the pure major enantiomer after column chromatography. Diastereomer ratio for all products is >20:1. [c]Determined by HPLC analysis using a chiral stationary phase. Me, methyl; Ph, phenyl

The stereochemical outcome of the mixed double cycloaddition products **115** regarding the lower enantioselectivity indicated that the stereochemical course of the reaction is most probably not only controlled by a simple chiral ligand/metal complex mediated transformation but also by means of different processes. Usually in the double cycloaddition the first step should be the enantio-determining step, in which the chirality is induced by (*R*)-Fesulphos/AgOAc and the second step is a diastereoselective step that is a substrate-controlled transformation (Figure 31). If the stereochemical course of the double cycloaddition is

proceeding via this pathway, no differences in enantioselectivity should be noted for the double cycloaddition products **105** and the mixed cycloaddition products **115**.

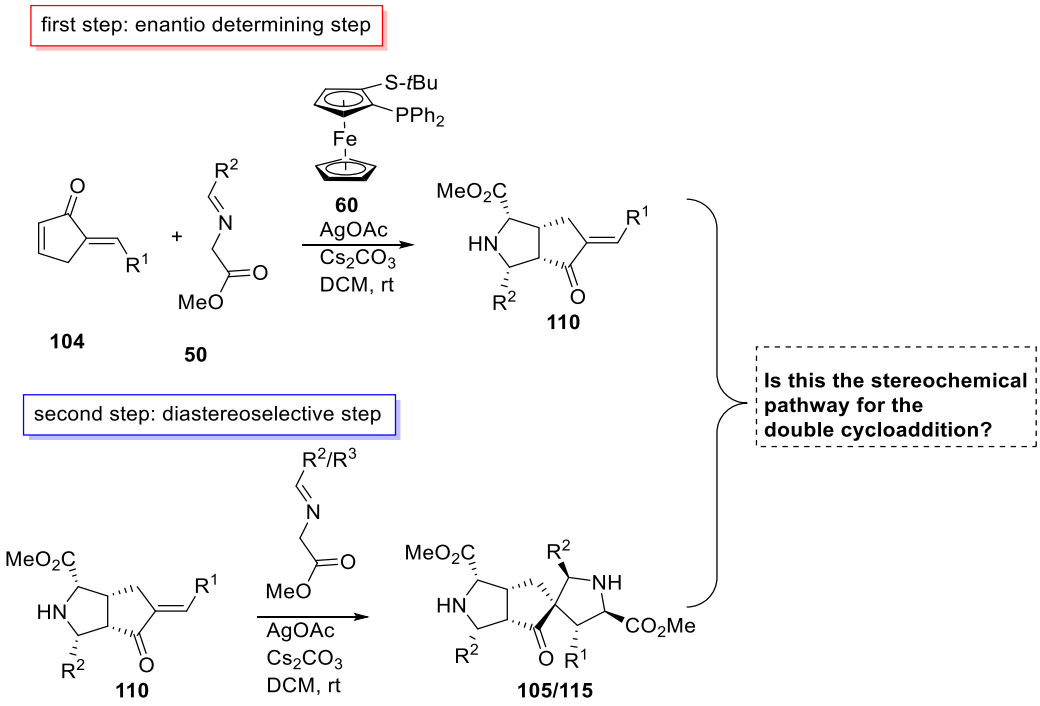


**Figure 31**: Questioning of the stereochemical pathway of the double cycloaddition.

## 3.5 Mechanistical studies of the stereochemical course of the double cycloaddition

In order to understand the differences in enantioslectivity of the double cycloaddition products **105** and the mixed double cycloaddition products **115** and to analyse the stereochemical course of the reaction, a detailed and stepwise investigation of the enantioselective reaction was performed. For mechanistical studies the enantioselective reaction of cyclic enone **104a** and imine **50a** was chosen as model reaction. The analysis was divided in two parts, the enantioselectivity of the mono addition as well the enantioselectivity of the second addition was investigated.

### 3.5.1 Mechanistical studies on the first step of the reaction sequence

In beginning of the mechanistical studies, first the enantioselectivity of the mono addition product **110a** was investigated as this is a key intermediate leading to the double cycloaddition product **105a** in the second cycloaddition. Upon treatment of cyclic enone **1a** with 1.1 equiv. of iminoester **2a** in the presence of (*R*)-Fesulphos **L1** (6.5 mol%), AgOAc (6 mol%) and $Cs_2CO_3$ (40 mol%) in DCM, monoadduct **4a** can be formed with varying enantioselectivity in the range of 80%-95% *e.e.* (Figure 32). The mono addition product **110a** shows lower enantioselectivity compared to the double cycloaddition product **105a** which is obtained with excellent enantioselectivity (99% *e.e.*). By increasing the ratio of the chiral ligand (*R*)-Fesulphos **60** over the Lewis acid AgOAc (2:1) the differences in eantioselectivity becomes more obvious, thus obtaining the mono adduct **110a** with only 80% e.e. but still excellent diastereoselectivity and high enantioselectivity for the double cycloaddition product **105a** regardless of the ratio of catalyst (*R*)-Fesulphos/AgOAc. The difference in enantioselectivity indicates at first stage that kind of a different process is involved in the asymmetric reaction resulting in different enantiomeric ratios for both products **105a** and **110a**. The higher enantioselectivity for the double adduct **105a** leads to the question whether it is involved in the catalytic process by incorporation to the chiral catalyst (*R*)-Fesulphos/AgOAc and thus generating a more selective catalyst which is responsible for the enhanced enantioselectivity of the double product **105a** over the mono adduct **110a.** In such a case the reaction would proceed through an asymmetric autoinduction process.

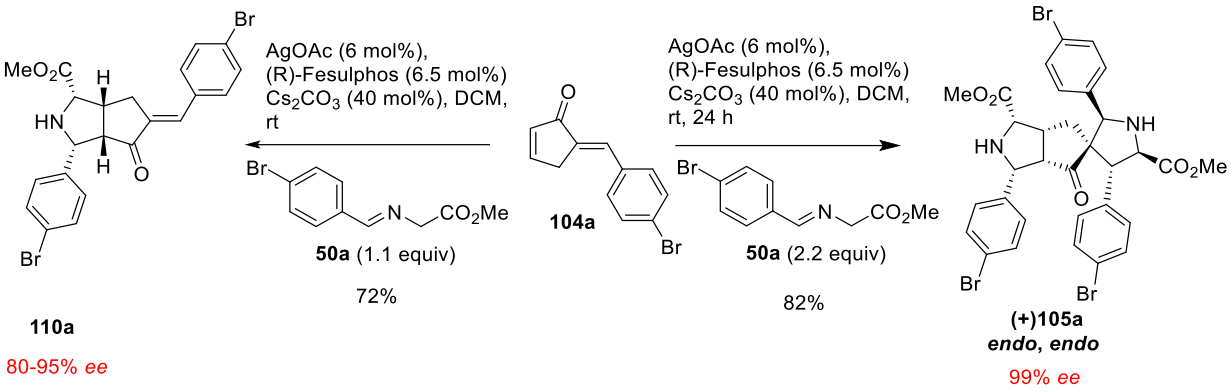


**Figure 32**: Differences in enantioelectivities between the mono adduct **110a** and the double adduct **105a**.

Asymmetric autoinduction[88-89] and asymmetric autocatalysis[90-91] are special and rare cases in asymmetric synthesis. The process of asymmetric autoinduction and asymmetric autocatalysis are outlined in Figure 33.

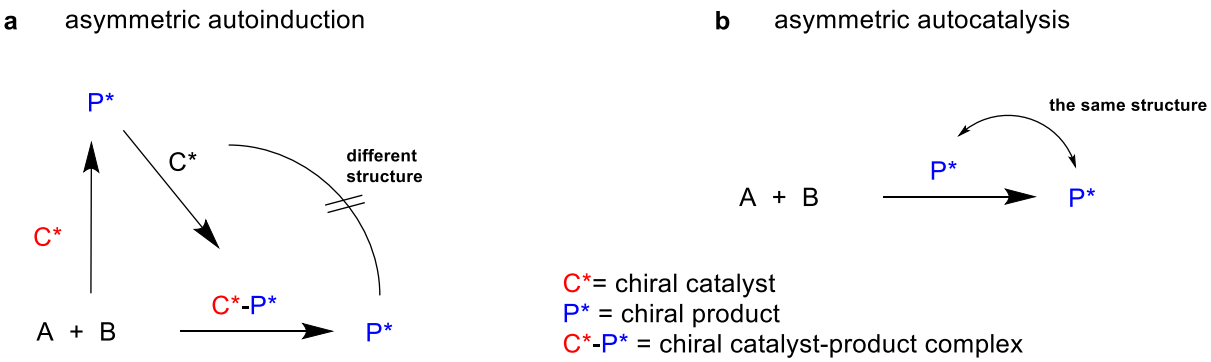


**Figure 33**: Schematic illustration of a) asymmetric autoinduction and b) asymmetric autocatalysis.

In asymmetric autoinduction, the product of the reaction is incorporated in the original enantioselective catalyst by generating a new, more active catalytic species thereby improving asymmetric induction by modifying the stereochemical course of the reaction. In such a process a change in enantioselectivity of the product during the course of the reaction should be observed, as at initial stage the reaction is catalyzed by the original chiral catalyst and over reaction time the product forms a new chiral complex with the chiral catalyst and thus modifying the stereochemical course of the reaction.[89] Wulff et al observed an asymmetric autoinduction in a VAPOL/Aluminium catalyzed Diels-Alder reaction (Figure 34).[92] A time-dependent increase in enantioselectivity of the Diels-Alder product could be observed by plotting the *e.e.* of the product as function of time.

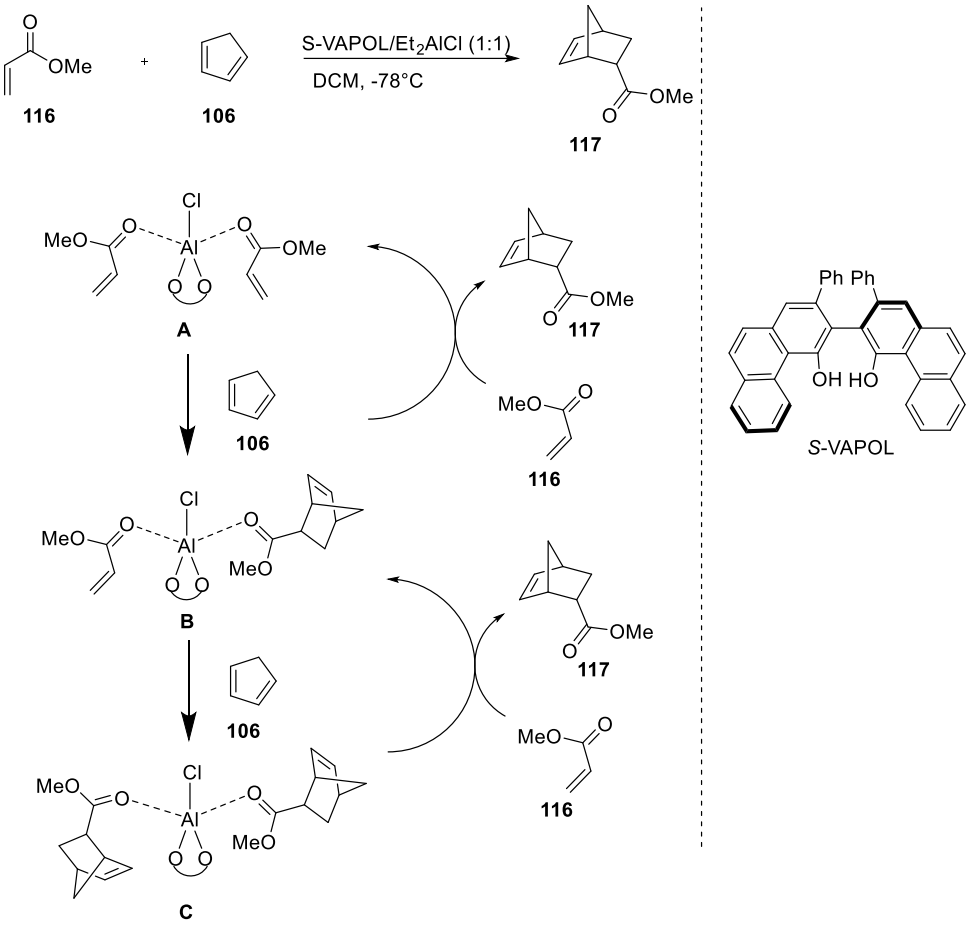


**Figure 34**: Asymmetric autoinduction in the Diels-Alder reaction between dienophile **116** and diene **106**.

In asymmetric autocatalysis the enantioenriched product in the reaction acts as a chiral catalyst for its own formation and modulates the stereochemical outcome with amplification of chirality. Only one example for asymmetric autocatalysis is known, which was described by Soai et al by addition of dialkylzinc reagents to pyridine-3-carbaldehyde **118** (Figure 35).[93-94] It was shown that the product of the reaction acts as catalyst by inducing enantioselectivity to its own formation with amplification of chirality. Only 0,28 % *e.e.* of the product as catalyst afforded its own formation with 88% *e.e.* (Figure 35).[93]

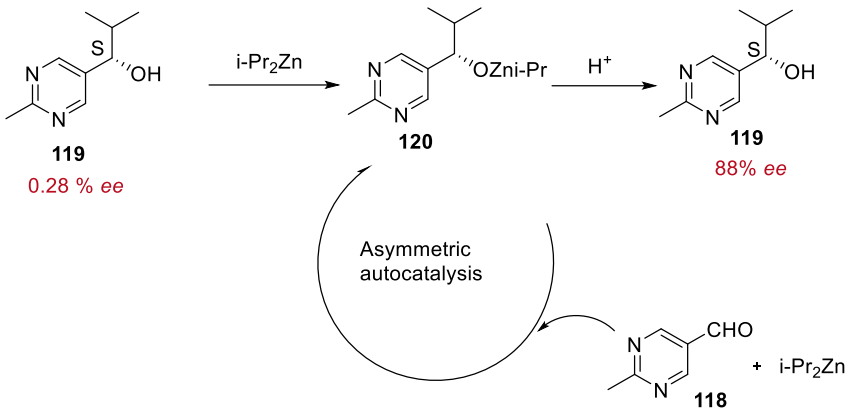


**Figure 35**: Asymmetric autocatalysis of addition of dialkylzinc to pyridine carbaldehyde **118**.

In order to determine whether the higher enantioselectivity of the double cycloaddition product **105a** over the mono adduct **110a** might be related to an asymmetric autoinduction mechanism, a time dependent experiment for the double cycloaddition between cyclic enone **104a** and imine **50a** was performed to determine whether changes in enantioselectivity can be observed over the course of the reaction. However, no changes could be observed and the product **105a** was isolated with unwaveringly high *e.e.* over the reaction regardless of the time which indicating that there is no asymmetric autoinduction in the double cycloaddition. Also to eliminate that an asymmetric autocatalytic process might occur in the double cycloaddition, the reaction of cyclic enone **104a** with imine **50a** was conducted with the product **105a** as catalyst (Figure 36). The product **105a** could potentially act as ligand to AgOAc but did not induce any chirality to its own formation as the product was obtained as racemic. Thus it was confirmed that no asymmetric autocatalysis proceeds in the mechanism.

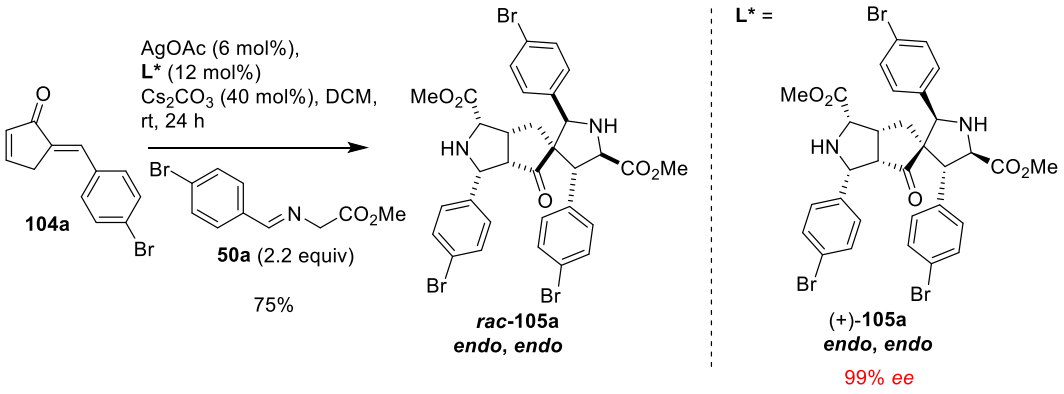


**Figure 36**: Double cycloaddition of in presence of chiral reaction product as chiral catalyst.

Further studies were conducted with the mono adduct **110a** to investigate the lower enantioselectivity. Based on the lower enantioselectivity of the mono adduct **110a** over the double adduct **105a** it was further hypothesized that a potential dynamic covalent process selectively on one enantiomer of the mono adduct **110a** might occur, which could explain the decreased enantioselectivity. With regard to this hypothesis, the formation of the mono adduct **110a** and the stereochemical outcome of the reaction was investigated by varying the reaction time of this reaction (Table 3.5).

**Table 3.5**: Time dependent studies on the enantioselectivity on the mono addition product **110a**.

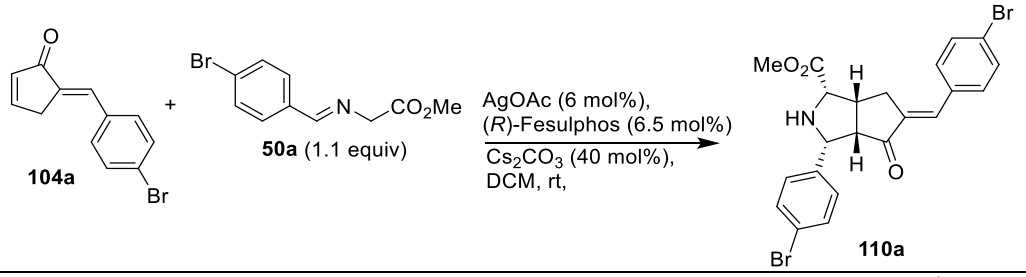


| Entry | Time (h) | e.e. [†] |
|---|---|---|
| 1 | 3 | 91 |
| 2 | 12 | 87 |
| 3 | 24 | 84 |
| 4[a] | 16 | 80 |

[a]12 mol% of (*R*)-Fesulphos was used. [†]Determined by HPLC analysis using a chiral stationary phase.

The results of the time-dependent studies on the stereochemical course of the reaction revealed that the enantioselectivity of the mono adduct **110a** decreases over the time. The decrease in enantioselectivity indicates that the main enantiomer of the reaction might be part of a dynamic covalent process over the course of the reaction in terms of a retro-cycloaddition, thus withdrawing the main enantiomer from the reaction equilibrium resulting in a decreased enantioselectivity over time. To prove the dynamic covalent mechanism in the reaction leading to a racemization process and further to confirm that it is an enantioselective (*R*)-Fesulphos/AgOAc-mediated reversible reaction, additional supporting experiments were performed (Figure 37). Enantioenriched mono adduct **110a** was treated with (*R*)-Fesulphos **60** (12 mol%), AgOAc (6 mol%) and $Cs_2CO_3$ (40 mol%) in DCM and a decrease of enantiomeric excess for the recovered mono adduct **110a** was observed (74% *e.e.*). In addition, racemic mono adduct **110a** was subjected to reaction under identical conditions and was recovered with -10% *e.e.* as an opposite enantiomer. These experiment further indicate that an enantioselective retro-

cycloaddition proceeds in the reaction confirming that the mono addition is a reversible process coupled with a kinetic resolution. Thus, selectively, one enantiomer of the mono addition product **110a**, the main enantiomer, matches with the chiral environment of the Ag/(*R*)-Fesulphos complex in a selective manner and undergoes a retro-cycloaddition. In this fashion a Ag/(*R*)-Fesulphos complex-mediated racemization occurs, converting the main enantiomer of **110a** to its opposite enantiomer over time. This dynamic covalent process of breaking and reforming of covalent bonds in the cycloaddition reaction in an asymmetric fashion is one aspect that could attribute to the low enantioselectivity of the mono addition product **110a** over the double cycloaddition product **105a**.

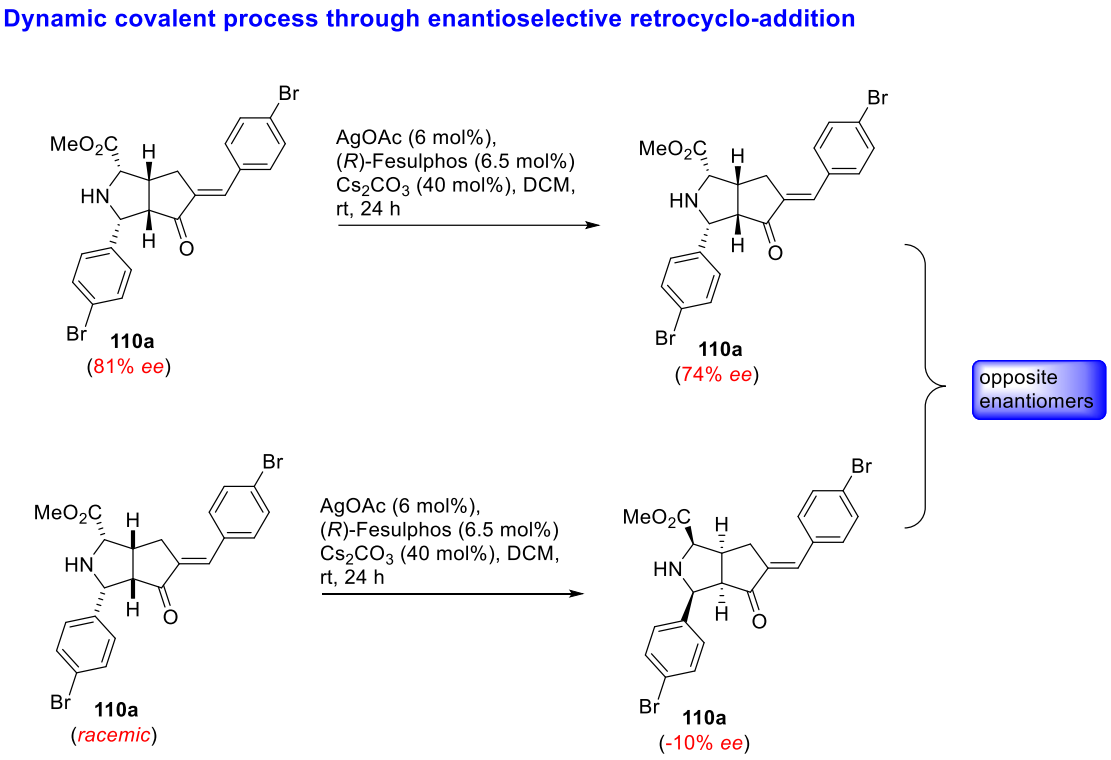


**Figure 37**: Enantioselective retro-cycloaddition of mono adduct **110a** via a dynamic covalent process.

### 3.5.2 Mechanistical studies on the second step of the reaction sequence

With the studies shown in the first step of the cycloaddition which revealed a dynamic covalent process in an enantioselective manner, the second cycloaddition in the reaction sequence from **110a** to **105a** was examined. Thus, the conversion of **110a** to **105a** under racemic as well as under chiral conditions was studied (Figure 38). Upon treatment of enantioenriched mono adduct (70% *e.e.*) under racemic conditions with 1.1 equiv. of imine **50a,** the double cycloaddition product **110a** was obtained with retained enantioselectivity, thus confirming that

the first step of the double cycloaddition is the enantio-determining step where the stereochemistry is set. However, subjecting the same enantioenriched mono adduct **110a** (70% *e.e.*) to reaction with imine **50a** under chiral conditions, surprisingly a drop in enantioselectivity for the double cycloaddition product **105a** (60% *e.e.*) was observed.

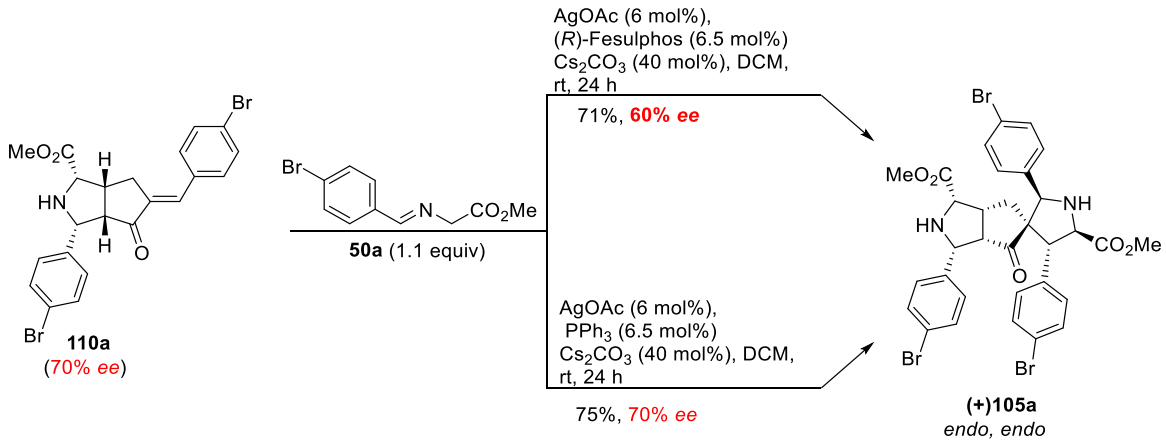


**Figure 38**: Reaction of mono adduct **110a** under racemic and chiral conditions and analysis of enantioselectivity of resulting double adduct **105a**.

To further elucidate the decrease in enantioselectivity under chiral conditions, also racemic mono adduct ***rac*-110a** was employed in the reaction with imine **50a** under chiral conditions and product **105a** was obtained with 20% *e.e.* (Figure 39) and was confirmed by crystal structure analysis.

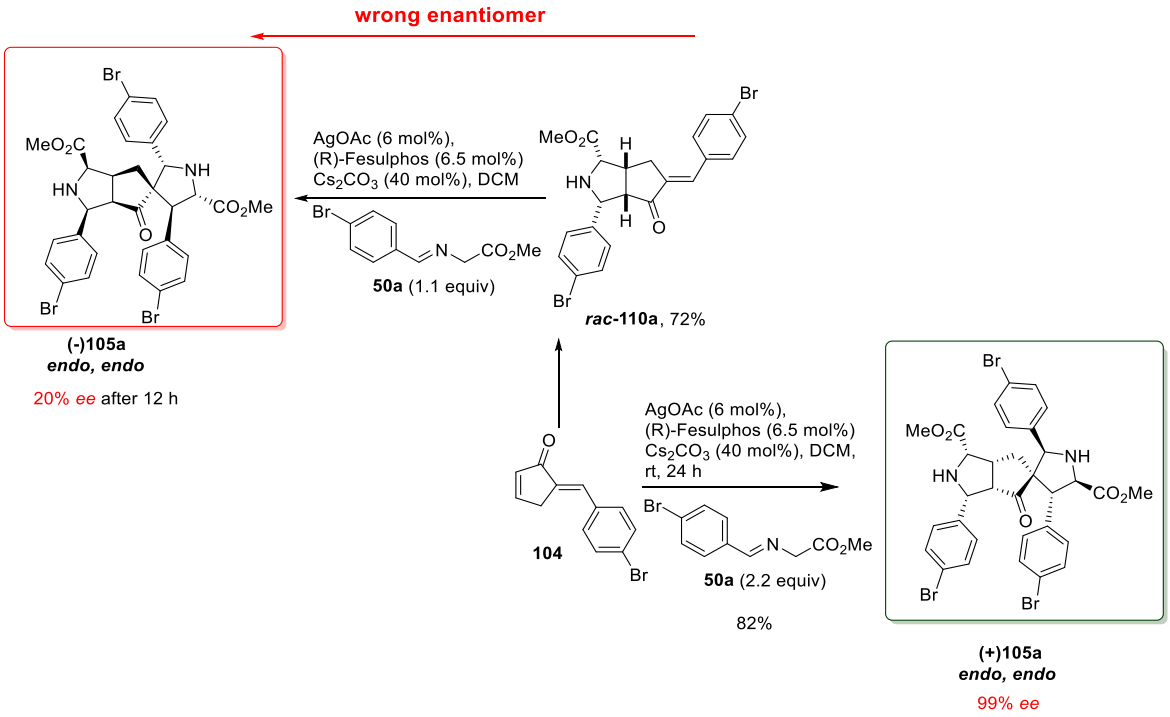


**Figure 39**: Formation of the wrong enantiomer upon treatment of ***rac*-110a** under chiral conditions.

To investigate why the wrong enantiomer of **105a** is obtained starting from the intermediate **110a** compared to the reaction starting from the cyclic enone **104a**, although the same set of reagents are used for the transformation, a time depended-kinetic experiment was performed. In this kinetic experiment, racemic mono adduct ***rac*-110a** was treated with imine **50a** under chiral conditions and the course of the reaction with regard to parameters like enantiomeric excess of the reaction products was analysed over time (Table 3.6) to verify whether an enantioselective retro-cycloaddition is the reason for this reaction outcome, as discussed above.

Table 3.6: Kinetic experiment for the chiral transformation of racemic mono adduct **110a**

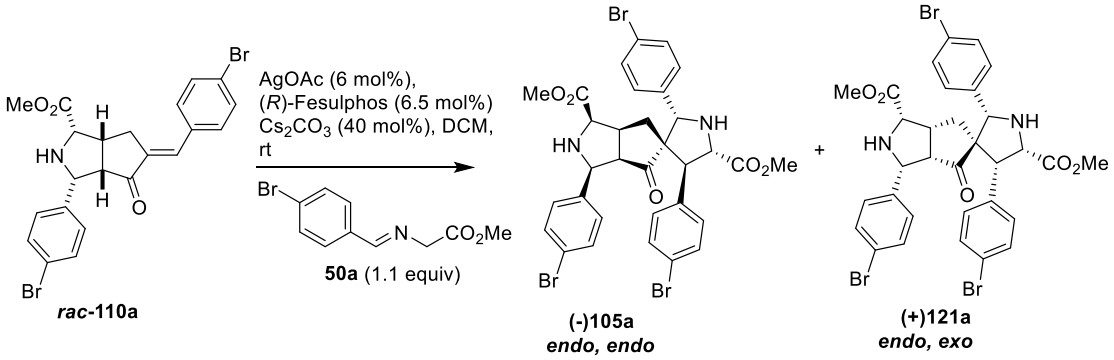


| time | (-)105a *e.e.* § (%) | (-)105a Yield‡ (%) | (+)121a *e.e.* § (%) | (+)121a Yield‡ (%) | Ratio**(-)105a**/(+)**121a** |
|---|---|---|---|---|---|
| 3 min | 40 | 29 | 37 | 47 | 1/1.5 |
| 7 min | 33 | 34 | 31 | 43 | 1/1.2 |
| 15 min | 30 | 45 | 29 | 42 | 1/1.2 |
| 1 h | 13 | 66 | 13 | 15 | 1/0.3 |

Reaction was performed in 6 ml of DCM and 0.2 mmol of SM. Each time 1.5 ml of the reaction mixture was taken, purified and analyzed. ‡Isolated yields of (-)**105a** and (+)**121a** after column chromatography based on **0.05 mmol SM (**4 aliquots were taken on specific time points from 0.2 mmol SM) mmol SM. §Determined by HPLC analysis on chiral phase.

In a very early stage of the reaction, full conversion of the racemic mono-adduct ***rac*-110a** is observed showing a fast reaction rate of that step. The racemic mono adduct **110a** is rapidly converted into two stereoisomers, the *endo,endo* -product (-)**110a** and the *endo, exo*-product **121a**. X-Ray analysis of the stereoisomer *endo,exo*-product **121a** revealed that it is formed through an *exo*-selective cycloaddition of the imine **50a** to the endo monoaddition product **110a** in which all the substituents of the *spiro*-cycle are on the same plane. Both stereoisomer, (-)**105** and (+)**121a** are formed with remarkable *e.e.* (40% and 37% *e.e.*) after three minutes (Table

3.6). Over the course of the reaction the *e.e.* of both product significantly drops down to 13% *e.e.* In addition, the ratio of the two stereoisomers changes over time, having in early stage of the reaction the e*ndo, exo*-(+)**121a** in excess over *endo, endo*-(-)**110a**, while throughout the reaction more *endo, endo*-(-)**110a** is formed and in parallel the yield of e*ndo, exo*-(+)**121a** is decreasing. In order to confirm the observation of this experiment a second kinetic studies was performed by subjecting racemic mono adduct ***rac*-110a** to cycloaddition with iminoester **50g** under same conditions and a similar trend was observed (Table 3.7).

Table 3.7: Kinetic experiment for the chiral transformation of racemic mono adduct **110c**

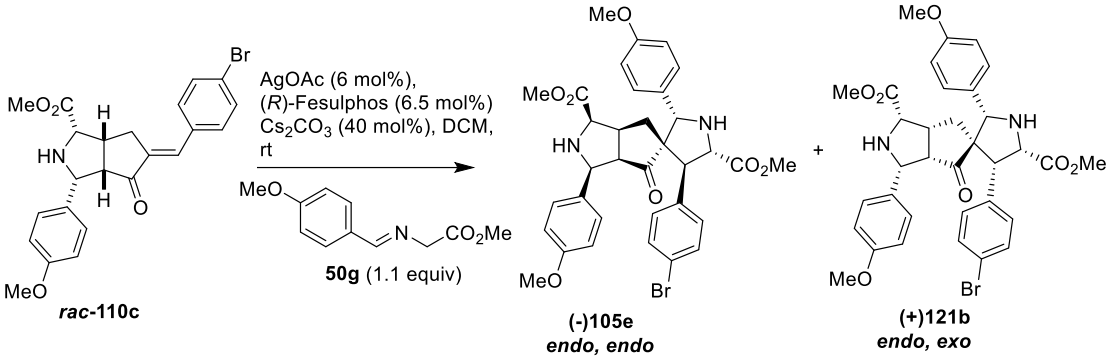


| | (-)-105e | | (+)-121b | | |
|---|---|---|---|---|---|
| time | *e.e.* § (%) | Yield‡ (%) | *e.e.* § (%) | Yield‡ (%) | Ratio**(-)105e**/(+)**121b** |
| 3 min | 55 | 31 | 55 | 47 | 1/1.5 |
| 7 min | 43 | 34 | 35 | 44 | 1/1.2 |
| 15 min | 40 | 34 | 35 | 44 | 1/1.2 |
| 30 min | 35 | 44 | 31 | 37 | 1.8/1 |
| 1 h | 11 | 80 | --- | --- | >20:1 |

Reaction was performed in 6 ml of DCM and 0.2 mmol of SM. Each time 1.5 ml of the reaction mixture was taken, purified and analyzed. ‡Isolated yields of (-)**105e** and **(+)121b** after column chromatography based on **0.05 mmol SM (**4 aliquots were taken on specific time points from 0.2 mmol SM) mmol SM. §Determined by HPLC analysis on chiral phase.

Since racemic mono addition product ***rac*-110** is converted to two stereoisomers, (-)**105** and (+)**121** with varying ratios over the course of the reaction, it implies the formation of kinetic and thermodynamically controlled products in a dynamic covalent process (Figure 40). The *endo, exo*-stereoisomer (+)**121** is the kinetically favored product and is formed faster than the thermodynamically more stable product *endo, endo*-(-)**105** which explains the excess of (+)**121** over the *endo, endo* product (-)**105** in early stages of the reaction. The change in ratio

throughout the course of the reaction indicates that the kinetically favored *endo*, *exo*-product (+)**121** is less stable and is converted into its more stable stereoisomer (+)**105**. The interconversion proceeds in an enantioselective fashion, thus the main enantiomer of the kinetically favored product (which is (+)**121**) is preferentially converted to its thermodynamically stable stereoisomer (+)**105**. Four products are formed in the reaction, two enantiomers of the kinetically favored product as well as two enantiomers of the thermodynamically favored product. In early stages of the reaction, the main enantiomer of the thermodynamically favored product is (-)**105**. Since (+)**105** is formed over the course of reaction by chiral catalyst mediated interconversion of the main enantiomer of the kinetic product (+)**121**, the *e.e.* of both products, (+)**121** and (-)**105** are decreased (Figure 40). Selectively, one enantiomer of the kinetically favored product matches with the chiral environment of the (*R*)-Fesulphos/AgOAc complex and undergoes a kinetic resolution in dynamic process.

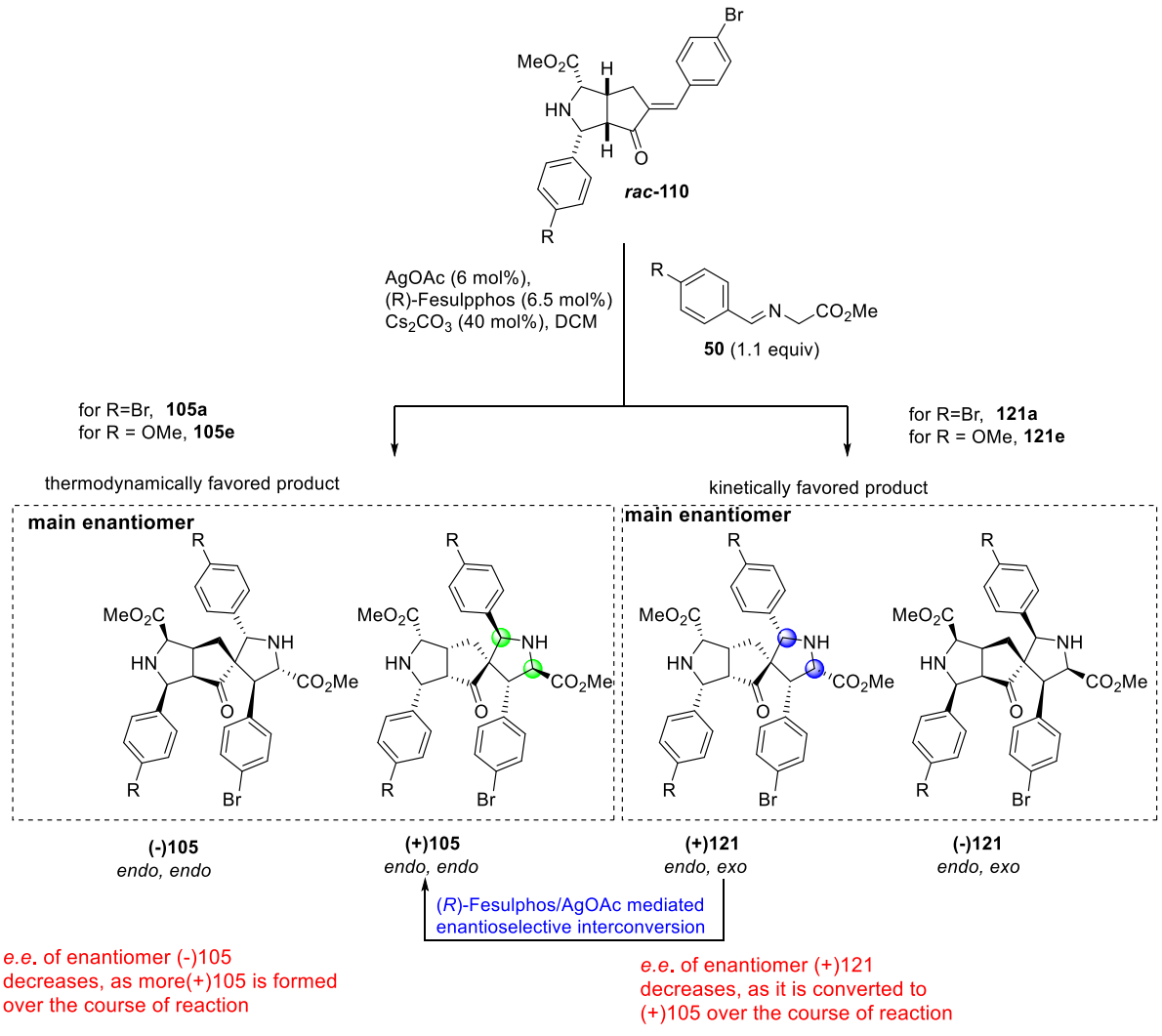


**Figure 40**: Illustration of the stereochemical outcome for the kinetic experiment mono adduct **110a**.

To further confirm the decrease in enantioselectivity and the changes in ratio of the kinetic experiment as a result of an interconversion of stereoisomers over time, more control experiments were conducted with *endo, exo*-product (+)**121a**. Compound (+)**121a** (37% *e.e.*) was employed to reaction with AgOAc (6 mol%), (*R*)-Fesulphos (6.5 mol%) and $Cs_2CO_3$ (40 mol%) and was partially converted to the more stable and thermodynamically favored *endo, endo*-product (+)**105a** with 59% *e.e.* (37%) while (+)**121a** was recovered with a decreased *e.e.* of 20% (Figure 41). This result illustrates that *endo, exo*-product (+)**121a** is not stable under these reaction conditions and can be converted by a (*R*)-Fesulphos/AgOAc-mediated transformation to its more stable stereoisomer. The lower *e.e.* of the recovered product (+)**121a** (20% *e.e.*) compared to its initial *e.e.* from outset of the reaction (37% *e.e.*) provided evidence that an enantioselective dynamic process is proceeding, as selectively the main enantiomer of the *endo, exo*-product (+)**121a** is interconverted to the stereoisomer (+)**105a**. This enantioselective dynamic process also explains the higher *e.e.* of the obtained *endo, endo* product (+)**105a** (59% *e.e.*) over the initial *e.e.* of the starting material.

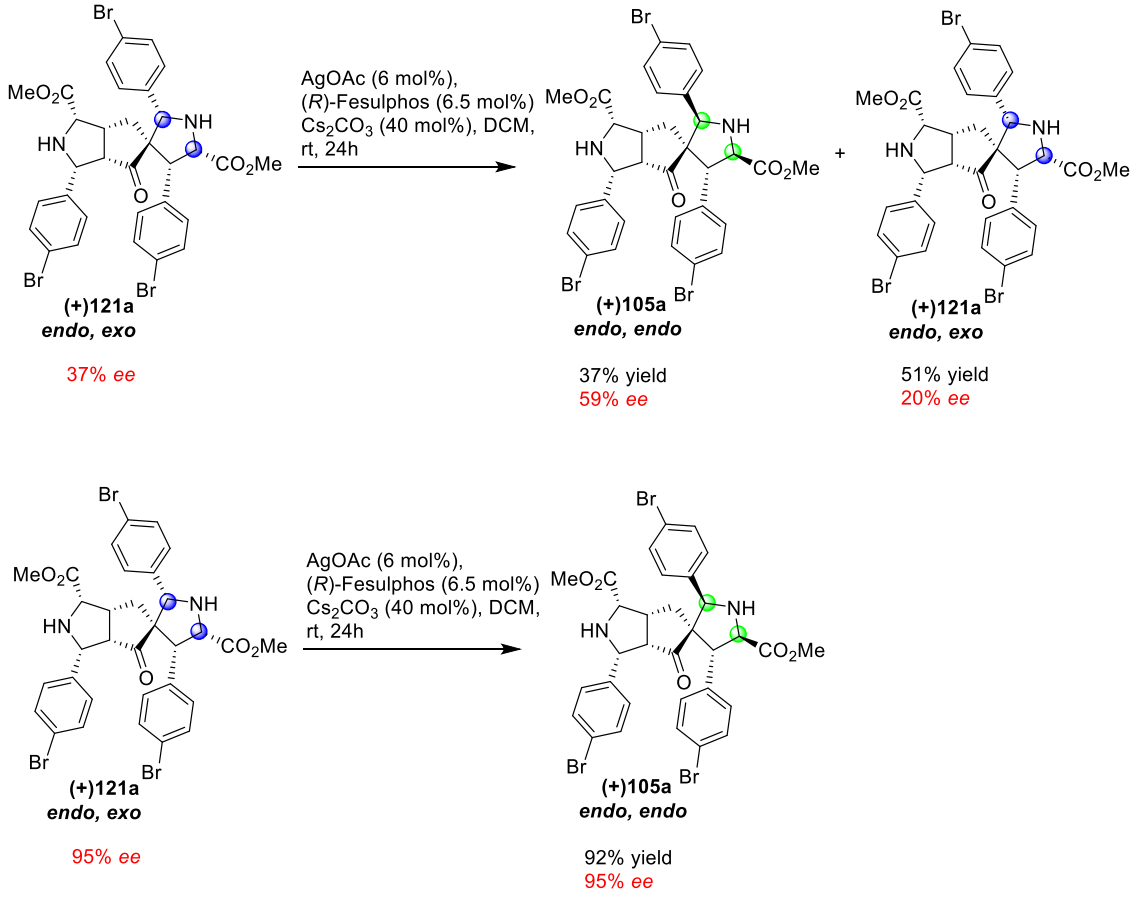


**Figure 42**: Enantioselective interconversion of (+)**121a** to its stereoisomer (+)**105a**.

By subjecting highly enantioenriched *endo, exo*-product (+)**121a** (95% *e.e.*) to AgOAc (6 mol%), (*R*)-Fesulphos (6.5 mol%) and $Cs_2CO_3$ (40 mol%) the more stable thermodynamically favored *endo, endo*-product (+)**105a** was obtained with very high *e.e.* (95% *e.e.*) and high yield (92%). The retention of *e.e.* and the very high yield confirm the highly enantioselective nature of the dynamic process (Figure 42).

To investigate the mechanism for the interconversion of the stereoisomers and to figure out through which intermediate the reaction proceeds additional experiments were conducted. In the transformation of the kinetic *endo, exo*-product (+)**121** to the more stable *endo, endo*-isomer **105**, two stereocenters of the *spiro*-cycle are inverted. As only changes in stereochemistry of the *spiro*-cycle occur, it might be possible that the reaction proceeds through a retrocyclo-addition reaction on the *spiro*-cyclic ring. Thus, the kinetically favoured *endo, exo*-product (+)**121a** (37%) *e.e.* was treated with iminoester **50g** (2 equiv.) in the presence of AgOAc (6 mol%), (*R*)-Fesulphos (6.5 mol%) and $Cs_2CO_3$ (40 mol%) in DCM. An imine exchange reaction was observed on the *spiro*-cycle providing *endo, endo*- product **115p** with 65% yield in 33% *e.e.* (Figure 43).

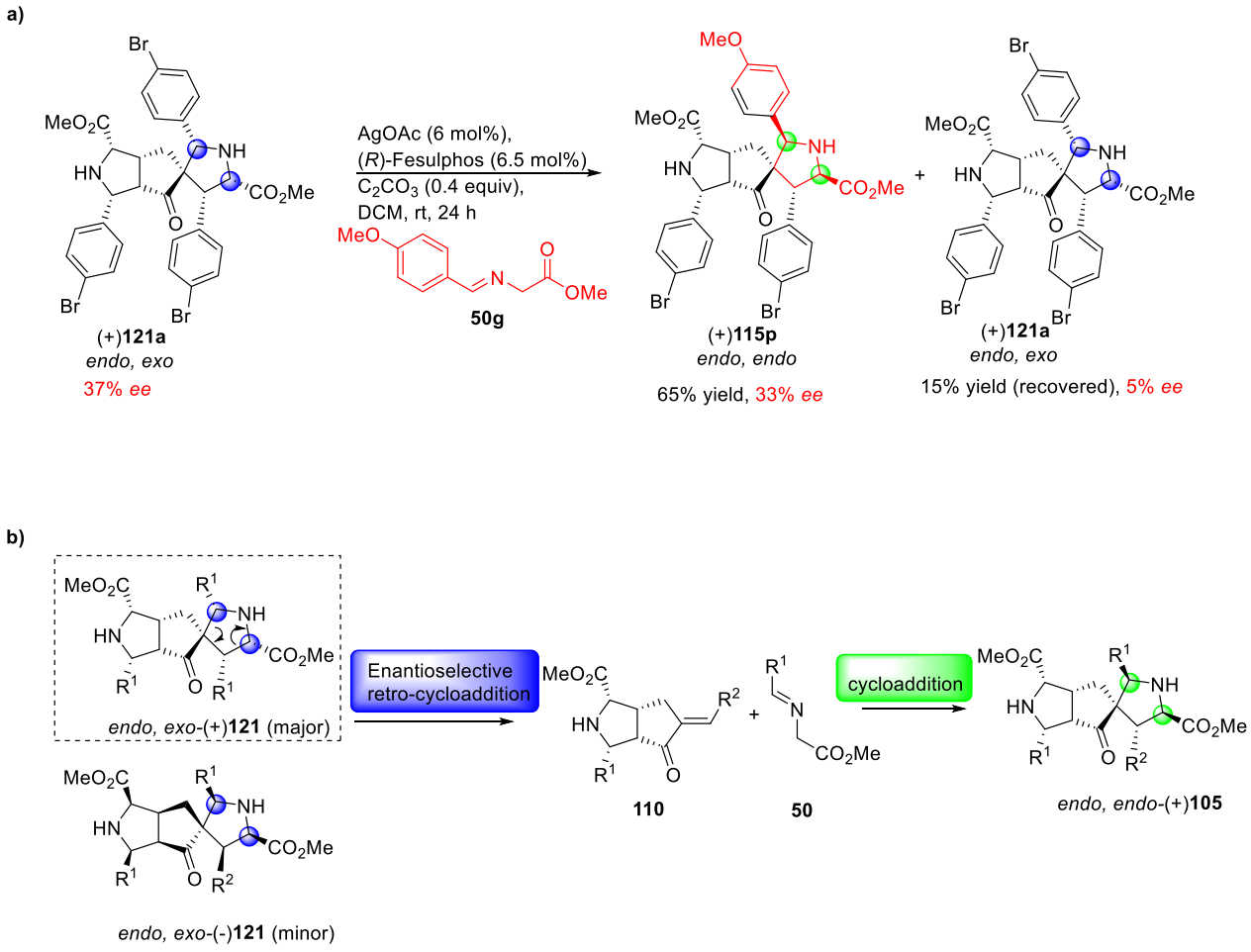


**Figure 43**: a) Imine exchange reaction on (+)**121a**; b) enantioselective dynamic covalent process.

The imine exchange reaction illustrates that the transformation of *endo, exo*-product (+)**121a** to *endo, endo*- product **115p** proceeds via retro-cycloaddition reaction by generation the mono adduct **110a** as an intermediate. An enantioselective (*R*)-Fesulphos/AgOAc-mediated retro-cycloaddition on the spiro-cyclic ring of the *endo, exo*-product proceeds, leading to the formation of mono adduct **110a**. Mono adduct **110a** is then trapped by the added imine in an *endo*-selective fashion to regenerate the spiro cycle in a 1,3-dipolar cycloaddition to afford *endo, endo*-product **115p**. The interconversion of the *endo, exo*-product **121** to its stereoisomer *endo, endo*-**105** is in general a dynamic covalent process in which covalent bonds are cleaved through an enantioselective retro cycloaddition generating mono adduct **110** and reformed again by cycloaddition (Figure 43).

To verify in general the thermodynamic stability of *endo, endo* product over its stereoisomer *endo, exo*-product, racemic *endo, endo*-**105a** was subjected to reaction with AgOAc (6 mol%), (*R*)-Fesulphos (6.5 mol%) and $Cs_2CO_3$ (40 mol%) with and without iminoester **50a** (Figure 44). Product **105a** was not converted to its stereoisomer and was fully recovered, confirming the relative lower energy of the product and thus the thermodynamic stability over its stereoisomer.

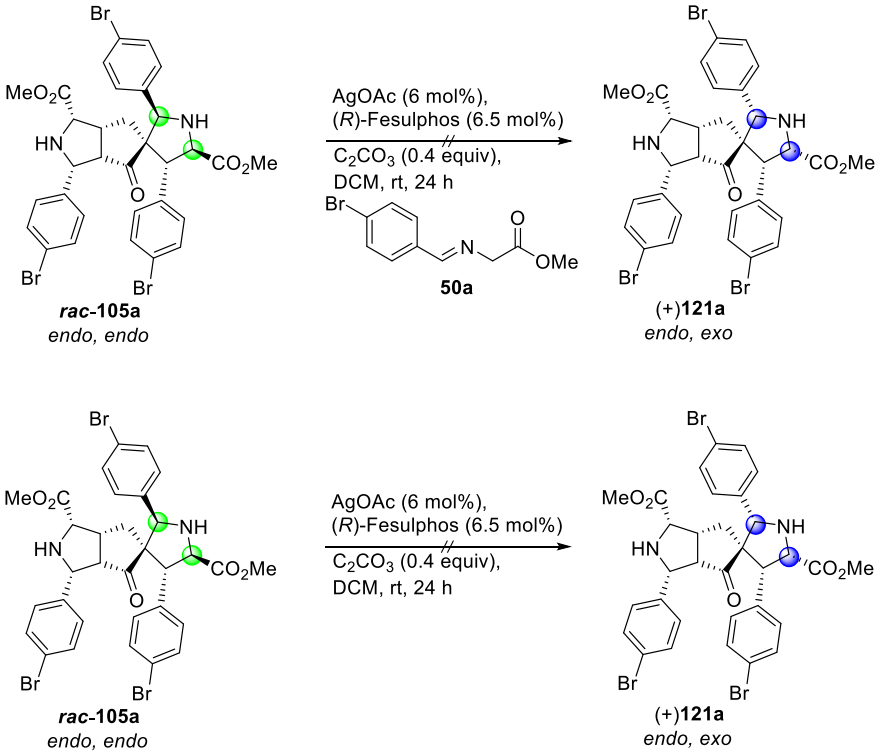


**Figure 44**: Control experiment to prove the stability of *endo, endo*-**105a** over *endo, exo*-**121a**.

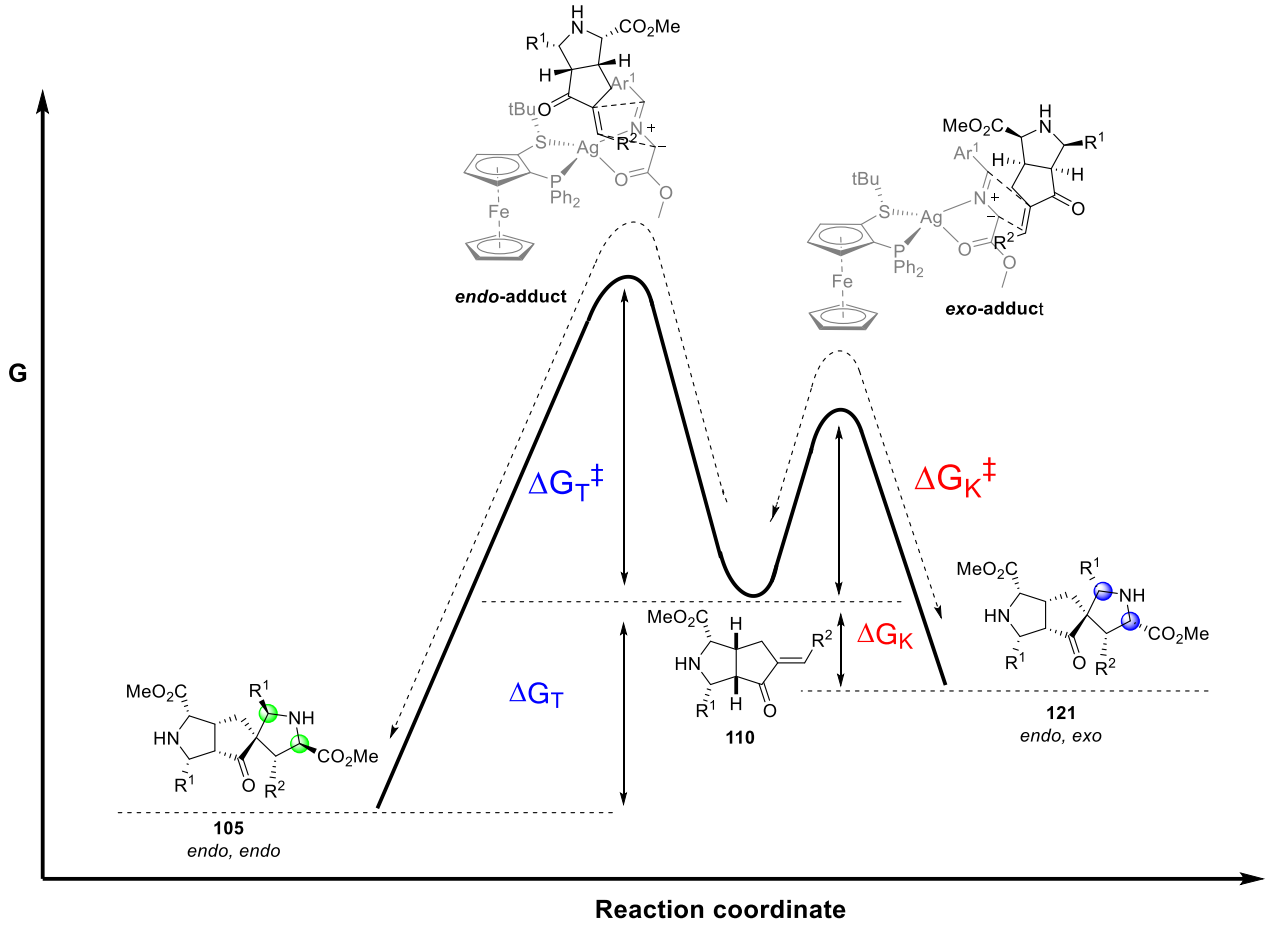


**Figure 45**: Energy diagram for *endo, endo* **105** and *endo, exo* **121**.

The energy barrier for the transition of the *endo, exo*-product **121** is lower with respect to the energy of the transition state for the *endo, endo*-product **105** (Figure 45). Thus, the mono adduct **110** is converted faster to *endo, exo*-product, which is the kinetically favoured, but higher in energy relative to the *endo, endo*-product **105**. The kinetic product **121** undergoes a retro-cycloaddition under the reaction conditions over the course of the reaction as it is non-stable and is converted back to the mono adduct **110**. An *endo*-selective cycloaddition occurs affording the *endo, endo*-product **105**, which is lower in energy compared to the stereoisomeric *endo, exo*-product **121**, and is the thermodynamically favoured product. A dynamic covalent process shifts the equilibrium towards the thermodynamically controlled pathway.

### 3.5.3 Summary of the mechanistical study

With regard to the performed detailed mechanistical studies on the first step as well as the second step of the reaction sequence, the double cycloaddition of cyclic enone **104** and imine **50** proceeds through a dynamic covalent process and can be divided into two cycles (Figure 46). In the reaction sequence of the double cycloaddition, first a (*R*)-Fesulphos/AgOAc catalyzed *endo*-selective cycloaddition occurs to generate the mono addition product **110** in which the chiral centers are set. The initial enantiopurity of the mono addition is >95% *e.e.*, however over time a selective (*R*)-Fesulphos/AgOAc mediated retro-cycloaddition of the main enantiomer of the mono addition product proceeds, inducing its decomposition. Thus the *e.e.* of the mono adduct is remarkably reduced from >95% *e.e.* to around 80% *e.e.* The selective decomposition of the main enantiomer shows that it matches well with the chiral environment of the (*R*)-Fesulphos/AgOAc complex. In the second cycle, a second cycloaddition occurs to the generated enantioenriched mono-adduct which leads to the formation of two diastereomers. Through an *exo*-selective cycloaddition to the mono adduct a kinetically favored non-stable *endo, exo*-product **121** is formed, as well as thermodynamically stable *endo, endo*-product **105** via an *endo*-based transition state. Here again, an enantioselective dynamic covalent process takes place in which the kinetic non-stable product **121** is interconverted to the thermodynamically more product **105** by means of a retro-cycloaddition through mono adduct **110** as intermediate. The double cycloaddition is an enantioselective dynamic covalent process, in which covalent bonds are broken and reformed again. Kinetic and thermodynamic products are formed in early stage of the reaction, while over the course of the reaction the equilibrium is shifted towards the thermodynamically controlled product. The double cycloaddition follows a thermodynamically controlled pathway and enables the interconversion of stereoisomers to reach the desired equilibrium.

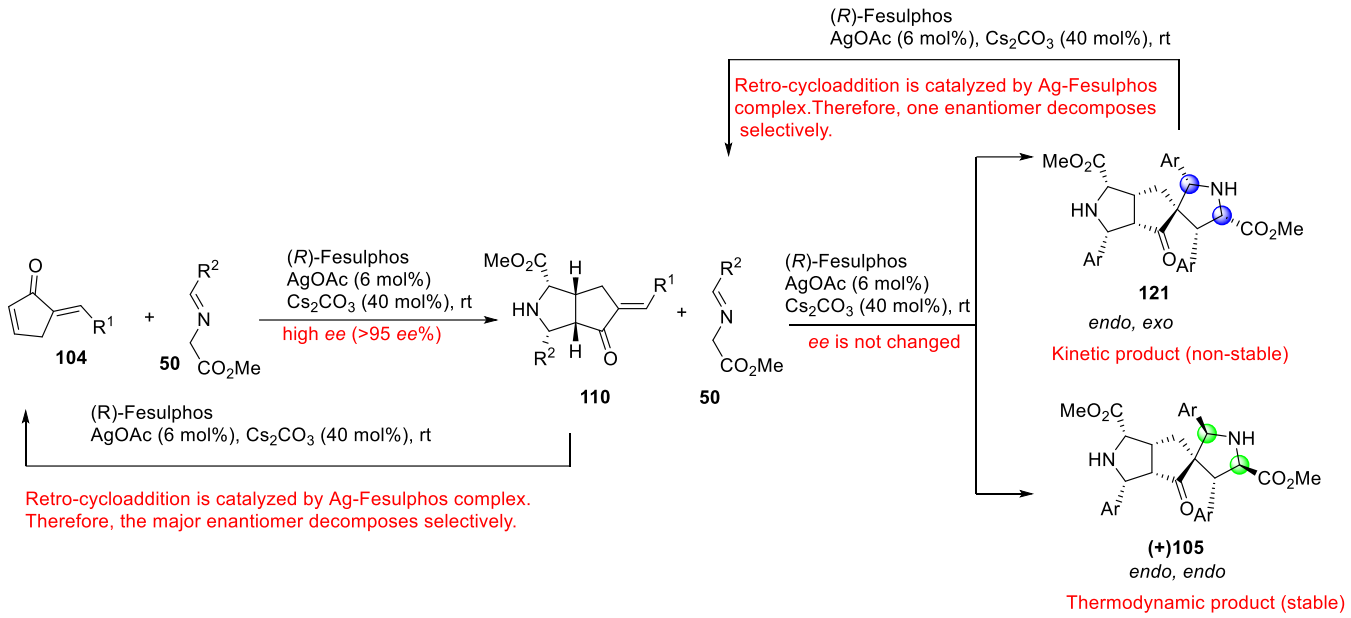


**Figure 46**: Illustration of the enantioselective dynamic covalent process in the double 1,3-dipolar cycloaddition of enone **104** with imine **50**.

## 3.6 Selective synthesis of the *endo, exo*-stereoisomer

The formation of the *endo, exo* stereoisomer in the double cycloaddition as a kinetically favoured but non-stable product in DCM lead to the question, whether a stereodivergent synthesis can be achieved, in which the kinetic *endo, exo*- product **121** can be obtained as main product by slowing down the interconversion to the thermodynamically favoured *endo, endo*-product **105**. For the stereodivergent synthesis it was ambitious to use the same chiral catalyst to achieve the switchable diastereoselectivity in the double cycloaddition of cyclic enone **104** and imine **50**. A solvent screening revealed that employing an aqueous solvent system THF:$H_2O$ (4:1) a distereodivergent synthesis for the double cycloaddition can be achieved, resulting in the formation of *endo, exo*-product **121** as the main diastereomer (Figure 47). Treatment of enone **104a** with 2.2 equiv. of iminoester **50a** in the presence of (*R*)-Fesulphos **60** (6.5 mol%) AgOAc (6 mol%) and $Cs_2CO_3$ (40 mol%) in this aqueous solvent system yields the *endo, exo*-product (+)**121a** (95% *e.e.*, 60% yield) as the main diastereomer relative to *endo, endo* product (+)**105a** (*d.r.* 4:1) (Figure 47), wherein in DCM as solvent the *endo, endo*-product (+)**105a** was selectively obtained as a result of a dynamic covalent process (see chapter 3.5). The substrate scope in aqueous solvent system was studied and is wide. Electron-donating substituents, electron-withdrawing groups as well as heterocycles are tolerated and the products are obtained with excellent enantioselectivity (89%-97% *e.e.*).

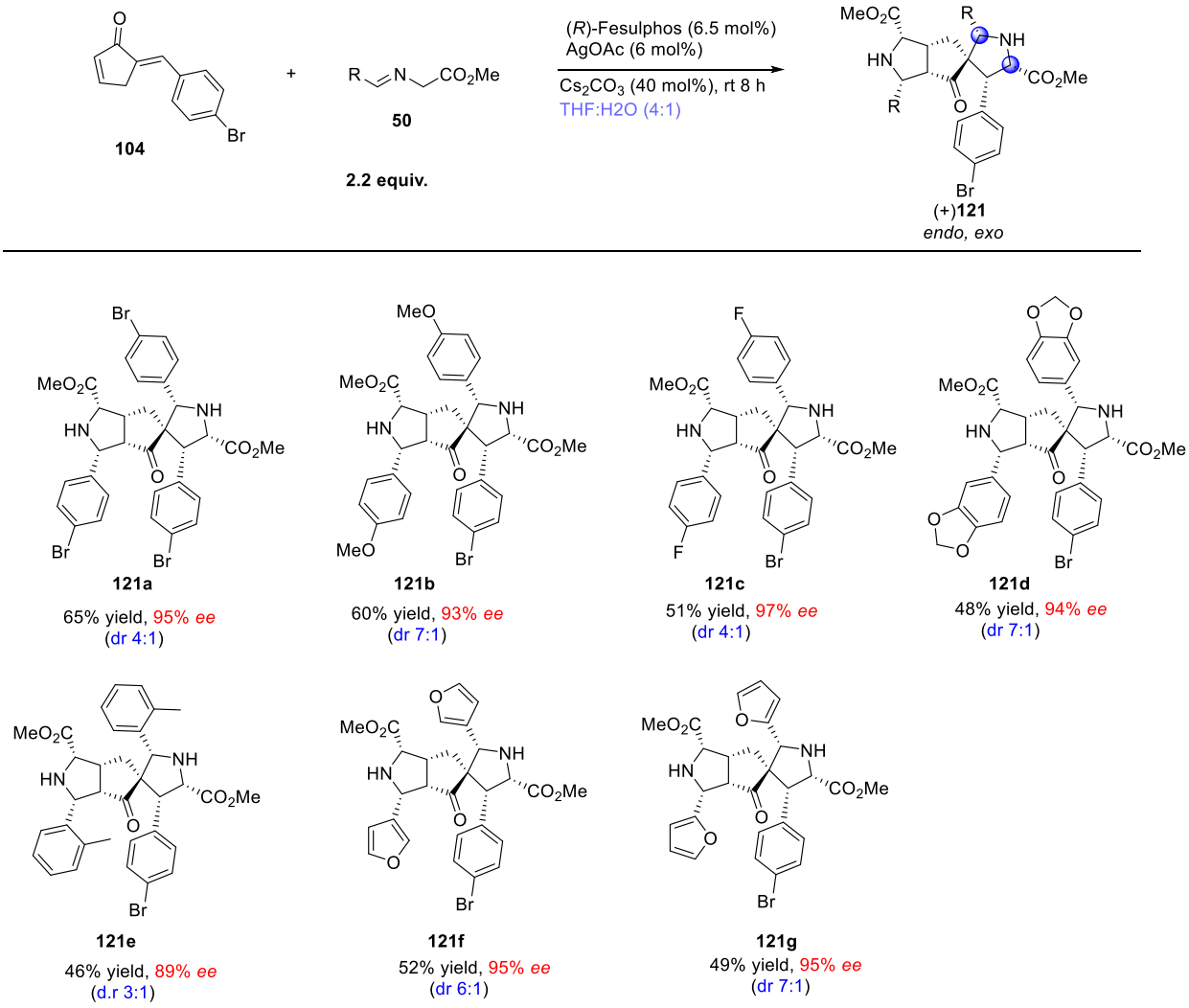


**Figure 47**: Substrate scope for the stereodivergent synthesis of *endo, exo*-diastereomer **121** in aqueous solvent system.

The aqueous environment might stabilize and favour the *exo*-selective transition state which results in inversion in diastereoselectivity compared to the same reaction DCM. In addition the interconversion of the kinetic *endo, exo*-product **121** to thermodynamically favoured *endo, endo*-product **105** is slower. The aqueous solvent system decreases the speed of the equilibrium process of the thermodynamically controlled pathway, thus the desired equilibrium is not reached it results in the kinetically controlled *endo, exo*-product **121** as a major diastereomer (Figure 48). However in DCM, the thermodynamically controlled equilibrium is reached faster as a result of a fast interconversion of the stereoisomers. The retro-cycloaddition of the kinetically favoured non-stable *endo, exo*-product **121** is accelerated in DCM, but the rate is decreased in the aqueous solvent system as a result of a slower retro-cycloaddition. The slower equilibrium process in THF:$H_2O$ enables a diastereodivergent transformation of cyclic enones **104** with imine **50** using the same set of reagents.

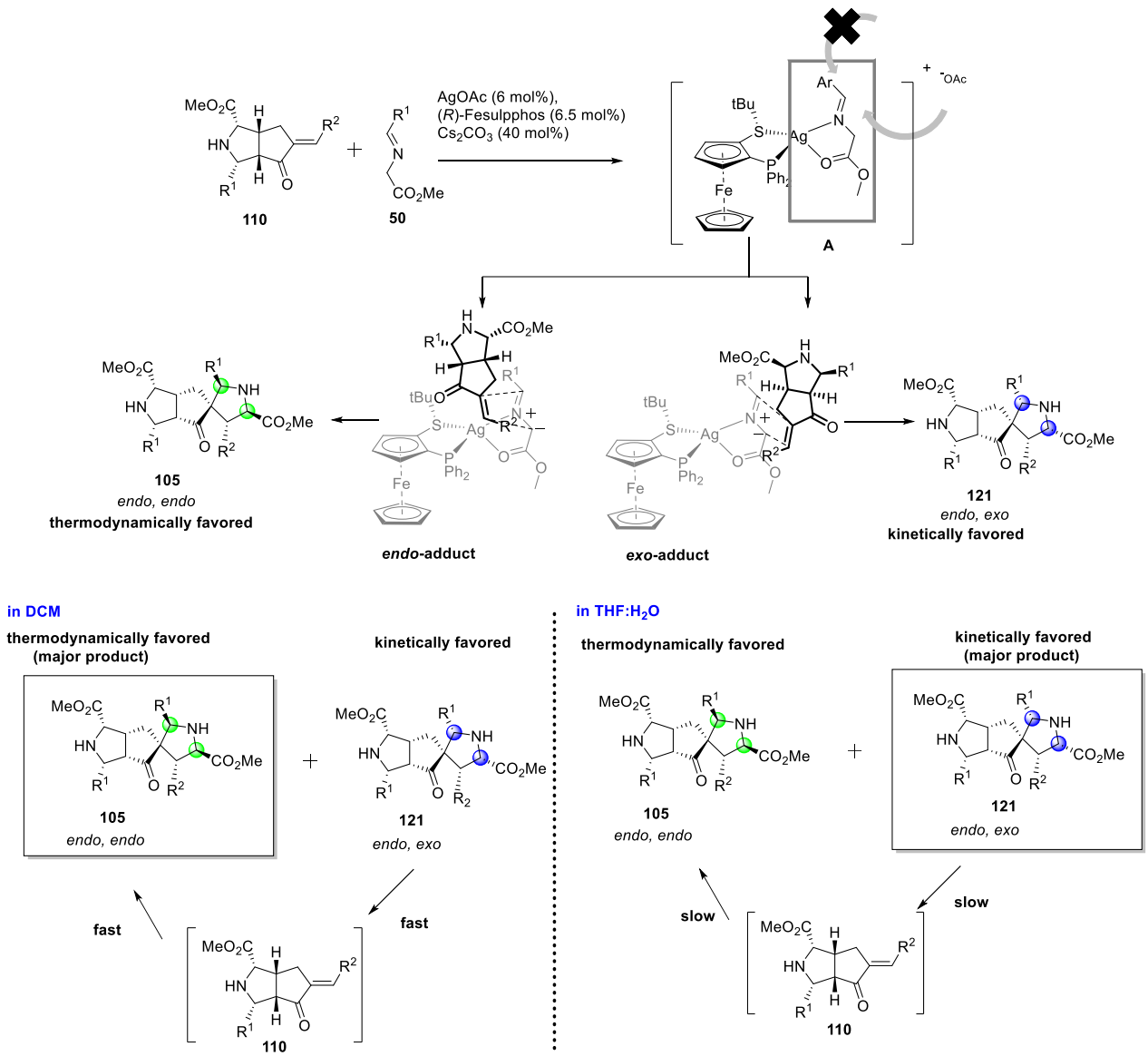


**Figure 48**: Proposed intermediates and transition states for formation of kinetically and thermodynamically favoured products **105** and **121** and differences in equilibrium in DCM and THF:$H_2O$.

## 3.7 Biological evaluation of the tricyclic double cycloaddition products

In the course of a program aimed at the synthesis of a pseudo NP compound class, two pyrrolidine fragments were combined in an unprecedented, novel and structurally complex manner via a double 1,3-dipolar cycloaddition. In total 88 compounds (including racemic and chiral) were submitted to the COMAS in Dortmund for cell-based screening for potential novel bioactivity. The screening results revealed that five of the submitted compounds show activity in autophagy (Figure 50).

Autophagy is an essential cellular and molecular mechanism inducing a self-degradative process which is fundamental for the proper and healthy function of cells.[95] It plays a wide and fundamental role in various physiological and pathophysiological issues as a survival mechanism.[96] The intracellular degradation process of autophagy includes, for instance, the removing of misfolded or aggregated proteins, abolishment of damaged or dysfunctional organelles such as mitochondria and additionally provides building blocks and energy for cellular renovation and homeostasis.[95, 97] The degradation process can be in a selective or non-selective fashion. In the autophagy machinery the whole process starts with an isolated membrane, a phagophore, enclosing a portion of portion of cytoplasma with organelles to form an autophagosome (Figure 49).[97] The outer membrane of the autophagosome latterly undergoes a fusion with the lysosome, thus proceeding the degradation of the inter content. Valuable by products such as amino acids of the degradation process are recovered and promoted back to the cytoplasma by lysosomal permeases and transporters which be re-used for metabolism.[95, 97]

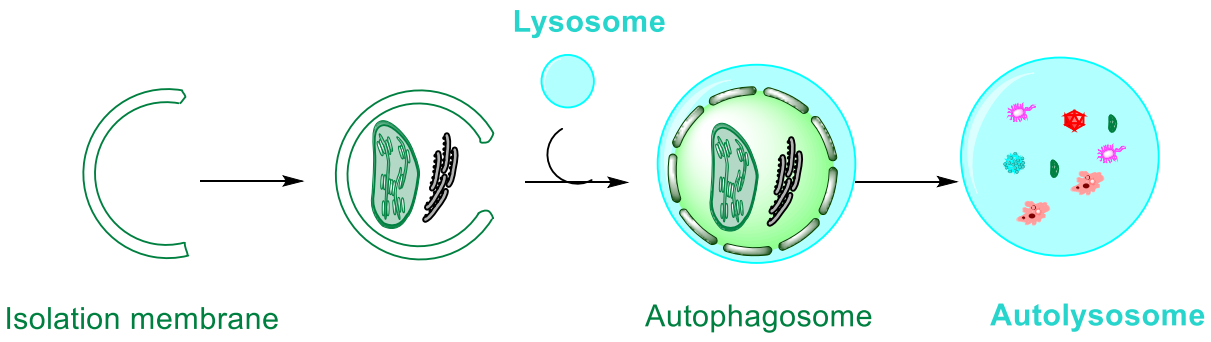


**Figure 49**: Schematic representation of autophagy intracellular degradation process (illustration according to reference[95]).

The most active compound turned out to be the double cycloaddition *endo, endo*-product **105a** with half-maximal inhibitory concentration ($IC_{50}$) of 3.12 ± 0.64 µM in the rapamycin-induced autophagy assay. In addition, *endo, endo*-product **115a** from the mixed double cycloaddition products exhibited a very similar inhibition with an $IC_{50}$ value of 3.77 ± 1.04 µM for autophagy. The double cycloaddition products with the combination of two pyrrolidine fragments in an unrelated fashion resulting in structurally complex tricyclic compounds display a new class of bioactive compounds that can be potential modulators of the autophagy pathway.

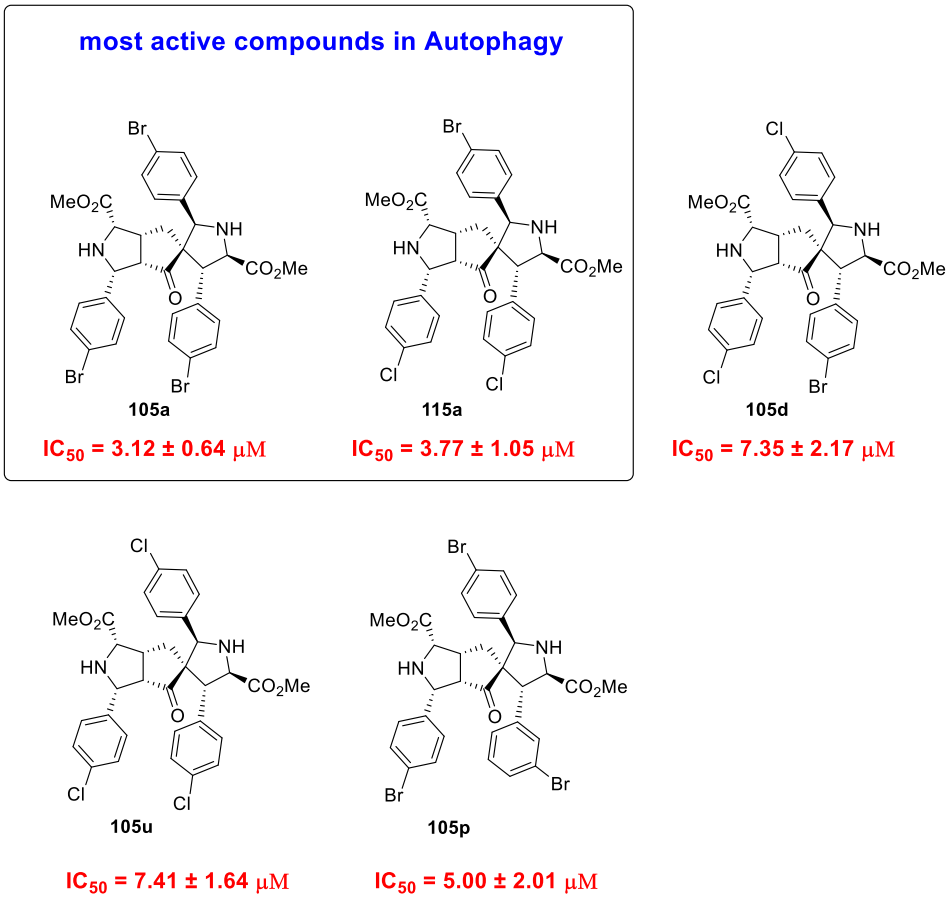


**Figure 50**: Results of the biological screening from COMAS and activity in autophagy.

## 3.8 Conclusion

In summary, the first enantioselective dynamic covalent process in double 1,3-dipolar cycloadditions has been discovered. A one pot tandem cycloaddition of azomethine ylides to α′-alkylidene-2-cyclopentenones provided highly complex tricyclic compounds with 8 stereocenters. High enantioselectivities and diastereoselectivities were obtained through a thermodynamically controlled equilibrium process. A stereodivergent synthesis was accomplished using the same set of reagents by employing an aqueous solvent system and an enantiodivergent synthesis was realized as a result of dynamic covalent process coupled to a kinetic resolution. Some of the corresponding double cycloaddition products displayed potential inhibition of the autophagy pathway.

# 4 Sequential 1,3-dipolar cycloaddition and dearomatization of indoles

## 4.1 Introduction

Indole alkaloids containing a pyrroloindoline moiety are important heterocyclic frameworks that are represented in the core structure of various NPs and bioactive molecules.[98-99] The privileged scaffolds of pyrroloindolines and their related NPs cover an impressive range of diverse biological properties including anticholinesterase[100], anti-inflammatory[101], and anticancer activities[102]. Their distinct structural features and well established bioactivity have inspired the development of various synthetic methods for to access pyrroloindolines.

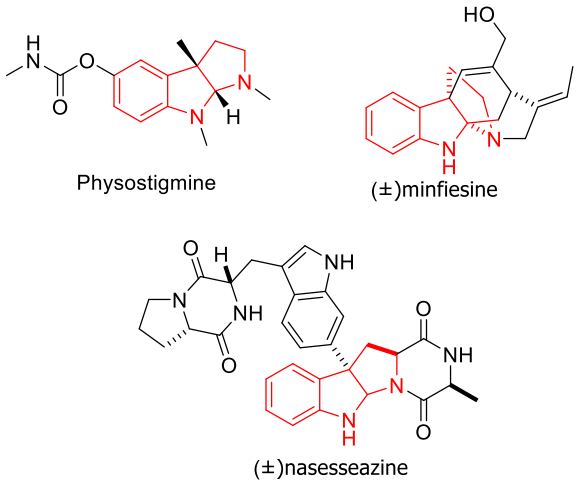


**Figure 51**: Selected examples of NPs containing a pyrroloindoline scaffold.

One of the most applied methods for the construction of indoline related scaffolds such as the pyrroloindoline is the dearomatization of indoles, in which the planar aromatic structure of indole is converted to indoline core motifs.[103] Thus, tryptamines and their derivatives were widely explored to generate pyrroloindolines by utilizing the C3-nucleophilicity of the indole ring and inducing a cascade cyclization with electrophiles. In this context, Reisman and co-workers reported an enantioselective synthesis of pyrroloindolines by a $SnCl_4$-mediated reaction of C3-substituted indole precursors **122** with acetamidoacrylate **123** (Figure 52).[104] A conjugated addition occurs via the C-3 nucleophilic center of the indole **122** followed by trapping the iminium ion in a cyclization process. Later, a rhodium-catalyzed [3+2] annulation for the generation of enantioenriched pyrroloindolines was reported by the group of Davis.[105] A convenient and mild method for the construction of pyrroloindolines was reported by Liao

and co-workers using α-haloamides **127** for a formal [3+2] cycloaddition via in situ generated aza-oxyallyl cation.[106]

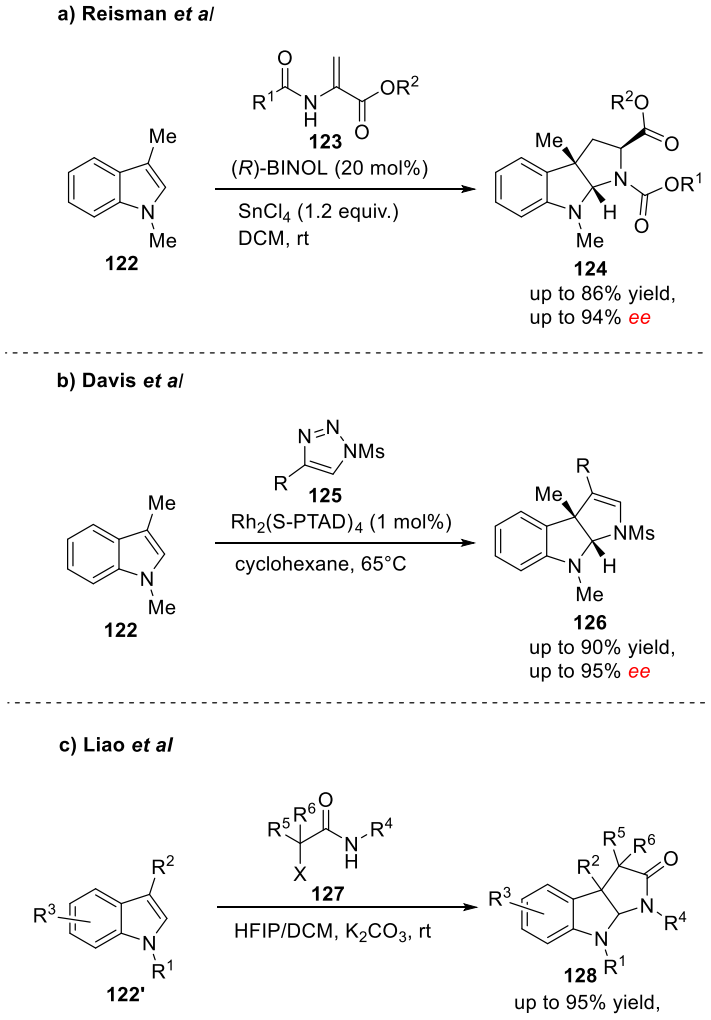


**Figure 52**: Reports on construction of pyrroloindolines via dearomatization of indoles.

## 4.2 Aim of the project

The pyrroloindoline core structure displays relevant structural features regarding bioactivity and is a relevant NP scaffold. With respect to the design principle of pseudo NPs the unrelated combination of pyrroloindoline scaffolds with other NP scaffolds might afford highly interesting compound classes with potential novel bioactivity. A synthetic strategy was designed for the combination of the pyrroloindoline scaffold with a pyrrolidine moity in a polycyclic manner, in which the pyrroloindoline moiety would be generated in a late stage (Figure 53). An asymmetric 1,3-dipolar cycloaddition of azomethine ylides **50** to cyclic enone **129** for the formation of a pyrrolidine scaffold should be employed by setting the stereogenic centers. Indole formation and subsequently a substrate-controlled diastereoselective

dearomatization strategy should afford a highly complex fused polycyclic compounds **132** with different NP scaffolds such as pyrrolidine, pyrroloindoline and cyclopentane.

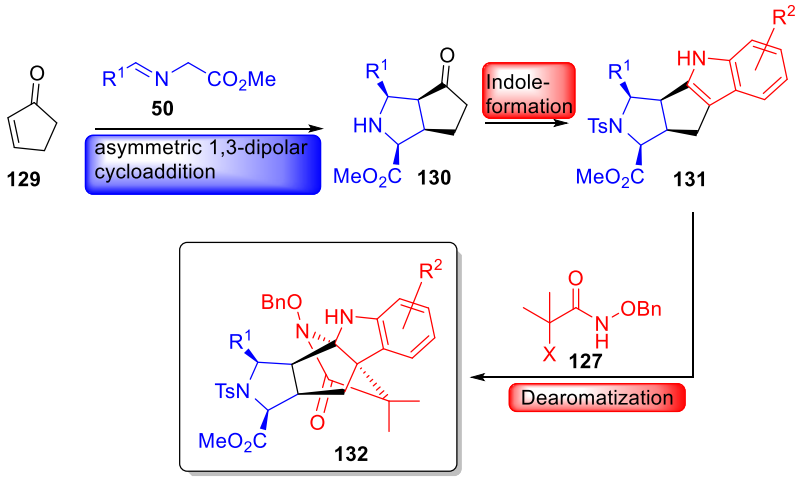


**Figure 53**: Synthetic strategy for the synthesis of polycyclic pyrroloindoline **130**.

## 4.3 Results and discussion

Based on the synthetic strategy cyclic enone **129** was subjected to an enantioselective 1,3-dipolar cycloaddition with iminoester **50a** to afford product **130** with 80% yield and 73% *e.e.* The nitrogen atom of the pyrrolidine was protected as a tosyl functionality by treating pyrrolidine **130** with TsCl in presence of $K_2CO_3$ as a base (Figure 54). The tosyl-protected product **133** was obtained with 85% yield under retention of the original *e.e.* (73% *e.e.*).

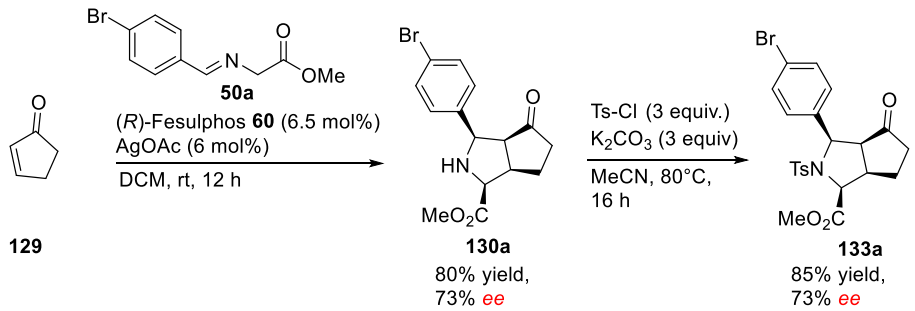


**Figure 54**: Synthesis of N-protected pyrrolidine **133a**.

Tosyl-protected product **131** was subjected to reaction with various aryl-hydrazine chlorides **134** in a Fischer-indole synthesis for the generation of different functionalized indoles **131** (Figure 55). Optimization revealed that employing melting **L-(+) tartaric acid** (TA)/**dimethyl urea** (DMU) (30:70) mixture afforded the best result in terms of reaction rate and yield according to a protocol of König and co-workers.[107] The low melting mixture TA/DMU serves as solvent and as catalyst.

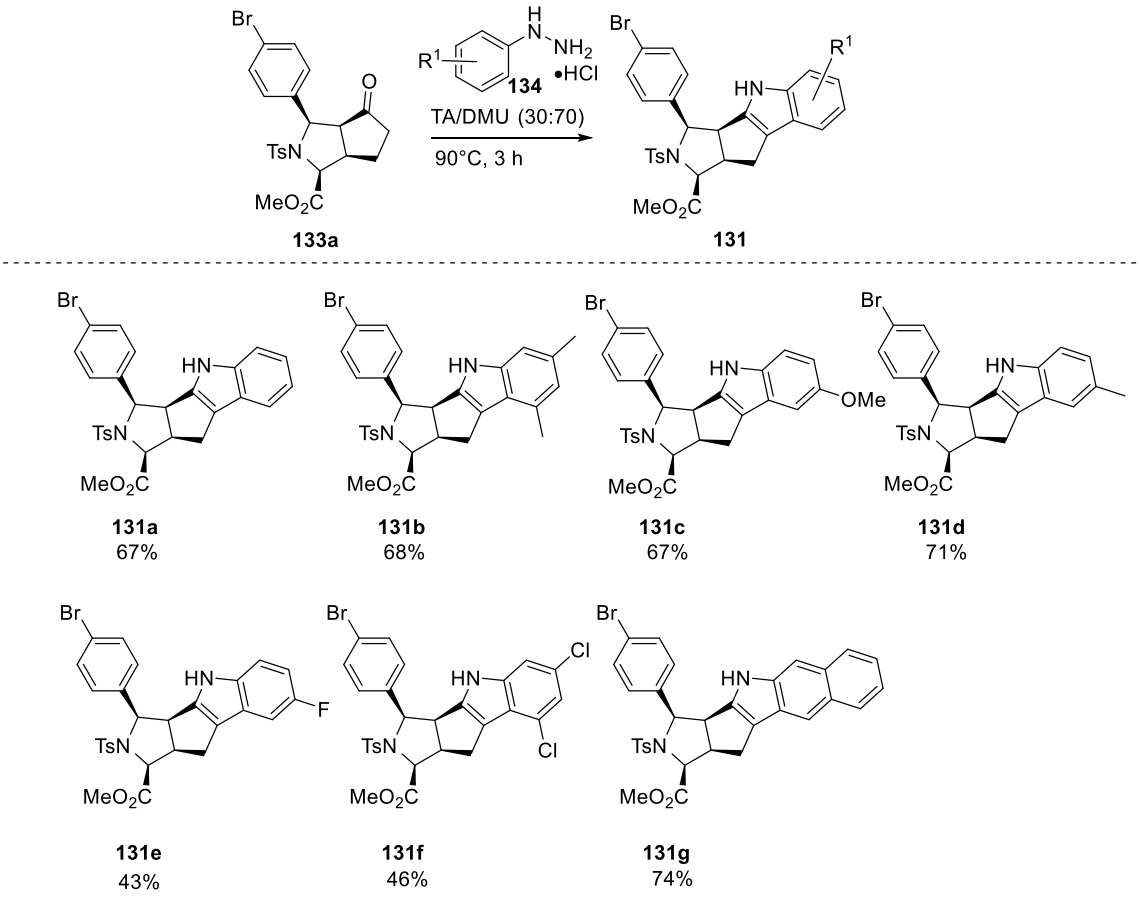


**Figure 55**: Scope of the Fischer-Indole synthesis in low melting mixture.

The yields for the indole formation in the applied low melting mixture range from 43-74%. Electron neutral and electron-donating substituents on the aromatic moiety of the aryl-hydrazine afforded higher yield in the corresponding Fischer indole-synthesis wherein electron withdrawing substituents such as fluorine or chlorine resulted in lower yields of the respective indole products (**131e** and **131f**). The lower yields in case of electron withdrawing substituents on the aryl-hydrazines is related to the reaction mechanism, as electron withdrawing groups hinder the [3,3]-sigmatropic shift for the ring closure.[108]

Indole products **131** were subjected to a dearomatization process to generate the pyrroloindoline scaffold from the planar aromatic indole. A formal [3+2]-cycloaddition was employed with α-haloamide **127** in presence of $K_2CO_3$ in HFIP/DCM mixture. An aza-oxyallyl cation[109] is generated *in situ* which undergoes a cycloaddition with the indole ring of **131**. Upon cycloaddition, two more stereocenters are created, which are quaternary stereocenters. The corresponding dearomatization products **132** are obtained with good yields and excellent diastereoselectivity (dr >20:1) (Figure 56).

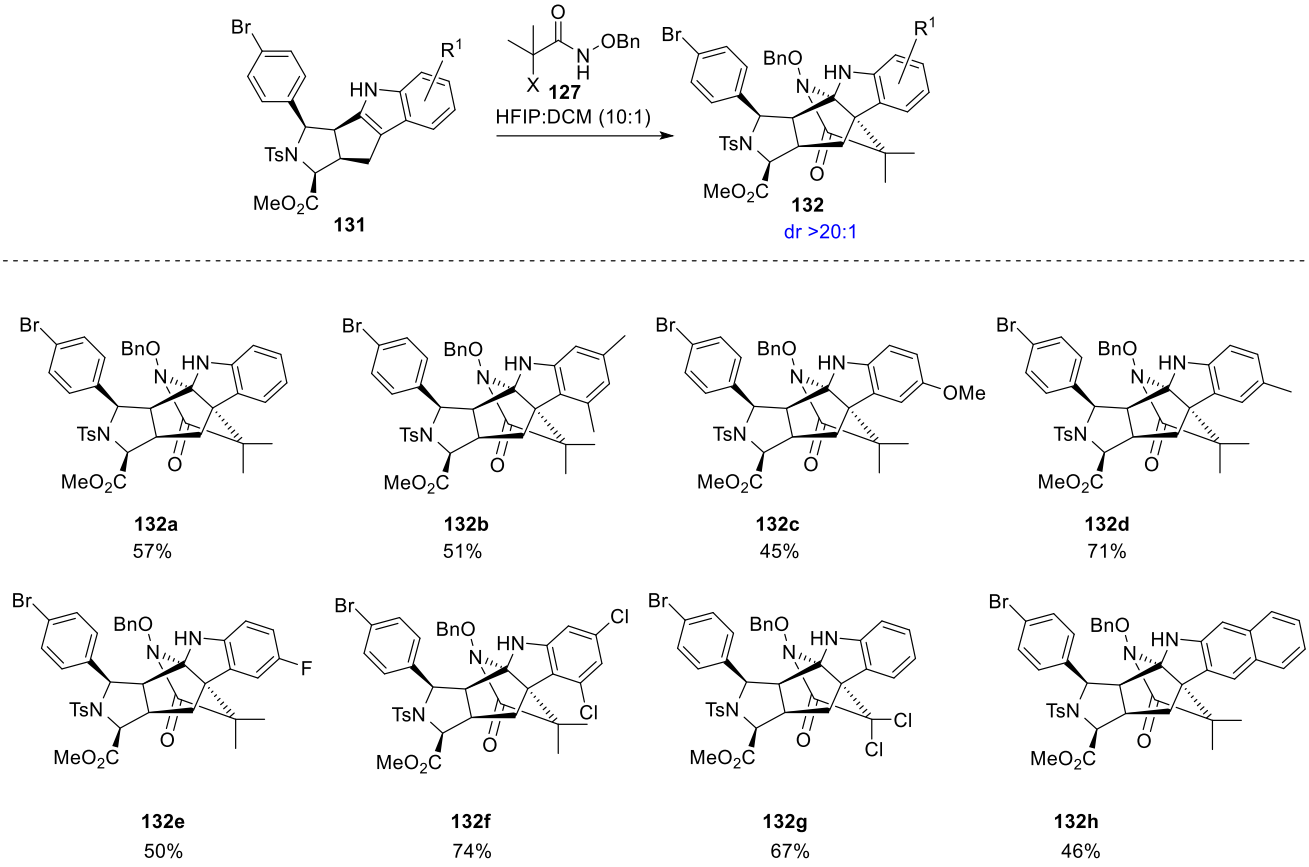


**Figure 56**: Reaction scope of the dearomatization for the formation of pyrroloindoline scaffold.

The diastereoselectivity of the dearomatization process is substrate controlled. The stereogenic centers are already set in the asymmetric 1,3-dipolar cycloaddition to generate the pyrrolidine **130a**. The approach of the *in situ* generated aza-oxyallyl cation **127'** proceeds selectively from the *si*-face as the *re*-face is sterically more hindered due to the substituents of the pyrrolidine ring. To avoid unfavourable interactions, the cycloaddition takes place from the opposite side with respect to the substituent of the pyrrolidine (Figure 57).

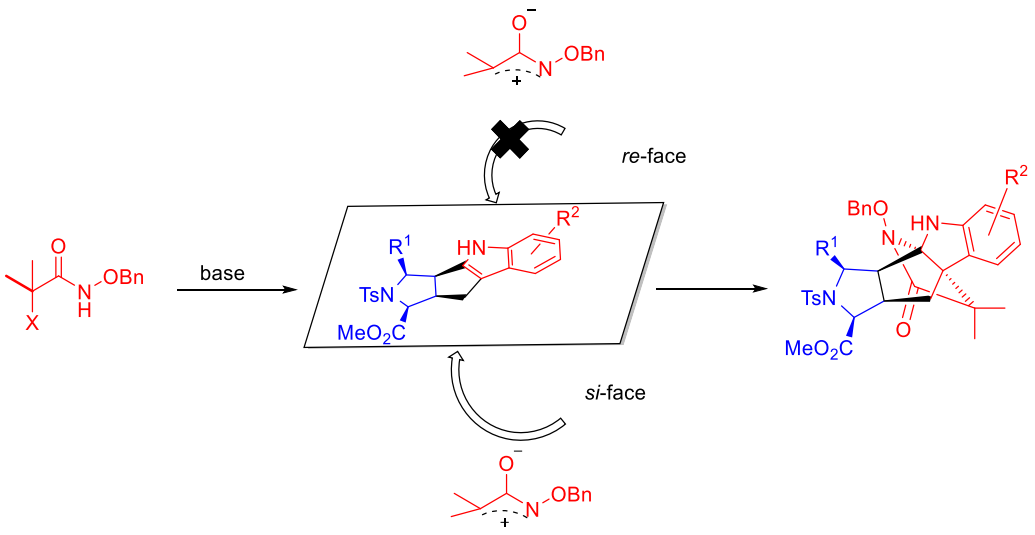


**Figure 57**: Proposed intermediates and transition states for the diastereoselctivity.

## 4.4 Conclusion

In summary, the combination of NP scaffolds such as pyrroloindoline and pyrrolidine was conducted resulting in complex polycyclic compounds. A substrate-controlled diastereoselctive dearomatization process generated two additional quaternary centers through a formal [3+2]-cycloaddition. The stereochemistry of the reaction was set in the beginning of the synthesis and enabled a stereo-controlled dearomatization. A pentacyclic fused pseudo NP compound collection was generated with up to 6 stereocenters and with high functional group tolerance. The successful synthesized compounds are currently undergoing biological evaluation at COMAS.

# 5 Summary of the Thesis

Pseudo NPs contain natural product (NP) derived fragments in novel, unrelated and structurally complex arrangements, which are not accessible by current biosynthetic pathways. Their structural features explore novel chemical and biological space which are unexploited and not covered by NPs. Towards the goal of synthesizing a novel pseudo NP compound library, the combination of different NP scaffolds in an enantioselective manner was intended.

The combination of two pyrrolidine fragments in an unprecedented fashion and different connection types was carried out by sequence of two subsequent asymmetric double 1,3-dipolar cycloaddition reactions of azomethine ylides to cyclopentenones containing an endocyclic and exocyclic double bond. Highly complex tricyclic compounds with up to eight stereocenters with excellent enantioselectivity and diastereoselectivity were obtained (Figure 58a). Owing differences in the reactivity of the endocyclic and exocyclic double bond of the cyclepentones, two different azomethine ylides were applied as well in a one pot process yielding structurally complex molecular entities albeit with lower enantioselectivity. Detailed mechanistical studies on the enantioselective course of the double 1,3-dipolar cycloaddition revealed that a dynamic covalent process proceeds during the reaction in thermodynamically controlled manner. Kinetically and thermodynamically favored stereoisomers were identified and conditions for a stereodivergent synthesis of the stereoisomers were established and carried out. Time-dependent analysis of the reaction course also enabled an enantiodivergent synthesis. Biological evaluation of the synthesized pseudo NP compound library showed activity in autophagy inhibition.

In the second part of the dissertation, the concept of the pseudo NP was applied to design highly complex polycyclic compounds through the combination of synthetic methods of the asymmetric 1,3-dipolar cycloadditions and diastereoselective dearomatizations of indoles (Figure 58b). Highly important NP fragments such as pyrrolidine and pyrrolindoline were combined in a fused fashion resulting in a structurally complex polycyclic compounds. The enantioselectivity was set during the asymmetric 1,3-dipolar cycloaddition in the first step of the synthetic sequence followed by a diastereoselective dearomatization of the indole moiety by a formal [3+2] cycloaddition to afford pyrroloindolines.

In both parts of the thesis, a rich library of a pyrrolidine-containing pseudo NPs was generated.

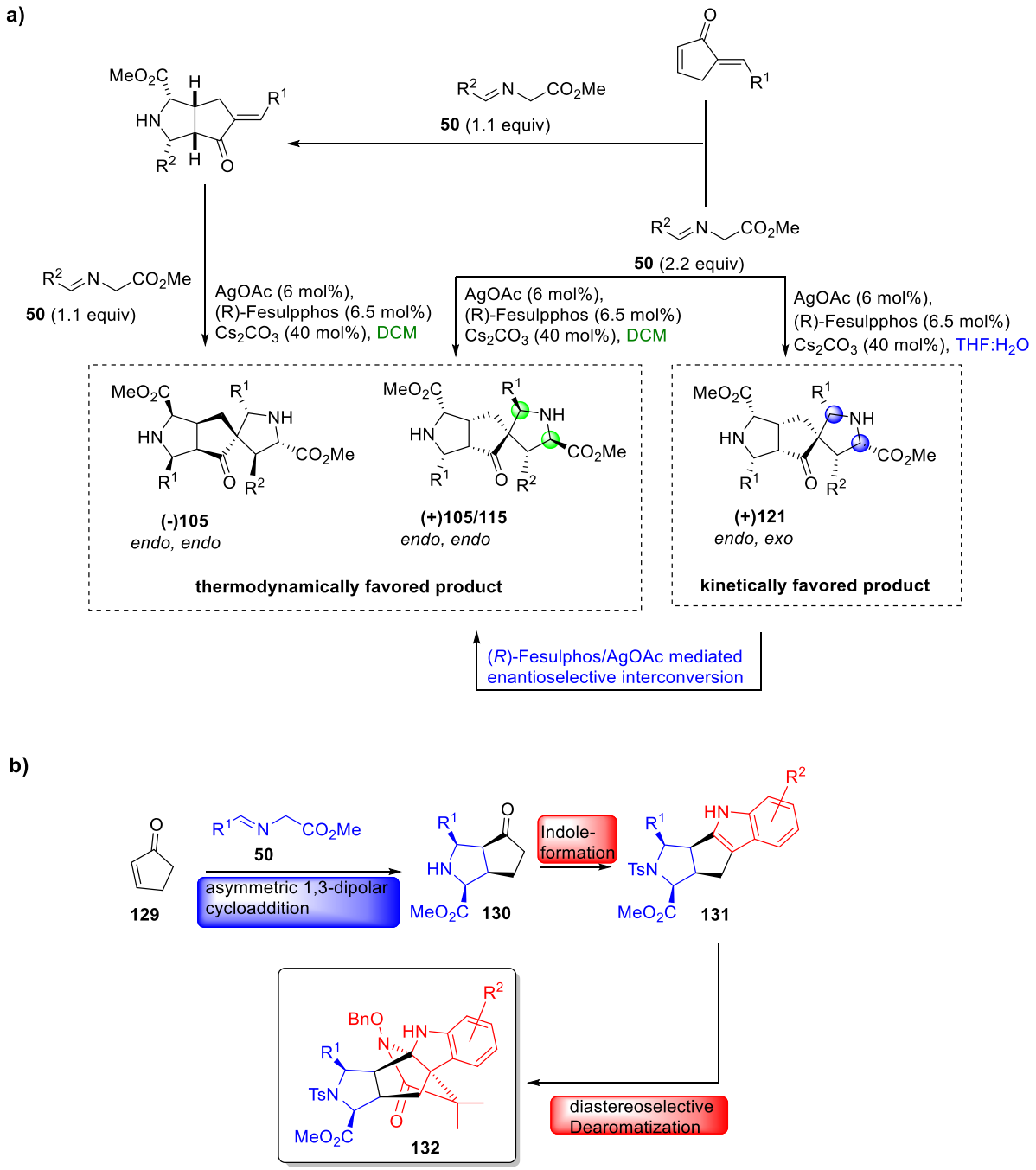


**Figure 58**: Summary of the Thesis.

# 6 Experimental section

## 6.1 General Information

Unless otherwise noted, all commercially available compounds were used as provided without further purifications. Dry solvents (THF, toluene, DCM) were used as commercially available. Solvents for chromatography were technical grade. Oxygen and/or moisture sensitive solutions were transferred using syringes and cannulas.

Analytical thin-layer chromatography (TLC) was performed on *Merck silica gel aluminium plates* with F-254 indicator. Compounds were visualized by irradiation with UV light or potassium permanganate staining. Column chromatography was performed using *silica gel Merck 60* (particle size 0.040-0.063 mm). Solvent mixtures are understood as volume/volume.

$^{1}$H-NMR and $^{13}$C-NMR were recorded on a *Bruker DRX400* (400 MHz), *Bruker DRX500* (500 MHz) and *INOVA500* (500 MHz) using $CDCl_3$ or $CD_2Cl_2$ as solvent. Data are reported in the following order: chemical shift (δ) values are reported in ppm with the solvent resonance as internal standard ($CDCl_3$: δ = 7.26 ppm for 1H, δ = 77.16 ppm for $^{13}$C; $CD_2Cl_2$: δ = 5.32 ppm for $^{1}$H, δ = 53.8 ppm for $^{13}$C); multiplicities are indicated br s (broadened singlet), s (singlet), d (doublet), t (triplet), q (quartet) m (multiplet); coupling constants (*J*) are given in Hertz (Hz).

Low resolution mass spectra (MS-ESI) were collected using a *Waters Corp. LC-MS system* (column: LC revers phase CC Nucleodur C4 Gravity, 5 µm from Macherey-Nagel) equipped with an *UV-Waters 2487 Dual Absorbance Detector* and *Waters Micromass ZQ 2000 ESCI+ Multi-Mode-Ionisation MS-Detector*.

High resolution mass spectra were recorded on a *LTQ Orbitrap* mass spectrometer coupled to an *Acceka HPLC*-System (HPLC column: *Hypersyl GOLD,* 50 mm x 1 mm, particle size 1.9 µm, ionization method: electron spray ionization). Fourier transform infrared spectroscopy (FT-IR) spectra were obtained with a *Bruker Tensor 27* spectrometer (ATR, neat) and are reported in terms of frequency of absorption ($cm^{-1}$). Optical rotations were measured in a *Schmidt + Haensch Polartronic HH8* polarimeter.

Fourier transform infrared spectroscopy (FT-IR) spectra were obtained with a *Bruker Tensor 27* spectrometer (ATR, neat) and are reported in terms of frequency of absorption ($cm^{-1}$).

The enantiomeric excesses were determined by HPCL analysis using a chiral stationary phase column (column: CHIRALCEL IC, eluent: (*iso*-hexane/ *iso*-propanol). The chiral HPLC methods were calibrated with the corresponding racemic mixtures. The ratio of diastereomers

was determined by $^{1}$H-NMR analysis via integration of characteristic signals of methyl esters. Chemical yields refer to pure isolated substances. Yields and enantiomeric excesses, diastereoselectivity are given in the tables. The chemicals and solvents were purchased from the companies Sigma-Aldrich, Acros Organic, ABCR and Alfa Aesar. (*Rp*)-2-(*tert*-Butylthio)-1-(diphenyl-phosphino)ferrocene (purity: 98%), were purchased from Sigma-Aldrich.

Optical rotations were measured in a *Schmidt + Haensch Polartronic HH8* polarimeter equipped with a sodium lamp source (589 nm), and were 73 reported as follows: $[\alpha]_D^{T\,°C}$ (c = g/100 mL, solvent).

## 6.2 Synthesis of iminoesters

General Procedure A

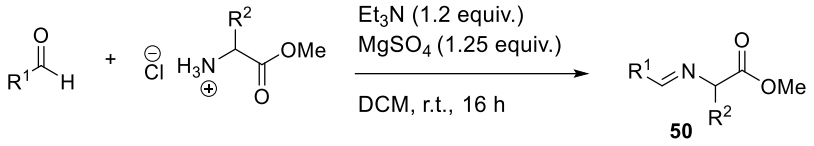


To a suspension of amino acid ester hydrochloride (1.2 equiv., 12 mmol) and $MgSO_4$ (1.25 equiv., 12.5 mmol) in DCM (15 mL) was added $Et_3N$ (1.2 equiv., 12 mmol). The mixture was stirred at ambient temperature for 1h. Then the corresponding aldehyde (1 equiv., 10 mmol) was added and the mixture was allowed to stir at ambient temperature overnight. The precipitate was removed by filtration and the filtrate was washed with water (15 mL). The aqueous phase was extracted two times with DCM (10 mL) and the combined organic layer was washed once with brine (15 mL), dried over $MgSO_4$ and concentrated. The iminoesters were used for 1,3-dipolar cycloadditions and NMR studies without further purification.

**Methyl (*E*)-2-((4-bromobenzylidene)amino)acetate (50a)[110]**

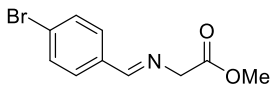


**50a**

colorless crystalline solid, 93% yield, **$^1$H NMR** (500 MHz, $CD_2Cl_2$) δ 8.24 (t, *J* = 1.4 Hz, 1H), 7.65 (d, *J* = 8.5 Hz, 2H), 7.58 (d, *J* = 8.5 Hz, 2H), 4.37 (d, *J* = 1.4 Hz, 2H), 3.74 (s, 3H). **$^{13}$C NMR** (126 MHz, $CD_2Cl_2$) δ 170.82, 164.41, 135.24, 132.42, 130.30, 126.04, 62.21, 52.49.

**Methyl (*E*)-2-((4-chlorobenzylidene)amino)acetate (50b)[110]**

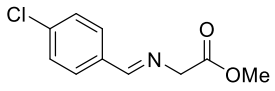


**50b**

colorless crystalline solid, 90% yield, **$^1$H NMR** (500 MHz, $CD_2Cl_2$) δ 8.25 (t, *J* = 1.4 Hz, 1H), 7.72 (d, *J* = 8.5 Hz, 2H), 7.42 (d, *J* = 8.5 Hz, 2H), 4.38 (d, *J* = 1.4 Hz, 2H), 3.74 (s, 3H). **$^{13}$C NMR** (126 MHz, $CD_2Cl_2$) δ 170.87, 164.29, 137.55, 134.85, 130.11, 129.45, 62.21, 52.49.

**Methyl (*E*)-2-((4-fluorobenzylidene)amino)acetate (50c)[111]**

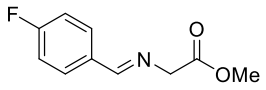


**50c**

colorless crystalline solid, 87% yield, **$^1$H NMR** (700 MHz, $CD_2Cl_2$) δ 8.25 (t, *J* = 1.5 Hz, 1H), 7.78 (d, *J* = 8.7, Hz, 2H), 7.13 (d, *J* = 8.7 Hz, 2H), 4.37 (d, *J* = 1.5 Hz, 2H), 3.74 (s, 3H). **$^{13}$C NMR** (176 MHz, $CD_2Cl_2$) δ 170.99, 165.87 (d, *J* = 250.7 Hz), 164.44, 164.18, 132.78 (d, *J* = 3.0 Hz), 130.92 (d, *J* = 8.8 Hz), 116.19 (d, *J* = 22.0 Hz), 62.21, 52.46.

**Methyl (*E*)-2-((3-bromobenzylidene)amino)acetate (50d)**

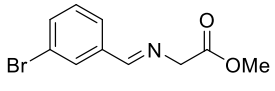


**50d**

colorless crystalline solid, 82% yield, **$^1$H NMR** (700 MHz, $CD_2Cl_2$) δ 8.23 (t, *J* = 1.4 Hz ,1H), 7.96 (s, 1H), 7.68-7.63 (m, 1H), 7.61 – 7.59 (m, 1H), 7.33 (t, *J* = 7.8 Hz, 1H), 4.39 (d, *J* = 1.4 Hz, 2H), 3.75 (s, 3H). **$^{13}$C NMR** (176 MHz, $CD_2Cl_2$) δ 170.77, 164.06, 138.36, 134.55, 131.38, 130.83, 127.80, 123.37, 62.20, 52.52.

**Methyl (*E*)-2-((2-bromobenzylidene)amino)acetate (50e)**

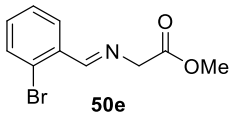


**50e**

colorless crystalline solid, 80% yield, **$^{1}$H NM**R (700 MHz, $CD_2Cl_2$) δ 8.66 (d, *J* = 1.5 Hz, 1H), 8.05 (dd, *J* = 8.0, 1.8 Hz, 1H), 7.60 (dd, *J* = 8.0, 1.8 Hz, 1H), 7.40 – 7.37 (m, 1H), 7.32-7.28 (m, 1H), 4.44 (d, *J* = 1.5 Hz, 2H), 3.75 (s, 3H). **$^{13}$C NMR** (176 MHz, $CD_2Cl_2$) δ 170.79, 164.54, 134.70, 133.66, 132.93, 129.36, 128.28, 125.83, 62.29, 52.51.

**Methyl (*E*)-2-((4-methylbenzylidene)amino)acetate (50f)[112]**

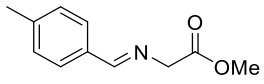


**50f**

yellow crystalline solid, 86% yield, **$^{1}$H NMR** (700 MHz, $CD_2Cl_2$) δ 8.24 (t, *J* = 1.4 Hz, 1H), 7.65 (d, *J* = 8.2 Hz, 2H), 7.24 (d, *J* = 8.2 Hz, 2H), 4.36 (d, *J* = 1.4 Hz, 2H), 3.74 (s, 3H), 2.39 (s, 3H). **$^{13}$C NMR** (176 MHz, $CD_2Cl_2$) δ 171.18, 165.52, 142.30, 133.76, 129.92, 128.83, 62.39, 52.42, 21.81.

**Methyl (*E*)-2-((4-methoxybenzylidene)amino)acetate (50g)[112]**

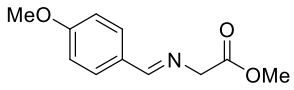


**50g**

yellow crystalline solid, 78% yield, **$^{1}$H NMR** (700 MHz, $CD_2Cl_2$) δ 8.24 (d, *J* = 1.4 Hz, 1H), 7.74 (d, *J* = 8.8 Hz, 2H), 6.98 (d, *J* = 8.8 Hz, 2H), 4.38 (d, *J* = 1.4 Hz, 2H), 3.88 (s, 3H), 3.78 (s, 3H). **$^{13}$C NMR** (176 MHz, $CD_2Cl_2$) δ 171.30, 164.85, 162.71, 130.48, 129.27, 114.56, 62.33, 55.93, 52.39.

**Methyl (*E*)-2-((4-nitrobenzylidene)amino)acetate (50h)**

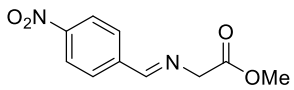


**50h**

red oild, 77% yield, **$^{1}$H NMR** (700 MHz, $CD_2Cl_2$) δ 8.39 (t, *J* = 1.4 Hz, 1H), 8.27 (d, *J* = 8.8 Hz, 2H), 7.96 (d, *J* = 8.8 Hz, 2H), 4.46 (d, *J* = 1.4 Hz, 2H), 3.76 (s, 3H). **$^{13}$C NMR** (176 MHz, $CD_2Cl_2$) δ 170.46, 163.56, 141.70, 129.66, 124.41, 62.27, 52.60.

**Methyl (*E*)-2-((naphthalen-2-ylmethylene)amino)acetate (50i)[112]**

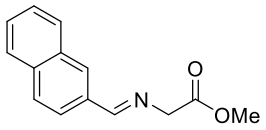


**50i**

colorless crystalline solid, 75% yield, **$^1$H NMR** (700 MHz, $CD_2Cl_2$) δ 8.44 (t, *J* = 1.4 Hz, 1H), 8.10 – 8.09 (m, 1H), 8.02 (dd, *J* = 8.5, 1.7 Hz, 1H), 7.94 – 7.92 (m, 1H), 7.89-7.84 (m, 2H), 7.59 – 7.53 (m, 2H), 4.45 (d, *J* = 1.4 Hz, 2H), 3.77 (s, 3H). **$^{13}$C NMR** (176 MHz, $CD_2Cl_2$) δ 171.10, 165.66, 135.50, 134.06, 133.61, 131.11, 129.22, 129.07, 128.39, 128.00, 127.15, 124.15, 62.45, 52.48.

**Methyl (*E*)-2-((furan-2-ylmethylene)amino)acetate (50j)[111]**

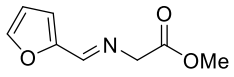


**50j**

brown oil, 80% yield, **$^1$H NMR** (400 MHz, $CD_2Cl_2$): δ 8.07 (t, *J* = 1.3 Hz, 1H), 7.56 (d, *J* = 5.8 Hz, 1H), 6.85 (d, *J* = 5.5 Hz, 1H), 6.52 (dd, *J* = 5.8, 5.5 Hz, 1H), 4.33 (d, *J* = 1.3 Hz, 2H), 3.74 (s, 3H). **$^{13}$C NMR** (101 MHz, (CD2Cl2): δ 170.87, 153.79, 151.98, 145.83, 115.54, 112.31, 62.23, 52.48.

**Methyl (*E*)-2-((furan-3-ylmethylene)amino)acetate (50k)**

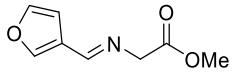


**50k**

brown oil, 76% yield, **$^1$H NMR** (700 MHz, $CD_2Cl_2$) δ 8.21 (s, *J* = 1.4 Hz, 1H), 7.78 (d, *J* = 4.1 Hz, 1H), 7.49 – 7.44 (m, 1H), 6.84 – 6.79 (m, 1H), 4.30 (d, *J* = 1.4 Hz, 2H), 3.73 (s, 3H). **$^{13}$C NMR** (176 MHz, $CD_2Cl_2$) δ 171.07, 157.31, 146.58, 144.85, 125.87, 108.23, 62.42, 52.42.

## 6.3 Synthesis of cyclic enone

General procedure B

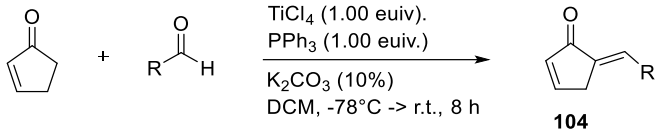


To a solution of the cyclic enone (1.0 equiv.) and triphenylphosphine (1.0 equiv.) in DCM (15 ml) was added titanium tetrachloride (1.0 equiv.) at -78 °C. After 15 min, the mixture was treated with RCHO (1.0-3.0 equiv.). The mixture was allowed to warm to room temperature over 8 h and then treated with 10% aqueous $K_2CO_3$. The organic layer was concentrated in vacuum and the residue was purified by flash chromatography on silica gel (petroleum ether/EtOAc) to give alkylidene cyclic enone **104**.

**(*E*)-5-(4-bromobenzylidene)cyclopent-2-en-1-one (104a)[87, 113]**

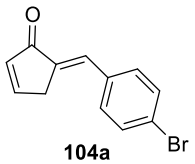


yellow amorphous solid, 90% yield, **$^1$H NMR** (400 MHz, $CD_2Cl_2$) δ 7.66-7.70 (m, 1H), 7.55 (d, *J* = 8.5 Hz, 2H), 7.43 (d, *J* = 8.5 Hz, 2H), 7.33 (s, 1H), 6.48 (m, 1H), 3.54 (d, *J* = 6.5 Hz, 2H). **$^{13}$C NMR** (126 MHz, $CD_2Cl_2$) δ 196.83, 157.39, 135.12, 134.26, 133.28, 132.05, 131.78, 129.98, 123.61, 34.21.

**(*E*)-5-(3-bromobenzylidene)cyclopent-2-en-1-one (104b)**

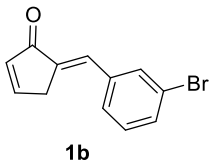


yellow amorphous solid, 72% yield, **$^1$H NMR** (500 MHz, $CD_2Cl_2$) δ 7.76 – 7.70 (m, 2H), 7.58 – 7.48 (m, 2H), 7.33 (d, *J* = 7.9 Hz, 1H), 7.26 (d, *J* = 7.9 Hz, 1H), 6.45 – 6.42 (m, 1H), 3.56 (d, *J* = 6.3 Hz, 2H). **$^{13}$C NMR** (126 MHz, $CD_2Cl_2$) δ 197.23, 158.10, 137.96, 135.62, 134.45, 133.32, 132.71, 130.95, 130.14, 129.51, 123.34, 34.68.

**(*E*)-5-(2-bromobenzylidene)cyclopent-2-en-1-one (104c)**

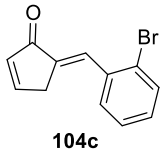


**104c**

brown amorphous solid, 56% yield, **$^{1}$H NMR** (500 MHz, $CD_2Cl_2$) δ 7.69 – 7.58 (m, 3H), 7.33 – 7.29 (m, 3H), 6.44-6.40 (m, 1H), 3.49 (d, *J* = 6.5 Hz, 2H). **$^{13}$C NMR** (126 MHz, $CD_2Cl_2$) δ 205.56, 158.46, 150.79, 138.25, 135.75, 133.92, 130.95, 130.42, 130.31, 128.10, 127.96, 34.09.

**(*E*)-5-(4-methylbenzylidene)cyclopent-2-en-1-one (104d)[87, 113]**

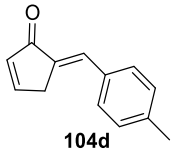


**104d**

white amorphous solid, 79% yield, **$^{1}$H NMR** (500 MHz, $CD_2Cl_2$) δ 7.68 (s, 1H), 7.51 (d, *J* = 8.2 Hz, 2H), 7.31 (d, *J* = 6.2 Hz, 1H), 7.25 (d, *J* = 8.2 Hz, 2H), 6.42-6.38 (m, 1H), 3.56 (d, *J* = 6.2 Hz, 2H), 2.38 (s, 3H). **$^{13}$C NMR** (126 MHz, $CD_2Cl_2$) δ 197.65, 157.67, 140.60, 134.13, 132.97, 132.27, 131.86, 130.95, 130.14, 34.94, 21.71.

**(*E*)-5-(4-chlorobenzylidene)cyclopent-2-en-1-one (104e)[113]**

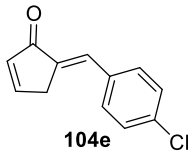


**104e**

yellow amorphous solid, 84% yield, **$^{1}$H NMR** (500 MHz, $CD_2Cl_2$) δ 7.73 – 7.67 (m, 1H), 7.54 (d, *J* = 8.6 Hz, 2H), 7.41 (d, *J* = 8.6 Hz, 2H), 7.29 (s, 1H), 6.42-6.39 (m, 1H), 3.54 (d, *J* = 6.3 Hz, 2H). **$^{13}$C NMR** (126 MHz, $CD_2Cl_2$) δ 197.34, 157.89, 135.65, 134.39, 133.66, 132.10, 130.43, 129.59, 34.73.

**(*E*)-5-(4-methoxybenzylidene)cyclopent-2-en-1-one (104f)**

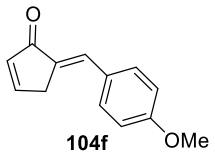


**104f**

yellow amorphous solid, 75% yield, **$^{1}$H NMR** (500 MHz, $CD_2Cl_2$) δ 7.83(d, *J* = 8.4 Hz, 1H), 7.67 (s, 1H), 7.57 (d, *J* = 8.3 Hz, 2H), 6.96 (d, *J* = 8.3 Hz, 2H), 6.41 – 6.38 (m, 1H), 3.84 (s,

3H), 3.55 (d, *J* = 6.5 Hz, 2H). **$^{13}$C NMR** (126 MHz, $CD_2Cl_2$) δ 197.64, 157.34, 135.73, 132.69, 132.31, 131.61, 128.42, 114.86, 114.80, 55.91, 34.93.

**(*E*)-5-(4-nitrobenzylidene)cyclopent-2-en-1-one (104g)**

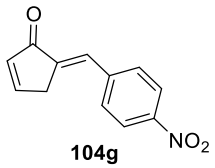


104g

brown amorphous solid, 53% yield, **$^{1}$H NMR** (500 MHz, $CD_2Cl_2$) δ 8.26 (d, *J* = 8.8 Hz, 2H), 7.75 (m, 3H), 7.39 (s, 1H), 6.50 – 6.43 (m, 1H), 3.61 (d, *J* = 6.3 Hz, 2H). **$^{13}$C NMR** (126 MHz, $CD_2Cl_2$) δ 196.94, 158.44, 148.20, 142.18, 136.69, 135.64, 131.33, 129.14, 124.47, 34.66.

**(*E*)-5-(naphthalen-2-ylmethylene)cyclopent-2-en-1-one (104h)**

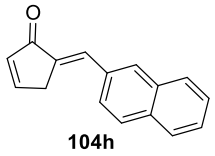


104h

white amorphous solid, 66% yield, **$^{1}$H NMR** (500 MHz, $CD_2Cl_2$) δ 8.00 – 7.85 (m, 4H), 7.77 – 7.70 (m, 2H), 7.63 – 7.47 (m, 3H), 6.45-6.40 (m, 1H), 3.69 (d, *J* = 6.2 Hz, 2H). **$^{13}$C NMR** (126 MHz, $CD_2Cl_2$) δ 197.54, 157.91, 135.72, 134.28, 133.87, 133.44, 133.39, 131.95, 131.77, 129.03, 128.99, 128.16, 127.79, 127.20, 54.22, 35.02.

**(*E*)-5-(2,2-dimethylpropylidene)cyclopent-2-en-1-one (104i)**

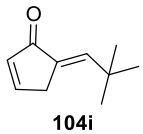


104i

colorless oil, 48% yield, **$^{1}$H NMR** (500 MHz, $CD_2Cl_2$) δ 7.69 (s, 1H), 6.55 (d, *J* = 6.0 Hz, 1H), 6.33-6.31 (m, 1H), 3.37 (d, *J* = 6.2 Hz, 2H), 1.18 (s, 9H). **$^{13}$C NMR** (126 MHz, $CD_2Cl_2$) δ 198.19, 158.46, 145.76, 135.40, 130.67, 83.02, 33.46, 29.93.

**(*E*)-5-(4-bromobenzylidene)-3-methylcyclopent-2-en-1-one (104j)**

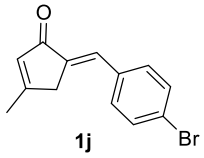


**1j**

white amorphous solid, 57% yield, **$^{1}$H NMR** (500 MHz, $CD_2Cl_2$) δ 7.56 (d, *J* = 8.5 Hz, 2H), 7.45 (d, *J* = 8.5 Hz, 2H), 7.19 (s, 1H), 6.15 (s, 1H), 3.43 (s, 2H), 2.22 (s, 3H). **$^{13}$C NMR** (126 MHz, $CD_2Cl_2$) δ 197.22, 172.37, 135.60, 135.02, 132.51, 132.17, 131.77, 128.65, 123.77, 38.85, 19.45.

## 6.4 Synthesis of double cycloaddition *endo, endo*-products

General Procedure C

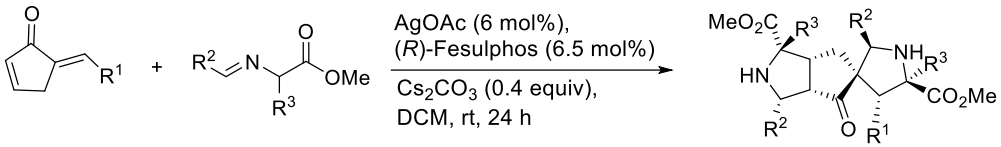


**104** **50** **105**

(*Rp*)-2-(*tert*-Butylthio)-1-(diphenylphosphino)ferrocene (6.5 mol%, 7.8 μmol) and silver acetate (6 mol%, 7.2 μmol) were dissolved in DCM (2mL) and stirred at ambient temperature for 15 min. To the resulting solution iminoester **50** (2.2 equiv., 0.26 mmol), $Cs_2CO_3$ (40 mol%, 48 μmol) and enone **104** (1.0 equiv., 0.12 mmol) were added and the mixture was allowed to stir at ambient temperature for at least 24 h (until all *endo, exo* diastereomer is converted to *endo, endo* isomer). The crude mixture was directly charged onto silica gel and the product was isolated using *n*-pentane / acetone as eluent.

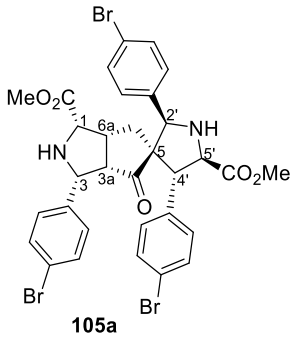


**105a**

**Dimethyl (1*S*,2′*R*,3*R*,3*aS*,4'*R*,5*R*,5′*R*,6*aR*)-2',3,4'-tris(4-bromophenyl)-4-oxohexahydro-1*H*-spiro[cyclopenta[*c*]pyrrole-5,3'-pyrrolidine]-1,5'-dicarboxylate (105a)**

yellow amorphous solid, 81% yield, **$^{1}$H NMR** (700 MHz, $CD_2Cl_2$) δ 7.53 (d, *J* = 7.5 Hz, 2H), 7.47 (d, *J* = 7.5 Hz, 2H), 7.42 (d, *J* = 8.0 Hz, 2H), 7.15 (d, *J* = 8.0 Hz, 2H), 7.05 (d, *J* = 7.9 Hz, 2H), 6.97 (d, *J* = 7.9 Hz, 2H), 4.25 (s, 1H), 4.14 (d, *J* = 10.7 Hz, 1H), 3.97 (d, *J* = 7.1 Hz, 1H), 3.75 (d, *J* = 7.6 Hz, 1H), 3.66 (s, 3H), 3.60 (s, 3H), 3.43 (d, *J* = 7.1 Hz, 1H), 2.63 – 2.59 (m, 1H), 2.03-1.99 (m, 1H), 1.75 (dd, *J* = 13.6, 7.6 Hz, 1H), 1.59 (dd, *J* = 13.6, 7.6 Hz, 1H); **$^{13}$C NMR** (176 MHz, $CD_2Cl_2$) δ 216.65, 173.27, 171.55, 138.97, 138.88, 137.94, 132.34, 132.20, 131.47, 130.20, 130.05, 122.86, 121.72, 121.52, 74.72, 68.28, 66.97, 63.99, 63.12, 55.87, 55.32, 52.66, 52.26, 40.28, 34.47.

**HRMS**: calcd. for $[M+H]^+$ $C_{32}H_{29}{}^{79}Br_3N_2O_5$ = 758.97127, found: 758.96994; calcd. for $[M+H]^+$ $C_{32}H_{29}{}^{79}Br^{81}Br_2N_2O_5$ = 762.96703, found: 762.96584; calcd. for $[M+H]^+$ $C_{32}H_{29}{}^{79}Br_2{}^{81}BrN_2O_5$ = 760.96902, found: 760.96789; calcd. for $[M+H]^+$ $C_{32}H_{29}{}^{81}Br_3N_2O_5$ = 764.96554, found: 764.96380.

**HPLC** conditions: CHIRALPAK IC column, *iso*-propanol/ *iso*-hexane = 30/70, flow rate = 0.5 mL min$^{-1}$, minor enantiomer: $t_R$ = 19.79 min; major enantiomer: $t_R$ = 26.32 min; (99% e.e.); CHIRALPAK IA column, *iso*-propanol/ *iso*-hexane = 15/85, flow rate = 0.5 mL min$^{-1}$, minor enantiomer: $t_R$ = 86.05 min; major enantiomer: $t_R$ = 51.16 min; (99% e.e.).

**$[\alpha]^{20}_{D}$** = + 41.1° (c = 0.19, $CHCl_3$).

**FT-IR:** $\tilde{\nu}$ 3431, 2884, 2765, 2521, 2315, 1644, 1615, 1461, 1092, 1156, 1075 cm$^{-1}$.

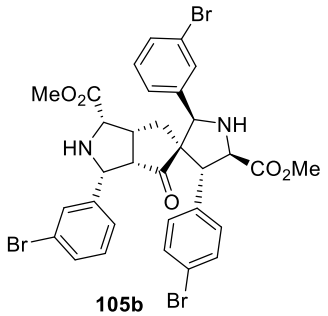


**105b**

**Dimethyl*(1S,2'R,3R,3aS,4'R,5R,5'R,6aR)*-2',3-bis(3-bromophenyl)-4'-(4-bromophenyl)-4-oxohexahydro-1*H*-spiro[cyclopenta[*c*]pyrrole-5,3'-pyrrolidine]-1,5'-dicarboxylate (105b)**

white amorphous solid, 72% yield, **$^{1}$H NMR** (400 MHz, ($CD_2Cl_2$): δ 7.55 (d, *J* = 8.4 Hz, 2H), 7.46 (d, *J* = 8.4 Hz, 1H), 7.43-7.42 (m, 1H), 7.41 – 7.40 (m, 1H), 7.32 (d, *J* = 7.5 Hz, 1H), 7.24 – 7.17 (m, 3H), 7.11 (d, *J* = 7.5 Hz, 2H), 7.01 (d, *J* = 7.5 Hz, 1H), 4.23 (s, 1H), 4.14 (d, *J* = 10.7 Hz, 1H), 3.99 (d, *J* = 7.1 Hz, 1H), 3.75 (d, *J* = 8.9 Hz, 1H), 3.66 (s, 3H), 3.60 (s, 3H), 3.48 (d, *J* = 7.1 Hz, 1H), 2.63 – 2.58 (m, 1H), 2.05 (dd, *J* = 13.7, 8.9 Hz, 1H), 1.59 (dd, *J* = 13.7, 10.6 Hz, 1H), 1.28 – 1.24 (m, 1H); **$^{13}$C NMR** (101 MHz, ($CD_2Cl_2$): δ 216.59, 173.20, 171.45, 142.31, 141.24, 139.12, 132.30, 132.12, 131.49, 131.45, 131.04, 130.92, 130.87, 130.10, 127.47, 127.15, 123.11, 122.61, 121.69, 74.78, 68.28, 66.99, 64.04, 63.17, 55.97, 55.38, 52.61, 52.26, 40.16, 34.53.

**HRMS**: calcd. for $[M+H]^+$ $C_{32}H_{29}{}^{79}Br_3N_2O_5$ = 758.97121, found: 758.96994; calcd. for $[M+H]^+$ $C_{32}H_{29}{}^{79}Br^{81}Br_2N_2O_5$ = 762.96571, found: 762.96584; calcd. for $[M+H]^+$ $C_{32}H_{29}{}^{79}Br_2{}^{81}BrN_2O_5$ = 760.96842, found: 760.96789; calcd. for $[M+H]^+$ $C_{32}H_{29}{}^{81}Br_3N_2O_5$ = 764.96422, found: 764.96380.

**HPLC** conditions: CHIRALPAK IC column, *iso*-propanol/ *iso*-hexane = 30/70, flow rate = 0.5 mL $min^{-1}$, minor enantiomer: $t_R$ = 22.14 min; major enantiomer: $t_R$ = 86.39 min; (91% e.e.).

**$[\alpha]^{20}_D$** = + 136.2° (c = 0.2, $CHCl_3$).

**FT-IR:** $\tilde{\nu}$ 3457**,** 2952, 2361, 1732, 1489, 1434, 1362, 1206, 1159, 1073, 1023$cm^{-1}$.

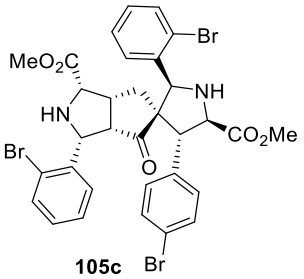


105c

**Dimethyl (1*S*,2'*S*,3*R*,3*aS*,4'*R*,5*R*,5'*R*,6*aR*)-2',3-bis(2-bromophenyl)-4'-(4-bromophenyl)-4-oxohexahydro-1*H*-spiro[cyclopenta[*c*]pyrrole-5,3'-pyrrolidine]-1,5'-dicarboxylate (105c)**

white amorphous solid, 65% yield, **$^{1}$H NMR** (400 MHz, ($CD_2Cl_2$): δ 7.61 (dd, *J* = 8.5, 1.3 Hz, 1H), 7.54 – 7.49 (m, 3H), 7.35 – 7.30 (m, 1H), 7.29 – 7.23 (m, 2H), 7.21 – 7.12 (m, 3H), 7.02 (d, *J* = 8.5 Hz, 2H), 4.95 (s, 1H), 4.38 (d, *J* = 10.6 Hz, 1H), 3.99 (d, *J* = 7.7 Hz, 1H), 3.77 (d, *J* = 5.8 Hz, 1H), 3.65 (s, 3H), 3.57 (s, 3H), 3.44 (d, *J* = 7.7 Hz, 1H), 2.87 – 2.81 (m, 1H), 2.68 (bs, 1H), 2.35 – 2.27 (m, 1H), 2.05 – 1.92 (m, 2H), 1.44 (dd, *J* = 13.4, 10.6 Hz, 1H); **$^{13}$C NMR** (101 MHz, ($CD_2Cl_2$): δ 216.17, 173.19, 171.61, 139.28, 139.10, 137.85, 133.70, 132.52, 132.13, 131.45, 130.21, 129.99, 129.14, 128.58, 128.53, 127.70, 125.02, 124.92, 121.53, 71.13, 68.87, 66.67, 63.46, 62.89, 55.22, 52.93, 52.58, 52.16, 39.76, 33.79.

**HRMS**: calcd. for $[M+H]^+$ $C_{32}H_{29}{}^{79}Br_3N_2O_5$ = 758.97121, found: 758.96994; calcd. for $[M+H]^+$ $C_{32}H_{29}{}^{79}Br^{81}Br_2N_2O_5$ = 762.96571, found: 762.96584; calcd. for $[M+H]^+$ $C_{32}H_{29}{}^{79}Br_2{}^{81}BrN_2O_5$ = 760.96842, found: 760.96789; calcd. for $[M+H]^+$ $C_{32}H_{29}{}^{81}Br_3N_2O_5$ = 764.96422, found: 764.96380.

**HPLC** conditions: CHIRALPAK IC column, *iso*-propanol/ *iso*-hexane = 40/60, flow rate = 0.5 mL $min^{-1}$, minor enantiomer: $t_R$ = 23.47 min; major enantiomer: $t_R$ = 28.45 min**;** (98% e.e.).

**[α]**$^{20}{}_D$= + 136.1° (c = 0.3, $CHCl_3$).

**FT-IR:** $\tilde{\nu}$ 3447, 2877, 2758, 2359, 1771, 1733,1653, 1206, 1181, 1129, 1119 $cm^{-1}$.

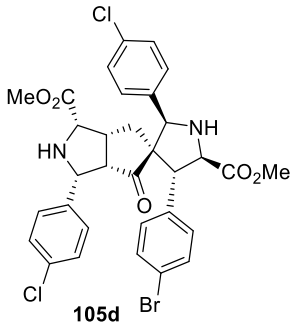


105d

**Dimethyl (1S,2'*R*,3*R*,3*aS*,4'*R*,5*R*,5'*R*,6*aR*)-4'-(4-bromophenyl)-2',3-bis(4-chlorophenyl)-4-oxohexahydro-1*H*-spiro[cyclopenta[*c*]pyrrole-5,3'-pyrrolidine]-1,5'-dicarboxylate (105d)**

white amorphous solid, 81% yield, **$^{1}$H NMR** (400 MHz, ($CD_2Cl_2$): δ 7.53 (d, *J* = 8.4 Hz, 2H), 7.31 (d, *J* = 8.5 Hz, 2H), 7.26 (d, *J* = 8.5 Hz, 2H), 7.21 (d, *J* = 8.4 Hz, 2H), 7.06 (d, *J* = 8.4 Hz, 2H), 7.02 (d, *J* = 8.4 Hz, 2H), 4.26 (s, 1H), 4.15 (d, *J* = 10.8 Hz, 1H), 3.97 (d, *J* = 7.2 Hz, 1H), 3.75 (d, *J* = 8.2 Hz, 1H), 3.66 (s, 3H), 3.59 (s, 3H), 3.44 (d, *J* = 7.2 Hz, 1H), 2.64 – 2.58 (m, 1H), 2.05 – 2.00 (m, 1H), 1.78-1.73 (m, 1H), 1.59 (dd, *J* = 13.5, 8.2 Hz, 1H); **$^{13}$C NMR** (101 MHz, ($CD_2Cl_2$): δ 216.67, 173.27, 171.55, 139.00, 138.37, 137.45, 134.66, 133.38, 132.18, 131.46, 129.88, 129.70, 129.36, 128.49, 121.70, 74.70, 68.31, 66.99, 63.95, 63.11, 55.90, 55.34, 52.60, 52.24, 40.28, 34.38.

**HRMS**: calcd. for $[M+H]^+$ $C_{32}H_{29}{}^{79}Br^{35}Cl_2N_2O_5$ = 671.07186, found: 671.07097; calcd. for $[M+H]^+$ $C_{32}H_{29}{}^{81}Br^{35}Cl_2N_2O_5$ = 673.06864, found: 673.06892; calcd. for $[M+H]^+$ $C_{32}H_{29}{}^{81}Br^{35}Cl^{37}ClN_2O_5$ = 675.06609, found: 675.06597.

**HPLC** conditions: CHIRALPAK IC column, *iso*-propanol/ *iso*-hexane = 30/70, flow rate = 0.5 mL min$^{-1}$, minor enantiomer: $t_R$ = 18.25 min; major enantiomer: $t_R$ = 25.29 min; (99% e.e.).

**$[\alpha]^{20}_{D}$** = + 131.1° (c = 0.2, $CHCl_3$).

**FT-IR:** $\tilde{\nu}$ 3651, 2525, 2159, 2029, 1976, 1788, 1589, 1425, 1236, 1123, 1023 cm$^{-1}$.

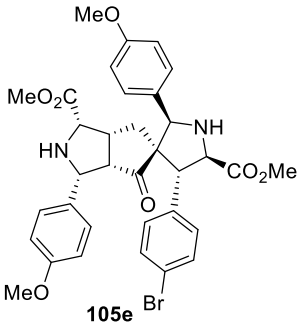


105e

**Dimethyl (1*S*,2'*R*,3*R*,3*aS*,4'*R*,5*R*,5'*R*,6*aR*)-4'-(4-bromophenyl)-2',3-bis(4-methoxyphenyl)-4-oxohexahydro-1*H*-spiro[cyclopenta[*c*]pyrrole-5,3'-pyrrolidine]-1,5'-dicarboxylate (105e)**

white amorphous solid, 60% yield, **$^{1}$H NMR** (400 MHz, $CD_2Cl_2$): δ 7.54 (d, *J* = 8.4 Hz, 2H), 7.16 (d, *J* = 8.6 Hz, 2H), 7.09 (d, *J* = 8.4 Hz, 2H), 6.96 (d, *J* = 8.6 Hz, 2H), 6.86 (d, *J* = 17.4, 8.6 Hz, 2H), 6.84 (d, *J* = 8.6 Hz, 2H) 4.20 (s, 1H), 4.10 (d, *J* = 10.5 Hz, 1H), 3.93 (d, *J* = 7.3 Hz, 1H), 3.82 (s, 3H), 3.80 (s, 3H), 3.76 (d, *J* = 7.3 Hz, 1H), 3.70 (d, *J* = 5.8 Hz, 1H), 3.64 (s, 3H), 3.59 (s, 3H), 3.44 (d, *J* = 7.3 Hz, 1H), 2.61 – 2.55 (m, 1H), 2.13 (d, *J* = 5.8 Hz, 1H), 1.96 (m, 1H), 1.75 -1.70 (m, 1H), 1.56 (dd, *J* = 13.5, 10.5 Hz, 1H); **$^{13}$C NMR** (101 MHz, ($CD_2Cl_2$): δ 217.03, 172.75, 171.27, 159.67, 158.98, 139.10, 131.95, 131.56, 131.04, 130.92, 128.95, 128.80, 120.96, 113.91, 113.12, 74.89, 67.76, 66.88, 63.94, 62.59, 55.64, 55.37, 55.20, 55.14, 51.93, 51.59, 40.15, 34.04.

**HRMS**: calcd. for $[M+H]^+$ $C_{34}H_{35}{}^{79}BrN_2O_7$ = 663.16997, found: 663.17004; calcd. for $[M+H]^+$ $C_{34}H_{35}{}^{81}BrN_2O_7$ = 665.16801, found: 665.16799.

**HPLC** conditions: CHIRALPAK IA column, *iso*-propanol/ *iso*-hexane = 60/40, flow rate = 0.5 mL $min^{-1}$, minor enantiomer: $t_R$ = 31.99 min; major enantiomer: $t_R$ = 23.59 min; (98% e.e.).

**$[\alpha]^{20}_{D}$** = + 157.6° (c = 0.2, $CHCl_3$).

**FT-IR:** $\tilde{\nu}$ 3475, 2439, 2379, 2342, 1640, 1544, 1303, 1288 ,1278, 1246, 1033 $cm^{-1}$.

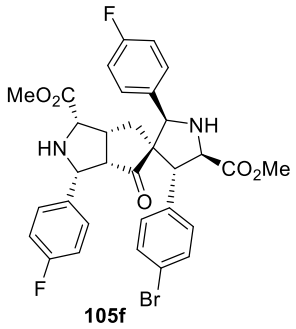


105f

**Dimethyl (1*S*,2'*R*,3*R*,3*aS*,4'*R*,5*R*,5'*R*,6*aR*)-4'-(4-bromophenyl)-2',3-bis(4-fluorophenyl)-4-oxohexahydro-1*H*-spiro[cyclopenta[*c*]pyrrole-5,3'-pyrrolidine]-1,5'-dicarboxylate (105f)**

white amorphous solid, 75% yield, **$^{1}$H NMR** (400 MHz, ($CD_2Cl_2$): δ 7.53 (d, *J* = 8.0 Hz, 2H), 7.25 (d, *J* = 8.0, 2H), 7.08 – 7.02 (m, 6H), 6.99-6.96 (m, 2H), 4.27 (s, 1H), 4.15 (d, *J* = 10.6 Hz, 1H), 3.97 (d, *J* = 7.3 Hz, 1H), 3.74 (d, *J* = 7.6 Hz, 1H), 3.66 (s, 3H), 3.59 (s, 3H), 3.44 (d, *J* = 7.3 Hz, 1H), 2.63 - 2.59 (m, 1H), 2.00 -1.97 (m, 1H), 1.77 (dd, *J* = 13.5, 7.6 Hz, 1H), 1.60 (dd, *J* = 13.5, 10.6 Hz, 1H); **$^{13}$C NMR** (101 MHz, ($CD_2Cl_2$): δ 216.94, 173.27, 171.63, 163.92 (d, *J* = 246.8 Hz), 162.52 (d, *J* = 246.4 Hz), 139.10, 135.46 (d, *J* = 3 Hz), 134.58 (d, *J* = 3.1 Hz), 132.18, 131.49, 130.20 (d, *J* = 8.1 Hz), 129.88 (d, *J* = 8 Hz), 121.69, 116.15 (d, *J* = 21.5 Hz), 115.20 (d, *J* = 21.4 Hz), 74.76, 68.26, 67.04, 64.00, 63.11, 55.90, 55.46, 52.58, 52.24, 40.36, 34.55.

**$^{19}$F NMR** (565 MHz, $CD_2Cl_2$) δ -113.6 (m), -115.4 (m).

**HRMS**: calcd. for $[M+H]^+$ $C_{32}H_{29}{}^{79}BrF_2N_2O_5$ = 639.12962, found: 639.13007; calcd. for $[M+H]^+$ $C_{32}H_{29}{}^{81}BrF_2N_2O_5$ = 641.12732, found: 641.12802.

**HPLC** conditions: CHIRALPAK IC column, *iso*-propanol/ *iso*-hexane = 30/70, flow rate = 0.5 mL $min^{-1}$, minor enantiomer: $t_R$ = 18.43 min; major enantiomer: $t_R$ = 27.01 min**;** (98% e.e.).

**$[\alpha]^{20}_D$** = + 144.1° (c = 0.1, $CHCl_3$).

**FT-IR:** $\tilde{\nu}$ 3458, 2922, 2385, 1732, 1604, 1508, 1218, 1145, 1089, 1010 $cm^{-1}$.

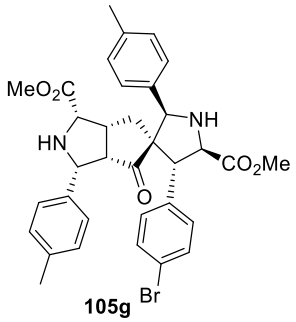


105g

**Dimethyl (1*S*,2'*R*,3*R*,3*aS*,4'*R*,5*R*,5'*R*,6*aR*)-4'-(4-bromophenyl)-4-oxo-2',3-di-*p*-tolylhexahydro-1*H*-spiro[cyclopenta[*c*]pyrrole-5,3'-pyrrolidine]-1,5'-dicarboxylate (105g)**

white amorphous solid, 63% yield, **$^{1}$H NMR** (400 MHz, ($CD_2Cl_2$): δ 7.46 (d, *J* = 8.4 Hz, 2H), 7.06 – 6.99 (m, 8H), 6.83 (d, *J* = 8.0 Hz, 2H), 4.12 (s, 1H), 4.01 (d, *J* = 10.8 Hz, 1H), 3.86 (d, *J* = 7.4 Hz, 1H), 3.61 (d, *J* = 5.9 Hz, 1H), 3.56 (s, 3H), 3.50 (s, 3H), 3.34 (d, *J* = 7.4 Hz, 1H), 2.54 – 2.46 (m, 1H), 2.28 (s, 3H), 2.25 (s, 3H), 1.91 – 1.86 (m, 1H), 1.67 – 1.63 (m, 1H), 1.48 (dd, *J* = 13.4, 10.8 Hz, 1H).

**$^{13}$C NMR** (101 MHz, ($CD_2Cl_2$): δ 217.41, 173.30, 171.83, 139.66, 138.91, 137.68, 136.60, 135.17, 132.14, 131.52, 129.85, 129.09, 128.27, 128.25, 121.54, 75.81, 68.55, 67.56, 64.87, 63.24, 56.36, 56.06, 52.50, 52.18, 40.79, 34.55, 29.65, 21.41.

**HRMS**: calcd. for $[M+H]^+$ $C_{34}H_{35}{}^{79}BrN_2O_5$ = 631.18013, found: 631.18021; calcd. for $[M+H]^+$ $C_{34}H_{35}{}^{81}BrN_2O_5$ = 633.17791, found: 633.17816.

**HPLC** conditions: CHIRALPAK IC column, *iso*-propanol/ *iso*-hexane = 80/20, flow rate = 0.5 mL $min^{-1}$, minor enantiomer: $t_R$ = 23.13 min; major enantiomer: $t_R$ = 66.36 min; (93% e.e.).

**$[\alpha]^{20}_D$**= + 95.9° (c = 0.22, CHCl3).

**FT-IR:** $\tilde{\nu}$ 3384, 2966, 2867, 2161, 2032, 1735, 1587, 1436, 1206, 1106, 1011 $cm^{-1}$.

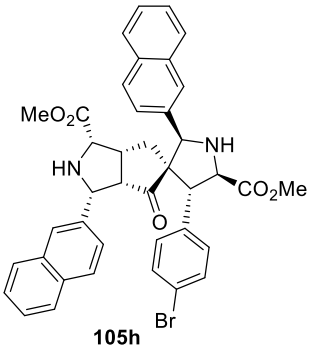


105h

**Dimethyl (1*S*,2'*R*,3*R*,3*aS*,4'*R*,5*R*,5'*R*,6*aR*)-4'-(4-bromophenyl)-2',3-di(naphthalen-2-yl)-4-oxohexahydro-1*H*-spiro[cyclopenta[*c*]pyrrole-5,3'-pyrrolidine]-1,5'-dicarboxylate (105h)**

white amorphous solid, 66% yield, **$^{1}$H NMR** (400 MHz, $CD_2Cl_2$): δ 7.87 – 7.85 (m, 3H), 7.83 (d, *J* = 8.5 Hz, 1H), 7.80 (d, *J* = 8.0 Hz, 1H), 7.77 (d, *J* = 8.5 Hz, 1H), 7.74 (s, 1H), 7.60 (s, 1H), 7.57 (d, *J* = 8.0 Hz, 2H), 7.53 – 7.47 (m, 4H), 7.35 (dd, *J* = 8.4, 1.8 Hz, 1H), 7.12 – 7.10 (m, 3H), 4.44 (s, 1H), 4.25 (d, *J* = 10.6 Hz, 1H), 3.98 (d, *J* = 7.0 Hz, 1H), 3.72 (d, *J* = 5.9 Hz, 1H), 3.69 (s, 3H), 3.44 (d, *J* = 7.0 Hz, 1H), 3.36 (s, 3H), 2.66 – 2.59 (m, 1H), 2.02 (dd, *J* = 13.5, 8.7 Hz, 1H), 1.90 -1.84 (m, 1H), 1.73 (dd, *J* = 13.5, 10.6 Hz, 1H).

**$^{13}$C NMR** (176 MHz, ($CD_2Cl_2$): δ 216.47, 172.67, 171.21, 138.97, 136.91, 135.41, 133.30, 133.13, 133.01, 131.65, 130.93, 128.41, 128.05, 127.73, 127.66, 127.62, 127.13, 127.03, 126.49, 126.39, 126.01, 125.72, 125.63, 125.53, 121.05, 75.25, 67.97, 66.81, 64.21, 62.70, 55.68, 55.29, 51.74, 51.67, 40.07, 34.06.

**HRMS**: calcd. for $[M+H]^+$ $C_{40}H_{35}{}^{79}BrN_2O_5$ = 703.18101, found: 703.18021; calcd. for $[M+H]^+$ $C_{40}H_{35}{}^{81}BrN_2O_5$ = 705.17876, found: 705.17816.

**HPLC** conditions: CHIRALPAK IA column, *iso*-propanol/ *iso*-hexane = 60/40, flow rate = 0.5 mL min$^{-1}$, minor enantiomer: $t_R$ = 70.97 min; major enantiomer: $t_R$ = 42.85 min; (96% e.e.).

**$[\alpha]^{20}_{D}$** = + 168.8° (c = 0.22, $CHCl_3$).

**FT-IR:** $\tilde{\nu}$ 3364, 2956, 2867, 2159, 2031, 1731, 1489, 1208, 1088, 1012 cm$^{-1}$.

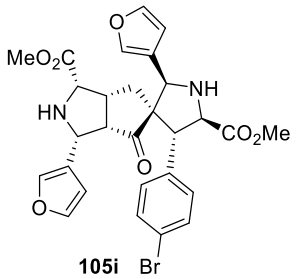


105i

**Dimethyl (1*S*,2'*S*,3*R*,3*aS*,4'*R*,5*R*,5'*R*,6*aR*)-4'-(4-bromophenyl)-2',3-di(furan-2-yl)-4-oxohexahydro-1*H*-spiro[cyclopenta[*c*]pyrrole-5,3'-pyrrolidine]-1,5'-dicarboxylate (105i)**

white amorphous solid, 40% yield **$^{1}$H NMR** (400 MHz, $CD_2Cl_2$): δ 7.51 – 7.46 (m, 3H), 7.40 (m, 1H), 7.23 – 7.22 (m, 2H), 6.99 (d, *J* = 8.5 Hz, 1H), 6.30 (dd, *J* = 1.9, 0.9 Hz, 2H), 6.11 (dd, *J* = 1.9, 0.9 Hz, 1H), 4.24 (d, *J* = 10.7 Hz, 1H), 4.20 (s, 1H), 3.90 (d, *J* = 7.1 Hz, 1H), 3.76 (d, *J* = 5.7 Hz, 1H), 3.64 (s, 3H), 3.63 (s, 3H), 3.34 (d, *J* = 7.1 Hz, 1H), 2.76 - 2.72 (m, 1H), 2.44 -2.39 (m, 1H), 1.65 -1.61 (m, 1H), 1.49 (dd, *J* = 13.6, 10.7 Hz, 1H).

**$^{13}$C NMR** (126 MHz, $CD_2Cl_2$) δ 218.09, 173.09, 171.76, 144.31, 143.32, 141.46, 140.34, 139.57, 132.15, 131.33, 125.31, 123.13, 121.54, 110.98, 109.74, 67.87, 67.56, 67.25, 63.23, 56.80, 56.30, 56.15, 52.61, 52.23, 41.37, 34.16.

**HRMS**: calcd. for $[M+H]^+$ $C_{28}H_{27}{}^{79}BrN_2O_7$ = 583.10702, found: 583.10744; calcd. for $[M+H]^+$ $C_{28}H_{27}{}^{81}BrN_2O_7$ = 585.10472, found: 585.10539.

**HPLC** conditions: CHIRALPAK IC column, *iso*-propanol/ *iso*-hexane = 50/50, flow rate = 0.5 mL min$^{-1}$, minor enantiomer: $t_R$ = 31.04 min; major enantiomer: $t_R$ = 67.54 min; (96% e.e.).

**$[\alpha]^{20}_{D}$**= + 78.5° (c = 0.12, CHCl3).

**FT-IR:** $\tilde{\nu}$ 3458, 2932, 2885, 2159, 2029,1765, 1532, 1302, 1056 cm$^{-1}$.

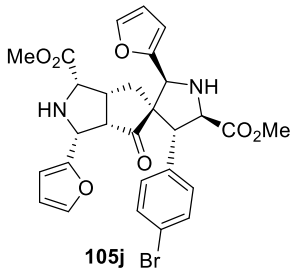


105j

**Dimethyl (1*S*,2'*R*,3*R*,3*aS*,4'*R*,5*R*,5'*R*,6*aR*)-4'-(4-bromophenyl)-2',3-di(furan-3-yl)-4-oxohexahydro-1*H*-spiro[cyclopenta[*c*]pyrrole-5,3'-pyrrolidine]-1,5'-dicarboxylate (105j)**

white amorphous solid, 45% yield $^{1}$H NMR (600 MHz, $CD_2Cl_2$) δ 7.52 (d, *J* = 8.4 Hz, 2H), 7.39 – 7.38 (m, 1H), 7.36 – 7.34 (m, 1H), 7.11 (d, *J* = 8.4 Hz, 2H), 6.37 (dd, *J* = 3.4, 1.8 Hz, 1H), 6.34 (dd, *J* = 3.4, 1.8 Hz, 1H), 6.30 (d, *J* = 3.3 Hz, 1H), 6.15 (d, *J* = 3.3 Hz, 1H), 4.34-4.32 (m, 2H) 3.95 (d, *J* = 6.5 Hz, 1H), 3.76 (d, *J* = 5.7 Hz, 1H), 3.64 (s, 6H), 3.55 (d, *J* = 6.5 Hz, 1H), 2.72 – 2.67 (m, 1H), 2.51 – 2.47 (m, 1H), 1.62 – 1.55 (m, 2H).

**$^{13}$C NMR** (151 MHz, $CD_2Cl_2$) δ 216.64, 173.18, 171.46, 151.93, 151.60, 142.91, 142.46, 139.70, 132.17, 131.25, 121.60, 111.38, 110.93, 108.96, 108.75, 68.15, 67.16, 67.09, 63.45, 58.95, 55.89, 55.78, 52.63, 52.38, 42.25, 32.66.

**HRMS**: calcd. for $[M+H]^+$ $C_{28}H_{27}{}^{79}BrN_2O_7$ = 583.10769, found: 583.10744; calcd. for $[M+H]^+$ $C_{28}H_{27}{}^{81}BrN_2O_7$ = 585.10504, found: 585.10539.

**HPLC conditions**: CHIRALPAK IC column, *iso*-propanol/ *iso*-hexane = 50/50, flow rate = 0.5 mL min$^{-1}$, minor enantiomer: $t_R$ = 27.54 min; major enantiomer: $t_R$ = 74.1 min; (95% e.e.

**$[\alpha]^{20}_D$** = + 41.1° (c = 0.21, $CHCl_3$).

**FT-IR:** $\tilde{\nu}$ 3449, 2942, 2863, 2158, 2049,1766, 1529, 1299, 1184, 1056, cm$^{-1}$.

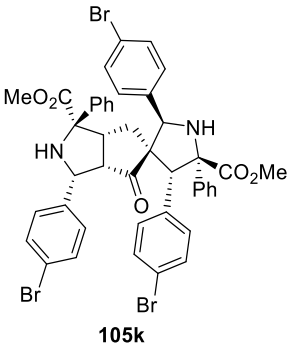


**105k**

**Dimethyl (1*R*,2'*R*,3*R*,3*aS*,4'*R*,5*R*,5'*S*,6*aR*)-2',3,4'-tris(4-bromophenyl)-4-oxo-1,5'-diphenylhexahydro-1*H*-spiro[cyclopenta[*c*]pyrrole-5,3'-pyrrolidine]-1,5'-dicarboxylate (105k)**

white amorphous solid, 21% yield**, $^{1}$H NMR** (700 MHz, $CD_2Cl_2$) δ 7.66 (d, *J* = 8.4 Hz, 2H), 7.61 (d, *J* = 7.2 Hz, 2H), 7.58 (d, *J* = 8.4 Hz, 2H), 7.34 – 7.22 (m, 10H), 6.98 (d, *J* = 7.2 Hz, 2H), 6.94 (d, *J* = 8.5 Hz, 2H), 6.51 (d, *J* = 8.5 Hz, 2H), 4.26 (s, 1H), 4.10 (d, *J* = 12.0 Hz, 1H), 3.94 – 3.89 (m, 2H), 3.67 (s, 3H), 3.31 (s, 3H), 2.53 – 2.50 (m, 1H), 2.39 (m, 1H), 2.30 (m, 1H), 1.75 (dd, *J* = 13.4, 12.0 Hz, 1H), 1.65 (m, 1H).

**$^{13}$C NMR** (176 MHz, $CD_2Cl_2$) δ 217.20, 173.93, 172.38, 144.25, 139.95, 137.92, 137.08, 136.68, 133.14, 132.47, 131.96, 131.54, 129.78, 129.30, 128.95, 128.57, 128.05, 127.79, 126.78, 126.14, 123.22, 122.21, 121.22, 75.05, 73.95, 71.37, 69.96, 66.14, 61.76, 55.36, 53.17, 52.82, 45.25, 31.62.

**HRMS**: calcd. for $[M+H]^+$ $C_{44}H_{38}{}^{79}Br^{81}Br_2N_2O_5$ = 915.02844, found: 915.02915; calcd. for $[M+H]^+$ $C_{44}H_{38}{}^{81}Br_3N_2O_5$ = 917.02640, found: 917.02760.

**HPLC conditions**: CHIRALPAK IC column, *iso*-propanol/ *iso*-hexane = 3/97, flow rate = 0.5 mL min$^{-1}$, minor enantiomer: $t_R$ = 26.61 min; major enantiomer: $t_R$ = 18.76 min; (91% e.e.).

**$[\alpha]^{20}_D$** = + 76.1° (c = 0.21, CHCl3).

**FT-IR: $\tilde{\nu}$** 3651, 2523, 2159, 2030, 1976, 1733, 1510, 1508, 1221, 1010 cm$^{-1}$.

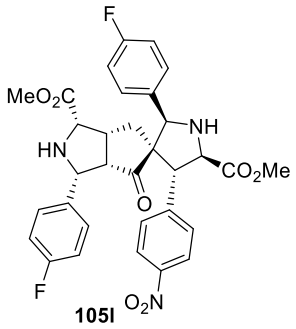


**105l**

**Dimethyl (1*S*,2'*R*,3*R*,3*aS*,4'*R*,5*R*,5'*R*,6*aR*)-2',3-bis(4-fluorophenyl)-4'-(4-nitrophenyl)-4-oxohexahydro-1*H*-spiro[cyclopenta[*c*]pyrrole-5,3'-pyrrolidine]-1,5'-dicarboxylate (105l)**

yellow amorphous solid, 80% yield, **$^{1}$H NMR** (600 MHz, $CD_2Cl_2$) δ 8.30 – 8.22 (m, 2H), 7.39 – 7.34 (m, 2H), 7.30 – 7.24 (m, 2H), 7.11 – 6.98 (m, 6H), 4.32 (s, 1H), 4.17 (dd, *J* = 10.8, 3.7 Hz, 1H), 4.04-4.02 (m, 1H), 3.75-3.73 (m, 1H), 3.63 (s, 3H), 3.62 – 3.60 (m, 1H), 3.60 (s, 3H), 2.82 (m, 1H), 2.67 – 2.60 (m, 1H), 2.06 (bs, 1H), 2.02 – 1.97 (m, 1H), 1.83 – 1.79 (m, 1H), 1.60 – 1.52 (m, 1H).

**$^{13}$C NMR** (151 MHz, $CD_2Cl_2$) δ 215.81, 172.35, 170.92, 163.52 (d, *J* = 247 Hz), 162.91(d, *J* = 244.9 Hz), 147.20, 147.03, 134.82 (d, *J* = 2.5 Hz), 133.82 (d, *J* = 3.0 Hz), 130.10, 129.70 (d, *J* = 8.5 Hz), 129.22 (d, *J* = 7.9 Hz), 123.67, 115.67 (d, *J* = 21.5 Hz), 114.66 (d, *J* = 21.4 Hz), 74.24, 67.60, 66.27, 63.28, 62.41, 55.03, 54.95, 52.09, 51.68, 39.65, 33.99.

**$^{19}$F NMR** (565 MHz, $CD_2Cl_2$) δ -113.9 (m), -115.7 (m).

**HRMS**: calcd. for $[M+H]^+$ $C_{32}H_{29}F_2N_3O_7$ = 606.20604, found: 606.20463.

**HPLC** conditions: CHIRALPAK IC column, *iso*-propanol/ *iso*-hexane = 80/20, flow rate = 0.5 mL min$^{-1}$, minor enantiomer: $t_R$ = 24.63 min; major enantiomer: $t_R$ = 34.95 min; (95% e.e.).

**$[\alpha]^{20}_{D}$** = + 152.3° (c = 0.13, $CHCl_3$).

**FT-IR:** $\tilde{\nu}$ 3651, 2529, 2159, 2030, 1976, 1725, 1509, 1345, 1218, 1137, 1052 cm$^{-1}$.

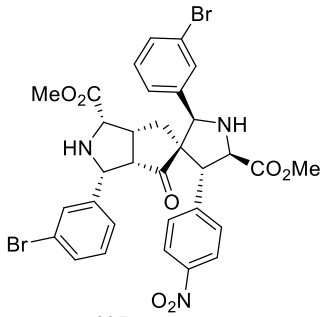


105m

**Dimethyl (1*S*,2'*R*,3*R*,3*aS*,4'*R*,5*R*,5'*R*,6*aR*)-2',3-bis(3-bromophenyl)-4'-(4-nitrophenyl)-4-oxohexahydro-1*H*-spiro[cyclopenta[*c*]pyrrole-5,3'-pyrrolidine]-1,5'-dicarboxylate (105m)**

white amorphous solid, 72%, **$^{1}$H NMR** (600 MHz, $CD_2Cl_2$) δ 8.26 (d, *J* = 8.7 Hz, 2H), 7.48 – 7.39 (m, 5H), 7.31 (d, *J* = 1.9 Hz, 1H), 7.26 – 7.17 (m, 3H), 7.02 (dd, *J* = 8.7, 1.9 Hz, 1H), 4.29 (s, 1H), 4.16 (d, *J* = 10.6 Hz, 1H), 4.06 (d, *J* = 7.2 Hz, 1H), 3.76 (d, *J* = 5.7 Hz, 1H), 3.63 (s, 3H), 3.60 (s, 3H), 2.68 – 2.60 (m, 1H), 2.07 (d, *J* = 7.2 Hz, 1H), 1.81 (dd, *J* = 13.6, 10.6 Hz, 1H), 1.58 – 1.51 (m, 2H).

**$^{13}$C NMR** (151 MHz, $CD_2Cl_2$) δ 215.98, 172.82, 171.32, 147.76, 147.47, 142.23, 141.08, 132.27, 131.55, 131.10, 130.99, 130.71, 130.67, 130.13, 127.47, 127.21, 124.39, 123.17, 122.66, 74.80, 68.24, 66.77, 63.89, 63.02, 55.67, 55.41, 52.71, 52.29, 40.06, 34.56.

**HRMS**: calcd. for $[M+H]^+$ $C_{32}H_{29}{}^{79}Br_2N_3O_7$ = 726.04689, found: 726.04450; calcd. for $[M+H]^+$ $C_{32}H_{29}{}^{79}Br^{81}BrN_3O_7$ = 728.04469, found: 728.04246; calcd. for $[M+H]^+$ $C_{32}H_{29}{}^{81}Br_2N_3O_7$ = 730.04311, found: 730.04041.

**HPLC** conditions: CHIRALPAK IA column, *iso*-propanol/ *iso*-hexane = 30/70, flow rate = 0.5 mL min$^{-1}$, minor enantiomer: $t_R$ = 66.37 min; major enantiomer: $t_R$ = 45.82 min; (91% e.e.).

**[α]$^{20}$ D**= + 130.1° (c = 0.23, $CHCl_3$).

**FT-IR:** $\tilde{\nu}$ 3587, 2524, 2159, 2030, 1733, 1648, 1518, 1345, 1205, 1153, 1085 cm$^{-1}$.

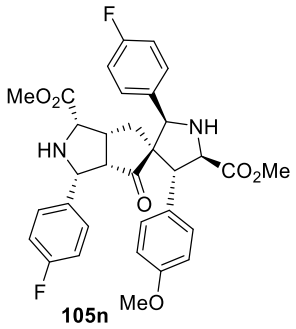


105n

**Dimethyl (1*S*,2'*R*,3*R*,3*aS*,4'*R*,5*R*,5'*R*,6*aR*)-2',3-bis(4-fluorophenyl)-4'-(4-methoxyphenyl)-4-oxohexahydro-1*H*-spiro[cyclopenta[*c*]pyrrole-5,3'-pyrrolidine]-1,5'-dicarboxylate (105n)**

white amorphous solid, 65%, **$^{1}$H NMR** (700 MHz, $CD_2Cl_2$) δ 7.25 (d, *J* = 8.6, 2H), 7.09 (d, *J* = 8.6 Hz, 2H), 7.05 – 6.98 (m, 6H), 6.93 (d, *J* = 8.6 Hz, 2H), 4.27 (s, 1H), 4.14 (d, *J* = 10.8 Hz, 1H), 3.96 (d, *J* = 7.4 Hz, 1H), 3.84 (s, 3H), 3.73 (d, *J* = 5.8 Hz, 1H), 3.65 (s, 3H), 3.59 (s, 3H), 3.42 (d, *J* = 7.4 Hz, 1H), 2.63 – 2.57 (m, 1H), 2.00 – 1.97 (m, 1H), 1.80 – 1.75 (m, 1H), 1.63 (dd, *J* = 13.6, 10.8 Hz, 1H).

**$^{13}$C NMR** (176 MHz, $CD_2Cl_2$) δ 217.48, 173.58, 171.71, 163.86 (d, *J* = 246.5 Hz), 163.32 (d, *J* = 244.7 Hz), 159.42, 135.54 (d, *J* = 3.1 Hz), 134.82 (d, *J* = 3.0 Hz), 131.92, 130.72, 130.19 (d, *J* = 8.1 Hz), 130.02 (d, *J* = 8.0 Hz), 116.07 (d, *J* = 21.5 Hz), 115.18 (d, *J* = 21.4 Hz), 114.37, 74.91, 68.66, 67.47, 64.12, 63.18, 56.13, 55.79, 55.58, 52.48, 52.18, 40.44, 34.66; HRMS: calcd. for $[M+H]^+$ $C_{33}H_{32}F_2N_2O_6$ = 591.23147, found: 591.23012.

**$^{19}$F NMR** (565 MHz, $CD_2Cl_2$) δ -114.4 (m), -115.9 (m).

**HPLC** conditions: CHIRALPAK IC column, *iso*-propanol/ *iso*-hexane = 30/70, flow rate = 0.5 mL $min^{-1}$, minor enantiomer: $t_R$ = 24.52 min; major enantiomer: $t_R$ = 50.30 min; (98% e.e.).

**$[\alpha]^{20}_D$** = + 146.7° (c = 0.1, $CHCl_3$).

**FT-IR:** $\tilde{\nu}$ 3527, 2511, 2477, 1755, 1585, 1558, 1297, 1166, 1097, 1012 $cm^{-1}$.

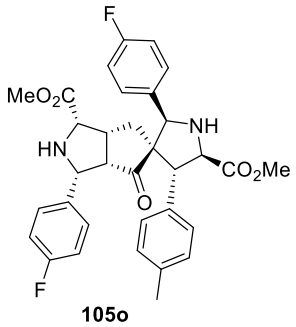


105o

**Dimethyl *(1S,2'R,3R,3aS,4'R,5R,5'R,6aR)*-2',3-bis(4-fluorophenyl)-4-oxo-4'-(*p*-tolyl)hexahydro-1*H*-spiro[cyclopenta[*c*]pyrrole-5,3'-pyrrolidine]-1,5'-dicarboxylate (105o)**

white amorphous solid, 60%, **$^{1}$H NMR** (600 MHz, $CD_2Cl_2$) δ 7.27 – 7.24 (m, 2H), 7.22 (d, *J* = 7.9 Hz, 2H), 7.08 – 6.96 (m, 8H), 4.27 (s, 1H), 4.14 (d, *J* = 10.7 Hz, 1H), 3.99 (d, *J* = 7.3 Hz, 1H), 3.72 (d, *J* = 5.7 Hz, 1H), 3.64 (s, 3H), 3.62 (d, *J* = 7.3Hz, 1H), 3.59 (s, 3H), 2.61 -2.53 (m, 1H), 2.39 (s, 3H), 2.01 -1.95 (m, 1H), 1.75 (m, 1H), 1.62 (dd, *J* = 13.6, 10.7 Hz, 1H).

**$^{13}$C NMR** (151 MHz, $CD_2Cl_2$) δ 217.52, 173.54, 171.71, 163.97 (d, *J* = 246.5 Hz), 163.42 (d, *J* = 244.7 Hz), 137.59, 136.94, 135.52 (d, *J* = 2.9 Hz), 134.71 (d, *J* = 3.2 Hz), 130.18 (d, *J* = 8.1 Hz), 130.02 (d, *J* = 8.0 Hz), 129.73, 129.56, 116.08 (d, *J* = 21.4 Hz), 115.19 (d, *J* = 21.4 Hz), 74.93, 68.57, 67.41, 64.13, 63.16, 56.14, 55.93, 52.48, 52.16, 40.44, 34.62, 21.39.

**$^{19}$F NMR** (565 MHz, $CD_2Cl_2$) δ -114.3 (m), -115.9 (m).

**HRMS**: calcd. for $[M+H]^+$ $C_{33}H_{32}F_2N_2O_5$ = 575.23641, found: 575.23520.

**HPLC** conditions: CHIRALPAK IC column, *iso*-propanol/ *iso*-hexane = 30/70, flow rate = 0.5 mL min$^{-1}$, minor enantiomer: $t_R$ = 18.23 min; major enantiomer: $t_R$ = 143.3 min; (98% e.e.).

**$[\alpha]^{20}_{D}$** = + 41.1° (c = 0.15, $CHCl_3$).

**FT-IR:** $\tilde{\nu}$ 3498, 2511, 2159, 2049, 2022, 1731, 1508, 1218, 1035, 1011 cm$^{-1}$.

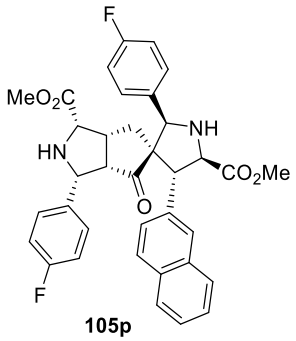


105p

**Dimethyl (1*S*,2'*R*,3*R*,3*aS*,4'*R*,5*R*,5'*R*,6*aR*)-2',3-bis(4-fluorophenyl)-4'-(naphthalen-2-yl)-4-oxohexahydro-1*H*-spiro[cyclopenta[*c*]pyrrole-5,3'-pyrrolidine]-1,5'-dicarboxylate (105p)**

brown amorphous solid, 65%, **$^{1}$H NMR** (500 MHz, $CD_2Cl_2$) δ 7.92 – 7.88 (m, 3H), 7.61 (d, *J* = 1.9 Hz, 1H), 7.58 – 7.50 (m, 2H), 7.34 (dd, *J* = 8.5, 1.9 Hz, 1H), 7.31 – 7.27 (m, 2H), 7.09 – 6.94 (m, 6H), 4.39 (s, 1H), 4.16-4.14 (m, 2H), 3.71 (d, *J* = 5.7 Hz, 1H), 3.66 (d, *J* = 7.3 Hz, 1H), 3.57 (s, 3H), 3.52 (s, 3H), 2.83 (bs, 1H), 2.66 – 2.57 (m, 1H), 2.03 – 1.98 (m, 1H), 1.83 (m, 1H), 1.67 (dd, *J* = 13.6, 10.7 Hz, 1H).

**$^{13}$C NMR** (126 MHz, $CD_2Cl_2$) δ 217.24, 173.54, 171.60, 163.15 (d, *J* = 246.5 Hz), 162.57 (d, *J* = 244.6 Hz), 137.35, 135.44 (d, *J* = 3.0 Hz), 134.73 (d, *J* = 3.2 Hz), 133.91, 133.14, 130.21 (d, *J* = 8.1 Hz), 129.96 (d, *J* = 8.0 Hz), 128.71, 128.61, 128.32, 128.20, 127.50, 126.89, 126.56, 116.12 (d, *J* = 21.5 Hz), 115.19 (d, *J* = 21.4 Hz), 74.92, 68.66, 67.13, 64.05, 63.08, 56.33, 55.93, 52.54, 52.08, 40.45, 34.62.

**$^{19}$F NMR** (565 MHz, $CD_2Cl_2$) δ -114.3 (m), -115.9 (m).

**HRMS**: calcd. for $[M+H]^+$ $C_{36}H_{32}F_2N_2O_5$ = 611.23648, found: 611.23520;

**HPLC** conditions: CHIRALPAK IC column, *iso*-propanol/ *iso*-hexane = 30/70, flow rate = 0.5 mL min$^{-1}$, minor enantiomer: $t_R$ = 20.03 min; major enantiomer: $t_R$ = 44.11 min; (95% e.e.).

**$[\alpha]^{20}_D$** = + 168.4° (c = 0.17, $CHCl_3$).

**FT-IR:** $\tilde{\nu}$ 3402, 2460, 2108, 1680, 1588, 1398, 1212, 1187, 1078, 1019 cm$^{-1}$**.**

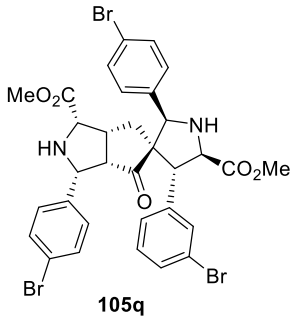


105q

**Dimethyl (1*S*,2'*R*,3*R*,3*aS*,4'*R*,5*R*,5'*R*,6*aR*)-4'-(3-bromophenyl)-2',3-bis(4-bromophenyl)-4-oxohexahydro-1*H*-spiro[cyclopenta[*c*]pyrrole-5,3'-pyrrolidine]-1,5'-dicarboxylate (105q)**

white amorphous solid, 81% yield, **$^{1}$H NMR** (400 MHz, $CD_2Cl_2$) δ 7.50 – 7.44 (m, 5H), 7.33 – 7.27 (m, 2H), 7.18 – 7.11 (m, 3H), 6.97 (d, *J* = 8.4 Hz, 2H), 4.24 (s, 1H), 4.13 (d, *J* = 10.2 Hz, 1H), 3.99 (d, *J* = 7.2 Hz, 1H), 3.78 – 3.74 (m, 1H), 3.66 (s, 3H), 3.61 (s, 3H), 3.45 (d, *J* = 7.2 Hz, 1H), 2.75 (s, 1H), 2.68 – 2.58 (m, 1H), 2.00 (dd, *J* = 13.5, 10.2 Hz, 1H), 1.78 (m, 1H), 1.61 – 1.52 (m, 2H).

**$^{13}$C NMR** (101 MHz, $CD_2Cl_2$) δ 216.49, 173.14, 171.57, 142.24, 138.82, 137.91, 132.64, 132.33, 131.52, 131.02, 130.68, 130.26, 130.07, 128.45, 123.10, 122.87, 121.55, 74.87, 68.29, 66.84, 64.07, 63.17, 55.75, 55.52, 52.68, 52.23, 40.25, 34.73.

**HRMS**: calcd. for $[M+H]^+$ $C_{32}H_{29}{}^{79}Br_3N_2O_5$ = 758.97254, found: 758.96994; calcd. for $[M+H]^+$ $C_{32}H_{29}{}^{79}Br^{81}Br_2N_2O_5$ = 762.96848, found: 762.96584; calcd. for $[M+H]^+$ $C_{32}H_{29}{}^{79}Br_2{}^{81}BrN_2O_5$ = 760.97050, found: 760.96789; calcd. for $[M+H]^+$ $C_{32}H_{29}{}^{81}Br_3N_2O_5$ = 764.96625, found: 764.96380.

**HPLC** conditions: CHIRALPAK IC column, *iso*-propanol/ *iso*-hexane = 30/70, flow rate = 0.5 mL min$^{-1}$, minor enantiomer: $t_R$ = 18.90min; major enantiomer: $t_R$ = 32.07 min; (91% e.e.).

**$[\alpha]^{20}_{D}$** = + 107.8° (c = 0.24, $CHCl_3$).

**FT-IR:** $\tilde{\nu}$ 3488, 2511, 2159, 2057, 2014, 1732, 1659, 1428, 1211, 1142, 1089 cm$^{-1}$.

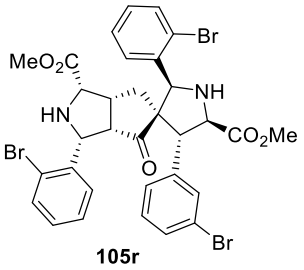


105r

**Dimethyl (1*S*,2'*S*,3*R*,3*aS*,4'*R*,5*R*,5'*R*,6*aR*)-2',3-bis(2-bromophenyl)-4'-(3-bromophenyl)-4-oxohexahydro-1*H*-spiro[cyclopenta[*c*]pyrrole-5,3'-pyrrolidine]-1,5'-dicarboxylate (105r)**

white amorphous solid, 60% yield, **$^{1}$H NMR** (700 MHz, $CD_2Cl_2$) δ 7.61 (dd, *J* = 8.0, 1.3 Hz, 1H), 7.53 (dd, *J* = 8.0, 1.3 Hz, 1H), 7.48 – 7.46 (m, 1H), 7.35 – 7.32 (m, 2H), 7.29 – 7.15 (m, 6H), 7.11 (m, 1H), 4.93 (s, 1H), 4.37 (d, *J* = 10.2 Hz, 1H), 4.01 (d, *J* = 8.0 Hz, 1H), 3.76 (d, *J* = 6.0 Hz, 1H), 3.65 (s, 3H), 3.58 (s, 3H), 3.46 (d, *J* = 8.0 Hz, 1H), 2.89 – 2.84 (m, 1H), 2.30 – 2.24 (m, 1H), 2.05 – 2.01 (m, 1H), 1.40 (dd, *J* = 13.4, 10.2 Hz, 1H).

**$^{13}$C NMR** (176 MHz, $CD_2Cl_2$) δ 216.03, 173.00, 171.65, 142.33, 139.26, 137.78, 133.74, 132.81, 132.55, 130.88, 130.67, 130.25, 130.14, 129.18, 128.68, 128.56, 128.31, 127.84, 125.08, 124.89, 122.98, 71.42, 68.95, 66.50, 63.55, 62.92, 55.50, 52.80, 52.62, 52.14, 39.74, 34.15.

**HRMS**: calcd. for $[M+H]^+$ $C_{32}H_{30}{}^{79}Br_2{}^{81}BrN_2O_5$ = 759.97549, found: 759.97264; calcd. for $[M+H]^+$ $C_{32}H_{30}{}^{79}Br{}^{81}Br_2N_2O_5$ = 761.97320, found: 761.97059; calcd. for $[M+H]^+$ $C_{32}H_{30}{}^{81}Br_3N_2O_5$ = 763.97095, found: 763.96855.

**HPLC** conditions: CHIRALPAK IC column, *iso*-propanol/ *iso*-hexane = 30/70, flow rate = 0.5 mL min$^{-1}$, minor enantiomer: $t_R$ = 19.44 min; major enantiomer: $t_R$ = 39.94 min; (91% e.e.).

**$[\alpha]^{20}_D$** = + 131.2° (c = 0.35, $CHCl_3$).

**FT-IR:** $\tilde{\nu}$ 3476, 2508, 2129, 2156, 1998, 1734, 1642, 1208, 1112, 1021 cm$^{-1}$.

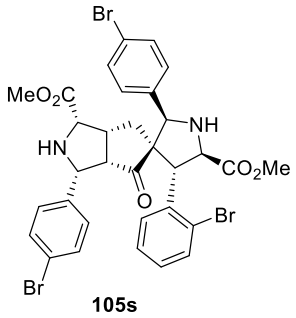


105s

**Dimethyl (1*S*,2'*S*,3*R*,3*aS*,4'*R*,5*R*,5'*R*,6*aR*)-2',3-bis(2-bromophenyl)-4'-(3-bromophenyl)-4-oxohexahydro-1*H*-spiro[cyclopenta[*c*]pyrrole-5,3'-pyrrolidine]-1,5'-dicarboxylate (105s)**

white amorphous solid, 80% yield, **$^{1}$H NMR** (600 MHz, $CD_2Cl_2$) δ 7.66 (dd, *J* = 8.1, 1.3 Hz, 1H), 7.49 (d, *J* = 8.4 Hz, 2H), 7.46 (d, *J* = 8.1 Hz, 1H), 7.43 (d, *J* = 8.4 Hz, 2H), 7.41 – 7.38 (m, 1H), 7.22 – 7.15 (m, 5H), 4.30 (s, 1H), 4.21 (d, *J* = 4.8 Hz, 1H), 4.04 (d, *J* = 10.2 Hz, 1H), 3.88 (d, *J* = 4.8 Hz, 1H), 3.66 (m, 4H), 3.58 (s, 3H), 2.90 (bs, 1H), 2.50 – 2.43 (m, 1H), 2.10 (bs, 1H), 1.81 – 1.78 (m, 1H), 1.68 – 1.60 (m, 2H).

**$^{13}$C NMR** (151 MHz, $CD_2Cl_2$) δ 216.98, 173.62, 171.50, 140.91, 138.27, 137.11, 133.62, 132.48, 131.35, 130.35, 130.13, 130.07, 129.33, 128.63, 126.10, 123.02, 121.50, 74.99, 68.33, 64.61, 63.63, 55.99, 52.75, 52.07, 40.17, 33.90.

**HRMS**: calcd. for $[M+H]^+$ $C_{32}H_{29}{}^{79}Br_3N_2O_5$ = 758.96994, found: 758.97286; calcd. for $[M+H]^+$ $C_{32}H_{30}{}^{79}Br_2{}^{81}BrN_2O_5$ = 760.96789, found: 760.97090; calcd. for $[M+H]^+$ $C_{32}H_{20}{}^{81}Br_3N_2O_5$ = 764.96380, found: 764.96625.

**HPLC** conditions: CHIRALPAK IC column, *iso*-propanol/ *iso*-hexane = 30/70, flow rate = 0.5 mL min$^{-1}$, minor enantiomer: $t_R$ = 21.32 min; major enantiomer: $t_R$ = 39.24 min; (95% e.e.).

**$[\alpha]^{20}_D$** = + 22.1° (c = 0.1, $CHCl_3$).

**FT-IR:** $\tilde{\nu}$ 3335, 2512, 2187, 2156, 2011, 1728, 1648, 1203, 1098 cm$^{-1}$.

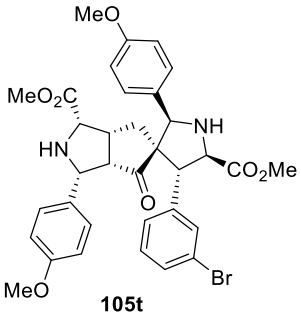


**105t**

**Dimethyl (1*S*,2'*R*,3*R*,3*aS*,4'*R*,5*R*,5'*R*,6*aR*)-4'-(3-bromophenyl)-2',3-bis(4-methoxyphenyl)-4-oxohexahydro-1*H*-spiro[cyclopenta[*c*]pyrrole-5,3'-pyrrolidine]-1,5'-dicarboxylate (105t)**

white amorphous solid, 55% yield, **$^{1}$H NMR** (600 MHz, $CD_2Cl_2$) δ 7.49 – 7.47 (m, 1H), 7.35 (d, *J* = 10.3 Hz, 1H), 7.30 (m, 1H), 7.16-7.12 (m, 3H), 6.95 (d, *J* = 8.6 Hz, 2H), 6.86 (dd, *J* = 10.3, 8.6 Hz, 4H), 4.19 (s, 1H), 4.09 (d, *J* = 10.7 Hz, 1H), 3.95 (d, *J* = 7.5 Hz, 1H), 3.82 (s, 3H), 3.80 (s, 3H), 3.70 (d, *J* = 5.7 Hz, 1H), 3.65 (s, 3H), 3.60 (s, 3H), 3.44 (d, *J* = 7.5 Hz, 1H), 2.75 (bs, 1H), 2.64 – 2.57 (m, 1H), 2.01 (bs, 1H), 1.94 (dd, *J* = 10.7, 8.9 Hz, 1H), 1.78 – 1.74 (m, 1H), 1.55 – 1.51 (m, 1H).

**$^{13}$C NMR** (151 MHz, $CD_2Cl_2$) δ 217.44, 173.17, 171.87, 160.23, 159.55, 142.83, 132.74, 131.54, 130.86, 130.63, 130.06, 129.61, 129.41, 128.45, 122.99, 114.46, 113.73, 75.62, 68.36, 67.32, 64.54, 63.17, 56.16, 56.09, 55.77, 55.73, 52.55, 52.15, 40.73, 34.88; **HRMS**: calcd. for $[M+H]^+$ $C_{34}H_{35}{}^{79}BrN_2O_7$ = 663.17181, found: 663.17004; calcd. for $[M+H]^+$ $C_{34}H_{35}{}^{81}BrN_2O_7$ = 665.17000, found: 665.16799.

**HPLC** conditions: CHIRALPAK IC column, *iso*-propanol/ *iso*-hexane = 80/20, flow rate = 0.5 mL min$^{-1}$, minor enantiomer: $t_R$ = 27.41 min; major enantiomer: $t_R$ = 51.85 min; (91% e.e.).

**$[\alpha]^{20}_{D}$** = + 128.2° (c = 0.12, $CHCl_3$).

**FT-IR:** $\tilde{\nu}$ 3412, 2512, 2167, 2114, 1766, 1598, 1225, 1181, 1103, 1036 cm$^{-1}$.

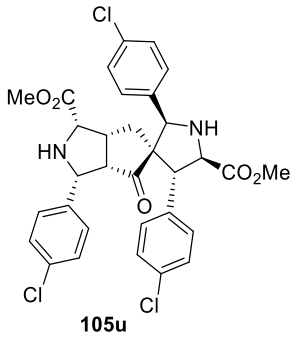


105u

**Dimethyl (1*S*,2′*R*,3*R*,3*aS*,4'*R*,5*R*,5'*R*,6*aR*)-2',3,4'-tris(4-chlorophenyl)-4-oxohexahydro-1*H*-spiro[cyclopenta[*c*]pyrrole-5,3'-pyrrolidine]-1,5'-dicarboxylate (105u)**

white amorphous solid, 80% yield, **$^{1}$H NMR** (500 MHz, $CD_2Cl_2$) δ 7.38 (d, *J* = 8.4 Hz, 2H), 7.31 (d, *J* = 8.5 Hz, 2H), 7.27 (d, *J* = 8.4 Hz, 2H), 7.21 (d, *J* = 8.5 Hz, 2H), 7.12 (d, *J* = 8.5 Hz, 2H), 7.02 (d, *J* = 8.5 Hz, 2H), 4.26 (s, 1H), 4.15 (d, *J* = 10.7 Hz, 1H), 3.97 (d, *J* = 7.1 Hz, 1H), 3.75 (d, *J* = 5.7 Hz, 1H), 3.65 (s, 3H), 3.59 (s, 3H), 3.45 (d, *J* = 7.1 Hz, 1H), 2.75 (bs, 1H), 2.63 – 2.57 (m, 1H), 2.07 – 1.99 (m, 1H), 1.78 – 1.73 (m, 1H), 1.59 (dd, *J* = 13.5, 10.7 Hz, 1H).

**$^{13}$C NMR** (126 MHz, $CD_2Cl_2$) δ 216.74, 173.28, 171.54, 138.47, 138.35, 137.38, 134.62, 133.54, 133.34, 131.08, 129.85, 129.68, 129.34, 129.19, 128.47, 74.66, 68.34, 67.02, 63.90, 63.07, 55.87, 55.26, 52.60, 52.24, 40.23, 34.45.

**HRMS**: calcd. for $[M+H]^+$ $C_{32}H_{30}{}^{35}Cl_3N_2O_5$ = 627.12301, found: 627.12148; calcd. for $[M+H]^+$ $C_{32}H_{30}{}^{35}Cl_2{}^{37}ClN_2O_5$ = 629.12023, found: 629.11853; calcd. for $[M+H]^+$ $C_{32}H_{30}{}^{35}Cl^{37}Cl_2N_2O_5$ = 631.11700, found: 631.11558.

**HPLC** conditions: CHIRALPAK IC column, *iso*-propanol/ *iso*-hexane = 30/70, flow rate = 0.5 mL min$^{-1}$, minor enantiomer: $t_R$ = 35.56 min; major enantiomer: $t_R$ = 56.67 min; (95% e.e.).

**[α]$^{20}$ D**= + 95.6° (c = 0.18, $CHCl_3$).

**FT-IR:** $\tilde{\nu}$ 3357, 2360, 2238, 1732, 1491, 1434, 1207, 1108, 1089, 1013, cm$^{-1}$.

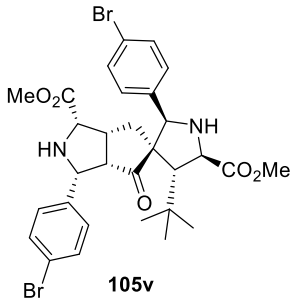


105v

**Dimethyl (1*S*,2′*R*,3*R*,3*aS*,4'*R*,5*R*,5'*R*,6*aR*)-2',3-bis(4-bromophenyl)-4'-(tert-butyl)-4-oxohexahydro-1*H*-spiro[cyclopenta[*c*]pyrrole-5,3'-pyrrolidine]-1,5'-dicarboxylate (15v)**

white amorphous solid, 21% yield, **$^{1}$H NMR** (700 MHz, $CD_2Cl_2$) δ 7.44 (d, *J* = 8.5 Hz, 2H), 7.40 (d, *J* = 8.4 Hz, 2H), 7.14 (d, *J* = 8.4 Hz, 2H), 7.10 (d, *J* = 8.5 Hz, 2H), 4.16 (d, *J* = 10.3 Hz, 1H), 4.03 (s, 1H), 3.78 (s, 3H), 3.70 (d, *J* = 7.1 Hz, 1H), 3.66 (s, 3H), 2.58 – 2.51 (m, 1H), 2.46 (dd, *J* = 13.0, 10.3 Hz, 1H), 2.36 (d, *J* = 7.1 Hz, 1H), 2.16 (d, *J* = 7.0 Hz, 1H), 2.14 – 2.07 (m, 1H), 1.91-1.89 (m, 1H), 0.98 (s, 9H).

**$^{13}$C NMR** (176 MHz, $CD_2Cl_2$) δ 216.64, 175.27, 172.00, 138.81, 138.44, 132.23, 131.23, 130.34, 129.83, 122.73, 121.33, 75.49, 68.56, 64.03, 63.60, 58.94, 54.79, 52.52, 52.33, 40.39, 34.42, 33.74, 30.10.

**HRMS**: calcd. for $[M+H]^+$ $C_{30}H_{35}{}^{79}Br_2N_2O_5$ = 661.09072, found: 661.09165; calcd. for $[M+H]^+$ $C_{30}H_{35}{}^{79}Br^{81}BrN_2O_5$ = 663.08868, found: 663.08948; calcd. for $[M+H]^+$ $C_{30}H_{35}{}^{81}Br_2N_2O_5$ = 665.08663, found: 665.08771.

**HPLC** conditions: CHIRALPAK IC column, *iso*-propanol/ *iso*-hexane = 30/70, flow rate = 0.5 mL min$^{-1}$, minor enantiomer: $t_R$ = 40.02 min; major enantiomer: $t_R$ = 40.02 min; (94% e.e.).

**[α]$^{20}$ D**= 15.0° (c = 0.1, $CHCl_3$).

**FT-IR:** $\tilde{\nu}$ 3185, 2535, 2441, 2031, 1617, 1534, 1211, 1189, 1089 cm$^{-1}$.

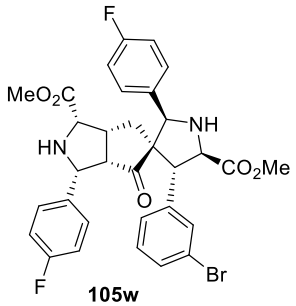


105w

**Dimethyl (1*S*,2'*R*,3*R*,3*aS*,4'*R*,5*R*,5'*R*,6*aR*)-4'-(3-bromophenyl)-2',3-bis(4-fluorophenyl)-4-oxohexahydro-1*H*-spiro[cyclopenta[*c*]pyrrole-5,3'-pyrrolidine]-1,5'-dicarboxylate (105w)**

white solid, 75%, **$^{1}$H NMR** (600 MHz, $CD_2Cl_2$) δ 7.48 (d, *J* = 8.6 Hz, 1H), 7.33-7.31 (m, 1H), 7.30-7.28 (m, 1H), 7.28 – 7.24 (m, 2H), 7.14 – 7.13 (m, 1H), 7.06 – 7.01 (m, 6H), 4.27 (s, 1H), 4.14 (d, *J* = 10.6 Hz, 1H), 3.99 (d, *J* = 7.4 Hz, 1H), 3.74 (d, *J* = 5.8 Hz, 1H), 3.66 (s, 3H), 3.60 (s, 3H), 3.46 (d, *J* = 7.4 Hz, 1H), 2.75 (s, 1H), 2.65 – 2.59 (m, 1H), 2.05 (bs, 1H), 1.97 – 1.94 (m, 1H), 1.79 (dd, *J* = 13.6, 10.6 Hz 1H), 1.59-1.54 (m, 1H).

**$^{13}$C NMR** (151 MHz, $CD_2Cl_2$) δ 216.79, 173.14, 171.65, 164.02 (d, *J* = 246.7 Hz), 163.44 (d, *J* = 244.7 Hz), 142.36, 135.40 (d, *J* = 2.9 Hz), 134.56 (d, *J* = 3.1 Hz), 132.67, 130.98, 130.66, 130.28 (d, *J* = 8.2 Hz), 129.90 (d, *J* = 8.0 Hz), 128.45, 123.06, 116.14 (d, *J* = 21.5 Hz), 115.26 (d, *J* = 21.4 Hz), 74.93, 68.26, 66.91, 64.05, 63.14, 55.76, 55.66, 52.60, 52.21, 40.33, 34.83.

**$^{19}$F NMR** (565 MHz, $CD_2Cl_2$) δ -114.1 (m), -114.8 (m).

**HRMS**: calcd. for $[M+H]^+$ $C_{32}H_{30}{}^{79}BrF_2N_2O_5$ = 639.13182, found: 639.13007; calcd. for $[M+H]^+$ $C_{32}H_{30}{}^{81}BrF_2N_2O_5$ = 641.13007, found: 641.12802.

**HPLC** conditions: CHIRALPAK IC column, *iso*-propanol/ *iso*-hexane = 30/70, flow rate = 0.5 mL min$^{-1}$, minor enantiomer: $t_R$ = 22.39 min; major enantiomer: $t_R$ = 41.27 min; (95% e.e.).

**$[\alpha]^{20}_D$** = + 138.5° (c = 0.2, $CHCl_3$).

**FT-IR:** $\tilde{\nu}$ 3312, 2412, 2067, 2014, 1734, 1558, 1223, 1103, 1025 cm$^{-1}$.

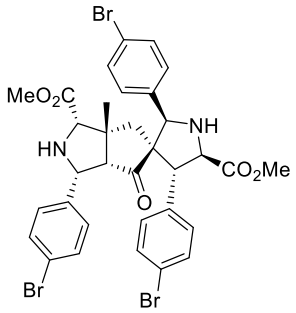


105x

**Dimethyl (1*R*,2'*R*,3*S*,3*aR*,4'*R*,5*R*,5'*R*,6*aS*)-1,2',4'-tris(4-bromophenyl)-3*a*-methyl-6-oxohexahydro-1*H*-spiro[cyclopenta[*c*]pyrrole-5,3'-pyrrolidine]-3,5'-dicarboxylate (105x)**

white amorphous solid, 40% yield; **$^{1}$H NMR** (700 MHz, $CD_2Cl_2$) δ 7.53 (d, *J* = 8.5 Hz, 2H), 7.45-7.42 (m, 4H), 7.16 – 7.09 (m, 6H), 4.21 (s, 1H), 4.19 (d, *J* = 9.1 Hz, 1H), 4.02 (d, *J* = 5.5 Hz, 1H), 3.60 (s, 3H), 3.57 (s, 3H), 3.54 (d, *J* = 5.5 Hz, 1H), 3.44 (s, 1H), 2.00 (d, *J* = 9.1 Hz, 1H), 1.88 (d, *J* = 14.8 Hz, 1H), 1.54 (s, 2H), 1.43 (d, *J* = 14.8 Hz, 1H), 0.98 (s, 3H).

**$^{13}$C NMR** (176 MHz, $CD_2Cl_2$) δ 218.44, 173.66, 171.60, 139.40, 138.09, 137.65, 132.24, 132.07, 131.94, 131.43, 130.81, 129.58, 122.88, 121.69, 121.39, 74.26, 72.00, 66.94, 66.65, 65.10, 64.26, 55.99, 52.86, 52.09, 46.81, 40.22, 26.90.

**HRMS**: calcd. for $[M+H]^+$ $C_{33}H_{32}{}^{79}Br_2{}^{81}BrN_2O_5$ = 774.98354, found: 774.98395; calcd. for $[M+H]^+$ $C_{33}H_{32}{}^{79}Br^{81}Br_2N_2O_5$ = 776.98149, found: 776.98137.

**HPLC** conditions: CHIRALPAK IC column, *iso*-propanol/ *iso*-hexane = 15/85, flow rate = 0.5 mL min$^{-1}$, minor enantiomer: $t_R$ = 37.47 min; major enantiomer: $t_R$ = 50.97 min; (94% e.e.).

**$[\alpha]^{20}_D$** = + 125.8° (c = 0.18, $CHCl_3$).

**FT-IR:** $\tilde{\nu}$ 3332, 2360, 2159, 2030, 1715, 1655, 1453, 1215, 1122, 1095, cm$^{-1}$.

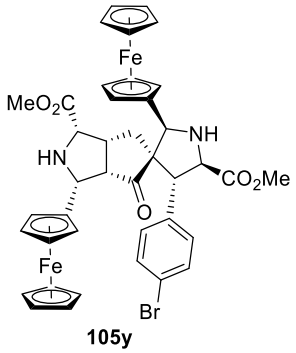


105y

**Dimethyl (1*S*,2'*R*,3*R*,3*aS*,4'*R*,5*R*,5'*R*,6*aR*)-2',3,4'-tris(4-chlorophenyl)-4-oxohexahydro-1*H*-spiro[cyclopenta[*c*]pyrrole-5,3'-pyrrolidine]-1,5'-dicarboxylate 105y)**

white amorphous solid, 48% yield; **$^{1}$H NMR** (500 MHz, $CD_2Cl_2$) δ 7.46 (d, *J* = 8.5 Hz, 2H), 7.01 (d, *J* = 8.5 Hz, 2H), 4.21 (s, 5H), 4.17 (dd, *J* = 2.5, 1.3 Hz, 1H), 4.14 (dd, *J* = 2.7, 1.3 Hz, 1H), 4.13 – 4.12 (m, 1H), 4.11 – 4.10 (m, 3H), 4.08 (s, 5H), 4.03 (dd, *J* = 2.7, 1.3 Hz, 1H), 3.90 (s, 1H), 3.81 (d, *J* = 6.2 Hz, 1H), 3.78 (d, *J* = 2.5 Hz, 1H), 3.75 – 3.74 (m, 1H), 3.66 (s, 3H), 3.60 (s, 3H), 3.17 (d, *J* = 6.2 Hz, 1H), 2.77 – 2.72 (m, 1H), 2.09 – 2.06 (m, 1H), 1.47 – 1.37 (m, 2H).

**$^{13}$C NMR** (126 MHz, $CD_2Cl_2$) δ 217.04, 173.95, 172.32, 139.95, 131.95, 131.33, 121.22, 87.66, 85.56, 70.52, 69.77, 69.45, 69.42, 69.11, 69.03, 68.93, 68.50, 68.08, 67.81, 67.43, 67.09, 66.09, 65.61, 63.06, 60.83, 56.73, 55.99, 52.47, 52.26, 42.33, 33.48.

**HRMS**: calcd. for $[M+H]^+$ $C_{40}H_{40}{}^{79}Br^{56}Fe_2N_2O_5$ = 819.08140, found: 819.08073; calcd. for $[M+H]^+$ $C_{40}H_{40}{}^{79}Br^{54}Fe^{56}FeN_2O_5$ = 817.08607, found: 817.08544; calcd. for $[M+H]^+$ $C_{40}H_{40}{}^{81}Br^{54}Fe^{57}FeN_2O_5$ = 820.08448, found: 820.08390; calcd. For $[M+H]^+$ $C_{40}H_{40}{}^{81}Br^{56}Fe_2N_2O_5$ = 821.07935, found: 821.07887; calcd. for $[M+H]^+$ $C_{40}H_{40}{}^{79}Br^{57}Fe^{58}FeN_2O_5$ = 822.08019, found: 822.08132.

**HPLC** conditions: CHIRALPAK IC column, *iso*-propanol/ *iso*-hexane = 15/85, flow rate = 0.5 mL min$^{-1}$, minor enantiomer: $t_R$ = 37.47 min; major enantiomer: $t_R$ = 50.97 min; (94% e.e.).

**$[\alpha]^{20}$ D**= + 98.5° (c = 0.18, $CHCl_3$).

**FT-IR: $\tilde{\nu}$** 3344, 2947, 2847, 1732, 1488, 1436, 1245, 1220, 1151, 1104, 1007, 967 cm$^{-1}$.

## 6.5 Synthesis of mono cycloaddition products

General Procedure D

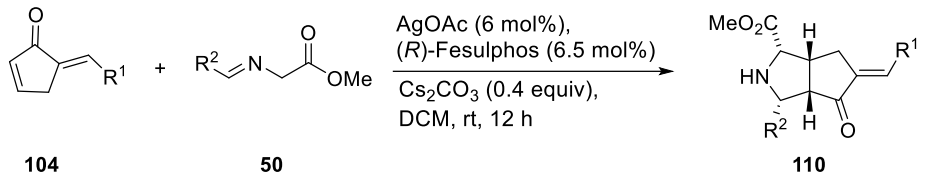


**104** **50** **110**

(*Rp*)-2-(*tert*-Butylthio)-1-(diphenylphosphino)ferrocene (6.5 mol%, 7.8 µmol) and silver acetate (6 mol%, 7.2 µmol) were dissolved in DCM (2mL) stirred at ambient temperature for 15 min. To the resulting solution were added iminoester **50** (1.1 equiv., 0.13 mmol), $Cs_2CO_3$ (40 mol%, 48 µmol) and enone **104** (1.00 equiv., 0.12 mmol) and the mixture was allowed to stir at ambient temperature for 12 h. The crude mixture was directly charged onto silica gel and the product was isolated using *n*-pentane / acetone as eluent.

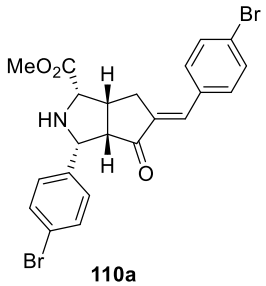


**110a**

**Methyl (1*S*,3*R*,3*aS*,6*aR*)-5-((*E*)-4-bromobenzylidene)-3-(4-bromophenyl)-4-oxooctahydrocyclopenta[*c*]pyrrole-1-carboxylate (110a)**

white amorphous solid, 72% yield, **$^{1}$H NMR** (500 MHz, $CD_2Cl_2$) δ 7.56 (d, *J* = 8.5 Hz, 2H), 7.41 – 7.35 (m, 4H), 7.20 (d, *J* = 8.5 Hz, 2H), 7.01-6.97 (m, 1H), 4.53 (d, *J* = 10.4 Hz, 1H), 4.14 (d, *J* = 5.5 Hz, 1H), 3.83 (s, 3H), 3.31 – 3.07 (m, 3H), 2.78 (m, 1H), 2.41 (bs, 1H).

**$^{13}$C NMR** (126 MHz, $CD_2Cl_2$) δ 206.19, 172.11, 138.99, 138.01, 134.86, 132.71, 132.45, 131.58, 131.44, 129.93, 124.22, 121.58, 64.99, 64.54, 56.31, 52.51, 40.72, 31.95.

**HRMS**: calcd. for $[M+H]^+$ $C_{22}H_{20}{}^{79}Br_2NO_3$ = 503.98039, found: 503.98045; calcd. for $[M+H]^+$ $C_{22}H_{20}{}^{79}Br^{81}BrNO_3$ = 505.97827, found: 505.97840; calcd. for $[M+H]^+$ $C_{22}H_{20}{}^{81}Br_2NO_3$ = 507.97602, found: 507.97635.

**HPLC conditions**: CHIRALPAK IC column, *iso*-propanol/ *iso*-hexane = 30/70, flow rate = 0.5 mL min$^{-1}$, minor enantiomer: $t_R$ = 40.63 min; major enantiomer: $t_R$ = 28.16min; (81% e.e.); CHIRALPAK IA column, *iso*-propanol/ *iso*-hexane = 15/85, flow rate = 0.5 mL min$^{-1}$, minor enantiomer: $t_R$ = 36.68 min; major enantiomer: $t_R$ = 93.25 min.

**$[\alpha]^{20}_D$** = + 251.5° (c = 0.2, $CHCl_3$).

**FT-IR:** $\tilde{\nu}$ 3378, 2514, 2058, 1744, 1525, 1488, 1221, 1155, 1093, 1008 cm$^{-1}$.

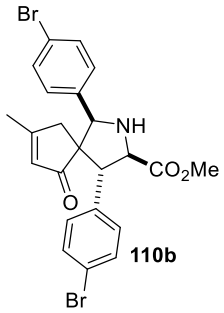


***rac*-Methyl (1*R*,3*R*,4*R*,5*R*)-1,4-bis(4-bromophenyl)-8-methyl-6-oxo-2-azaspiro[4.4]non-7-ene-3-carboxylate (110b)**

white amorphous solid, 57% yield, **$^{1}$H NMR** (600 MHz, $CD_2Cl_2$) δ 7.50 (d, *J* = 8.4 Hz, 2H), 7.41 (d, *J* = 8.4 Hz, 2H), 7.13 (d, *J* = 8.4 Hz, 4H), 5.36 (s, 1H), 4.30 (s, 1H), 4.14 (d, *J* = 7.0 Hz, 1H), 3.75 (s, 3H), 3.73 (d, *J* = 7.0 Hz, 1H), 3.21 (s, 1H), 2.34-2.31 (m, 2H), 1.81 (s, 3H).

**$^{13}$C NMR** (151 MHz, $CD_2Cl_2$) δ 209.95, 176.94, 173.23, 140.54, 137.13, 132.42, 131.81, 131.14, 129.18, 128.99, 122.32, 121.55, 73.05, 67.66, 64.79, 55.57, 52.76, 42.62, 19.40.

**HRMS**: calcd. for $[M+H]^+$ $C_{23}H_{22}{}^{79}Br_2NO_3$ = 517.99610, found: 517.99637; calcd. for $[M+H]^+$ $C_{22}H_{20}{}^{79}Br^{81}BrNO_3$ = 519.99405, found: 519.99406.

**FT-IR:** $\tilde{\nu}$ 3558, 2508, 2025, 1987, 1756, 1548, 1234, 1198, 1081, 1036 $cm^{-1}$.

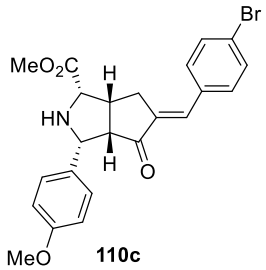


**Methyl (1*S*,3*R*,3*aS*,6*aR*)-5-((*E*)-4-bromobenzylidene)-3-(4-methoxyphenyl)-4-oxooctahydrocyclopenta[*c*]pyrrole-1-carboxylate (110c)**

yellow amorphous solid, 61% yield, **$^{1}$H NMR** (500 MHz, $CD_2Cl_2$) δ 7.56 (d, *J* = 8.5 Hz, 2H), 7.38 (d, *J* = 8.5 Hz, 2H), 7.18 (d, *J* = 8.7 Hz, 2H), 6.99 (t, *J* = 3.0 Hz, 1H), 6.79 (d, *J* = 8.7 Hz, 2H), 4.51 (d, *J* = 10.5 Hz, 1H), 4.12 (d, *J* = 5.4 Hz, 1H), 3.83 (s, 3H), 3.76 (s, 3H), 3.27 – 3.21 (m, 1H), 3.16 – 3.08 (m, 2H), 2.79 (ddd, *J* = 18.1, 7.0, 3.4 Hz, 1H).

**$^{13}$C NMR** (126 MHz, $CD_2Cl_2$) δ 206.61, 172.31, 159.50, 138.30, 134.97, 132.67, 132.43, 131.54, 131.06, 129.23, 124.09, 113.79, 65.51, 64.49, 56.70, 55.62, 52.48, 41.07, 31.84.

**HRMS**: calcd. for $[M+H]^+$ $C_{23}H_{23}{}^{79}BrNO_4$ = 456.08010, found: 456.08050; calcd. for $[M+H]^+$ $C_{23}H_{23}{}^{81}BrNO_4$ = 458.07800, found: 458.07845.

**HPLC conditions**: CHIRALPAK IC column, *iso*-propanol/ *iso*-hexane = 50/50, flow rate = 0.5 mL $min^{-1}$, minor enantiomer: $t_R$ = 66.88 min; major enantiomer: $t_R$ = 49.92 min; (69% e.e.).

**[α]**$^{20}$ D= + 166.2° (c = 0.1, CHCl3).

**FT-IR:** $\tilde{\nu}$ 2926, 2835, 1737, 1707, 1614, 1511, 1487, 1303, 1244, 1172, 1132, 1031 $cm^{-1}$.

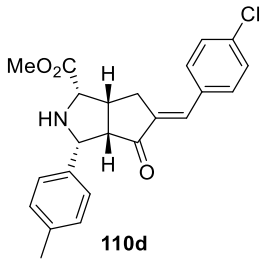


**110d**

**Methyl (1*S*,3*R*,3*aS*,6*aR*)-5-((*E*)-4-chlorobenzylidene)-4-oxo-3-(*p*-tolyl)octahydrocyclopenta[*c*]pyrrole-1-carboxylate (110d)**

white amorphous solid, 74% yield, **$^1$H NMR** (500 MHz, $CD_2Cl_2$) δ 7.48 – 7.37 (m, 4H), 7.15 (d, *J* = 7.9 Hz, 2H), 7.08 (d, *J* = 7.9 Hz, 2H), 7.02-6.99 (m, 1H), 4.52 (d, *J* = 10.4 Hz, 1H), 4.12 (d, *J* = 5.5 Hz, 1H), 3.83 (s, 3H), 3.29 – 3.08 (m, 3H), 2.86 – 2.78 (m, 1H), 2.30 (s, 3H).

**$^{13}$C NMR** (126 MHz, $CD_2Cl_2$) δ 206.47, 172.28, 138.13, 137.74, 136.52, 135.67, 134.57, 132.46, 130.99, 129.44, 129.24, 128.06, 65.88, 64.59, 56.73, 52.48, 41.14, 31.79, 21.39.

**HRMS**: calcd. for $[M+H]^+$ $C_{23}H_{23}{}^{35}ClNO_3$ = 396.13610, found: 396.13610; calcd. for $[M+H]^+$ $C_{23}H_{23}{}^{37}ClNO_3$ = 398.13316, found: 398.13315.

**HPLC conditions**: CHIRALPAK IC column, *iso*-propanol/ *iso*-hexane = 30/70, flow rate = 0.5 mL $min^{-1}$, minor enantiomer: $t_R$ = 39.63 min; major enantiomer: $t_R$ = 40.63 min; (84% e.e.).

**[α]$^{20}$ D**= + 265.2° (c = 0.1, $CHCl_3$).

**FT-IR:** $\tilde{\nu}$ 3458, 2514, 2058, 1723, 1511, 1487, 1221, 1123, 1088, 1025 $cm^{-1}$.

## 6.6 Synthesis of mixed double cycloaddition *endo, endo*-products

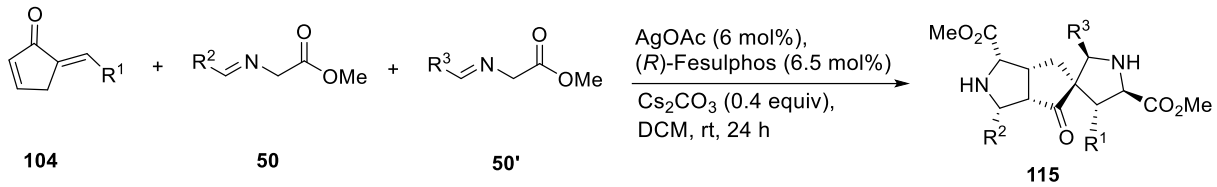


(*Rp*)-2-(tert-Butylthio)-1-(diphenylphosphino)ferrocene (6.5 mol%, 7.8 μmol) and silver acetate (6 mol%, 7.2 μmol) were dissolved in DCM (2mL) and stirred at ambient temperature for 15 min. To the resulting solution iminoester **50** (1.1 equiv., 0.13 mmol), Cs2CO3 (40 mol%, 48 μmol) and enone **104** (1 equiv., 0.12 mmol) were added and the mixture was allowed to stir at ambient temperature for 3 h followed by addition of second iminoester **50'** (1.1 equiv., 0.13 mmol). The reaction mixture was stirred at ambient temperature for at least 24 h. The crude mixture was directly charged onto silica gel and the product was isolated using n-pentane / acetone as eluent.

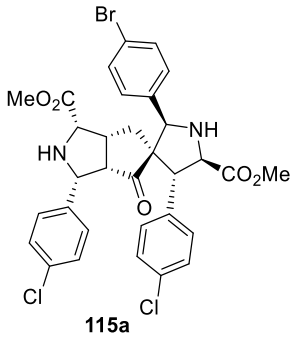


115a

**Dimethyl (1*S*,2'*R*,3*R*,3*aS*,4'*R*,5*R*,5'*R*,6*aR*)-2'-(4-bromophenyl)-3,4'-bis(4-chlorophenyl)-4-oxohexahydro-1*H*-spiro[cyclopenta[*c*]pyrrole-5,3'-pyrrolidine]-1,5'-dicarboxylate (115a)**

white amorphous solid, 77% yield, **$^{1}$H NMR** (400 MHz, $CD_2Cl_2$) δ 7.47 (d, *J* = 8.4 Hz, 2H), 7.38 (d, *J* = 8.5 Hz, 2H), 7.27 (d, *J* = 8.5 Hz, 2H), 7.13-7.11 (m, 4H), 7.02 (d, *J* = 8.4 Hz, 2H), 4.25 (s, 1H), 4.15 (d, *J* = 10.6 Hz, 1H), 3.95 (d, *J* = 7.2 Hz, 1H), 3.75 (d, *J* = 5.6 Hz, 1H), 3.65 (s, 3H), 3.59 (s, 3H), 3.45 (d, *J* = 7.2 Hz, 1H), 2.77 (s, 1H), 2.66 – 2.59 (m, 1H), 2.09 – 1.99 (m, 2H), 1.76 (m, 1H), 1.59 (*J* = 13.6, 10.6 Hz, 1H).

**$^{13}$C NMR** (101 MHz, $CD_2Cl_2$) δ 216.68, 173.29, 171.55, 138.48, 138.37, 137.98, 133.59, 133.38, 132.33, 131.11, 130.20, 129.71, 129.21, 128.49, 122.84, 74.76, 68.35, 67.05, 63.96, 63.11, 55.91, 55.28, 52.60, 52.24, 40.28, 34.50.

**HRMS**: calcd. for $[M+H]^+$ $C_{32}H_{29}{}^{79}Br^{35}Cl_2N_2O_5$ = 671.07191, found: 671.07097; calcd. for $[M+H]^+$ $C_{32}H_{29}{}^{81}Br^{35}Cl\ N_2O_5$ = 673.06915, found: 673.06892; calcd. for $[M+H]^+$ $C_{32}H_{29}{}^{81}Br^{37}Cl^{35}ClN_2O_5$ = 675.06689, found: 675.06597.

**HPLC** conditions: CHIRALPAK IC column, *iso*-propanol/ *iso*-hexane = 40/60, flow rate = 0.5 mL min$^{-1}$, minor enantiomer: $t_R$ = 15.28 min; major enantiomer: $t_R$ = 21.02 min; (85% e.e.).

**$[\alpha]^{20}_{D}$** = + 65.6° (c = 0.2, $CHCl_3$).

**FT-IR:** $\tilde{\nu}$ 3423**,** 2528 ,2159, 2030, 1955, 1578, 1496, 1215, 1105, 1032 cm$^{-1}$.

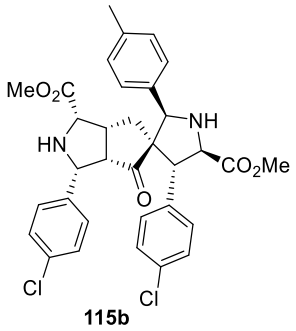


**115b**

**Dimethyl (1*S*,2'*R*,3*R*,3*aS*,4'*R*,5*R*,5'*R*,6*aR*)-3,4'-bis(4-chlorophenyl)-4-oxo-2'-(*p*-tolyl)hexahydro-1*H*-spiro[cyclopenta[*c*]pyrrole-5,3'-pyrrolidine]-1,5'-dicarboxylate (115b)**

white amorphous solid, 65% yield, **$^{1}$H NMR** (600 MHz, $CD_2Cl_2$) δ 7.38 (d, *J* = 8.4 Hz, 2H), 7.27 (d, *J* = 8.4 Hz, 2H), 7.15 – 7.11 (m, 6H), 7.03 (d, *J* = 8.4 Hz, 2H), 4.22 (s, 1H), 4.13 (d, *J* = 10.7 Hz, 1H), 3.98 (s, 1H), 3.95 (d, *J* = 7.1 Hz, 1H), 3.73 (d, *J* = 5.8 Hz, 1H), 3.65 (s, 3H), 3.60 (s, 3H), 3.42 (d, *J* = 7.1 Hz, 1H), 2.63 – 2.57 (m, 1H), 2.33 (s, 3H), 2.03 – 1.97 (m, 1H), 1.76 – 1.73 (m, 1H), 1.56 (dd, *J* = 13.4, 10.7 Hz, 1H).

**$^{13}$C NMR** (151 MHz, $CD_2Cl_2$) δ 217.14, 173.36, 171.66, 138.95, 138.90, 138.57, 135.22, 133.47, 133.33, 131.09, 129.88, 129.73, 129.17, 128.47, 128.21, 75.51, 68.47, 67.29, 63.92, 63.12, 55.96, 55.75, 52.56, 52.21, 40.36, 34.52, 21.41.

**HRMS**: calcd. for $[M+H]^+$ $C_{33}H_{32}{}^{35}Cl_2N_2O_5$ = 607.17639, found: 607.17610; calcd. for $[M+H]^+$ $C_{33}H_{32}{}^{35}Cl^{37}ClN_2O_5$ = 609.17367, found: 609.17315; calcd. for $[M+H]^+$ $C_{33}H_{32}{}^{37}Cl_2N_2O_5$ = 611.17036, found: 611.17020.

**HPLC** conditions: CHIRALPAK IC column, *iso*-propanol/ *iso*-hexane = 40/60, flow rate = 0.5 mL min$^{-1}$, minor enantiomer: $t_R$ = 21.61 min; major enantiomer: $t_R$ = 55.35 min; (82% e.e.).

**$[\alpha]^{20}_{D}$** = + 57.9° (c = 0.2, $CHCl_3$).

**FT-IR:** $\tilde{\nu}$ 3325, 2958, 2315, 2087, 1734, 1505, 1487, 1148, 1091, 1013, cm$^{-1}$.

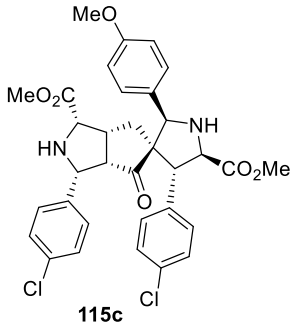


**115c**

**Dimethyl (1*S*,2'*R*,3*R*,3*aS*,4'*R*,5*R*,5'*R*,6*aR*)-3,4'-bis(4-chlorophenyl)-2'-(4-methoxyphenyl)-4-oxohexahydro-1*H*-spiro[cyclopenta[*c*]pyrrole-5,3'-pyrrolidine]-1,5'-dicarboxylate (115c)**

white amorphous solid, 55% yield, **$^{1}$H NMR** (600 MHz, $CD_2Cl_2$) δ 7.38 (d, *J* = 8.4 Hz, 2H), 7.27 (d, *J* = 8.4 Hz, 2H), 7.16 (d, *J* = 8.6 Hz, 2H), 7.12 (d, *J* = 8.4 Hz, 2H), 7.03 (d, *J* = 8.4 Hz, 2H), 6.85 (d, *J* = 8.6 Hz, 2H), 4.21 (s, 1H), 4.13 (d, *J* = 10.6 Hz, 1H), 3.94 (d, *J* = 7.1 Hz, 1H), 3.79 (s, 3H), 3.73 (d, *J* = 5.8 Hz, 1H), 3.64 (s, 3H), 3.60 (s, 3H), 3.42 (d, *J* = 7.1 Hz, 1H), 2.77 (bs, 1H), 2.64 – 2.58 (m, 1H), 1.99 (dd, *J* = 13.5, 10.6 Hz, 1H), 1.77– 1.71 (m, 1H), 1.55 (dd, *J* = 13.5, 10.6 Hz, 1H).

**$^{13}$C NMR** (151 MHz, $CD_2Cl_2$) δ 217.30, 173.38, 171.66, 160.24, 138.96, 138.59, 133.44, 133.33, 131.07, 130.11, 129.74, 129.48, 129.17, 128.47, 114.50, 75.29, 68.29, 67.26, 63.92, 63.14, 55.93, 55.77, 55.71, 52.55, 52.20, 40.35, 34.62.

**HRMS**: calcd. for $[M+H]^+$ $C_{33}H_{33}{}^{35}Cl_2N_2O_6$ = 623.18971 found: 623.18958; calcd. for $[M+H]^+$ $C_{33}H_{33}{}^{35}Cl^{37}ClN_2O_6$ = 625.26857 found: 625.26765.

**HPLC** conditions: CHIRALPAK IC column, *iso*-propanol/ *iso*-hexane = 40/60, flow rate = 0.5 mL min$^{-1}$, minor enantiomer: $t_R$ = 20.96 min; major enantiomer: $t_R$ = 26.49 min; (83% e.e.).

**$[\alpha]^{20}_{D}$**= + 123.8° (c = 0.2, $CHCl_3$).

**FT-IR:** $\tilde{\nu}$ 3496, 2475, 2437, 1827, 1754, 1542, 1228, 1165, 1102, 102 5cm$^{-1}$.

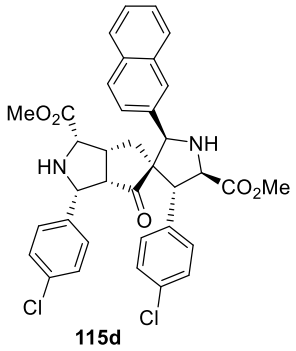


115d

**Dimethyl (1*S*,2'*R*,3*R*,3*aS*,4'*R*,5*R*,5'*R*,6*aR*)-3,4'-bis(4-chlorophenyl)-2'-(naphthalen-2-yl)-4-oxohexahydro-1*H*-spiro[cyclopenta[*c*]pyrrole-5,3'-pyrrolidine]-1,5'-dicarboxylate (115d)**

white amorphous solid, 63% yield, **$^{1}$H NMR** (600 MHz, $CD_2Cl_2$) δ 7.87 – 7.81 (m, 3H), 7.75 – 7.74 (m, 1H), 7.53 – 7.48 (m, 2H), 7.40 (d, *J* = 8.5 Hz, 2H), 7.36 (dd, *J* = 8.5, 1.9 Hz, 1H), 7.25 (d, *J* = 8.4 Hz, 2H), 7.16 (d, *J* = 8.4 Hz, 2H), 6.99 (d, *J* = 8.4 Hz, 2H), 4.45 (s, 1H), 4.07 – 4.02 (m, 2H), 3.68 – 3.65 (m, 4H), 3.63 (s, 3H), 3.53 (d, *J* = 7.3 Hz, 1H), 2.68 – 2.62 (m, 1H), 1.94 - 1.90 (m, 1H), 1.89 -1.85 (m, 1H), 1.64 – 1.54 (m, 2H).

**$^{13}$C NMR** (151 MHz, $CD_2Cl_2$) δ 216.83, 173.36, 171.62, 138.69, 138.45, 136.12, 133.84, 133.66, 133.54, 133.32, 131.17, 129.73, 129.20, 128.98, 128.59, 128.45, 128.18, 127.57, 126.97, 126.06, 75.72, 68.69, 67.28, 63.91, 63.09, 55.86, 55.69, 52.61, 52.23, 40.34, 34.64.

**HRMS**: calcd. for $[M+H]^+$ $C_{36}H_{32}{}^{35}Cl_2N_2O_5$ = 643.17790, found: 643.17610; calcd. for $[M+H]^+$ $C_{36}H_{32}{}^{35}Cl^{37}ClN_2O_5$ = 645.17539, found: 645.17315; calcd. for $[M+H]^+$ $C_{36}H_{32}{}^{37}Cl_2N_2O_5$ = 647.17179, found: 647.17020.

**HPLC** conditions: CHIRALPAK IC column, *iso*-propanol/ *iso*-hexane = 60/40, flow rate = 0.5 mL min$^{-1}$, minor enantiomer: $t_R$ = 18.98 min; major enantiomer: $t_R$ = 30.45 min; (89% e.e.).

**$[\alpha]^{20}_{D}$** = + 102.7° (c = 0.22, $CHCl_3$).

**FT-IR:** $\tilde{\nu}$ 3415, 2348, 2109, 1735, 1732, 1496, 1211, 1172, 1097, 1048, cm$^{-1}$.

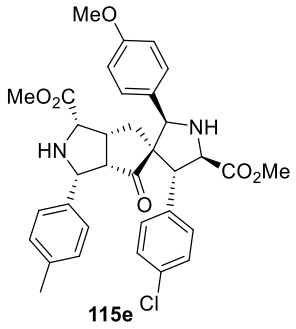


115e

**Dimethyl (1*S*,2'*R*,3*R*,3*aS*,4'*R*,5*R*,5'*R*,6*aR*)-4'-(4-chlorophenyl)-2'-(4-methoxyphenyl)-4-oxo-3-(*p*-tolyl)hexahydro-1*H*-spiro[cyclopenta[*c*]pyrrole-5,3'-pyrrolidine]-1,5'-dicarboxylate (115e)**

yellow amorphous solid, 70% yield, **$^{1}$H NMR** (600 MHz, $CD_2Cl_2$) δ 7.39 (d, *J* = 8.4 Hz, 2H), 7.15 (dd, *J* = 8.7 Hz, 2H), 7.14 (d, *J* = 8.4 Hz, 2H) 7.12 (d, *J* = 8.4 Hz, 2H), 6.92 (d, *J* = 8.7 Hz, 2H), 6.85 (d, *J* = 8.7 Hz, 2H), 4.19 (s, 1H), 4.10 (d, *J* = 10.7 Hz, 1H), 3.94 (d, *J* = 7.3 Hz, 1H), 3.80 (s, 3H), 3.70 (d, *J* = 5.8 Hz, 1H), 3.64 (s, 3H), 3.59 (s, 3H), 3.44 (d, *J* = 7.3 Hz, 1H), 2.61 – 2.56 (m, 1H), 2.36 (s, 3H), 1.98-1.96 (m, 1H), 1.73-1.69 (m, 1H), 1.55 (dd, *J* = 13.7, 10.7 Hz, 1H).

**$^{13}$C NMR** (151 MHz, $CD_2Cl_2$) δ 217.65, 173.30, 171.82, 160.23, 139.18, 137.69, 136.60, 133.40, 131.13, 129.98, 129.53, 129.16, 129.09, 128.25, 114.47, 75.50, 68.39, 67.54, 64.86, 63.24, 56.34, 55.93, 55.77, 52.49, 52.16, 40.76, 34.62, 21.46.

**HRMS**: calcd. for $[M+H]^+$ $C_{34}H_{35}{}^{35}ClN_2O_6$ = 603.22708, found: 603.22564; calcd. for $[M+H]^+$ $C_{34}H_{35}{}^{37}ClN_2O_6$ = 605.22458, found: 605.22269.

**HPLC** conditions: CHIRALPAK IC column, *iso*-propanol/ *iso*-hexane = 80/20, flow rate = 0.5 mL min$^{-1}$, minor enantiomer: $t_R$ = 24.02 min; major enantiomer: $t_R$ = 57.97 min; (89% e.e.).

**$[\alpha]^{20}_{D}$** = + 114.1° (c = 0.22, $CHCl_3$).

**FT-IR:** $\tilde{\nu}$ 3339, 2448, 2021, 1735, 1589, 1496, 1235, 1115, 1078, 1023 cm$^{-1}$.

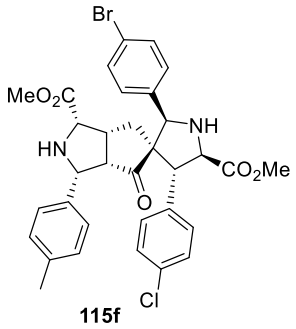


115f

**Dimethyl (1*S*,2'*R*,3*R*,3*aS*,4'*R*,5*R*,5'*R*,6*aR*)-2'-(4-bromophenyl)-4'-(4-chlorophenyl)-4-oxo-3-(*p*-tolyl)hexahydro-1*H*-spiro[cyclopenta[*c*]pyrrole-5,3'-pyrrolidine]-1,5'-dicarboxylate (115f)**

white amorphous solid, 65% yield, **$^{1}$H NMR** (400 MHz, $CD_2Cl_2$) δ 7.47 (d, *J* = 8.5 Hz, 2H), 7.39 (d, *J* = 8.5 Hz, 2H), 7.17 – 7.09 (m, 6H), 6.92 (d, *J* = 8.0 Hz, 2H), 4.23 (s, 1H), 4.12 (d, *J* = 10.6 Hz, 1H), 3.98 (d, *J* = 7.3 Hz, 1H), 3.72 (d, *J* = 5.7 Hz, 1H), 3.65 (s, 3H), 3.58 (s, 3H), 3.47 (d, *J* = 7.3 Hz, 1H), 2.78 (bs, 1H), 2.64 – 2.50 (m, 1H), 2.36 (s, 3H), 2.08 – 1.93 (m, 2H), 1.79 – 1.73 (m, 1H), 1.59 (dd, *J* = 13.7, 10.6 Hz, 1H).

**$^{13}$C NMR** (101 MHz, $CD_2Cl_2$) δ 217.00, 173.22, 171.72, 138.72, 137.86, 137.73, 136.40, 133.53, 132.29, 131.17, 130.26, 129.20, 129.10, 128.22, 122.82, 75.00, 68.45, 67.33, 64.89, 63.21, 56.30, 55.52, 52.53, 52.19, 40.66, 34.51, 21.46.

**HRMS**: calcd. for $[M+H]^+$ $C_{33}H_{32}{}^{79}Br^{35}ClN_2O_5$ = 651.12765, found: 651.12559; calcd. for $[M+H]^+$ $C_{33}H_{32}{}^{81}Br^{35}ClN_2O_5$ = 653.12541, found: 653.12354; calcd. for $[M+H]^+$ $C_{33}H_{32}{}^{81}Br^{37}ClN_2O_5$ = 655.12220, found: 655.12059.

**HPLC** conditions: CHIRALPAK IC column, *iso*-propanol/ *iso*-hexane = 30/70, flow rate = 0.5 mL min$^{-1}$, minor enantiomer: $t_R$ = 24.85 min; major enantiomer: $t_R$ = 55.27 min; (90% e.e.).

**$[\alpha]^{20}$ D**= + 78.5° (c = 0.2, $CHCl_3$).

**FT-IR:** $\tilde{\nu}$ 3520, 2485, 2415, 1871, 1745, 1663, 1453, 1295, 1081, 1022 cm$^{-1}$.

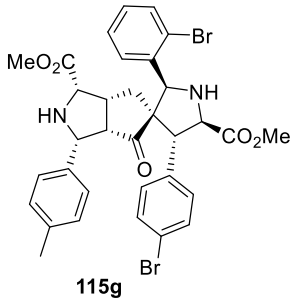


115g

**Dimethyl (1*S*,2'*S*,3*R*,3*aS*,4'*R*,5*R*,5'*R*,6*aR*)-2'-(2-bromophenyl)-4'-(4-bromophenyl)-4-oxo-3-(*p*-tolyl)hexahydro-1*H*-spiro[cyclopenta[*c*]pyrrole-5,3'-pyrrolidine]-1,5'-dicarboxylate (115g)**

white amorphous solid, 55% yield, **$^{1}$H NMR** (500 MHz, $CD_2Cl_2$) δ 7.60 (dd, *J* = 8.0, 1.3 Hz, 1H), 7.55 (d, *J* = 8.5 Hz, 2H), 7.37 – 7.27 (m, 2H), 7.24 – 7.15 (m, 2H), 7.11 (d, *J* = 8.5 Hz, 3H), 6.89 (d, *J* = 8.0 Hz, 2H), 4.96 (s, 1H), 4.13 (d, *J* = 10.7 Hz, 1H), 3.99-3.97 (m, 2H), 3.73 (d, *J* = 5.7 Hz, 1H), 3.66 (s, 3H), 3.59 (s, 3H), 3.47 (d, *J* = 7.7 Hz, 1H), 2.81 – 2.73 (m, 1H), 2.36 (s, 3H), 2.15 – 1.99 (m, 1H), 1.59 (dd, *J* = 13.6, 10.7 Hz , 1H).

**$^{13}$C NMR** (176 MHz, $CD_2Cl_2$) δ 216.54, 172.59, 171.18, 138.74, 137.36, 137.15, 135.93, 133.16, 131.63, 131.04, 129.58, 129.47, 128.55, 127.98, 127.66, 124.65, 121.10, 70.77, 68.38, 66.78, 64.37, 62.57, 55.87, 55.03, 51.97, 51.59, 40.26, 33.26, 20.89.

**HRMS**: calcd. for $[M+H]^+$ $C_{33}H_{32}{}^{79}Br_2N_2O_5$ = 695.07740, found: 695.07507; calcd. for $[M+H]^+$ $C_{33}H_{32}{}^{79}Br^{81}BrN_2O_6$ = 697.07539, found: 697.07303; calcd. for $[M+H]^+$ $C_{33}H_{32}{}^{81}Br_2N_2O_6$ = 699.07348, found: 699.07098.

**HPLC** conditions: CHIRALPAK IA column, *iso*-propanol/ *iso*-hexane = 15/85, flow rate = 0.5 mL min$^{-1}$, minor enantiomer: $t_R$ = 41.58 min; major enantiomer: $t_R$ = 45.36 min; (90% e.e.).

**$[\alpha]^{20}_D$** = + 44.6° (c = 0.18, $CHCl_3$).

**FT-IR:** $\tilde{\nu}$ 3368, 2360, 2355, 1732, 1492, 1434, 1207, 1152, 1090, 1010, cm$^{-1}$.

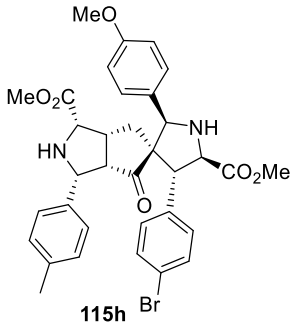


115h

**Dimethyl (1*S*,2'*R*,3*R*,3*aS*,4'*R*,5*R*,5'*R*,6*aR*)-4'-(4-bromophenyl)-2'-(4-methoxyphenyl)-4-oxo-3-(*p*-tolyl)hexahydro-1*H*-spiro[cyclopenta[*c*]pyrrole-5,3'-pyrrolidine]-1,5'-dicarboxylate (115h)**

white amorphous solid, 59% yield, **$^{1}$H NMR** (400 MHz, $CD_2Cl_2$) δ 7.54 (d, *J* = 8.7 Hz, 2H), 7.15 (d, *J* = 8.7 Hz, 2H), 7.12-7.09 (m, 4H), 6.92 (d, *J* = 8.8 Hz, 2H), 6.85 (d, *J* = 8.8 Hz, 2H), 4.19 (s, 1H), 4.10 (d, *J* = 10.7 Hz, 1H), 3.93 (d, *J* = 7.3 Hz, 1H), 3.80 (s, 3H), 3.70 (d, *J* = 5.7 Hz, 1H), 3.64 (s, 3H), 3.59 (s, 3H), 3.42 (d, *J* = 7.3 Hz, 1H), 2.78 (bs, 1H), 2.63 – 2.54 (m, 1H), 2.36 (s, 3H), 2.03 – 1.94 (m, 1H), 1.73 (m, 1H), 1.56 (dd, *J* = 13.7, 10.7 Hz, 1H).

**$^{13}$C NMR** (101 MHz, $CD_2Cl_2$) δ 217.61, 173.29, 171.82, 160.24, 139.70, 137.69, 136.61, 132.14, 131.50, 130.01, 129.53, 129.09, 128.25, 121.53, 114.48, 75.53, 68.35, 67.50, 64.86, 63.25, 56.34, 56.00, 55.77, 52.49, 52.17, 40.78, 34.62, 21.46.

**HRMS**: calcd. for $[M+H]^+$ $C_{34}H_{35}{}^{79}BrN_2O_6$ = 647.17683, found: 647.17513; calcd. for $[M+H]^+$ $C_{34}H_{35}{}^{81}BrN_2O_6$ = 649.17514, found: 649.17308.

**HPLC** conditions: CHIRALPAK IA column, *iso*-propanol/ *iso*-hexane = 20/80, flow rate = 0.5 mL min$^{-1}$, minor enantiomer: $t_R$ = 53.22 min; major enantiomer: $t_R$ = 47.58 min; (89% e.e.).

**$[\alpha]^{20}_{D}$** = + 127.5° (c = 0.2, $CHCl_3$).

**FT-IR:** $\tilde{\nu}$ 3652, 2534 ,2159, 2030, 1976, 1733, 1513, 1489, 1434, 1205, 1121, 1074, 1010 cm$^{-1}$.

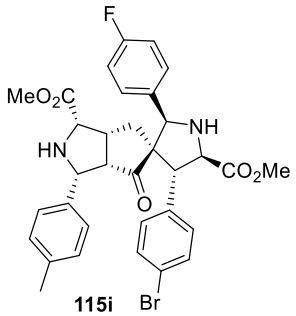


**115i**

white amorphous solid, 78% yield, **$^{1}$H NMR** (600 MHz, $CD_2Cl_2$) δ 7.54 (d, *J* = 8.4 Hz, 2H), 7.24 (dd, *J* = 8.4, 2H), 7.12 – 7.08 (m, 4H), 7.03 (d, *J* = 8.1 Hz, 2H), 6.92 (d, *J* = 8.1 Hz, 2H), 4.25 (s, 1H), 4.11 (d, *J* = 10.7 Hz, 1H), 3.96 (d, *J* = 7.3 Hz, 1H), 3.71 (d, *J* = 5.7 Hz, 1H), 3.65 (s, 3H), 3.58 (s, 3H), 3.45 (d, *J* = 7.3 Hz, 1H), 2.77 (bs, 1H), 2.62 – 2.55 (m, 1H), 2.36 (s, 3H), 2.03 (bs, 1H), 2.01 – 1.95 (m, 1H), 1.78 – 1.74 (m, 1H), 1.59 (dd, *J* = 13.5, 10.7 Hz, 1H).

**$^{13}$C NMR** (151 MHz, $CD_2Cl_2$) δ 216.63, 172.67, 171.17, 163.45 (d, *J* = 246.7 Hz), 138.78, 137.16, 135.87, 133.87 (d, *J* = 3.1 Hz), 131.60, 130.95, 129.67 (d, *J* = 8.1 Hz), 128.53, 127.66, 121.06, 115.55 (d, *J* = 21.5 Hz), 74.45, 67.74, 66.73, 64.30, 62.66, 55.72, 55.09, 51.96, 51.64, 40.10, 33.98, 20.89.

**$^{19}$F NMR** (565 MHz, $CD_2Cl_2$) δ -114.2 (m).

**HRMS**: calcd. for $[M+H]^+$ $C_{33}H_{33}{}^{79}BrFN_2O_5$ = 635.15514, found: 635.15578; calcd. for $[M+H]^+$ $C_{33}H_{33}{}^{81}BrFN_2O_5$= 637.15309, found: 637.15414.

**HPLC** conditions: CHIRALPAK IC column, *iso*-propanol/ *iso*-hexane = 30/70, flow rate = 0.5 mL min$^{-1}$, minor enantiomer: $t_R$ = 18.50 min; major enantiomer: $t_R$ = 44.05 min; (90% e.e.).

**$[\alpha]^{20}_{D}$**= + 115.5° (c = 0.2, $CHCl_3$).

**FT-IR:** $\tilde{\nu}$ 3448, 2515, 2159, 2030, 1732, 1513, 1435, 1248, 1183, 1031 cm$^{-1}$.

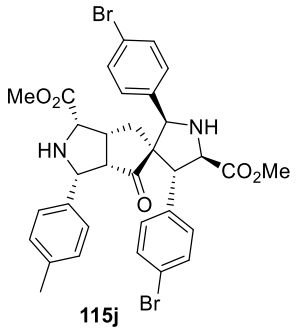


115j

**Dimethyl (1*S*,2'*R*,3*R*,3*aS*,4'*R*,5*R*,5'*R*,6*aR*)-2',4'-bis(4-bromophenyl)-4-oxo-3-(*p*-tolyl)hexahydro-1*H*-spiro[cyclopenta[*c*]pyrrole-5,3'-pyrrolidine]-1,5'-dicarboxylate (115j)**

white amorphous solid, 72% yield, **$^{1}$H NMR** (700 MHz, $CD_2Cl_2$) δ 7.54 (d, *J* = 8.4 Hz, 2H), 7.46 (d, *J* = 8.4 Hz, 2H), 7.15 (d, *J* = 8.0 Hz, 2H), 7.12-7.08 (m, 4H), 6.92 (d, *J* = 8.0 Hz, 2H), 4.23 (s, 1H), 4.12 (d, *J* = 10.8 Hz, 1H), 3.99 (s, 1H), 3.97 (d, *J* = 7.3 Hz, 1H), 3.72 (d, *J* = 5.8 Hz, 1H), 3.65 (s, 3H), 3.58 (s, 3H), 3.45 (d, *J* = 7.3 Hz, 1H), 2.62 – 2.57 (m, 1H), 2.36 (s, 3H), 2.03 – 1.98 (m, 1H), 1.78 – 1.74 (m, 1H), 1.59 (dd, *J* = 13.6, 10.8 Hz, 1H).

**$^{13}$C NMR** (176 MHz, $CD_2Cl_2$) δ 216.98, 173.18, 171.71, 139.21, 137.80, 137.73, 136.39, 132.30, 132.18, 131.52, 130.25, 129.11, 128.22, 122.84, 121.67, 74.97, 68.39, 67.26, 64.89, 63.22, 56.30, 55.56, 52.55, 52.21, 40.67, 34.48, 21.46.

**HRMS**: calcd. for $[M+H]^+$ $C_{33}H_{32}{}^{79}Br_2N_2O_5$ = 695.07740, found: 695.07507; calcd. for $[M+H]^+$ $C_{33}H_{32}{}^{79}Br^{81}BrN_2O_5$ = 697.06780, found: 697.07531; calcd. for $[M+H]^+$ $C_{33}H_{32}{}^{81}Br_2N_2O_5$ = 699.07358, found: 699.07098.

**HPLC** conditions: CHIRALPAK IC column, *iso*-propanol/ *iso*-hexane = 30/70, flow rate = 0.5 mL min$^{-1}$, minor enantiomer: $t_R$ = 25.90 min; major enantiomer: $t_R$ = 58.02 min; (87% e.e.).

**$[\alpha]^{20}$ D**= + 74.7° (c = 0.36, $CHCl_3$).

**FT-IR:** $\tilde{\nu}$ 3378, 2514, 2159, 2058, 1733, 1515, 1455, 1221, 1109, 1015 cm$^{-1}$.

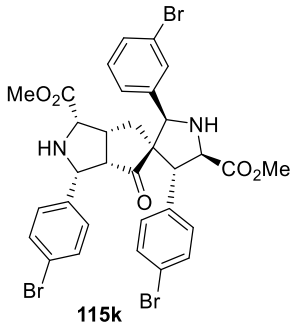


115k

**Dimethyl (1*S*,2'*R*,3*R*,3*aS*,4'*R*,5*R*,5'*R*,6*aR*)-2'-(3-bromophenyl)-3,4'-bis(4-bromophenyl)-4-oxohexahydro-1*H*-spiro[cyclopenta[*c*]pyrrole-5,3'-pyrrolidine]-1,5'-dicarboxylate (115k)**

white amorphous solid, 69% yield, **$^{1}$H NMR** (500 MHz, $CD_2Cl_2$) δ 7.53 (d, *J* = 8.4 Hz, 1H), 7.48 – 7.39 (m, 4H), 7.25 – 7.13 (m, 2H), 7.04 (d, *J* = 8.4 Hz, 1H), 6.94 (d, *J* = 8.3 Hz, 1H), 4.24 (s, 1H), 4.15 (d, *J* = 10.6 Hz, 1H), 3.99 (d, *J* = 7.5 Hz, 1H), 3.78 (d, *J* = 5.5 Hz, 1H), 3.67 (s, 2H), 3.60 (s, 2H), 2.76 (s, 0H), 2.70 – 2.63 (m, 1H), 2.10 – 2.00 (m, 2H), 1.83 – 1.78 (m, 1H), 1.61 (dd, *J* = 13.4, 10.8 Hz, 1H).

**$^{13}$C NMR** (126 MHz, $CD_2Cl_2$) δ 216.22, 173.21, 171.53, 141.59, 138.76, 138.56, 132.14, 132.03, 131.53, 131.43, 130.85, 130.17, 130.06, 127.11, 123.07, 121.72, 121.49, 74.50, 68.35, 66.75, 63.97, 63.06, 55.75, 55.08, 52.66, 52.29, 40.22, 34.38.

**HRMS**: calcd. for $[M+H]^+$ $C_{32}H_{29}{}^{79}Br_3N_2O_5$ = 758.96994, found: 758.97047; calcd. for $[M+H]^+$ $C_{32}H_{29}{}^{79}Br_2{}^{81}BrN_2O_5$ = 760.96789, found: 760.96839; calcd. for $[M+H]^+$ $C_{32}H_{29}{}^{79}Br^{81}Br_2N_2O_5$ = 762.96584, found: 762.96640; calcd. for $[M+H]^+$ $C_{32}H_{29}{}^{81}Br_3N_2O_5$ = 764.96380, found: 764.96363.

**HPLC** conditions: CHIRALPAK IA column, *iso*-propanol/ *iso*-hexane = 70/30, flow rate = 0.5 mL min$^{-1}$, minor enantiomer: $t_R$ = 21.04 min; major enantiomer: $t_R$ = 27.46 min; (89% e.e.).

**$[\alpha]^{20}_D$** = + 148.6° (c = 0.2, $CHCl_3$).

**FT-IR:** $\tilde{\nu}$ 3343, 2921, 2850, 2160, 2035, 1731, 1592, 1568 ,1487, 1434, 1373, 1206, 1072, 1009 cm$^{-1}$.

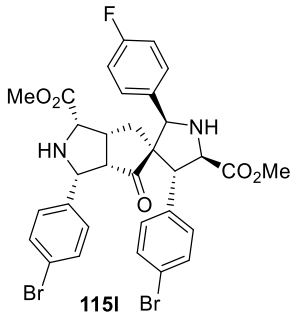


115l

**Dimethyl (1*S*,2'*R*,3*R*,3*aS*,4'*R*,5*R*,5'*R*,6*aR*)-3,4'-bis(4-bromophenyl)-2'-(4-fluorophenyl)-4-oxohexahydro-1*H*-spiro[cyclopenta[*c*]pyrrole-5,3'-pyrrolidine]-1,5'-dicarboxylate (115l)**

white amorphous solid, 72% yield,**$^{1}$H NMR** (500 MHz, $CD_2Cl_2$) δ 7.53 (d, *J* = 8.4 Hz, 2H), 7.42 (d, *J* = 8.4 Hz, 2H), 7.28 – 7.23 (m, 2H), 7.09 – 7.03 (m, 4H), 6.97 (d, *J* = 8.2 Hz, 2H), 4.27 (s, 1H), 4.13 (d, *J* = 10.7 Hz, 1H), 3.96 (d, *J* = 7.2 Hz, 1H), 3.74 (d, *J* = 6.0 Hz, 1H), 3.65 (s, 3H), 3.60 (s, 3H), 3.43 (d, *J* = 7.2 Hz, 1H), 2.76 (bs, 1H), 2.63 – 2.56 (m, 1H), 2.08 – 1.97 (m, 2H), 1.78 – 1.73 (m, 1H), 1.60 – 1.56 (m, 1H).

**$^{13}$C NMR** (126 MHz, $CD_2Cl_2$) δ 216.88, 173.31, 171.55, 163.17 (d, *J* = 246.8 Hz), 139.00 (d, *J* = 22.1 Hz), 138.91, 134.52, 134.49, 132.16, 131.43, 130.17, 130.10, 130.04, 121.57 (d, *J* = 20.5 Hz), 116.07 (d, J = 21.5 Hz), 114.31, 74.73, 68.17, 66.99, 63.93, 63.08, 55.82, 55.38, 52.63, 52.25, 40.23, 34.49.

**HRMS**: calcd. for $[M+H]^+$ $C_{32}H_{30}{}^{79}Br_2FN_2O_5$ = 699.05000, found: 699.05037; calcd. for $[M+H]^+$ $C_{32}H_{30}{}^{79}Br^{81}BrFN_2O_5$ = 701.04796, found: 701.04822; calcd. for $[M+H]^+$ $C_{32}H_{30}{}^{81}Br_2FN_2O_5$ = 703.04591, found: 703.04631.

**HPLC** conditions: CHIRALPAK IA column, *iso*-propanol/ *iso*-hexane = 70/30, flow rate = 0.5 mL min$^{-1}$, minor enantiomer: $t_R$ = 27.32 min; major enantiomer: $t_R$ = 20.59 min; (90% e.e.).

**$[\alpha]^{20}_{D}$** = + 157.6° (c = 0.2, $CHCl_3$).

**FT-IR:** $\tilde{\nu}$ 3343, 2922, 2852, 1731, 1611, 1511, 1488, 1434 ,1375, 1209, 1074,1009 cm$^{-1}$.

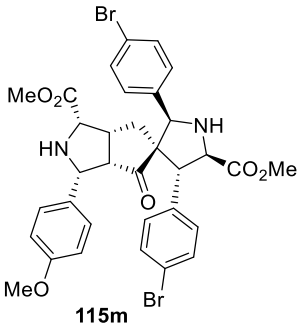


115m

**Dimethyl (1*S*,2'*R*,3*R*,3*aS*,4'*R*,5*R*,5'*R*,6*aR*)-2',4'-bis(4-bromophenyl)-3-(4-methoxyphenyl)-4-oxohexahydro-1*H*-spiro[cyclopenta[*c*]pyrrole-5,3'-pyrrolidine]-1,5'-dicarboxylate (115m)**

white amorphous solid, 60% yield, **$^{1}$H NMR** (500 MHz, $CD_2Cl_2$) δ 7.54 (d, *J* = 8.4 Hz, 2H), 7.46 (d, *J* = 8.4 Hz, 2H), 7.15 (d, *J* = 8.5 Hz, 2H), 7.08 (d, *J* = 8.5 Hz, 2H), 6.94 (d, *J* = 8.7 Hz, 2H), 6.82 (d, *J* = 8.7 Hz, 2H), 4.23 (s, 1H), 4.12 (d, *J* = 10.7 Hz, 1H), 3.96 (d, *J* = 7.3 Hz, 1H), 3.81 (s, 3H), 3.72 (d, *J* = 5.7 Hz, 1H), 3.65 (s, 3H), 3.58 (s, 3H), 3.46 (d, *J* = 7.2 Hz, 1H), 2.78 (bs, 1H), 2.64 – 2.57 (m, 1H), 2.08 – 1.96 (m, 2H), 1.79 – 1.73 (m, 1H), 1.60 (dd, *J* = 13.5, 10.6 Hz, 1H).

**$^{13}$C NMR** (126 MHz, $CD_2Cl_2$) δ 217.02, 173.22, 171.72, 159.52, 139.16, 137.86, 132.27, 132.16, 131.49, 131.37, 130.21, 129.32, 122.79, 121.64, 113.66, 74.87, 68.37, 67.21, 64.48, 63.07, 56.14, 55.69, 55.48, 52.55, 52.21, 40.57, 34.43.

**HRMS**: calcd. for $[M+H]^+$ $C_{33}H_{33}{}^{79}Br_2N_2O_6$ = 711.06999, found: 711.07037; calcd. for $[M+H]^+$ $C_{33}H_{33}{}^{79}Br^{81}BrN_2O_6$ = 713.06794, found: 713.06830; calcd. for $[M+H]^+$ $C_{33}H_{33}{}^{81}Br_2N_2O_6$ = 715.06590, found: 715.06661.

**HPLC** conditions: CHIRALPAK IA column, *iso*-propanol/ *iso*-hexane = 70/30, flow rate = 0.5 mL min$^{-1}$, minor enantiomer: $t_R$ = 48.61 min; major enantiomer: $t_R$ = 59.88 min; (90% e.e.).

**[α]$^{20}$ D**= + 177.6° (c = 0.2, CHCl3).

**FT-IR:** $\tilde{\nu}$ 3342, 2921, 2851, 2160, 2036, 1731, 1612, 1511 ,1435, 1245, 1075, 1009 cm$^{-1}$.

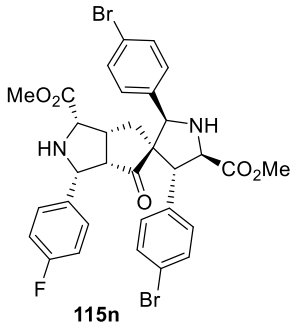


115n

**Dimethyl (1*S*,2'*R*,3*R*,3*aS*,4'*R*,5*R*,5'*R*,6*aR*)-2',4'-bis(4-bromophenyl)-3-(4-fluorophenyl)-4-oxohexahydro-1*H*-spiro[cyclopenta[*c*]pyrrole-5,3'-pyrrolidine]-1,5'-dicarboxylate (115n)**

white amorphous solid, 70% yield, **$^{1}$H NMR** (500 MHz, $CD_2Cl_2$) δ 7.53 (d, *J* = 8.4 Hz, 2H), 7.47 (d, *J* = 8.4 Hz, 2H), 7.15 (d, *J* = 8.5 Hz, 2H), 7.06 (d, *J* = 8.5 Hz, 2H), 7.03 – 6.96 (m, 4H), 4.24 (s, 1H), 4.16 (d, *J* = 10.7 Hz, 1H), 3.97 (d, *J* = 7.2 Hz, 1H), 3.75 (d, *J* = 5.7 Hz, 1H), 3.66 (s, 3H), 3.58 (s, 3H), 3.44 (d, *J* = 7.2 Hz, 1H), 2.76 (bs, 1H), 2.66 – 2.59 (m, 1H), 2.06 – 2.01 (m, 2H), 1.81 – 1.75 (m, 1H), 1.60 (dd, *J* = 13.5, 10.7 Hz, 2H).

**$^{13}$C NMR** (126 MHz, $CD_2Cl_2$) δ 216.75, 173.24, 171.59, 162.58 (d, *J* = 244.8 Hz), 138.94, 137.95, 135.40, 135.38, 132.22 (d, *J* = 17.0 Hz), 131.47, 130.17, 129.83 (d, *J* = 8.0 Hz), 122.80, 121.68, 115.11 (d, *J* = 21.4 Hz), 74.71, 68.32, 67.00, 63.96, 63.04, 55.85, 55.34, 52.57, 52.24, 40.30, 34.45.

**HRMS**: calcd. for $[M+H]^+$ $C_{32}H_{30}{}^{79}Br_2FN_2O_5$ = 699.05000, found: 699.05022; calcd. for $[M+H]^+$ $C_{32}H_{30}{}^{79}Br^{81}BrFN_2O_5$ = 701.04796, found: 701.04813; calcd. for $[M+H]^+$ $C_{32}H_{30}{}^{81}Br_2FN_2O_5$ = 703.04591, found: 703.04628.

**HPLC** conditions: CHIRALPAK IA column, *iso*-propanol/ *iso*-hexane = 70/30, flow rate = 0.5 mL min$^{-1}$, minor enantiomer: $t_R$ = 19.92 min; major enantiomer: $t_R$ = 27.10 min; (89% e.e.).

**$[\alpha]^{20}_{D}$** = + 157.6° (c = 0.2, $CHCl_3$).

**FT-IR:** $\tilde{\nu}$ 2922, 2851, 2161, 1732, 1604, 1508, 1489 ,1434, 1214, 1075, 1009 cm$^{-1}$.

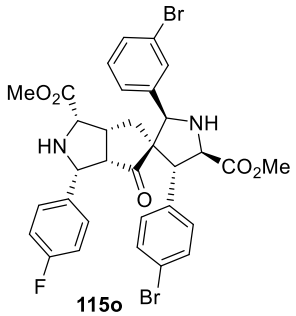


**115o**

**Dimethyl (1*S*,2'*R*,3*R*,3*aS*,4'*R*,5*R*,5'*R*,6*aR*)-2'-(3-bromophenyl)-4'-(4-bromophenyl)-3-(4-fluorophenyl)-4-oxohexahydro-1*H*-spiro[cyclopenta[*c*]pyrrole-5,3'-pyrrolidine]-1,5'-dicarboxylate (115o)**

white amorphous solid, 75% yield, **$^{1}$H NMR** (500 MHz, $CD_2Cl_2$) δ 7.53 (d, *J* = 8.5 Hz, 2H), 7.47 – 7.42 (m, 2H), 7.25 – 7.20 (m, 2H), 7.05 (d, *J* = 8.4 Hz, 2H), 7.01 – 6.95 (m, 4H), 4.25 (s, 1H), 4.16 (d, *J* = 4.0 Hz, 1H), 3.99 (d, *J* = 7.7 Hz, 1H), 3.78 (d, *J* = 4.0 Hz, 1H), 3.68 (s, 3H), 3.59 (s, 3H), 3.47 (d, *J* = 7.7 Hz, 1H), 2.76 (bs, 1H), 2.71 – 2.65 (m, 1H), 2.12 – 2.02 (m, 2H), 1.84 – 1.80 (m, 1H), 1.62 (dd, *J* = 13.5, 10.7 Hz, 1H).

**$^{13}$C NMR** (126 MHz, $CD_2Cl_2$) δ 216.28, 173.19, 171.59, 162.57 (d, *J* = 244.8 Hz), 141.65, 138.54, 135.31, 132.13, 132.01, 131.58, 131.43, 130.83, 129.86 (d, *J* = 7.9 Hz), 127.12, 123.05, 121.72, 115.11 (d, *J* = 21.3 Hz), 74.50, 71.96, 68.42, 66.79, 63.99, 63.03, 55.77, 55.11, 52.60, 52.27, 40.29, 34.40.

**HRMS**: calcd. for $[M+H]^+$ $C_{32}H_{30}{}^{79}Br_2FN_2O_5$ = 699.05000, found: 699.05028; calcd. for $[M+H]^+$ $C_{32}H_{30}{}^{79}Br^{81}BrFN_2O_5$ = 701.04796, found: 701.04814; calcd. for $[M+H]^+$ $C_{32}H_{30}{}^{81}Br_2FN_2O_5$ = 703.04591, found: 703.04587.

**HPLC** conditions: CHIRALPAK IA column, *iso*-propanol/ *iso*-hexane = 70/30, flow rate = 0.5 mL min$^{-1}$, minor enantiomer: $t_R$ = 21.01 min; major enantiomer: $t_R$ = 68.05 min; (89% e.e.).

**$[\alpha]^{20}_{D}$** = + 157.6° (c = 0.2, $CHCl_3$).

**FT-IR:** $\tilde{\nu}$ 2922, 2852, 1732, 1568, 1508, 1489, 1210, 1154 ,1074, 1037, 1010, 965 cm$^{-1}$.

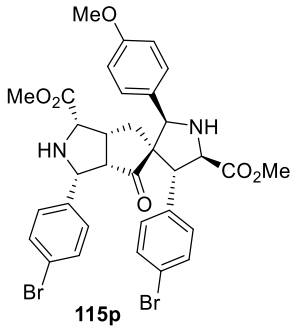


115p

**Dimethyl (1*S*,2'*R*,3*R*,3*aS*,4'*R*,5*R*,5'*R*,6*aR*)-3,4'-bis(4-bromophenyl)-2'-(4-methoxyphenyl)-4-oxohexahydro-1*H*-spiro[cyclopenta[*c*]pyrrole-5,3'-pyrrolidine]-1,5'-dicarboxylatewhite (115p)**

white amorphous solid, 37% yield, $^{1}$H NMR (600 MHz, $CDCl_3$) δ 7.46 (d, *J* = 7.4 Hz, 2H), 7.36 (d, *J* = 8.4 Hz, 2H), 7.07-7.10 (m, 4H), 6.99 (d, *J* = 8.4 Hz, 2H), 6.78 (d, *J* = 7.6 Hz, 2H), 4.28 (s, 1H), 4.13 (d, *J* = 10.8 Hz, 1H), 4.06 – 4.03 (m, 1H), 3.74 (s, 3H), 3.69 (d, *J* = 5.5 Hz, 1H), 3.61 (s, 3H), 3.59 (s, 3H), 3.34 (d, *J* = 4.8 Hz, 1H), 2.41-2.48 (m, 1H), 2.09 – 2.06 (m, 1H), 1.63 – 1.56 (m, 1H).

**$^{13}$C NMR** (151 MHz, $CDCl_3$) δ 217.46, 172.26, 171.15, 160.11, 138.29, 138.07, 132.09, 131.30, 130.75, 129.38, 129.12, 121.74, 121.47, 114.54, 67.09, 66.11, 63.48, 62.80, 55.98, 55.45, 52.88, 52.20, 39.92, 32.07, 29.85.

**HRMS**: calcd. for $[M+H]^+$ $C_{33}H_{33}{}^{79}Br_2N_2O_6$ = 711.06998, found: 711.06999; calcd. for $[M+H]^+$ $C_{33}H_{33}{}^{79}Br^{81}BrN_2O_6$ = 713.06794, found: 713.06794; calcd. for $[M+H]^+$ $C_{33}H_{33}{}^{81}Br_2N_2O_6$ = 715.06616, found: 715.06590;

**HPLC** conditions: CHIRALPAK IA column, *iso*-propanol/ *iso*-hexane = 40/60, flow rate = 0.5 mL min$^{-1}$, minor enantiomer: $t_R$ = 25.78 min; major enantiomer: $t_R$ = 33.09 min; (33% e.e.). (through imine exchange reaction, see experimental studies).

**FT-IR:** $\tilde{\nu}$ 3344, 2922, 2851, 1731, 1611, 1514, 1488, 1435, 1408, 1284, 1207, 1073, 964 cm$^{-1}$.

## 6.7 Synthesis of double cycloaddition *endo, exo*-products

General Procedure F

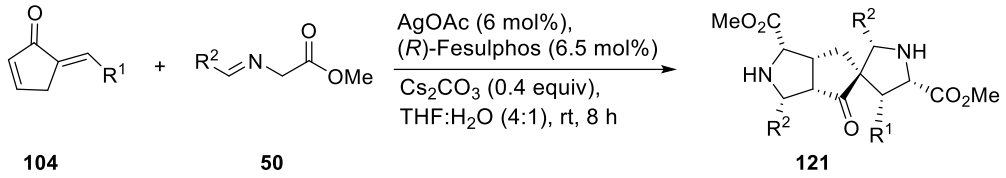


(*Rp*)-2-(*tert*-Butylthio)-1-(diphenylphosphino)ferrocene (6.5 mol%, 7.8 µmol) and silver acetate (6 mol%, 7.2 µmol) were dissolved in THF:H2O (4:1) (2.5 mL total volume) and stirred at ambient temperature for 15 min. To the resulting solution iminoester **50** (2.2 equiv., 0.26 mmol), $Cs_2CO_3$ (40 mol%, 48 µmol) and enone **104** (1 equiv., 0.12 mmol) were added and the mixture was allowed to stir at ambient temperature for 8 h. The crude mixture was directly charged onto silica gel and the product was isolated using n-pentane / acetone as eluent.

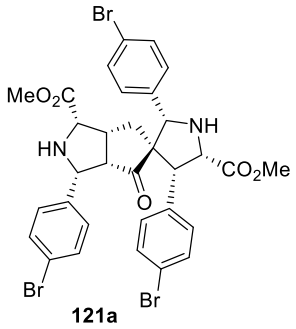


121a

**Dimethyl (1*S*,2'*S*,3*R*,3*aS*,4'*R*,5*R*,5'*S*,6*aR*)-2',3,4'-tris(4-bromophenyl)-4-oxohexahydro-1*H*-spiro[cyclopenta[*c*]pyrrole-5,3'-pyrrolidine]-1,5'-dicarboxylate (121a)**

white amorphous solid, 65% yield, **$^{1}$H NMR** (600 MHz, $CDCl_3$) δ 7.52 (d, *J* = 7.7 Hz, 2H), 7.45 (d, *J* = 8.4 Hz, 2H), 7.37 (d, *J* = 7.8 Hz, 2H), 7.28 (d, *J* = 7.8 Hz, 2H), 7.00 (d, *J* = 8.4 Hz, 2H), 6.83 (d, *J* = 8.0 Hz, 2H), 4.20 (d, *J* = 10.0 Hz, 2H), 4.04 (s, 1H), 3.76 (d, *J* = 9.3 Hz, 1H), 3.63 (s, 3H), 3.36 (s, 3H), 2.68-2.61 (m, 1H), 1.93 (dd, *J* = 13.9, 7.5 Hz, 1H), 1.65-1.62 (m, 1H), 1.60-1.53 (m, 2H).

**$^{13}$C NMR** (151 MHz, $CDCl_3$) δ 219.28, 172.27, 170.98, 137.18, 136.61, 131.96, 131.89, 131.50, 131.35, 131.33, 129.28, 129.20, 122.77, 121.67, 121.50, 70.86, 66.53, 64.34, 63.77, 63.20, 55.56, 54.28, 52.03, 51.87, 39.62, 30.71.

**HRMS**: calcd. for $[M+H]^+$ $C_{32}H_{30}{}^{79}Br_3N_2O_5$ = 758.97018, found: 758.96994; calcd. for $[M+H]^+$ $C_{32}H_{30}{}^{79}Br^{81}Br_2N_2O_5$ = 762.96627, found: 762.96584.

**HPLC** conditions: CHIRALPAK IC column, *iso*-propanol/ *iso*-hexane = 30/70, flow rate = 0.5 mL min$^{-1}$, minor enantiomer: $t_R$ = 19.89 min; major enantiomer: $t_R$ = 29.13 min; (95% e.e.); CHIRALPAK IA column, *iso*-propanol/ *iso*-hexane = 15/85, flow rate = 0.5 mL min$^{-1}$, minor enantiomer: $t_R$ = 72.52 min; major enantiomer: $t_R$ = 90.37 min; (95% e.e.).

**$[\alpha]^{20}_{D}$** = + 187.6° (c = 0.2, $CHCl_3$).

**FT-IR:** $\tilde{\nu}$ 3329, 2921, 2851, 1738, 1724, 1485, 1441, 1367, 1206, 1125, 1072, 1009 cm$^{-1}$.

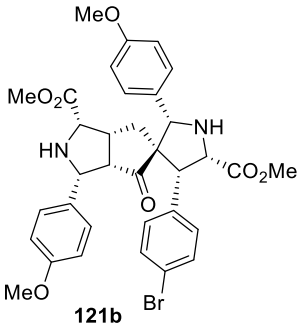


**121b**

**Dimethyl (1*S*,2'*S*,3*R*,3*aS*,4'*R*,5*R*,5'*S*,6*aR*)-4'-(4-bromophenyl)-2',3-bis(4-methoxyphenyl)-4-oxohexahydro-1*H*-spiro[cyclopenta[*c*]pyrrole-5,3'-pyrrolidine]-1,5'-dicarboxylate (121b)**

white amorphous solid, 60% yield, **$^{1}$H NMR** (600 MHz, $CD_2Cl_2$) δ 7.47 (d, *J* = 8.4 Hz, 2H), 7.32 (d, *J* = 8.1 Hz, 2H), 7.11 (d, *J* = 8.5 Hz, 2H), 6.92 (d, *J* = 8.9 Hz, 2H), 6.90 – 6.83 (m, 2H), 6.80 (d, *J* = 8.7 Hz, 2H), 4.16 (dd, *J* = 12.0, 9.8 Hz, 2H), 4.02 (s, 1H), 3.84 (s, 3H), 3.83 (s, 3H), 3.71 (d, *J* = 9.2 Hz, 1H), 3.57 (s, 3H), 3.32 (s, 3H), 2.65 – 2.60 (m, 2H), 1.84 (ddd, *J* = 13.9, 7.8, 1.2 Hz, 1H), 1.35 – 1.26 (m, 2H).

**$^{13}$C NMR** (151 MHz, $CD_2Cl_2$) δ 220.61, 172.58, 171.75, 160.35, 159.42, 138.29, 132.46, 131.51, 131.32, 130.33, 129.30, 129.15, 121.56, 114.29, 113.73, 71.42, 66.95, 65.16, 64.58, 63.55, 56.41, 55.83, 55.72, 54.67, 52.03, 51.88, 40.45, 31.57.

**HRMS**: calcd. for $[M+H]^+$ $C_{34}H_{36}{}^{79}BrN_2O_7$ = 663.16971, found: 663.17004; calcd. for $[M+H]^+$ $C_{34}H_{36}{}^{81}BrN_2O_7$ = 665.16804, found: 665.16799.

**HPLC** conditions: CHIRALPAK IA column, *iso*-propanol/ *iso*-hexane = 80/20, flow rate = 0.5 mL min$^{-1}$, minor enantiomer: $t_R$ = 36.50 min; major enantiomer: $t_R$ = 64.39 min; (93% e.e.).

**$[\alpha]^{20}_{D}$** = + 197.6° (c = 0.2, $CHCl_3$).

**FT-IR:** $\tilde{\nu}$ 2923, 2851, 1733, 1567, 1508, 1489, 1210, 1154 ,1075, 1037, 1009, 965 cm$^{-1}$.

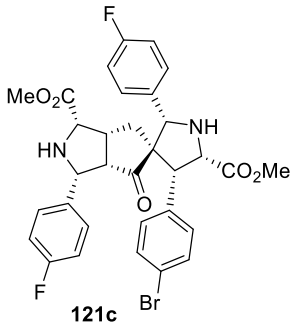


121c

**Dimethyl (1*S*,2'*S*,3*R*,3*aS*,4'*R*,5*R*,5'*S*,6*aR*)-4'-(4-bromophenyl)-2',3-bis(4-fluorophenyl)-4-oxohexahydro-1*H*-spiro[cyclopenta[*c*]pyrrole-5,3'-pyrrolidine]-1,5'-dicarboxylate (121c)**

white amorphous solid, 51% yield, **$^{1}$H NMR** (600 MHz, $CDCl_3$) δ 7.46 (d, *J* = 8.4 Hz, 2H), 7.41 – 7.37 (m, 2H), 7.09 (t, *J* = 8.2 Hz, 2H), 7.03 (d, *J* = 8.4 Hz, 2H), 6.97 – 6.90 (m, 4H), 4.25-4.20 (m, 2H), 4.08 (s, 1H), 3.76 (d, *J* = 9.4 Hz, 1H), 3.63 (s, 3H), 3.36 (s, 3H), 2.66-2.62 (m, 1H), 1.92 (dd, *J* = 13.7, 7.4 Hz, 1H), 1.56-150 (m, 1H), 1.46 – 1.41 (m, 1H), 1.28-1.23 (m, 1H).

**$^{13}$C NMR** (151 MHz, $CDCl_3$) δ 219.47, 172.24, 170.99, 162.99 (d, *J* = 248.0 Hz), 162.22 (d, *J* = 246.0 Hz), 136.73, 133.74, 133.20, 131.90, 131.77, 131.35, 129.14 (d, *J* = 7.8 Hz), 121.64, 115.80 (d, *J* = 21.3 Hz), 115.14 (d, *J* = 21.3 Hz), 71.55, 70.72, 66.54, 64.31, 63.80, 63.12, 55.63, 54.19, 52.02, 39.66, 30.77.

**HRMS**: calcd. for $[M+H]^+$ $C_{32}H_{30}{}^{79}BrF_2N_2O_5$ = 639.13007, found: 639.13014; calcd. for $[M+H]^+$ $C_{32}H_{30}{}^{81}BrF_2N_2O_5$ = 641.12818, found: 641.12811.

**HPLC** conditions: CHIRALPAK IC column, *iso*-propanol/ *iso*-hexane = 30/70, flow rate = 0.5 mL min$^{-1}$, minor enantiomer: $t_R$ = 17.01 min; major enantiomer: $t_R$ = 21.26 min; (97% e.e.).

**$[\alpha]^{20}_D$** = + 166.6° (c = 0.2, $CHCl_3$).

**FT-IR:** $\tilde{\nu}$ 3337, 2850, 1729, 1605, 1509, 1486, 1437, 1375, 1222, 1156, 1128, 1076, 1037, 1030, 1012 cm$^{-1}$.

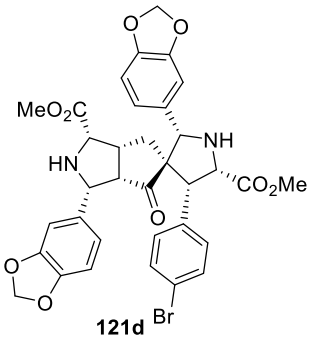


121d

**Dimethyl (1*S*,2'*S*,3*R*,3*aS*,4'*R*,5*R*,5'*S*,6*aR*)-2',3-bis(benzo[*d*][1,3]dioxol-5-yl)-4'-(4-bromophenyl)-4-oxohexahydro-1*H*-spiro[cyclopenta[*c*]pyrrole-5,3'-pyrrolidine]-1,5'-dicarboxylate (121d)**

white amorphous solid, 48% yield, **$^{1}$H NMR** (700 MHz, $CDCl_3$) δ 7.44 (d, *J* = 8.5 Hz, 2H), 7.10 (d, *J* = 8.5 Hz, 2H), 6.94 (s, 1H), 6.81 – 6.72 (m, 3H), 6.53 (dd, *J* = 8.0, 1.7 Hz, 1H), 6.47 (d, *J* = 1.7 Hz, 1H), 6.05 – 5.96 (m, 4H), 4.19 (dd, *J* = 10.0, 8.8 Hz, 2H), 4.00 (s, 1H), 3.74 (d, *J* = 9.2 Hz, 1H), 3.62 (d, *J* = 6.0 Hz, 1H), 3.59 (s, 3H), 3.32 (s, 3H), 2.71 – 2.65 (m, 1H), 1.88 (dd, *J* = 14.6, 8.4 Hz, 1H), 1.73 – 1.65 (m, 1H), 1.31 – 1.28 (m, 1H).

**$^{13}$C NMR** (176 MHz, $CDCl_3$) δ 220.39, 172.01, 171.15, 148.05, 147.90, 147.67, 147.10, 137.53, 132.33, 131.81, 131.35, 130.87, 121.41, 120.95, 120.90, 108.42, 108.12, 108.02, 107.99, 101.43, 101.23, 71.29, 66.57, 64.91, 64.17, 63.15, 55.99, 54.02, 51.91, 51.70, 40.00, 31.59.

**HRMS**: calcd. for $[M+H]^+$ $C_{34}H_{32}{}^{79}BrN_2O_9$ = 691.12857, found: 691.12859; calcd. for $[M+H]^+$ $C_{34}H_{32}{}^{81}BrN_2O_9$ = 693.12652, found: 693.12693.

**HPLC** conditions: CHIRALPAK IC column, *iso*-propanol/ *iso*-hexane = 80/20, flow rate = 0.5 mL $min^{-1}$, minor enantiomer: $t_R$ = 30.53 min; major enantiomer: $t_R$ = 59.65 min; (95% e.e.).

**$[\alpha]^{20}_D$** = + 147.6° (c = 0.2, $CHCl_3$).

**FT-IR:** $\tilde{\nu}$ 2886, 2160, 2035, 1727, 1502, 1485, 1442, 1388, 1238, 1205, 1118, 1035, 1010, 931 $cm^{-1}$.

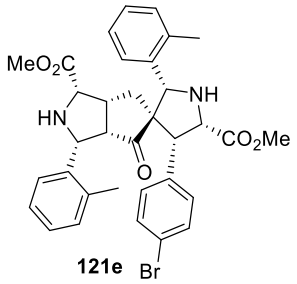


121e

**Dimethyl (1*S*,2'*S*,3*R*,3*aS*,4'*R*,5*R*,5'*S*,6*aR*)-4'-(4-bromophenyl)-4-oxo-2',3-di-*o*-tolylhexahydro-1*H*-spiro[cyclopenta[*c*]pyrrole-5,3'-pyrrolidine]-1,5'-dicarboxylate (121e)**

white amorphous solid, 46% yield, **$^{1}$H NMR** (700 MHz, $CDCl_3$) δ 7.80 – 7.74 (m, 1H), 7.36 (d, *J* = 8.4 Hz, 2H), 7.28 – 7.24 (m, 1H), 7.12 (dd, *J* = 4.0, 1.4 Hz, 2H), 7.09 (d, *J* = 7.5 Hz, 1H), 7.05 – 7.00 (m, 1H), 6.99 (d, *J* = 8.5 Hz, 2H), 6.89 (d, *J* = 7.6 Hz, 1H), 4.37 (s, 1H), 4.34 (d, *J* = 10.8 Hz, 1H), 4.11 (d, *J* = 8.9 Hz, 1H), 3.57 (d, *J* = 5.7 Hz, 1H), 3.53 (s, 3H), 3.48 (d, *J* = 8.5 Hz, 1H), 3.26 (s, 3H), 2.79-2.76 (m, 1H), 2.29 (s, 3H), 2.12 (s, 3H), 1.86 (dd, *J* = 14.0, 7.5 Hz, 1H), 1.63 – 1.58 (m, 1H), 1.29 – 1.24 (m, 1H).

**$^{13}$C NMR** (176 MHz, $CDCl_3$) δ 220.14, 172.07, 171.09, 136.89, 136.40, 135.80, 131.97, 131.84, 131.25, 131.21, 130.81, 130.08, 128.26, 128.21, 127.45, 126.38, 126.14, 125.18, 121.36, 65.97, 65.37, 64.08, 62.94, 61.41, 54.43, 53.77, 51.91, 51.73, 40.34, 31.24, 19.86, 19.57.

**HRMS**: calcd. for $[M+H]^+$ $C_{34}H_{36}{}^{79}BrN_2O_5$ = 631.18021, found: 631.18000; calcd. for $[M+H]^+$ $C_{34}H_{36}{}^{81}BrN_2O_5$ = 633.17816, found: 633.17805.

**HPLC** conditions: CHIRALPAK IC column, *iso*-propanol/ *iso*-hexane = 80/20, flow rate = 0.5 mL $min^{-1}$, minor enantiomer: $t_R$ = 28.40 min; major enantiomer: $t_R$ = 22.09 min; (89% e.e.).

**$[\alpha]^{20}_{D}$** = + 199.7° (c = 0.2, $CHCl_3$).

**FT-IR:** $\tilde{\nu}$ 3341, 2950, 1731, 1698, 1681, 1486, 1434, 1376, 1209, 1073, 1036, 1029, 1011 $cm^{-1}$.

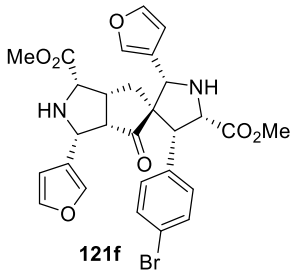


121f

**Dimethyl (1*S*,2'*S*,3*R*,3*aS*,4'*R*,5*R*,5'*S*,6*aR*)-4'-(4-bromophenyl)-2',3-di(furan-3-yl)-4-oxohexahydro-1*H*-spiro[cyclopenta[*c*]pyrrole-5,3'-pyrrolidine]-1,5'-dicarboxylate (121f)**

white amorphous solid, 52% yield, **$^{1}$H NMR** (700 MHz, $CDCl_3$) δ 7.48 – 7.47 (m, 2H), 7.40 (d, *J* = 8.5 Hz, 2H), 7.36 (t, *J* = 1.7 Hz, 1H), 6.94 – 6.92 (m, 3H), 6.45 (dd, *J* = 1.9, 0.9 Hz, 1H), 6.06 (dd, *J* = 1.8, 0.9 Hz, 1H), 4.28 (d, *J* = 11.8 Hz, 1H), 4.21 (d, *J* = 9.3 Hz, 1H), 4.09 (s, 1H), 3.73 – 3.70 (m, 2H), 3.65 (s, 3H), 3.35 (s, 3H), 2.81 – 2.78 (m, 1H), 2.28 – 2.21 (m, 1H), 1.93 – 1.87 (m, 1H), 1.44 – 1.40 (m, 1H).

**$^{13}$C NMR** (176 MHz, $CDCl_3$) δ 219.64, 172.32, 171.11, 143.92, 142.98, 140.61, 139.66, 136.55, 131.78, 131.27, 123.38, 122.56, 121.59, 110.31, 109.75, 66.14, 64.00, 63.91, 63.38, 57.42, 55.73, 54.79, 52.11, 51.86, 41.20, 30.47.

**HRMS**: calcd. for $[M+H]^+$ $C_{28}H_{28}{}^{79}BrN_2O_7$ = 583.10744, found: 583.10712; calcd. for $[M+H]^+$ $C_{28}H_{28}{}^{81}BrN_2O_7$ = 585.10539, found: 585.10539.

**HPLC** conditions: CHIRALPAK IC column, *iso*-propanol/ *iso*-hexane = 50/50, flow rate = 0.5 mL $min^{-1}$, minor enantiomer: $t_R$ = 27.54 min; major enantiomer: $t_R$ = 40.68 min; (95% e.e.).

**$[\alpha]^{20}_D$** = + 205.6° (c = 0.2, $CHCl_3$).

**FT-IR:** $\tilde{\nu}$ 2951, 1726, 1501, 1485, 1437, 1364, 1206, 1158, 1073, 1036, 1021, 1010, 873 $cm^{-1}$.

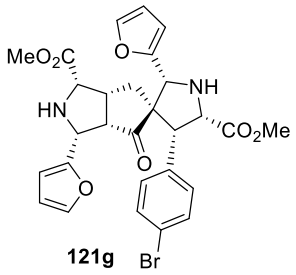


121g

**Dimethyl (1*S*,2'*R*,3*R*,3*aS*,4'*R*,5*R*,5'*S*,6*aR*)-4'-(4-bromophenyl)-2',3-di(furan-2-yl)-4-oxohexahydro-1*H*-spiro[cyclopenta[*c*]pyrrole-5,3'-pyrrolidine]-1,5'-dicarboxylate (121g)**

white amorphous solid, 49% yield, **$^{1}$H NMR** (700 MHz, $CDCl_3$) δ 7.46 – 7.41 (m, 3H), 7.29 (dd, *J* = 1.8, 0.8 Hz, 1H), 7.15 (d, *J* = 8.5 Hz, 2H), 6.44 – 6.41 (m, 2H), 6.32 (dd, *J* = 3.2, 1.9 Hz, 1H), 6.11 – 6.09 (m, 1H), 4.46 (d, *J* = 11.0 Hz, 1H), 4.30 (d, *J* = 8.7 Hz, 1H), 4.24 (s, 1H), 3.76 (d, *J* = 6.0 Hz, 1H), 3.72 (d, *J* = 8.7 Hz, 1H), 3.63 (s, 3H), 3.36 (s, 3H), 3.01 – 2.97 (m, 1H), 2.13 – 2.08 (m, 1H), 1.77 (ddd, *J* = 13.9, 7.6, 1.5 Hz, 1H), 1.39 (dd, *J* = 13.9, 11.0 Hz, 1H).

**$^{13}$C NMR** (176 MHz, $CDCl_3$) δ 218.91, 171.86, 170.59, 151.69, 150.43, 142.49, 142.30, 136.95, 131.83, 131.23, 121.52, 111.07, 110.76, 108.92, 108.69, 66.46, 64.52, 64.39, 63.50, 59.06, 55.66, 54.67, 52.20, 51.85, 41.63, 30.72.

**HRMS**: calcd. for $[M+H]^+$ $C_{28}H_{28}{}^{79}BrN_2O_7$ = 583.10744, found: 583.10718; calcd. for $[M+H]^+$ $C_{28}H_{28}{}^{81}BrN_2O_7$ = 585.10539, found: 585.10522.

**HPLC** conditions: CHIRALPAK IC column, *iso*-propanol/ *iso*-hexane = 50/50, flow rate = 0.5 mL $min^{-1}$, minor enantiomer: $t_R$ = 69.21 min; major enantiomer: $t_R$ = 29.62 min; (95% e.e.).

**$[\alpha]^{20}_D$** = + 197.6° (c = 0.2, $CHCl_3$).

**FT-IR:** $\tilde{\nu}$ 2951, 2159, 2034, 1730, 1505, 1485, 1435, 1363, 1205 ,1182, 1148, 1119, 1072, 953 $cm^{-1}$.

## 6.8 Synthesis of pyrrolidine fused indoles

### 6.8.1 Synthesis of indole precursor

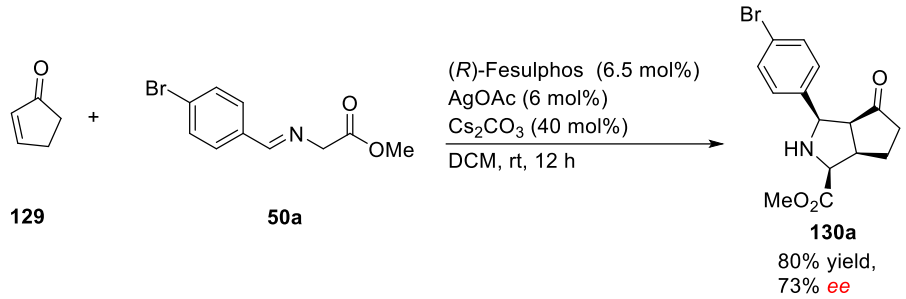


(*Rp*)-2-(*tert*-Butylthio)-1-(diphenylphosphino)ferrocene (6.5 mol%, 0.15 mmol) and silver acetate (6 mol%, 0.14 mmol) were dissolved in DCM (4:1) (10 mL) and stirred at ambient temperature for 15 min. To the resulting solution iminoester **50a** (1.1 equiv., 2.68 mmol), $Cs_2CO_3$ (40 mol%, 0.97 mmol) and enone **129** (1 equiv., 2.44 mmol) were added and the mixture was allowed to stir at ambient temperature for 12 h. The crude mixture was directly charged onto silica gel and the product was isolated using n-pentane / acetone (88:12) as white solid (80% yield).

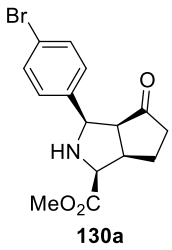


**Methyl (1*S*,3*R*)-3-(4-bromophenyl)-4-oxooctahydrocyclopenta[*c*]pyrrole-1-carboxylate (130a)**

**$^{1}$H NMR** (500 MHz, $CDCl_3$) δ 7.43 (d, *J* = 8.4 Hz, 2H), 7.24 (d, *J* = 8.4 Hz, 2H), 4.48 (d, *J* = 9.6 Hz, 1H), 4.15 (d, *J* = 6.7 Hz, 1H), 3.82 (s, 3H), 3.24 (ddd, *J* = 14.4, 8.2, 6.2 Hz, 1H), 2.92 (t, *J* = 8.9 Hz, 1H), 2.26 – 1.98 (m, 3H), 1.90 – 1.81 (m, 1H).

**$^{13}$C NMR** (126 MHz, $CDCl_3$) δ 216.90, 171.78, 137.13, 131.55, 129.01, 121.77, 64.38, 64.14, 55.31, 52.25, 42.39, 39.79, 23.95.

**HRMS**: calcd. for $[M+H]^+$ $C_{15}H_{17}{}^{79}BrNO_3$ = 338.03863, found: 338.03939; calcd. for $[M+H]^+$ $C_{15}H_{17}{}^{81}BrNO_3$ = 340.03659, found: 340.03699.

**$[\alpha]^{20}_D$** = + 65.6° (c = 0.4, $CHCl_3$).

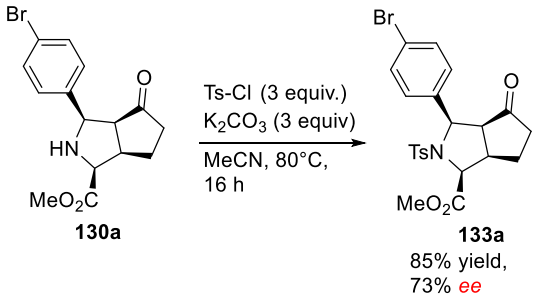


To a solution of 130a (1.80 g, 1.0 equiv, 5.32 mmol) in dry MeCN (20mL) was added $K_2CO_3$ (2.2 g, 3.0 equiv, 15.97 mmol) and TsCl (3.04 g, 3.0 equiv, 15.97 mmol) under argon atmosphere. The reaction solution was heated up to 80°C for 16 h. After cooling to rt, the reaction mixture was quenched with sat. $NaHCO_3$ (10 mL) and diluted with EtOAc (15 mL). The organic layer was washed with brine and sat $NaHCO_3$, dried over $MgSO_4$ and concentrated in vacuo. The crude product was purified by flash chromatography using *n*-pentane / acetone (85:15) to afford the desired product as a white solid (73% yield).

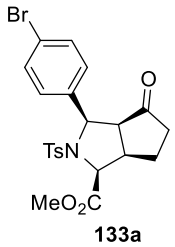


**Methyl (1*S*,3*R*)-3-(4-bromophenyl)-4-oxo-2-tosyloctahydrocyclopenta[*c*]pyrrole-1-carboxylate (133a)**

**$^1$H NMR** (500 MHz, $CDCl_3$) δ 7.58 (d, *J* = 8.3 Hz, 2H), 7.27 – 7.21 (m, 4H), 7.18 (dd, *J* = 8.6, 0.8 Hz, 2H), 5.14 (d, *J* = 11.0 Hz, 1H), 4.85 (d, *J* = 7.7 Hz, 1H), 3.89 (s, 3H), 3.24 (dq, *J* = 10.0, 8.2 Hz, 1H), 3.12 (ddd, *J* = 11.3, 8.5, 1.3 Hz, 1H), 2.39 (s, 3H), 2.04 – 1.80 (m, 3H), 1.70 – 1.63 (m, 1H).
**$^{13}$C NMR** (126 MHz, $CDCl_3$) δ 214.42, 170.62, 144.54, 136.26, 134.59, 131.28, 129.66, 129.59, 128.23, 121.74, 64.93, 64.47, 57.31, 52.72, 44.11, 38.53, 23.14, 21.70.
**HRMS**: calcd. for $[M+H]^+$ $C_{22}H_{23}{}^{79}BrNO_5S$ = 492.04748, found: 492.04749; calcd. for $[M+H]^+$ $C_{22}H_{23}{}^{81}BrNO_5S$ = 494.04544, found: 494.04534.
**$[\alpha]^{20}_D$** = + 77.3° (c = 0.3, $CHCl_3$).

### 6.8.2 Synthesis of indole and pyrrolidine fused polycyclic compound

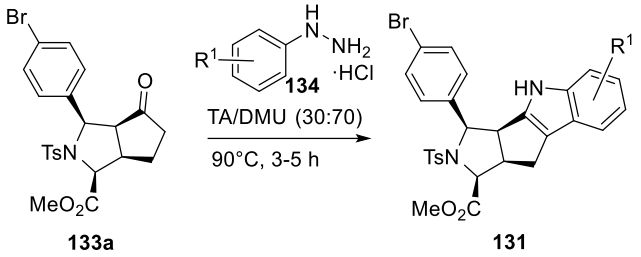


General Procedure G: This procedure was adapted from a protocol reported by König et. al.[107] To a microwave via equipped with a stir bar was added tartaric acid (122 mg) and dimethylurea (286 mg). The microwave vial was stirred and heated to 70°C. After all the solid had mealted (about 15 min), ketone 133a (100 mg, 0.20 mmol, 1.0 equiv.) and a phenyldydrazine hydrochlorid salt **134** (0.26 mmol, 1.3 equiv.) were added simultaneously to the heated solution. The reaction was then stirred at 90°C and monitored by LCMS. After full conversion of the starting material the reaction was quenched by adding water to the reaction while still heating. The was then cooled to room temperature, and the aqueous layer was extracted with DCM (3 x 5 mL). The combined organic layers were dried over $MgSO_4$ and concentrated. The crude product was purified by flash chromatography using *n*-pentane / acetone as eluent.

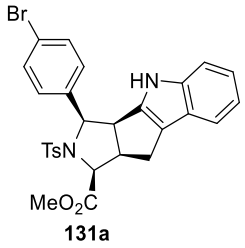


**Methyl (1*S*,3*R*)-3-(4-bromophenyl)-2-tosyl-2,3,3*a*,4,9,9*a*-hexahydro-1*H*-pyrrolo[3',4':4,5]cyclopenta[1,2-*b*]indole-1-carboxylate (131a)**

white amorphous solid, 67% yield, **$^1$H NMR** (500 MHz, $CDCl_3$) δ 7.52 (d, *J* = 8.4 Hz, 2H), 7.34 – 7.27 (m, 5H), 7.16 (d, *J* = 7.9 Hz, 2H), 7.05 – 6.97 (m, 3H), 6.40 (s, 1H), 5.10 (d, *J* = 8.4 Hz, 1H), 4.88 (d, *J* = 9.8 Hz, 1H), 4.19 – 4.14 (m, 1H), 3.65 – 3.61 (m, 1H), 3.46 (s, 3H), 3.01 (ddd, *J* = 15.1, 2.1, 1.0 Hz, 1H), 2.84 – 2.78 (m, 1H), 2.39 (s, 3H).

**$^{13}$C NMR** (126 MHz, $CDCl_3$) δ 170.98, 144.15, 141.25, 139.87, 137.58, 135.12, 131.24, 129.79, 129.50, 128.04, 123.59, 121.85, 121.67, 119.89, 119.81, 118.72, 111.74, 65.81, 64.92, 52.18, 51.43, 50.44, 31.11, 26.14, 21.69.

**HRMS**: calcd. for $[M+H]^+$ $C_{28}H_{26}{}^{79}BrN_2O_4S$ = 565.07912, found: 565.07931; calcd. for $[M+H]^+$ $C_{28}H_{26}{}^{81}BrN_2O_4S$ = 567.07707, found: 567.07714.

**$[\alpha]^{20}_D$** = + 44.3° (c = 0.12, $CHCl_3$).

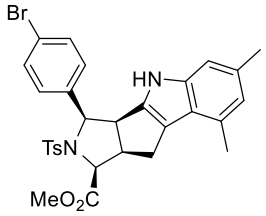


**131b**

**Methyl (1*S*,3*R*)-3-(4-bromophenyl)-6,8-dimethyl-2-tosyl-2,3,3*a*,4,9,9*a*-hexahydro-1*H*-pyrrolo[3',4':4,5]cyclopenta[1,2-*b*]indole-1-carboxylate (131b)**

white amorphous solid, 68% yield, **$^1$H NMR** (500 MHz, $CDCl_3$) δ 7.52 (d, *J* = 8.3 Hz, 2H), 7.34 – 7.27 (m, 4H), 7.16 (dt, *J* = 7.2, 0.9 Hz, 2H), 6.66 – 6.64 (m, 1H), 6.62 – 6.57 (m, 1H), 6.19 (s, 1H), 5.07 (d, *J* = 8.3 Hz, 1H), 4.88 (d, *J* = 9.9 Hz, 1H), 4.12 (dd, *J* = 8.3, 6.8 Hz, 1H), 3.61 – 3.54 (m, 1H), 3.48 (s,3), 3.15 (ddd, *J* = 15.1, 1.8, 1.0 Hz, 1H), 2.92 (ddd, *J* = 15.1, 6.8, 1.6 Hz, 1H), 2.43 (s, 3H), 2.39 (s, 3H), 2.30 (s, 3H).

**$^{13}$C NMR** (126 MHz, $CDCl_3$) δ 171.04, 144.10, 141.63, 138.32, 137.69, 135.24, 131.82, 131.22, 129.88, 129.49, 128.92, 128.07, 122.05, 121.82, 121.46, 119.52, 109.36, 65.93, 64.99, 52.15, 51.39, 50.55, 27.52, 21.68, 21.64, 19.05.

**HRMS**: calcd. for $[M+H]^+$ $C_{30}H_{30}{}^{79}BrN_2O_4S$ = 593.11042, found: 593.11062; calcd. for $[M+H]^+$ $C_{30}H_{30}{}^{81}BrN_2O_4S$ = 595.10837, found: 595.10856.

**$[\alpha]^{20}_D$** = + 52.6° (c = 0.15, $CHCl_3$).

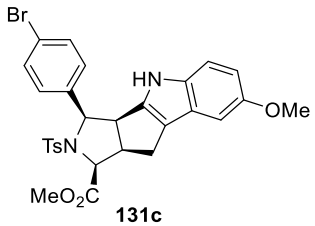


**131c**

**Methyl (1*S*,3*R*)-3-(4-bromophenyl)-7-methoxy-2-tosyl-2,3,3*a*,4,9,9*a*-hexahydro-1*H*-pyrrolo[3',4':4,5]cyclopenta[1,2-*b*]indole-1-carboxylate (131c)**

white amorphous solid, 67% yield, **$^{1}$H NMR** (500 MHz, $CDCl_3$) δ 7.52 (d, *J* = 8.3 Hz, 2H), 7.33 – 7.27 (m, 4H), 7.17 (d, *J* = 8.0 Hz, 2H), 6.92 (d, *J* = 8.8 Hz, 1H), 6.78 (d, *J* = 2.4 Hz, 1H), 6.68 (dd, *J* = 8.8, 2.4 Hz, 1H), 6.27 (s, 1H), 5.09 (d, *J* = 8.4 Hz, 1H), 4.87 (d, *J* = 9.8 Hz, 1H), 4.15 (dd, *J* = 8.4, 6.9 Hz, 1H), 3.78 (s, 3H), 3.60 (dd, *J* = 9.6, 2.3 Hz, 1H), 3.45 (s, 3H), 2.99 – 2.96 (m, 1H), 2.78 (ddd, *J* = 15.0, 7.0, 1.4 Hz, 1H), 2.39 (s, 3H).

**$^{13}$C NMR** (126 MHz, $CDCl_3$) δ 170.96, 154.25, 144.15, 140.73, 137.60, 136.38, 135.20, 131.24, 129.77, 129.51, 128.07, 124.00, 121.84, 119.59, 112.34, 111.42, 100.97, 65.86, 64.95, 55.95, 52.18, 51.40, 50.44, 26.07, 21.69.

**HRMS**: calcd. for $[M+H]^+$ $C_{29}H_{28}{}^{79}BrN_2O_5S$ = 595.08968, found: 595.08996; calcd. for $[M+H]^+$ $C_{29}H_{30}{}^{81}BrN_2O_5S$ = 597.08764, found: 597.08781.

**$[\alpha]^{20}_D$** = + 19.6° (c = 0.13, $CHCl_3$).

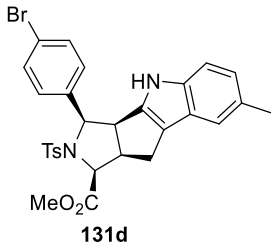


**131d**

**Methyl (1*S*,3*R*)-3-(4-bromophenyl)-7-methyl-2-tosyl-2,3,3*a*,4,9,9*a*-hexahydro-1*H*-pyrrolo[3',4':4,5]cyclopenta[1,2-*b*]indole-1-carboxylate (131d)**

white amorphous solid, 71% yield, **$^{1}$H NMR** (500 MHz, $CDCl_3$) δ 7.53 – 7.41 (m, 2H), 7.20 – 7.14 (m, 2H), 7.14 – 7.00 (m, 5H), 6.87 – 6.79 (m, 1H), 6.73 (dd, *J* = 7.2, 1.2 Hz, 1H), 6.04 (s, 1H), 5.04 (dd, *J* = 8.4, 0.9 Hz, 1H), 4.79 (dd, *J* = 9.9, 0.9 Hz, 1H), 4.09 (ddd, *J* = 8.3, 7.0, 1.3 Hz, 1H), 3.57 – 3.50 (m, 1H), 3.38 (s, 3H), 2.93 – 2.83 (m, 1H), 2.76 – 2.68 (m, 1H), 2.32 (s, 3H), 2.04 (s, 3H).

**$^{13}$C NMR** (126 MHz, $CDCl_3$) δ 170.83, 144.08, 140.63, 139.42, 137.92, 134.91, 131.03, 129.64, 129.44, 127.95, 122.90, 122.18, 121.62, 120.44, 119.95, 119.80, 116.38, 65.69, 65.04, 52.06, 51.41, 50.16, 26.24, 21.58, 16.02.

**HRMS**: calcd. for $[M+H]^+$ $C_{29}H_{28}{}^{79}BrN_2O_4S$ = 579.09477, found: 579.09505; calcd. for $[M+H]^+$ $C_{29}H_{28}{}^{81}BrN_2O_4S$ = 581.09272, found: 581.09289.

**$[\alpha]^{20}_D$** = + 21.8° (c = 0.11, $CHCl_3$).

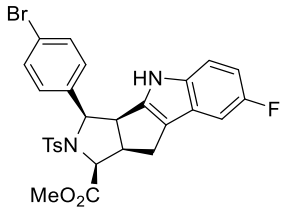


131e

**Methyl (1*S*,3*R*)-3-(4-bromophenyl)-7-fluoro-2-tosyl-2,3,3*a*,4,9,9*a*-hexahydro-1*H*-pyrrolo[3',4':4,5]cyclopenta[1,2-*b*]indole-1-carboxylate (131e)**

brown amorphous solid, 43% yield, **$^{1}$H NMR** (600 MHz, CDCl3) δ 7.55 – 7.46 (m, 2H), 7.30 (q, *J* = 8.6 Hz, 4H), 7.17 (d, *J* = 8.1 Hz, 2H), 6.95 (ddd, *J* = 16.7, 9.1, 3.4 Hz, 2H), 6.76 (td, *J* = 9.1, 2.5 Hz, 1H), 6.39 (s, 1H), 5.11 (d, *J* = 8.4 Hz, 1H), 4.88 (d, *J* = 9.8 Hz, 1H), 4.16 (dd, *J* = 8.4, 6.9 Hz, 1H), 3.64 – 3.57 (m, 1H), 3.47 (s, 3H), 2.97 (dd, *J* = 15.1, 2.7 Hz, 1H), 2.81 – 2.74 (m, 1H), 2.39 (s, 3H).
**$^{13}$C NMR** (151 MHz, $CDCl_3$) δ 170.93, 157.95 (d, *J* = 234.9 Hz), 144.21, 141.92, 137.65, 137.52, 135.13, 131.30, 129.73, 129.53, 128.05, 123.83, 123.76, 119.81 (d, *J* = 4.5 Hz), 112.26 (d, *J* = 9.7 Hz), 109.84 (d, *J* = 26.2 Hz), 103.77 (d, *J* = 23.6 Hz), 65.73, 64.84, 52.21, 51.42, 50.42, 26.00, 21.69.
**$^{19}$F NMR** (565 MHz, $CDCl_3$) δ -124.22 (td, *J* = 9.2, 4.2 Hz).
**HRMS**: calcd. for $[M+H]^+$ $C_{28}H_{25}{}^{79}BrFN_2O_4S$ = 583.06970, found: 583.06973; calcd. for $[M+H]^+$ $C_{28}H_{25}{}^{81}BrFN_2O_4S$ = 585.06765, found: 585.06751.
**$[\alpha]^{20}_{D}$** = + 81.3° (c = 0.44, $CHCl_3$).

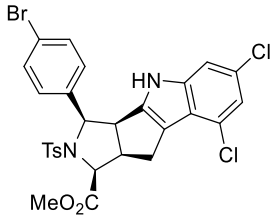


131f

**Methyl (1*S*,3*R*)-3-(4-bromophenyl)-6,8-dichloro-2-tosyl-2,3,3*a*,4,9,9*a*-hexahydro-1*H*-pyrrolo[3',4':4,5]cyclopenta[1,2-*b*]indole-1-carboxylate (131f)**

yellow amorphous solid, 46% yield, **$^{1}$H NMR** (500 MHz, $CDCl_3$) δ 7.67 (d, *J* = 8.3 Hz, 2H), 7.34 (d, *J* = 8.4 Hz, 2H), 7.23 (t, *J* = 8.6 Hz, 3H), 6.81 (s, 3H), 6.55 (s, 1H), 5.11 (d, *J* = 10.3 Hz, 1H), 4.78 (d, *J* = 7.4 Hz, 1H), 3.88 (s, 3H), 3.52 – 3.43 (m, 1H), 3.11 – 3.02 (m, 1H), 2.42 (s, 3H), 1.98 (d, *J* = 17.8 Hz, 1H), 1.83 – 1.73 (m, 1H).
**$^{13}$C NMR** (126 MHz, $CDCl_3$) δ 170.98, 159.96, 152.89, 146.58, 144.49, 137.69, 135.67, 134.36, 130.84, 129.92, 129.81, 129.27, 128.21, 121.21, 119.93, 111.29, 65.25, 64.29, 54.81, 52.69, 45.32, 26.60, 24.97, 21.75.

**HRMS**: calcd. for $[M+H]^+$ $C_{28}H_{23}{}^{79}BrCl_2N_2O_4S$ = 654.02366, found: 654.02382; calcd. for $[M+Na]^+$ $C_{28}H_{23}{}^{81}BrCl_2N_2O_4S$ = 656.01980, found: 656.01987.

**$[\alpha]^{20}_D$** = + 18.3° (c = 0.24, $CHCl_3$).

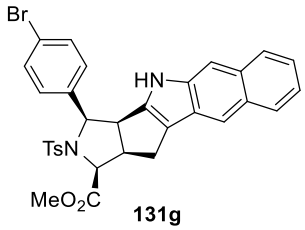


**131g**

**Methyl (1*S*,3*R*)-3-(4-bromophenyl)-2-tosyl-2,3,3*a*,4,11,11*a*-hexahydro-1*H*-benzo[f]pyrrolo[3',4':4,5]cyclopenta[1,2-*b*]indole-1-carboxylate (131g)**

white amorphous solid, 74% yield, **$^1$H NMR** (500 MHz, $CDCl_3$) δ 7.83 (dt, *J* = 8.0, 1.1 Hz, 1H), 7.57 (d, *J* = 8.3 Hz, 2H), 7.46 – 7.35 (m, 8H), 7.22 – 7.16 (m, 2H), 6.98 (s, 1H), 5.16 (d, *J* = 8.2 Hz, 1H), 4.88 (d, *J* = 9.9 Hz, 1H), 4.24 (ddd, *J* = 8.0, 6.6, 1.2 Hz, 1H), 3.65 – 3.57 (m, 1H), 3.37 (s, 3H), 3.08 (d, *J* = 1.5 Hz, 1H), 2.86 (ddd, *J* = 15.1, 6.7, 1.5 Hz, 1H), 2.40 (s, 3H). **$^{13}$C NMR** (126 MHz, $CDCl_3$) δ 170.81, 144.11, 137.99, 137.79, 135.25, 134.86, 131.18, 129.91, 129.70, 129.50, 128.80, 127.90, 125.56, 123.69, 121.89, 121.76, 121.23, 120.52, 119.10, 118.85, 118.68, 65.75, 64.95, 52.05, 51.51, 50.62, 26.11, 21.58.

**HRMS**: calcd. for $[M+H]^+$ $C_{32}H_{28}{}^{79}BrN_2O_4S$ = 615.09477, found: 615.09497; calcd. for $[M+H]^+$ $C_{32}H_{28}{}^{81}BrN_2O_4S$ = 617.09272, found: 617.09294.

**$[\alpha]^{20}_D$** = + 61.4° (c = 0.24, $CHCl_3$).

## 6.9 Synthesis of polycyclic pyrroloindoline by dearomatization

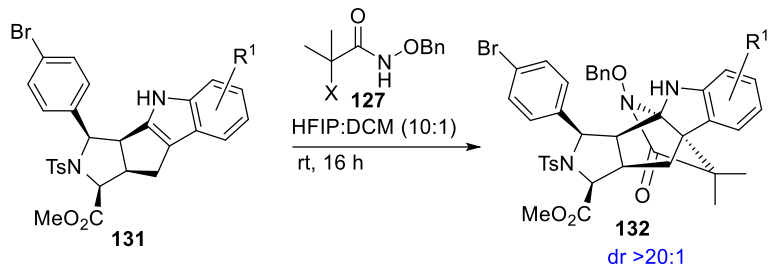


General Procedure H

Indole **131** (0.10mmol, 1.0 equiv) was dissolved in a solvent mixture (1.0 mL HFIP and 0.10 mL DCM) and then α-haloamide **127** (0.14 mmol, 1.4 equiv) and potassium carbonate (0.20 mmol, 2.0 equiv) were added. The mixture was stirred at room temperature until full conversion of the indole **131** (monitored by TLC). Then the reaction mixture was diluted with DCM (5 mL) and was filtered through a short pad of celite. The filtrate was concentrated under reduced pressure and was purified via flash column chromatography using *n*-pentane / acetone as eluent. The products were obtained as single diastereomer.

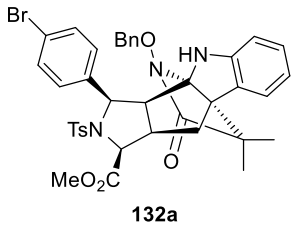


**Methyl (1*S*,3*R*,3*bS*,8*bR*)-12-(benzyloxy)-3-(4-bromophenyl)-10,10-dimethyl-11-oxo-2-tosyl-1,2,3,3*a*,9,9*a*-hexahydro-4*H*-3*b*,8*b*-(epiminoethano)pyrrolo[3',4':4,5]cyclopenta[1,2-*b*]indole-1-carboxylate (132a)**

white amorphous solid, 57% yield, **$^{1}$H NMR** (500 MHz, $CDCl_3$) δ 7.53 – 7.35 (m, 9H), 7.31 (d, *J* = 8.3 Hz, 2H), 7.02 – 6.90 (m, 2H), 6.74 – 6.64 (m, 1H), 6.59 (dd, *J* = 7.5, 1.3 Hz, 1H), 6.54 – 6.47 (m, 1H), 5.34 – 5.31 (m, 1H), 5.22 (d, *J* = 11.3 Hz, 1H), 5.02 – 4.93 (m, 2H), 4.58 (d, *J* = 7.2 Hz, 1H), 3.83 (s, 3H), 3.54 – 3.41 (m, 1H), 2.86 (dd, *J* = 13.3, 7.3 Hz, 1H), 2.30 (s, 3H), 2.10 (s, 1H), 1.45 (s, 3H), 1.23 (s, 3H)

**$^{13}$C NMR** (126 MHz, $CDCl_3$) δ 174.61, 170.85, 146.97, 144.03, 136.30, 135.82, 135.40, 130.26, 129.97, 129.66, 129.47, 129.31, 128.98, 128.86, 128.77, 128.20, 127.60, 123.51,

121.67, 119.06, 108.82, 93.92, 65.37, 63.80, 61.57, 53.95, 52.69, 46.36, 42.35, 37.47, 22.28, 21.59.

**HRMS**: calcd. for $[M+H]^+$ $C_{39}H_{39}{}^{79}BrN_3O_6S$ = 756.17375, found: 756.17435; calcd. for $[M+H]^+$ $C_{39}H_{39}{}^{81}BrN_3O_6S$ = 758.17170, found: 758.17246.

**$[\alpha]^{20}_D$** = + 44.7° (c = 0.14, $CHCl_3$).

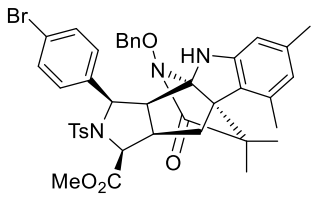


**132b**

**Methyl (1*S*,3*R*,3*bS*,8*bR*)-12-(benzyloxy)-3-(4-bromophenyl)-6,8,10,10-tetramethyl-11-oxo-2-tosyl-1,2,3,3*a*,9,9*a*-hexahydro-4*H*-3*b*,8*b*-(epiminoethano)pyrrolo[3',4':4,5]-cyclopenta[1,2-*b*]indole-1-carboxylate (132b)**

white amorphous solid, 51% yield, **$^1$H NMR** (500 MHz, $CDCl_3$) δ 7.50 – 7.34 (m, 9H), 7.28 (d, *J* = 8.3 Hz, 2H), 6.98 – 6.89 (m, 2H), 6.58 (s, 1H), 6.14 (s, 1H), 5.26 (d, *J* = 11.2 Hz, 1H), 5.03 – 4.90 (m, 3H), 4.59 (d, *J* = 7.1 Hz, 1H), 3.85 (s, 3H), 3.60 – 3.46 (m, 1H), 2.90 – 2.80 (m, 1H), 2.30 (s, 3H), 2.14 – 2.07 (m, 1H), 2.04 (s, 3H), 2.00 (s, 3H), 1.45 (s, 3H), 1.29 (s, 3H).

**$^{13}$C NMR** (126 MHz, $CDCl_3$) δ 174.28, 170.82, 147.70, 143.96, 138.55, 136.27, 135.88, 135.55, 132.12, 129.85, 129.74, 129.47, 129.28, 128.94, 128.87, 128.77, 128.16, 125.87, 121.90, 121.26, 107.30, 94.40, 78.20, 65.38, 63.79, 61.54, 53.64, 52.68, 45.95, 42.94, 28.10, 26.78, 22.12, 21.59, 19.53.

**HRMS**: calcd. for $[M+H]^+$ $C_{41}H_{43}{}^{79}BrN_3O_6S$ = 784.20505, found: 784.20575; calcd. for $[M+H]^+$ $C_{41}H_{43}{}^{81}BrN_3O_6S$ = 786.20300, found: 786.20392.

**$[\alpha]^{20}_D$** = + 77.2° (c = 0.34, $CHCl_3$).

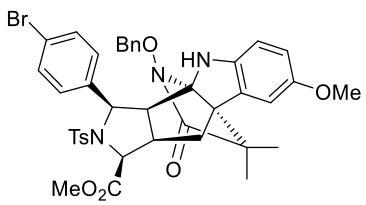


**132c**

**Methyl (1*S*,3*R*,3*bS*,8*bR*)-12-(benzyloxy)-3-(4-bromophenyl)-7-methoxy-10,10-dimethyl-11-oxo-2-tosyl-1,2,3,3*a*,9,9*a*-hexahydro-4*H*-3*b*,8*b*-(epiminoethano)pyrrolo-[3',4':4,5]-cyclopenta[1,2-*b*]indole-1-carboxylate (132c)**

white amorphous solid, 45% yield, **$^{1}$H NMR** (500 MHz, $CDCl_3$) δ 7.47 – 7.41 (m, 7H), 7.32 (d, *J* = 8.3 Hz, 2H), 6.98 – 6.94 (m, 2H), 6.67 (d, *J* = 8.9 Hz, 3H), 6.31 – 6.20 (m, 2H), 5.23 (d, *J* = 11.1 Hz, 1H), 4.99 (d, *J* = 11.1 Hz, 2H), 4.57 (d, *J* = 7.3 Hz, 1H), 3.84 (s, 3H), 3.67 (s, 3H), 3.45 – 3.42 (m, 1H), 2.87 – 2.83 (m, 1H), 2.30 (s, 3H), 2.22 (dd, *J* = 14.3, 7.0 Hz, 1H), 2.12 (t, *J* = 13.7 Hz, 1H), 1.22 (s, 3H), 0.70 (s, 3H).

**$^{13}$C NMR** (126 MHz, $CDCl_3$) δ 174.38, 170.84, 162.72, 154.05, 144.03, 136.12, 135.91, 135.46, 130.24, 129.93, 129.74, 129.29, 129.00, 128.83, 128.23, 121.81, 112.34, 110.72, 94.72, 78.12, 63.75, 61.58, 56.23, 54.11, 53.94, 52.68, 46.48, 42.36, 37.23, 36.68, 29.42, 27.55, 22.32, 21.58.

**HRMS**: calcd. for $[M+H]^+$ $C_{40}H_{41}{}^{79}BrN_3O_7S$ = 786.18431, found: 786.18492; calcd. for $[M+H]^+$ $C_{40}H_{41}{}^{81}BrN_3O_7S$ = 788.18226, found: 788.18306.

**$[\alpha]^{20}_{D}$** = + 33.4° (c = 0.3, $CHCl_3$).

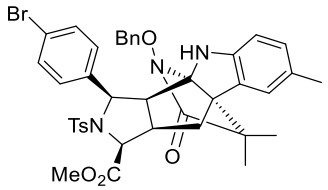


**132d**

**Methyl (1*S*,3*R*,3*bS*,8*bR*)-12-(benzyloxy)-3-(4-bromophenyl)-7,10,10-trimethyl-11-oxo-2-tosyl-1,2,3,3*a*,9,9*a*-hexahydro-4*H*-3*b*,8*b*-(epiminoethano)-pyrrolo[3',4':4,5]-cyclopenta-[1,2-*b*]indole-1-carboxylate (132d)**

white amorphous solid, 71% yield, **$^{1}$H NMR** (700 MHz, $CDCl_3$) δ 7.49 – 7.36 (m, 7H), 7.29 (d, *J* = 8.3 Hz, 2H), 6.98 – 6.92 (m, 2H), 6.64 – 6.60 (m, 2H), 6.54 – 6.44 (m, 3H), 5.24 (d, *J* = 11.7 Hz, 1H), 5.02 – 4.88 (m, 3H), 4.58 (d, *J* = 7.3 Hz, 1H), 3.81 (s, 3H), 3.50 (dd, *J* = 12.4, 7.5 Hz, 1H), 2.90 – 2.83 (m, 1H), 2.30 (s, 3H), 2.26 – 2.16 (m, 3H), 1.45 (s, 3H), 1.37 (s, 3H), 1.22 (s, 3H).

**$^{13}$C NMR** (126 MHz, $CDCl_3$) δ 174.95, 170.79, 146.34, 143.90, 136.48, 135.67, 135.60, 130.35, 129.91, 129.84, 129.79, 129.46, 129.38, 129.16, 128.98, 128.94, 128.77, 128.15, 121.28, 121.27, 119.46, 118.75, 94.01, 78.08, 65.70, 64.01, 61.63, 54.19, 52.62, 46.62, 42.57, 36.89, 21.58, 16.56.

**HRMS**: calcd. for $[M+H]^+$ $C_{40}H_{41}{}^{79}BrN_3O_6S$ = 770.18940, found: 770.18989; calcd. for $[M+H]^+$ $C_{40}H_{41}{}^{81}BrN_3O_6S$ = 772.18735, found: 772.18804.

**$[\alpha]^{20}_{D}$** = + 45.7° (c = 0.22, $CHCl_3$).

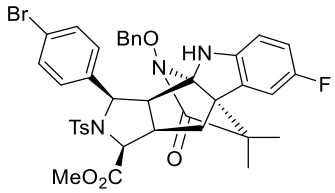


**132e**

**Methyl (1*S*,3*R*,3*bS*,8*bR*)-12-(benzyloxy)-3-(4-bromophenyl)-7-fluoro-10,10-dimethyl-11-oxo-2-tosyl-1,2,3,3*a*,9,9*a*-hexahydro-4*H*-3*b*,8*b*-(epiminoethano)-pyrrolo[3',4':4,5]-cyclopenta-[1,2-*b*]indole-1-carboxylate (132e)**

white amorphous solid, 50% yield, **$^1$H NMR** (500 MHz, $CDCl_3$) δ 7.51 – 7.36 (m, 8H), 7.32 (d, *J* = 8.4 Hz, 2H), 7.00 – 6.91 (m, 2H), 6.66 (s, 2H), 6.45 – 6.38 (m, 1H), 6.35 (dd, *J* = 8.1, 2.6 Hz, 1H), 5.30 – 5.22 (m, 1H), 5.04 – 4.90 (m, 2H), 4.58 (d, *J* = 7.2 Hz, 1H), 3.84 (s, 3H) 3.43 (ddd, *J* = 11.3, 7.4, 1.2 Hz, 1H), 2.87 – 2.83 (m, 1H), 2.31 (s, 3H), 2.24 – 2.17 (m, 1H), 2.08 (d, *J* = 13.7 Hz, 1H), 1.25 (s, 3H), 1.22 (s, 3H).

**$^{13}$C NMR** (126 MHz, $CDCl_3$) δ $^{13}$C NMR (126 MHz, $CDCl_3$) δ 174.35, 170.79, 157.30 (d, *J* = 236.9 Hz), 144.12, 143.07, 136.19, 135.62 (d, *J* = 62.6 Hz), 130.00, 129.74, 129.47, 129.37, 129.01, 128.88, 128.77, 128.21, 121.80, 113.99 (d, *J* = 23.4 Hz), 110.66 (d, *J* = 24.1 Hz), 109.18 (d, *J* = 8.3 Hz), 94.63, 78.05, 65.38, 63.67, 61.51, 53.98, 52.74, 46.28, 42.32, 37.27, 29.40, 27.59, 22.28, 21.60.

**HRMS**: calcd. for $[M+H]^+$ $C_{39}H_{38}{}^{79}BrN_3O_6S$ = 774.16432, found: 774.16515; calcd. for $[M+H]^+$ $C_{39}H_{38}{}^{81}BrN_3O_6S$ = 776.16228, found: 776.16325.

**$[\alpha]^{20}_D$** = + 53.5° (c = 0.24, $CHCl_3$).

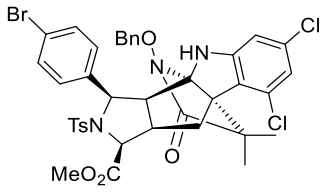


**132f**

**Methyl (1*S*,3*R*,3*bS*,8*bS*)-12-(benzyloxy)-3-(4-bromophenyl)-6,8-dichloro-10,10-dimethyl-11-oxo-2-tosyl-1,2,3,3*a*,9,9*a*-hexahydro-4*H*-3*b*,8*b*-(epiminoethano)-pyrrolo[3',4':4,5]-cyclopenta[1,2-*b*]indole-1-carboxylate (132f)**

white amorphous solid, 74% yield, **$^1$H NMR** (500 MHz, $CDCl_3$) δ 7.55 (d, *J* = 8.4 Hz, 2H), 7.49 – 7.37 (m, 4H), 7.21 – 7.17 (m, 5H), 7.08 (d, *J* = 8.5 Hz, 2H), 6.59 (t, *J* = 1.6 Hz, 2H), 5.00

– 4.93 (m, 3H), 4.67 (d, *J* = 7.4 Hz, 1H), 3.82 (s, 3H), 3.32 (t, *J* = 9.9 Hz, 1H), 2.86 – 2.81 (m, 1H), 2.40 (s, 3H), 1.71 (d, *J* = 11.2 Hz, 1H), 1.64 – 1.52 (m, 1H), 1.20 (s, 3H), 1.12 (s, 3H).

**$^{13}$C NMR** (126 MHz, $CDCl_3$) δ 170.73, 146.96, 144.47, 137.18, 135.90, 134.95, 134.53, 131.35, 129.70, 129.60, 129.47, 129.13, 128.99, 128.88, 128.79, 128.77, 128.24, 127.63, 127.17, 121.78, 78.00, 67.47, 65.34, 63.89, 55.73, 52.63, 44.84, 31.24, 29.40, 26.21, 25.29, 22.68, 21.73.

**HRMS**: calcd. for $[M+Na]^+$ $C_{39}H_{36}{}^{79}BrCl_2N_3O_6SNa$ = 845.12043, found: 845.12066; calcd. for $[M+Na]^+$ $C_{39}H_{36}{}^{81}BrCl_2N_3O_6SNa$ = 847.11438, found: 847.11451

**$[\alpha]^{20}_D$** = + 87.2° (c = 0.21, $CHCl_3$).

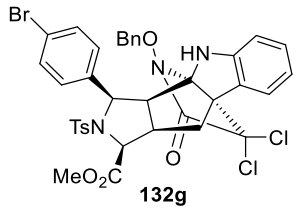


**132g**

**Methyl (1*S*,3*R*,3*bS*,8*bS*)-12-(benzyloxy)-3-(4-bromophenyl)-10,10-dichloro-11-oxo-2-tosyl-1,2,3,3*a*,9,9*a*-hexahydro-4*H*-3*b*,8*b*-(epiminoethano)-pyrrolo[3',4':4,5]-cyclopenta-[1,2-*b*]indole-1-carboxylate (132g)**

white amorphous solid, 67% yield, **$^1$H NMR** (500 MHz, $CDCl_3$) δ 7.47 – 7.39 (m, 4H), 7.37 – 7.33 (m, 4H), 6.99 (ddd, *J* = 21.4, 7.6, 1.1 Hz, 4H), 6.88 – 6.81 (m, 4H), 6.68 – 6.61 (m, 1H), 5.59 (dd, *J* = 7.9, 0.9 Hz, 1H), 5.12 (d, *J* = 11.1 Hz, 1H), 5.01 (d, *J* = 10.9 Hz, 1H), 4.92 (d, *J* = 11.1 Hz, 1H), 4.56 (d, *J* = 7.9 Hz, 1H), 3.70 (s, 3H), 3.33 (ddd, *J* = 10.8, 7.9, 1.1 Hz, 1H), 3.03 – 2.97 (m, 1H), 2.90 – 2.85 (m, 1H), 2.33 (s, 3H).

**$^{13}$C NMR** (126 MHz, $CDCl_3$) δ 170.60, 162.15, 146.56, 144.27, 135.67, 135.07, 135.05, 130.65, 130.27, 129.95, 129.71, 129.19, 128.97, 128.19, 128.02, 125.71, 121.93, 119.95, 109.99, 93.93, 85.73, 78.26, 71.63, 63.78, 61.88, 54.80, 52.64, 47.36, 38.57, 31.11, 21.63.

**HRMS**: calcd. for $[M+H]^+$ $C_{37}H_{33}{}^{79}Br^{35}Cl_2N_3O_6S$ = 796.06450, found: 796.06705; calcd. for $[M+H]^+$ $C_{37}H_{33}{}^{81}Br^{35}Cl_2N_3O_6S$ = 798.06245, found: 798.06473; calcd. for $[M+H]^+$ $C_{37}H_{33}{}^{81}Br^{37}Cl^{35}ClN_3O_6S$ = 800.05950, found: 800.06208; calcd. for $[M+H]^+$ $C_{37}H_{33}{}^{81}Br^{37}Cl_2N_3O_6S$ = 802.05655, found: 802.05574.

**$[\alpha]^{20}_D$** = + 31.7° (c = 0.33, $CHCl_3$).

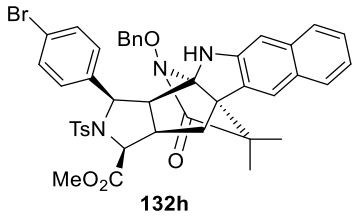


**132h**

**Methyl (1*S*,3*R*,3*bS*,10*bR*)-14-(benzyloxy)-3-(4-bromophenyl)-12,12-dimethyl-13-oxo-2-tosyl-1,2,3,3*a*,11,11*a*-hexahydro-4*H*-3*b*,10*b*-(epiminoethano)-benzo[*f*]pyrrolo-[3',4':4,5]-cyclopenta[1,2-*b*]indole-1-carboxylate (132h)**

white amorphous solid, 46% yield, **$^{1}$H NMR** (500 MHz, $CDCl_3$) δ 7.57 (d, *J* = 8.2 Hz, 1H), 7.50 (s, 7H), 7.43 – 7.36 (m, 2H), 7.29 – 7.27 (m, 1H), 7.23 – 7.16 (m, 3H), 7.11 (d, *J* = 8.2 Hz, 1H), 6.88 – 6.79 (m, 3H), 6.63 (dd, *J* = 8.3, 1.1 Hz, 1H), 5.33 – 5.24 (m, 1H), 5.02 (dd, *J* = 11.5, 3.5 Hz, 2H), 4.62 (d, *J* = 7.2 Hz, 1H), 3.82 (s, 3H), 3.66 – 3.61 (m, 1H), 2.96 – 2.91 (m, 1H), 2.35 – 2.30 (m, 1H), 2.22 (s, 3H), 2.18 (d, *J* = 2.7 Hz, 1H), 1.29 (s, 3H), 1.25 (s, 3H).

**$^{13}$C NMR** (126 MHz, $CDCl_3$) δ 174.93, 170.82, 143.82, 143.07, 136.64, 135.63, 135.28, 133.57, 130.48, 129.78, 129.47, 129.43, 129.04, 128.84, 128.78, 128.04, 128.02, 126.17, 124.57, 123.54, 121.87, 121.78, 120.94, 119.83, 119.79, 94.59, 78.23, 66.34, 64.00, 61.49, 54.16, 52.68, 46.16, 42.58, 27.75, 22.38, 21.52.

**HRMS**: calcd. for $[M+H]^+$ $C_{43}H_{41}{}^{79}BrN_3O_6S$ = 806.18940, found: 806.19024; calcd. for $[M+H]^+$ $C_{43}H_{41}{}^{81}BrN_3O_6S$ = 808.18735, found: 808.18854.

**$[\alpha]^{20}_D$** = + 65.7° (c = 0.27, $CHCl_3$).

## 6.10 Crystal Data

### 6.10.1 X-Ray analysis

The crystal structures of compounds (+**)105a**, (+)**105e**, (+)**105e**, **121a** and (+)**121b** was determined using the *Bruker D8 Venture* four-circle diffractometer equipped with a *PHOTON II* CPAD detector by *Bruker AXS GmbH*. The X-ray radiation was generated by the *IμS* microfocus source Mo (λ = 0.71073 Å) from *Incoatec GmbH* equipped with HELIOS mirror optics and a single-hole collimator by *Bruker AXS GmbH*. The selected single crystal of (+**)105a**, (+)**105e**, (+)**105e**, **121a** and (+)**121b** were covered with an inert oil (perfluoropolyalkyl ether) and mounted on the *MicroMount* from *MiTeGen*. The APEX 3 Suite (v.2018.7-2) software integrated with SAINT (integration) and SADABS (adsorption correction) programs by *Bruker AXS GmbH* were used for data collection. The processing and finalization of the crystal structure were performed using the Olex2 program. The crystal structures were solved by the ShelXT structure solution program using the Intrinsic Phasing option, which were further refined by the ShelXL refinement package using Least Squares minimization. The non-hydrogen atoms were anisotropically refined. The C-bound H atoms were placed in geometrically calculated positions, and a fixed isotropic displacement parameter was assigned to each atom according to the riding-model: C–H = 0.95–1.00 Å with *U*iso(H) = 1.5*U*eq($CH_3$) and 1.2*U*eq($CH_2$, CH) for other hydrogen atoms. The N-bound hydrogen atoms on N1, N2, N3 and N4 were located on the Difference-Fourier-Map and refined independently in every structure. The crystallographic data for the structures of (+)**105a**, (+)**105e**, (–)**105e**, **121a** and (+)**121b** has been published as supplementary publication number 1952338 [(+)**105a**], 2042023 [(+)**105e**], 2042025 [(–)**105e**], 2042027 (**121a**) and 20427026 [(+)**121b**] in the Cambridge Crystallographic Data Centre. A copy of these data can be obtained for free by applying to CCDC, 12 Union Road, Cambridge CB2 IEZ, UK, fax: 144-(0)1223-336033 or e-mail: deposit@ccdc.cam.ac.uk.

Crystal data and structure for (+)**105a**

CCDC Number: 1952338

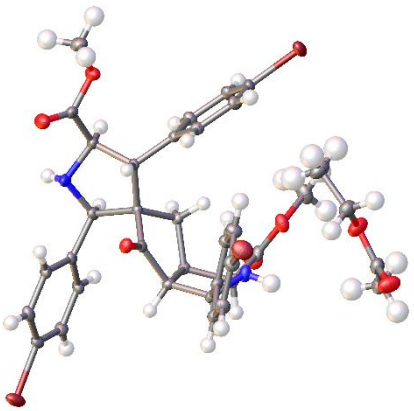

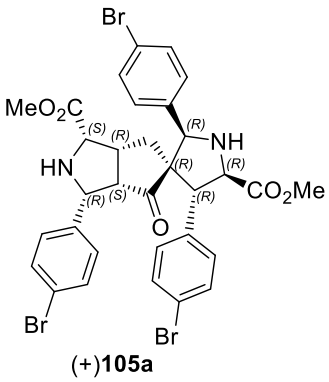


(+)**105a**

| Compound | (+)**105a** |
|---|---|
| Empirical formula | $C_{36}H_{37}Br_3N_2O_7$ |
| Formula weight | 849.40 |
| Temperature/K | 100.0 |
| Crystal system | orthorhombic |
| Space group | $P2_12_12_1$ |
| a/Å | 9.7769(5) |
| b/Å | 10.2614(5) |
| c/Å | 34.8336(18) |
| $\alpha$/° | 90 |
| $\beta$/° | 90 |
| $\gamma$/° | 90 |
| Volume/Å$^3$ | 3494.7(3) |
| Z | 4 |
| $\rho_{calc}$g/cm$^3$ | 1.614 |
| μ/mm$^{-1}$ | 3.514 |
| F(000) | 1712.0 |
| Crystal size/mm$^3$ | 0.278 × 0.278 × 0.191 |
| Radiation | MoKα ($\lambda$ = 0.71073) |
| 2Θ range for data collection/° | 4.138 to 61.998 |
| Index ranges | –14 ≤ h ≤ 14, –14 ≤ k ≤ 14, –50 ≤ l ≤ 50 |
| Reflections collected | 338322 |
| Independent reflections | 11129 [$R_{int}$ = 0.0425, $R_{sigma}$ = 0.0127] |
| Data/restraints/parameters | 11129/0/445 |
| Goodness-of-fit on F$^2$ | 1.086 |
| Final $R$ indexes [I>=2σ (I)] | $R_1$ = 0.0270, w$R_2$ = 0.0717 |
| Final $R$ indexes [all data] | $R_1$ = 0.0282, w$R_2$ = 0.0725 |
| Largest diff. peak/hole / e Å$^{-3}$ | 1.34/–0.57 |
| Flack parameter | –0.0002(13) |

Crystal data and structure for (+)**105e**

CCDC Number: 2042023

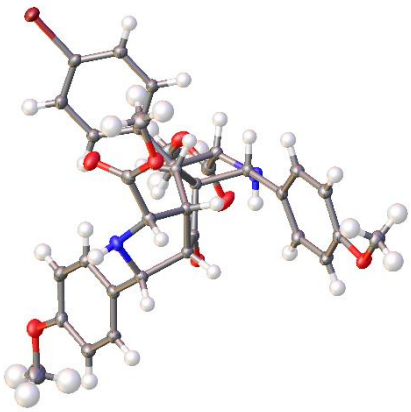

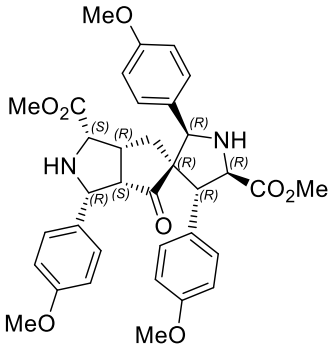


(+)**105e**

| Compound | (+)105**e** |
|---|---|
| Empirical formula | $C_{34}H_{35}BrN_2O_7$ |
| Formula weight | 663.55 |
| Temperature/K | 100.0 |
| Crystal system | orthorhombic |
| Space group | $P2_12_12_1$ |
| a/Å | 13.4421(15) |
| b/Å | 13.6093(14) |
| c/Å | 16.705(2) |
| $\alpha$/° | 90 |
| $\beta$/° | 90 |
| $\gamma$/° | 90 |
| Volume/Å$^3$ | 3055.9(6) |
| Z | 4 |
| $\rho_{calc}$g/cm$^3$ | 1.442 |
| $\mu$/mm$^{-1}$ | 1.398 |
| F(000) | 1376.0 |
| Crystal size/mm$^3$ | 0.722 × 0.186 × 0.176 |
| Radiation | MoK$\alpha$ ($\lambda$ = 0.71073) |
| 2$\Theta$ range for data collection/° | 3.86 to 57.998 |
| Index ranges | $-18 \le h \le 18$, $-18 \le k \le 18$, $-22 \le l \le 22$ |
| Reflections collected | 71862 |
| Independent reflections | 8123 [$R_{int}$ = 0.0429, $R_{sigma}$ = 0.0233] |
| Data/restraints/parameters | 8123/0/409 |
| Goodness-of-fit on F$^2$ | 1.053 |
| Final $R$ indexes [I>=2$\sigma$ (I)] | $R_1$ = 0.0265, w$R_2$ = 0.0694 |
| Final $R$ indexes [all data] | $R_1$ = 0.0285, w$R_2$ = 0.0709 |
| Largest diff. peak/hole / e Å$^{-3}$ | 1.10/–0.34 |
| Flack parameter | –0.0059(19) |

Crystal data and structure for (-)**105e**

CCDC Number: 2042025

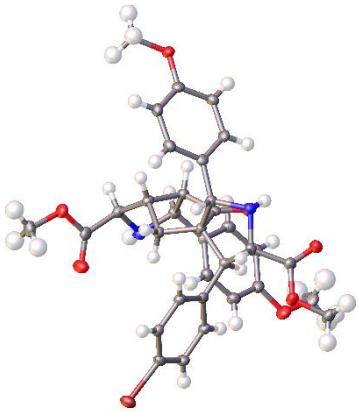

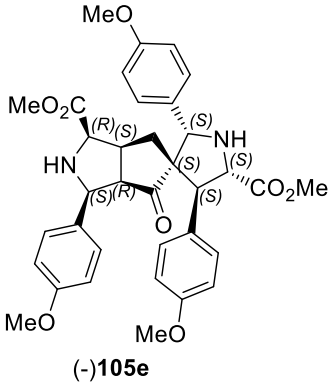


(-)**105e**

| Compound | (–)**105e** |
|---|---|
| Empirical formula | $C_{34}H_{35}BrN_2O_7$ |
| Formula weight | 663.55 |
| Temperature/K | 100.0 |
| Crystal system | orthorhombic |
| Space group | $P2_12_12_1$ |
| a/Å | 13.437(5) |
| b/Å | 13.616(9) |
| c/Å | 16.674(9) |
| $\alpha$/° | 90 |
| $\beta$/° | 90 |
| $\gamma$/° | 90 |
| Volume/Å$^3$ | 3050(3) |
| Z | 4 |
| $\rho_{calc}$g/cm$^3$ | 1.445 |
| μ/mm$^{-1}$ | 1.400 |
| F(000) | 1376.0 |
| Crystal size/mm$^3$ | 0.194 × 0.14 × 0.126 |
| Radiation | MoKα ($\lambda$ = 0.71073) |
| 2Θ range for data collection/° | 3.862 to 55.894 |
| Index ranges | –17 ≤ h ≤ 17, –17 ≤ k ≤ 17, –21 ≤ l ≤ 21 |
| Reflections collected | 37693 |
| Independent reflections | 7292 [$R_{int}$ = 0.0464, $R_{sigma}$ = 0.0375] |
| Data/restraints/parameters | 7292/0/409 |
| Goodness-of-fit on F$^2$ | 1.028 |
| Final $R$ indexes [I>=2σ (I)] | $R_1$ = 0.0317, w$R_2$ = 0.0667 |
| Final $R$ indexes [all data] | $R_1$ = 0.0401, w$R_2$ = 0.0699 |
| Largest diff. peak/hole / e Å$^{-3}$ | 0.75/–0.52 |
| Flack parameter | –0.005(3) |

Crystal data and structure for **121a**

CCDC Number: 2042027

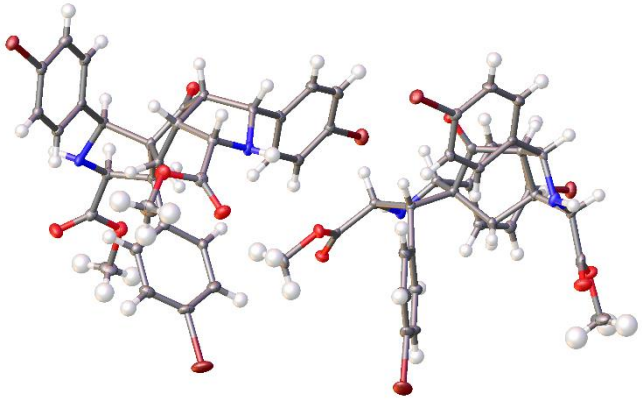

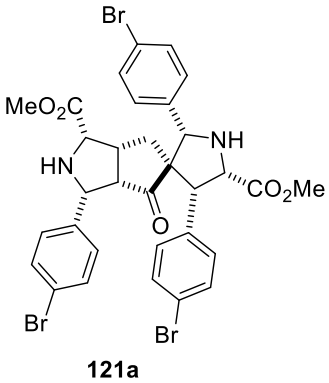


**121a**

| Compound | **121a** |
|---|---|
| Empirical formula | $C_{32}H_{29}Br_3N_2O_5$ |
| Formula weight | 761.30 |
| Temperature/K | 100.0 |
| Crystal system | triclinic |
| Space group | $P\bar{1}$ |
| a/Å | 11.2514(10) |
| b/Å | 15.8026(12) |
| c/Å | 19.7865(11) |
| $\alpha$/° | 80.520(2) |
| $\beta$/° | 81.241(3) |
| $\gamma$/° | 89.927(3) |
| Volume/Å$^3$ | 3428.5(4) |
| Z | 4 |
| $\rho_{calc}$g/cm$^3$ | 1.475 |
| $\mu$/mm$^{-1}$ | 3.569 |
| F(000) | 1520.0 |
| Crystal size/mm$^3$ | 0.343 × 0.29 × 0.206 |
| Radiation | MoK$\alpha$ ($\lambda$ = 0.71073) |
| 2$\Theta$ range for data collection/° | 3.624 to 54 |
| Index ranges | –14 ≤ h ≤ 14, –20 ≤ k ≤ 20, –25 ≤ l ≤ 25 |
| Reflections collected | 127028 |
| Independent reflections | 14914 [$R_{int}$ = 0.0313, $R_{sigma}$ = 0.0172] |
| Data/restraints/parameters | 14914/0/777 |
| Goodness-of-fit on F$^2$ | 1.110 |
| Final $R$ indexes [I>=2$\sigma$ (I)] | $R_1$ = 0.0424, w$R_2$ = 0.1060 |
| Final $R$ indexes [all data] | $R_1$ = 0.0439, w$R_2$ = 0.1066 |
| Largest diff. peak/hole / e Å$^{-3}$ | 1.55/–1.03 |
| Flack parameter | – |

Crystal data and structure for (+)**121b**

CCDC Number: 2042026

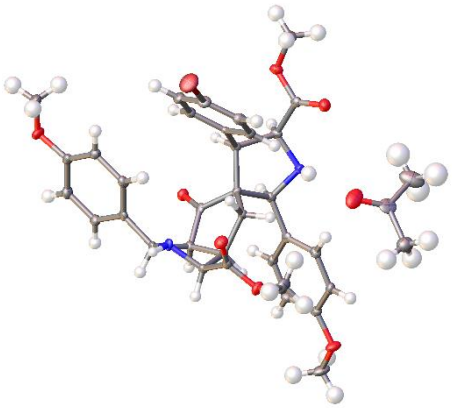

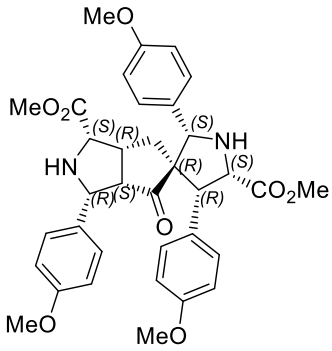


(+)**121b**

| Compound | **(+)121b** |
|---|---|
| Empirical formula | $C_{37}H_{41}BrN_2O_8$ |
| Formula weight | 721.63 |
| Temperature/K | 100.0 |
| Crystal system | hexagonal |
| Space group | $P6_1$ |
| a/Å | 11.267(3) |
| b/Å | 11.267(3) |
| c/Å | 47.013(17) |
| $\alpha$/° | 90 |
| $\beta$/° | 90 |
| $\gamma$/° | 120 |
| Volume/Å$^3$ | 5169(3) |
| Z | 6 |
| $\rho_{calc}$g/cm$^3$ | 1.391 |
| μ/mm$^{-1}$ | 1.248 |
| F(000) | 2256.0 |
| Crystal size/mm$^3$ | 0.358 × 0.1 × 0.066 |
| Radiation | MoKα ($\lambda$ = 0.71073) |
| 2Θ range for data collection/° | 4.52 to 51.992 |
| Index ranges | –13 ≤ h ≤ 13,<br>–13 ≤ k ≤ 13,<br>–57 ≤ l ≤ 57 |
| Reflections collected | 63799 |
| Independent reflections | 6763 [$R_{int}$ = 0.0753,<br>$R_{sigma}$ = 0.0361] |
| Data/restraints/parameters | 6763/1/447 |
| Goodness-of-fit on F$^2$ | 1.046 |
| Final *R* indexes [I>=2σ (I)] | $R_1$ = 0.0329,<br>w$R_2$ = 0.0630 |
| Final *R* indexes [all data] | $R_1$ = 0.0402,<br>w$R_2$ = 0.0657 |
| Largest diff. peak/hole / e Å$^{-3}$ | 0.26/–0.29 |
| Flack parameter | 0.005(3) |

## 6.11 Experimental studies on the double cycloaddition

### 6.11.1 Experimental studies on the stepwise addition

Double cycloaddition to obtain product **105a** was performed stepwise. Enone **104a** was treated with 1.1 equiv. of iminoester **50a** and after 3 h second addition of iminoester **50a** (1.1 equiv.) followed. The product was isolated and enantiomeric excess was determined by HPLC analysis on chiral phase (**IC** column).

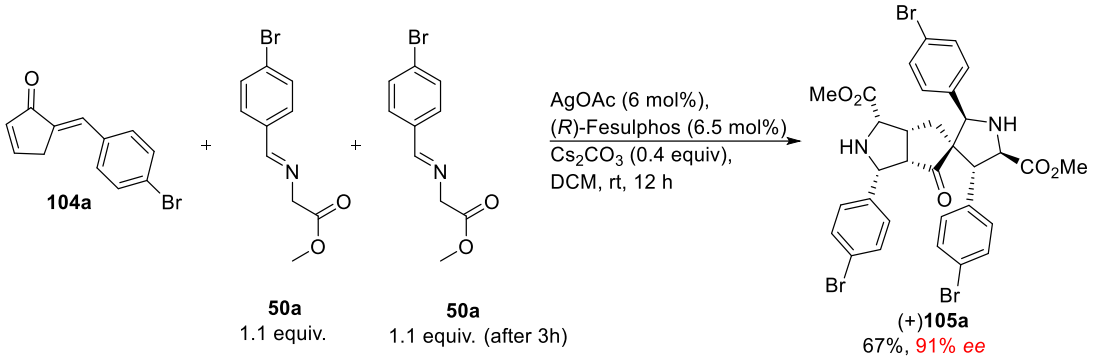


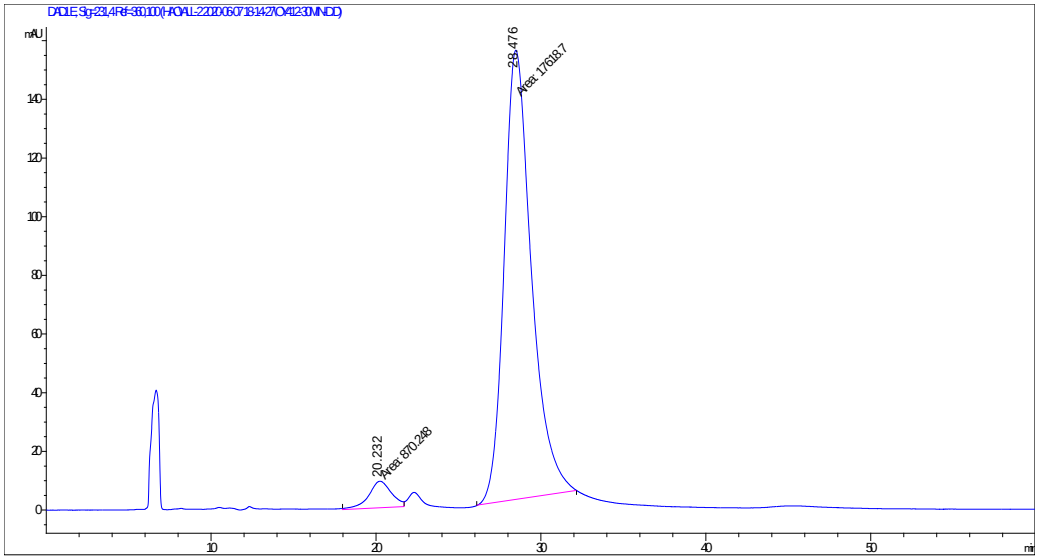


| # | Time | Area | Height | Width | Area% | Symmetry |
|---|---|---|---|---|---|---|
| 1 | 20.232 | 870.2 | 9.1 | 1.6025 | 4.707 | 0.96 |
| 2 | 28.476 | 17618.7 | 153.1 | 1.918 | 95.293 | 0.713 |

Double cycloaddition to obtain product **105a** was performed stepwise. Enone **104a** was treated with 1.1 equiv. of iminoester **50a** with ratio of AgOAc/(*R*)-Fesulphos (1:2) and after 3 h second addition of iminoester **50a** (1.1 equiv.) followed. The product was isolated and enantiomeric excess was determined by HPLC analysis on chiral phase (**IC** column).

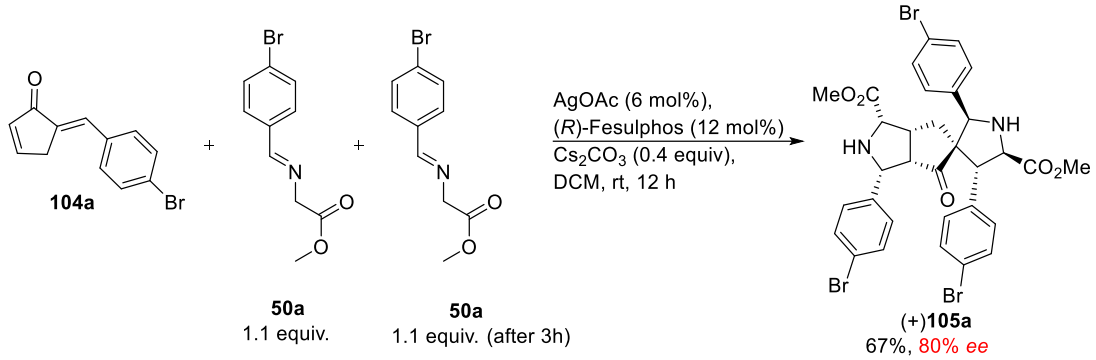


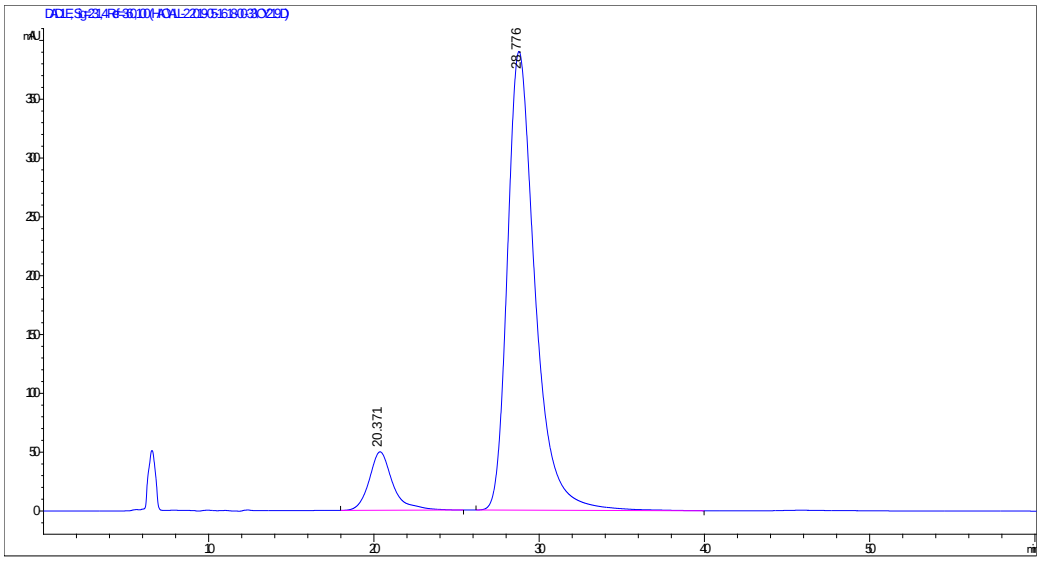


| # | Time | Area | Height | Width | Area% | Symmetry |
|---|---|---|---|---|---|---|
| 1 | 20.371 | 4912.9 | 49.7 | 1.4393 | 9.964 | 0.799 |
| 2 | 28.776 | 44392.6 | 389.2 | 1.9011 | 90.036 | 0.703 |

### 6.11.2 Experimental studies on the mono cycloaddition

Mono cycloaddition of enone **104a** was performed. Enone **104a** was treated with 1.1 equiv. of iminoester **50a** with ratio of AgOAc/(*R*)-Fesulphos **1:2**. The product **110a** was isolated after 3 h and enantiomeric excess was determined by HPLC analysis on chiral phase (**IA** column).

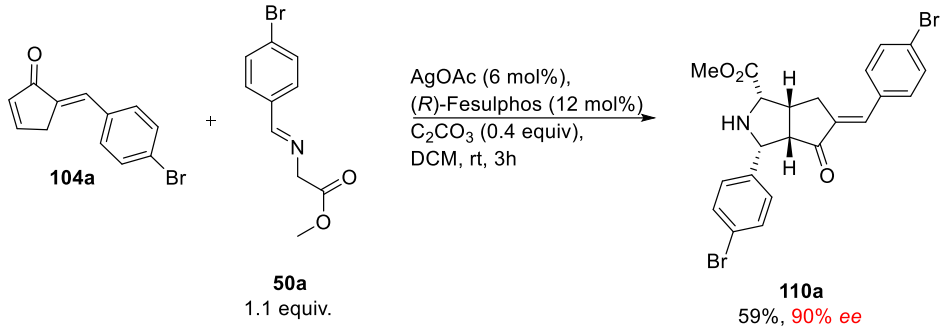


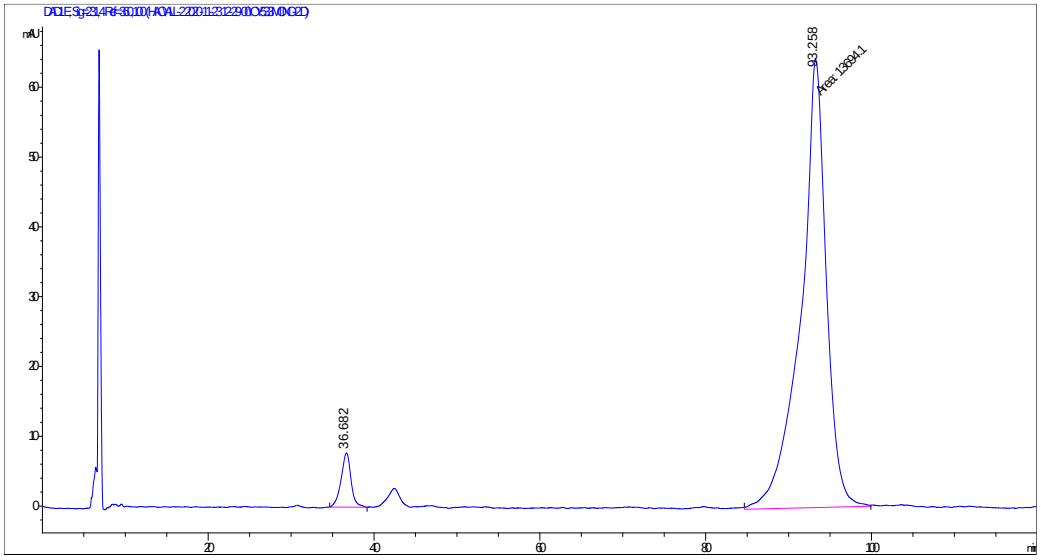


| # | Time | Area | Height | Width | Area% | Symmetry |
|---|---|---|---|---|---|---|
| 1 | 36.682 | 647.9 | 7.8 | 0.9873 | 4.518 | 1.142 |
| 2 | 93.258 | 13694.1 | 64.2 | 3.555 | 95.482 | 1.34 |

Mono cycloaddition of enone **104a** was performed. Enone **104a** was treated with 1.1 equiv. of iminoester **50a** with ratio of AgOAc/(*R*)-Fesulphos **1:2**. The product **110a** was isolated after 16 h and enantiomeric excess was determined by HPLC analysis on chiral phase (**IA** column).

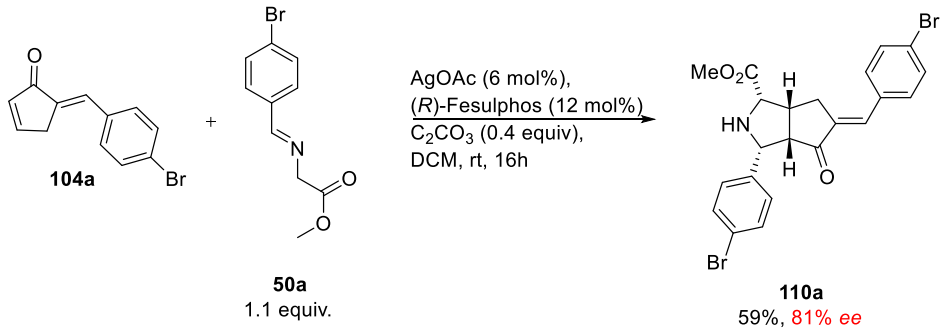


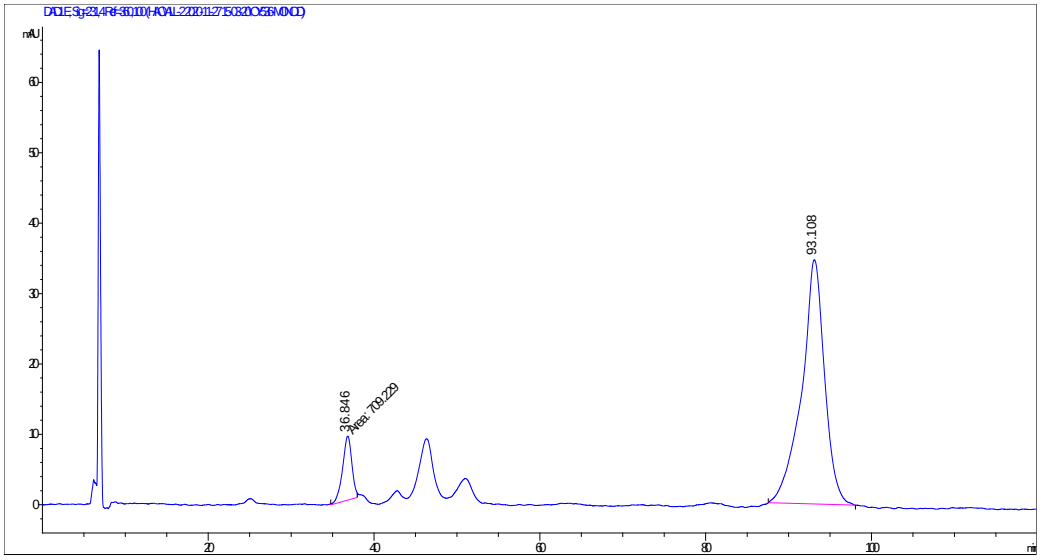


| # | Time | Area | Height | Width | Area% | Symmetry |
|---|---|---|---|---|---|---|
| 1 | 36.846 | 709.2 | 9.1 | 1.3 | 9.594 | 1.301 |
| 2 | 93.108 | 6683 | 34.7 | 2.2694 | 90.406 | 1.212 |

Mono cycloaddition of enone **104a** was performed. Enone **104a** was treated with 1.1 equiv. of iminoester **50a** with ratio of AgOAc/(*R*)-Fesulphos **1:1** and reaction was run for 3 h. The product **110a** was isolated and enantiomeric excess was determined by HPLC analysis on chiral phase (**IC** column).

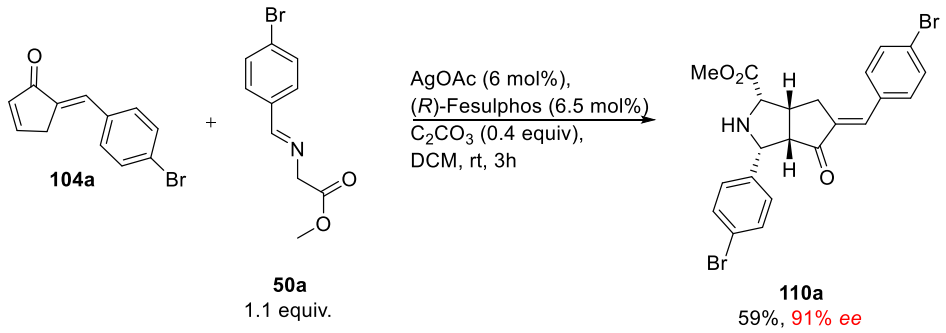


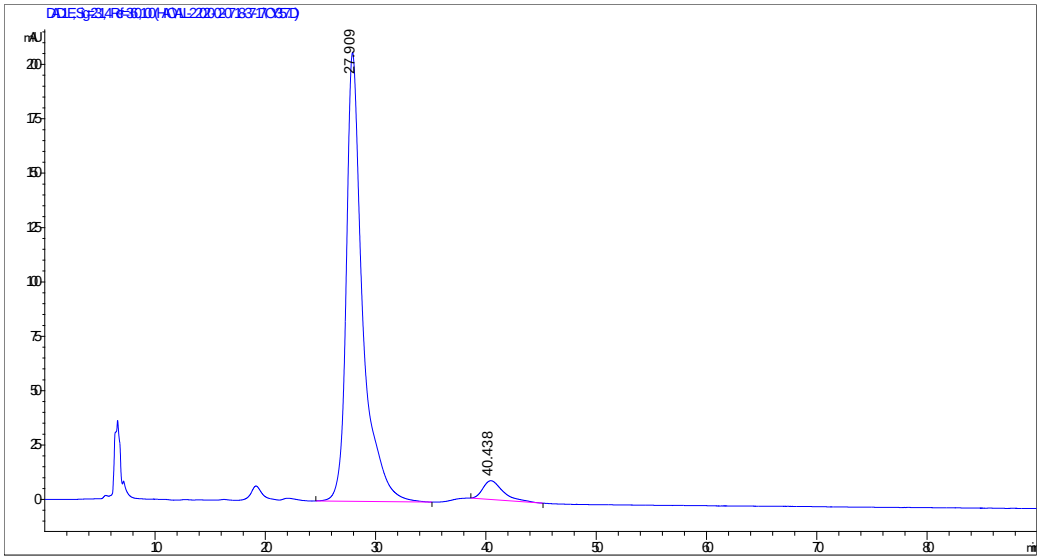


| # | Time | Area | Height | Width | Area% | Symmetry |
|---|---|---|---|---|---|---|
| 1 | 27.909 | 21239.8 | 206.4 | 1.4566 | 95.100 | 0.585 |
| 2 | 40.438 | 1094.5 | 8.6 | 1.4977 | 4.900 | 0.614 |

Mono cycloaddition of enone **104a** was performed. Enone **104a** was treated with 1.1 equiv. of iminoester **50a** with ratio of AgOAc/(*R*)-Fesulphos **1:1** and reaction was run for 12 h. The product **110a** was isolated and enantiomeric excess was determined by HPLC analysis on chiral phase (**IC** column).

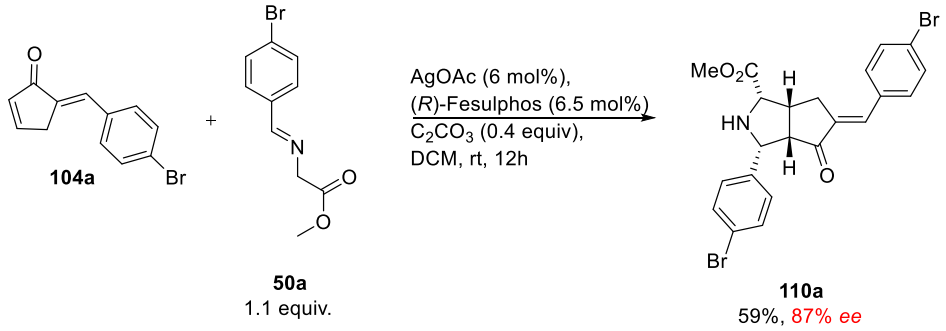


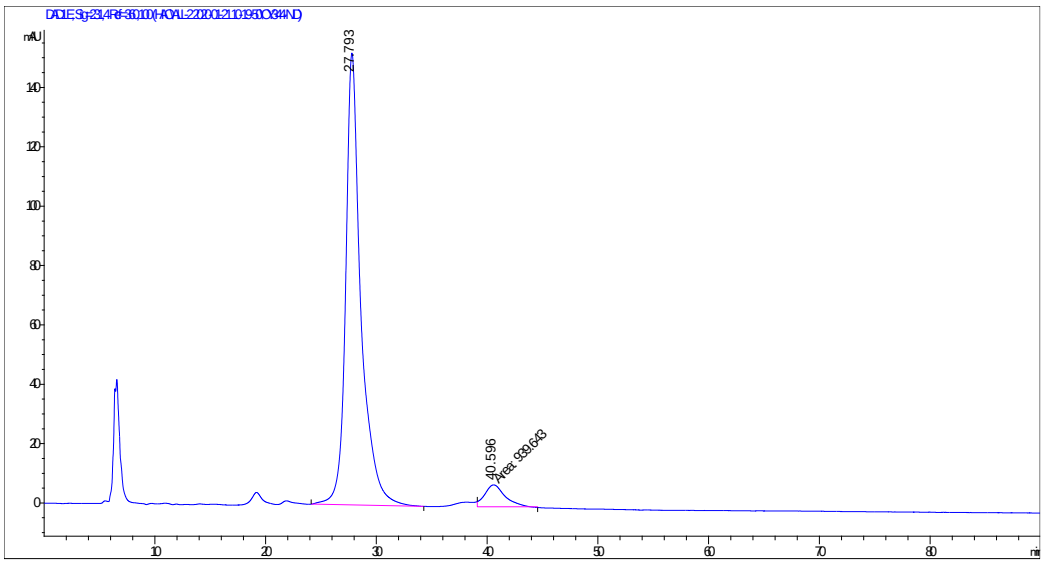


| # | Time | Area | Height | Width | Area% | Symmetry |
|---|---|---|---|---|---|---|
| 1 | 27.793 | 14550.7 | 152.3 | 1.3729 | 93.934 | 0.657 |
| 2 | 40.596 | 939.6 | 7.4 | 2.1229 | 6.066 | 0.773 |

Mono cycloaddition of enone **104a** was performed. Enone **104a** was treated with 1.1 equiv. of iminoester **50g**. Product **110c** was isolated and enantiomeric excess was determined by HPLC analysis on chiral phase (**IC** column)..

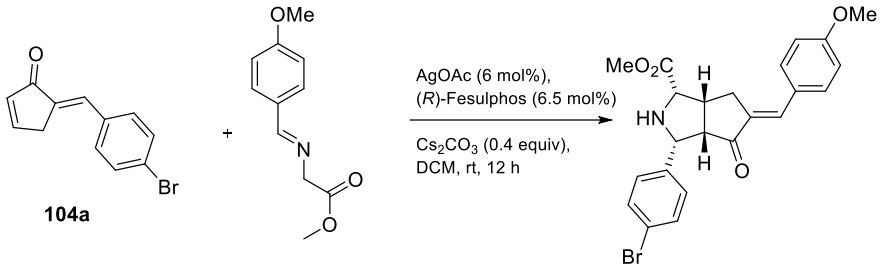


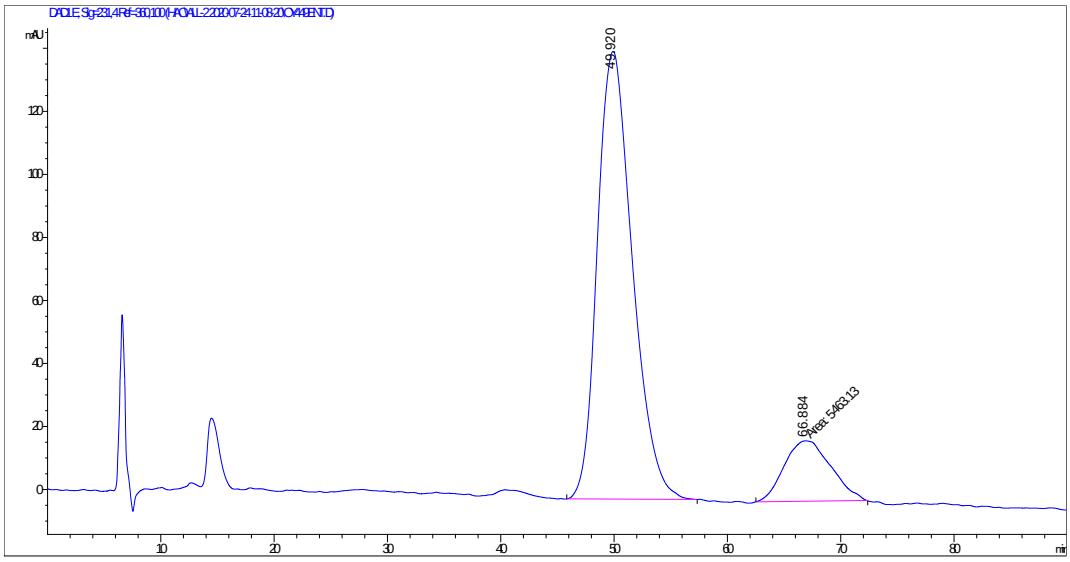


| # | Time | Area | Height | Width | Area% | Symmetry |
|---|---|---|---|---|---|---|
| 1 | 49.92 | 30572.2 | 142.1 | 2.6904 | 84.840 | 0.798 |
| 2 | 66.884 | 5463.1 | 19.2 | 4.7532 | 15.160 | 0.814 |

Racemic mono cycloaddition product **110a** was subjected to chiral conditions and was treated with AgOAc, (R)-Fesulphos and $Cs_2CO_3$. The product **110a** was isolated and enantiomeric excess was determined by HPLC analysis on chiral phase (**IA** column).. Mono cycloaddition product **110a** was recovered as opposite enantiomer, racemization occurs.

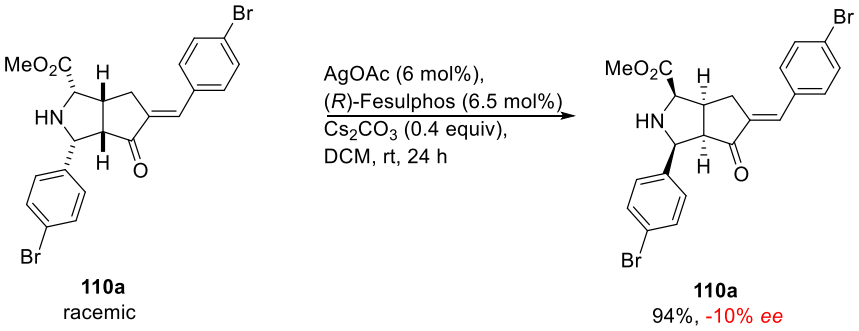


**110a**
racemic

**110a**
94%, -10% *ee*

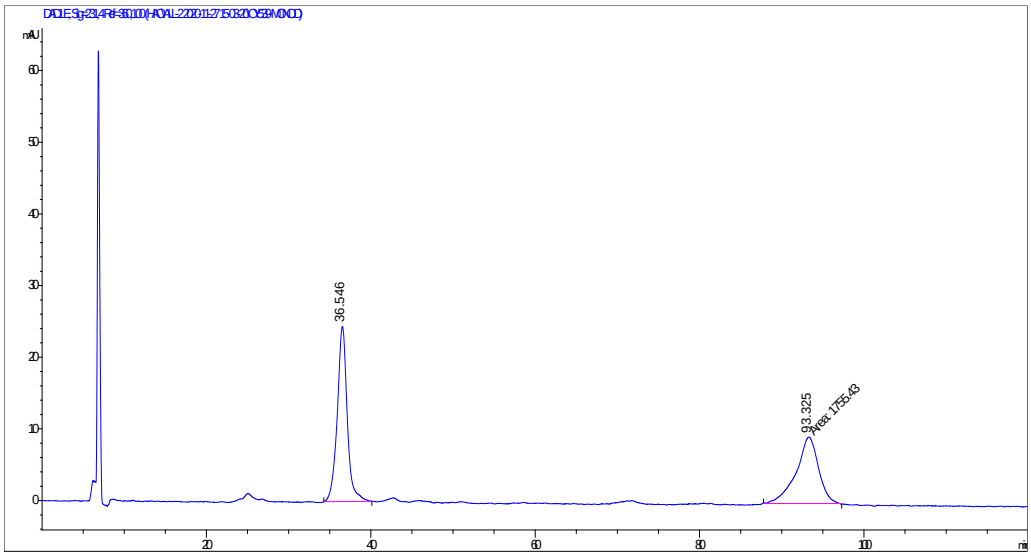


| # | Time | Area | Height | Width | Area% | Symmetry |
|---|---|---|---|---|---|---|
| 1 | 36.546 | 2061.6 | 24.4 | 1.1919 | 54.011 | 1.016 |
| 2 | 93.325 | 1755.4 | 9.3 | 3.1535 | 45.989 | 1.336 |

### 6.11.3 Experimental studies on the second cycloaddition

Enantioenriched mono cycloaddition product **110a** was treated with 1.1 equiv. of iminoester **50a** using achiral ligand $PPh_3$. The product **105a** was isolated and enantiomeric excess was determined by HPLC analysis on chiral phase (**IA** column).

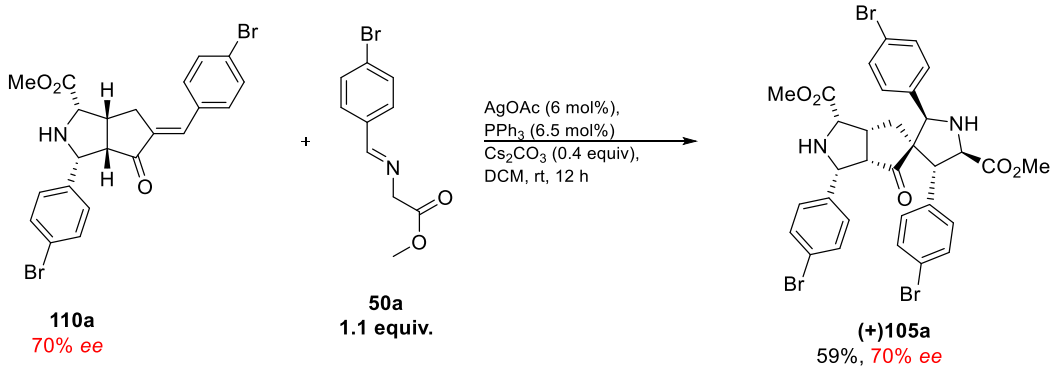


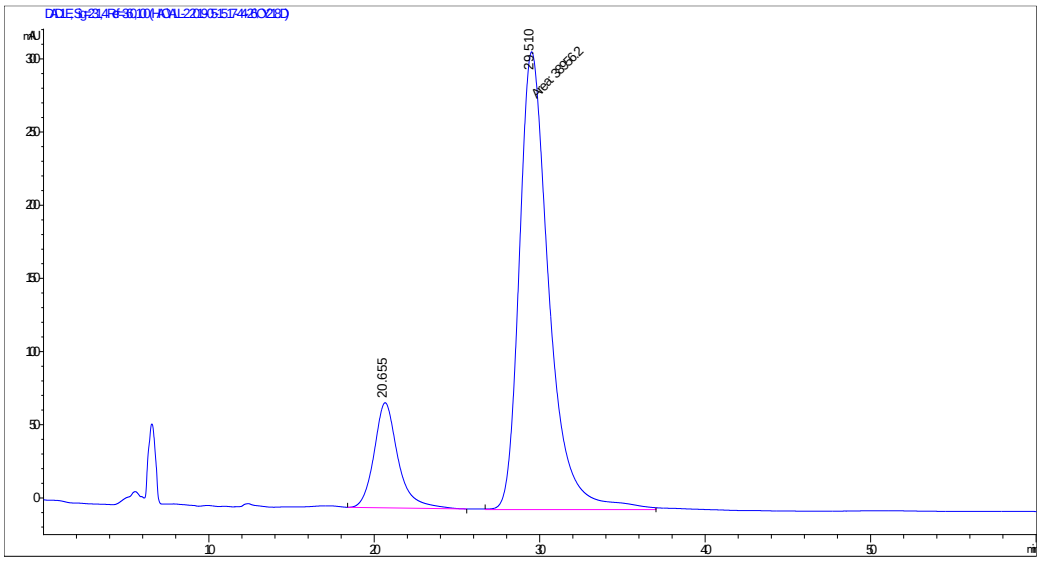


| # | Time | Area | Height | Width | Area% | Symmetry |
|---|---|---|---|---|---|---|
| 1 | 20.655 | 7067.4 | 72 | 1.6358 | 15.671 | 0.889 |
| 2 | 29.51 | 38029.9 | 311.4 | 2.0356 | 84.329 | 0.688 |

Enantioenriched mono cycloaddition product **110c** was treated with 1.1 equiv. of iminoester **50g**. The product was isolated and enantiomeric excess was determined by HPLC analysis on chiral phase (**IC** column).

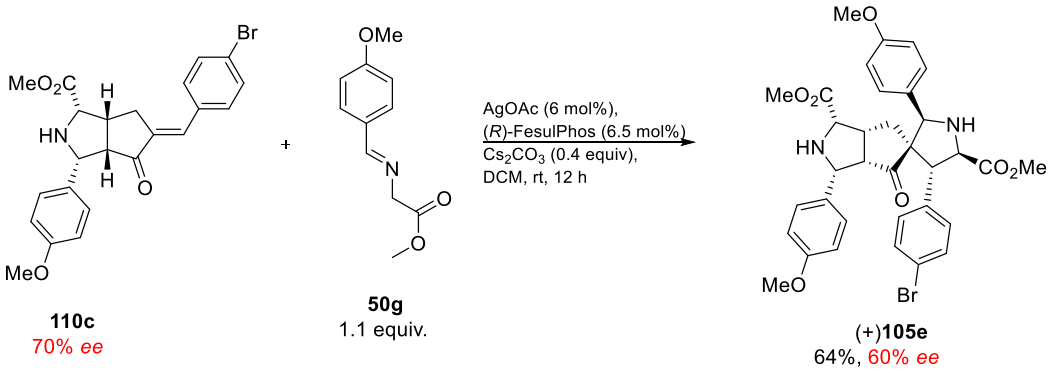


**110c**
70% *ee*

**50g**
1.1 equiv.

(+)**105e**
64%, 60% *ee*

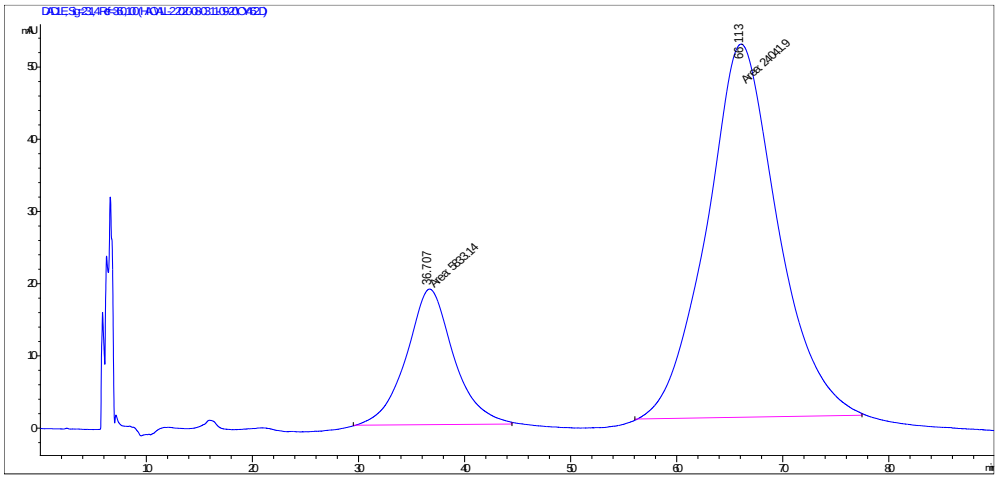


| # | Time | Area | Height | Width | Area% | Symmetry |
|---|---|---|---|---|---|---|
| 1 | 36.707 | 5833.1 | 18.8 | 5.1751 | 19.525 | 0.943 |
| 2 | 66.113 | 24041.9 | 51.7 | 7.7531 | 80.475 | 0.936 |

Enantioenriched mono cycloaddition product **110c** was treated with 1.1 equiv. of iminoester **50g** under racemic conditions. The product **105e** was isolated and enantiomeric excess was determined by HPLC analysis on chiral phase (**IC** column).

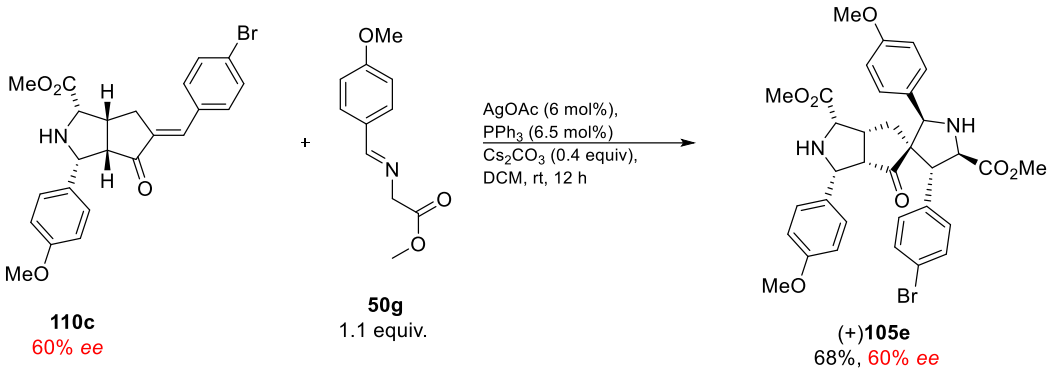


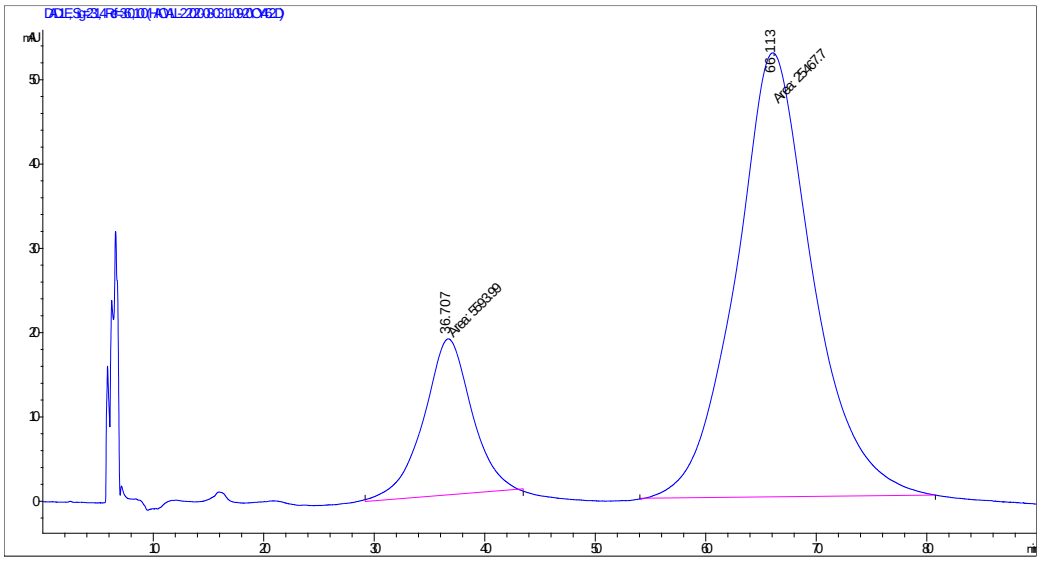


| # | Time | Area | Height | Width | Area% | Symmetry |
|---|---|---|---|---|---|---|
| 1 | 36.707 | 5594 | 18.5 | 5.0391 | 18.009 | 1.044 |
| 2 | 66.113 | 25467.7 | 52.7 | 8.0581 | 81.991 | 0.922 |

### 6.11.4 Experimental studies on the racemic mono adduct

Racemic mono cycloaddition product **110a** was treated with 1.1 equiv. of iminoester **50a**. The product was isolated and enantiomeric excess was determined by HPLC analysis on chiral phase (**IC** column). Opposite enantiomer compared double cycloaddition with enone **104a** was obtained.

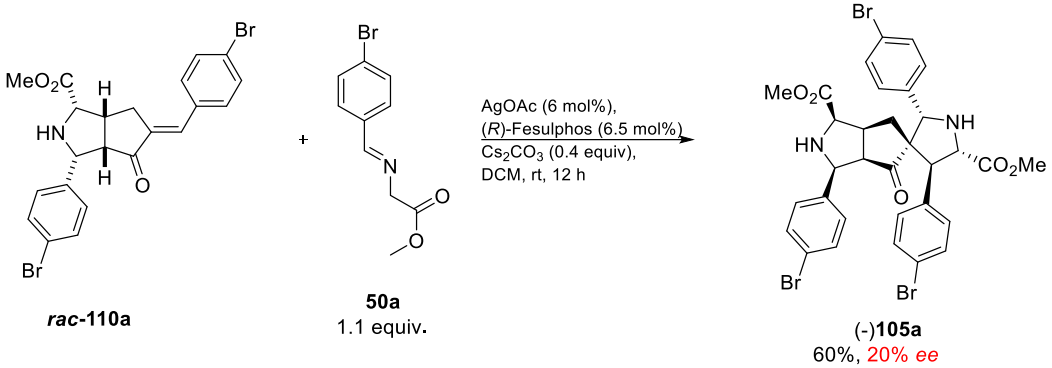


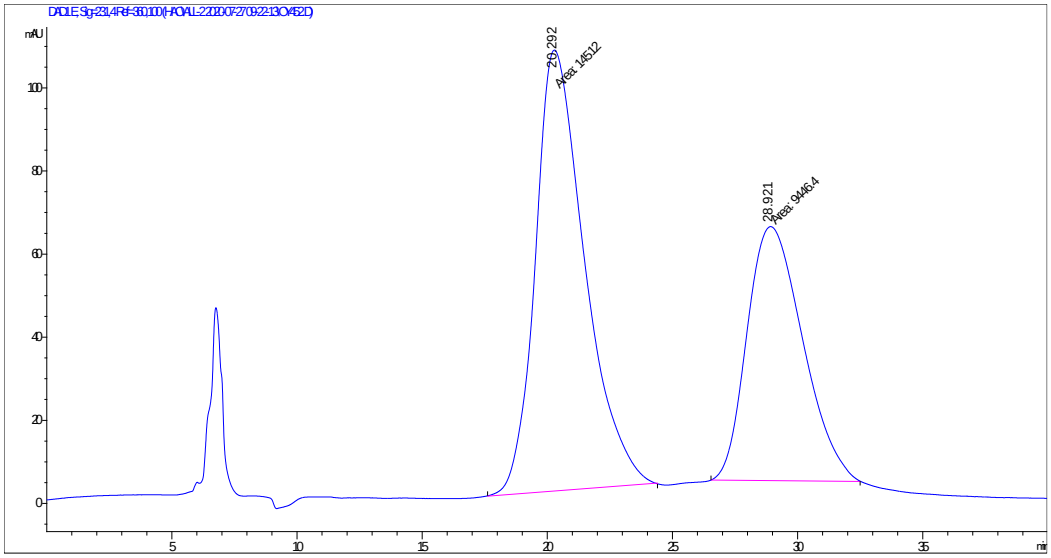


| # | Time | Area | Height | Width | Area% | Symmetry |
|---|---|---|---|---|---|---|
| 1 | 20.292 | 14512 | 106.1 | 2.2794 | 60.572 | 0.631 |
| 2 | 28.921 | 9446.4 | 61.1 | 2.5748 | 39.428 | 0.711 |

Racemic mono cycloaddition product **110c** was treated with 1.1 equiv. of iminoester **50g**. The product was isolated and enantiomeric excess was determined by HPLC analysis on chiral phase (**IC** column). Opposite enantiomer compared double cycloaddition with enone **104a** was obtained.

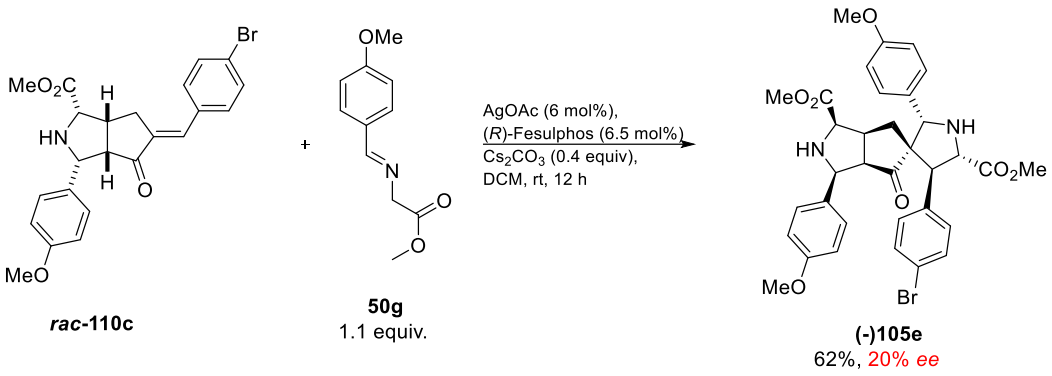


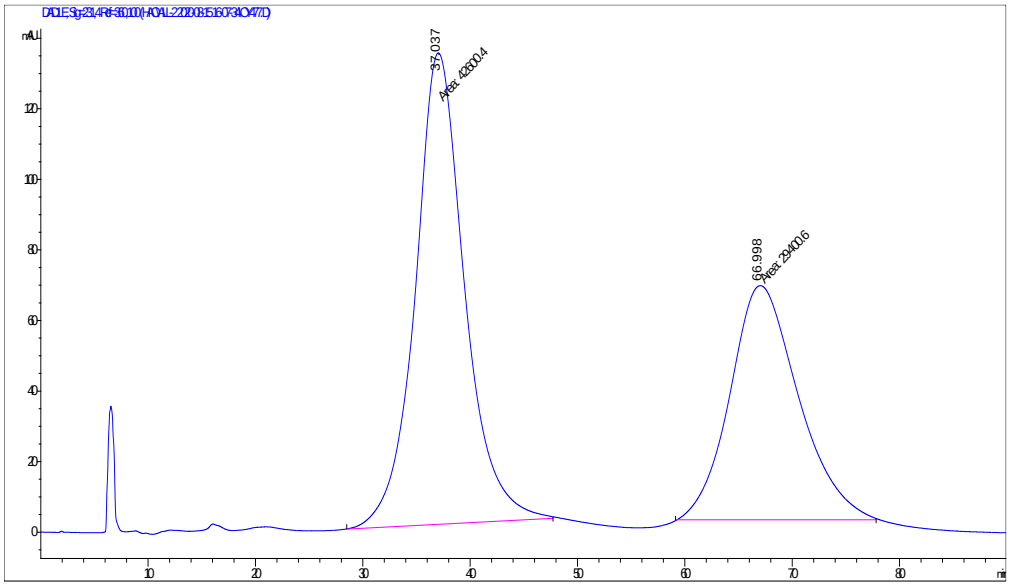


| # | Time | Area | Height | Width | Area% | Symmetry |
|---|---|---|---|---|---|---|
| 1 | 37.037 | 42600.4 | 133.6 | 5.3143 | 59.166 | 0.862 |
| 2 | 66.998 | 29400.6 | 66.4 | 7.381 | 40.834 | 0.767 |

# 7 References


[1] D. J. Newman, G. M. Cragg, *J. Nat. Prod.* **2007**, *70*, 461-477.

[2] S. Wetzel, R. S. Bon, K. Kumar, H. Waldmann, *Angew. Chem. Int. Ed.* **2011**, *50*, 10800-10826.

[3] G. Karageorgis, E. S. Reckzeh, J. Ceballos, M. Schwalfenberg, S. Sievers, C. Ostermann, A. Pahl, S. Ziegler, H. Waldmann, *Nat. Chem.* **2018**, *10*, 1103-1111.

[4] G. Karageorgis, D. J. Foley, L. Laraia, H. Waldmann, *Nat. Chem.* **2020**, *12*, 227-235.

[5] J. Adrio, J. C. Carretero, *Chem. Commun.* **2014**, *50*, 12434-12446.

[6] A. G. Taha, E. E. Elboray, Y. Kobayashi, T. Furuta, H. H. Abbas-Temirek, M. F. Aly, *J. Org. Chem.* **2020**.

[7] S. J. Rowan, S. J. Cantrill, G. R. Cousins, J. K. Sanders, J. F. Stoddart, *Angew. Chem. Int. Ed.* **2002**, *41*, 898-952.

[8] A. M. Edwards, R. Isserlin, G. D. Bader, S. V. Frye, T. M. Willson, H. Y. Frank, *Nature* **2011**, *470*, 163-165.

[9] M. Grigalunas, A. Burhop, A. Christoforow, H. Waldmann, *Curr. Opin. Chem. Biol.* **2020**.

[10] A. L. Harvey, *Drug Discovery Today* **2008**, *13*, 894-901.

[11] D. A. Dias, S. Urban, U. Roessner, *Metabolites* **2012**, *2*, 303-336.

[12] A. L. Harvey, R. Edrada-Ebel, R. J. Quinn, *Nat. Rev. Drug Discovery* **2015**, *14*, 111-129.

[13] J.-M. Ghuysen, *Int. J. Antimicrob. Agents* **1997**, *8*, 45-60.

[14] D. J. Newman, G. M. Cragg, *J. Nat. Prod.* **2012**, *75*, 311-335.

[15] D. H. Drewry, R. Macarron, *Curr. Opin. Chem. Biol.* **2010**, *14*, 289-298.

[16] A. G. Atanasov, B. Waltenberger, E.-M. Pferschy-Wenzig, T. Linder, C. Wawrosch, P. Uhrin, V. Temml, L. Wang, S. Schwaiger, E. H. Heiss, *Biotechnol. Adv.* **2015**, *33*, 1582-1614.

[17] G. M. Rishton, *Am. J. Cardiol.* **2008**, *101*, S43-S49.

[18] G. M. Cragg, S. A. Schepartz, M. Suffness, M. R. Grever, *J. Nat. Prod.* **1993**, *56*, 1657-1668.

[19] A. G. Atanasov, S. B. Zotchev, V. M. Dirsch, C. T. Supuran, *Nat. Rev. Drug Discovery* **2021**, 1-17.

[20] E. Zamir, P. I. Bastiaens, *Nat. Chem. Biol.* **2008**, *4*, 643-647.

[21] R. S. Bohacek, C. McMartin, W. C. Guida, *Med. Res. Rev.* **1996**, *16*, 3-50.

[22] C. M. Dobson, Nature Publishing Group, **2004**.

[23] R. S. Bon, H. Waldmann, *Acc. Chem. Res.* **2010**, *43*, 1103-1114.

[24] H. Van Hattum, H. Waldmann, *J. Am. Chem. Soc.* **2014**, *136*, 11853-11859.

[25] G. Karageorgis, H. Waldmann, *Synthesis-Stuttgart* **2018**, *51*, 55-66.

[26] M. A. Koch, A. Schuffenhauer, M. Scheck, S. Wetzel, M. Casaulta, A. Odermatt, P. Ertl, H. Waldmann, *Proc. Natl. Acad. Sci. U.S.A.* **2005**, *102*, 17272-17277.

[27] A. Schuffenhauer, P. Ertl, S. Roggo, S. Wetzel, M. A. Koch, H. Waldmann, *J. Chem. Inf. Model.* **2007**, *47*, 47-58.

[28] S. Wetzel, A. Schuffenhauer, S. Roggo, P. Ertl, H. Waldmann, *CHIMIA International Journal for Chemistry* **2007**, *61*, 355-360.

[29] G. S. Cremosnik, J. Liu, H. Waldmann, *Nat. Prod. Rep.* **2020**, *37*, 1497-1510.

[30] A. P. Antonchick, S. López-Tosco, J. Parga, S. Sievers, M. Schürmann, H. Preut, S. Höing, H. R. Schöler, J. Sterneckert, D. Rauh, *Chem. Biol.* **2013**, *20*, 500-509.

[31] J. Švenda, M. Sheremet, L. Kremer, L. Maier, J. O. Bauer, C. Strohmann, S. Ziegler, K. Kumar, H. Waldmann, *Angew. Chem. Int. Ed.* **2015**, *127*, 5688-5694.

[32] E. A. Crane, K. Gademann, *Angew. Chem. Int. Ed.* **2016**, *55*, 3882-3902.

[33] C. R. Pye, M. J. Bertin, R. S. Lokey, W. H. Gerwick, R. G. Linington, *Proc. Natl. Acad. Sci. U.S.A.* **2017**, *114*, 5601-5606.

[34] G. Karageorgis, D. J. Foley, L. Laraia, S. Brakmann, H. Waldmann, *Angew. Chem. Int. Ed.* **2021**.

[35] B. Over, S. Wetzel, C. Grütter, Y. Nakai, S. Renner, D. Rauh, H. Waldmann, *Nat. Chem.* **2013**, *5*, 21-28.

[36] M. Feher, J. M. Schmidt, *J. Chem. Inform. Comput. Sci.* **2003**, *43*, 218-227.

[37] F. Lovering, J. Bikker, C. Humblet, *J. Med. Chem.* **2009**, *52*, 6752-6756.

[38] R. Narayan, J. O. Bauer, C. Strohmann, A. P. Antonchick, H. Waldmann, *Angew. Chem. Int. Ed.* **2013**, *52*, 12892-12896.

[39] T. Schneidewind, S. Kapoor, G. Garivet, G. Karageorgis, R. Narayan, G. Vendrell-Navarro, A. P. Antonchick, S. Ziegler, H. Waldmann, *Cell Chem. Biol.* **2019**, *26*, 512-523. e515.

[40] H. Waldmann, G. Karageorgis, D. J. Foley, L. Laraia, S. Brakmann, *Angew. Chem. Int. Ed.* **2021**.

[41] C. Nájera, J. M. Sansano, in *Synthesis of Heterocycles via Cycloadditions I*, Springer, **2008**, pp. 117-145.

[42] L. M. Stanley, M. P. Sibi, *Chem. Rev.* **2008**, *108*, 2887-2902.

[43] T. Hashimoto, K. Maruoka, *Chem. Rev.* **2015**, *115*, 5366-5412.

[44] K. V. Gothelf, K. A. Jørgensen, *Chem. Rev.* **1998**, *98*, 863-910.

[45] E. Buchner, *Ber. Dtsch. Chem. Ges.* **1888**, *21*, 2637-2647.

[46] R. Huisgen, *Angew. Chem. Int. Ed.* **1963**, *2*, 633-645.

[47] R. Huisgen, *Angew. Chem. Int. Ed.* **1968**, *7*, 321-328.

[48] R. Woodward, R. Hoffmann, Weinheim/Deerfield Beach, **1970**.

[49] R. B. Woodward, R. Hoffmann, *J. Am. Chem. Soc.* **1965**, *87*, 395-397.

[50] K. Houk, J. Sims, C. R. Watts, L. Luskus, *J. Am. Chem. Soc.* **1973**, *95*, 7301-7315.

[51] K. Houk, J. Sims, R. Duke, R. Strozier, J. K. George, *J. Am. Chem. Soc.* **1973**, *95*, 7287-7301.

[52] R. Sustmann, in *Physical Organic Chemistry–2*, Elsevier, **1974**, pp. 569-593.

[53] R. Sustmann, *Tetrahedron Lett.* **1971**, *12*, 2717-2720.

[54] H. Pellissier, *Tetrahedron* **2007**, *16*, 3235-3285.

[55] R. Huisgen, G. Mloston, E. Langhals, *J. Am. Chem. Soc.* **1986**, *108*, 6401-6402.

[56] S. G. Pyne, A. S. Davis, N. Gates, J. Hartley, K. Lindsay, T. Machan, M. Tang, **2004**.

[57] R. Narayan, M. Potowski, Z.-J. Jia, A. P. Antonchick, H. Waldmann, *Acc. Chem. Res.* **2014**, *47*, 1296-1310.

[58] J. M. Longmire, B. Wang, X. Zhang, *J. Am. Chem. Soc.* **2002**, *124*, 13400-13401.

[59] A. S. Gothelf, K. V. Gothelf, R. G. Hazell, K. A. Jørgensen, *Angew. Chem. Int. Ed.* **2002**, *114*, 4410-4412.

[60] O. G. Mancheño, J. Priego, S. Cabrera, R. G. Arrayás, T. Llamas, J. C. Carretero, *J. Org. Chem.* **2003**, *68*, 3679-3686.

[61] S. Cabrera, R. G. Arrayás, J. C. Carretero, *J. Am. Chem. Soc.* **2005**, *127*, 16394-16395.

[62] A. P. Antonchick, C. Gerding-Reimers, M. Catarinella, M. Schürmann, H. Preut, S. Ziegler, D. Rauh, H. Waldmann, *Nat. Chem.* **2010**, *2*, 735.

[63] M. Potowski, M. Schürmann, H. Preut, A. P. Antonchick, H. Waldmann, *Nat. Chem. Biol.* **2012**, *8*, 428-430.

[64] M. Potowski, J. O. Bauer, C. Strohmann, A. P. Antonchick, H. Waldmann, *Angew. Chem. Int. Ed.* **2012**, *51*, 9512-9516.

[65] D. Seebach, *Angew. Chem. Int. Ed.* **1990**, *29*, 1320-1367.

[66] T. Maeda, H. Otsuka, A. Takahara, *Prog. Polym. Sci.* **2009**, *34*, 581-604.

[67] J. Hu, S. K. Gupta, J. Ozdemir, M. H. Beyzavi, *ACS Appl. Nano Mater.* **2020**, *3*, 6239-6269.

[68] J.-M. Lehn, A. V. Eliseev, *Science* **2001**, *291*, 2331-2332.

[69] P. T. Corbett, J. Leclaire, L. Vial, K. R. West, J.-L. Wietor, J. K. Sanders, S. Otto, *Chem. Rev.* **2006**, *106*, 3652-3711.

[70] F. B. Cougnon, J. K. Sanders, *Acc. Chem. Res.* **2012**, *45*, 2211-2221.

[71] Y. Jin, C. Yu, R. J. Denman, W. Zhang, *Chem. Soc. Rev.* **2013**, *42*, 6634-6654.

[72] P. Vongvilai, M. Angelin, R. Larsson, O. Ramström, *Angew. Chem. Int. Ed.* **2007**, *119*, 966-968.

[73] S. Xu, N. Giuseppone, *J. Am. Chem. Soc.* **2008**, *130*, 1826-1827.

[74] R. J. Lins, S. L. Flitsch, N. J. Turner, E. Irving, S. A. Brown, *Tetrahedron* **2004**, *60*, 771-780.

[75] D. G. Blackmond, *Cold Spring Harbor Perspect. Biol.* **2010**, *2*, a002147.

[76] D. G. Blackmond, *Chem. Rev.* **2019**, *120*, 4831-4847.

[77] I. P. Beletskaya, C. Nájera, M. Yus, *Chem. Rev.* **2018**, *118*, 5080-5200.

[78] M. P. Sibi, M. Liu, *Curr. Org. Chem.* **2001**, *5*, 719-755.

[79] M. Bartók, *Chem. Rev.* **2010**, *110*, 1663-1705.

[80] S. Krautwald, D. Sarlah, M. A. Schafroth, E. M. Carreira, *Science* **2013**, *340*, 1065-1068.

[81] H. Kagan, J. Fiaud, *Top. Stereochem.* **1988**, *18*, 249-330.

[82] J. M. Keith, J. F. Larrow, E. N. Jacobsen, *Adv. Synth. Catal.* **2001**, *343*, 5-26.

[83] H. Takayama, Z. J. Jia, L. Kremer, J. O. Bauer, C. Strohmann, S. Ziegler, A. P. Antonchick, H. Waldmann, *Angew. Chem. Int. Ed.* **2013**, *52*, 12404-12408.

[84] H.-F. Tu, P. Yang, Z.-H. Lin, C. Zheng, S.-L. You, *Nat. Chem.* **2020**, *12*, 838-844.

[85] M. Potowski, C. Merten, A. P. Antonchick, H. Waldmann, *Chem. Eur. J.* **2015**, *21*, 4913-4917.

[86] S. Cabrera, R. G. Arrayás, B. Martín-Matute, F. P. Cossío, J. C. Carretero, *Tetrahedron* **2007**, *63*, 6587-6602.

[87] T. Takanami, K. Suda, H. Ohmori, *Tetrahedron Lett.* **1990**, *31*, 677-680.

[88] A. H. Alberts, H. Wynberg, *J. Am. Chem. Soc.* **1989**, *111*, 7265-7266.

[89] K. P. Bryliakov, *ACS Catal.* **2019**, *9*, 5418-5438.

[90] K. Soai, T. Shibata, I. Sato, *Acc. Chem. Res.* **2000**, *33*, 382-390.

[91] K. Soai, I. Sato, T. Shibata, *Chem. Rec.* **2001**, *1*, 321-332.

[92] D. P. Heller, D. R. Goldberg, W. D. Wulff, *J. Am. Chem. Soc.* **1997**, *119*, 10551-10552.

[93] K. Soai, S. Niwa, H. Hori, *J. Chem. Soc., Chem. Commun.* **1990**, 982-983.

[94] S. V. Athavale, A. Simon, K. N. Houk, S. E. Denmark, *Nat. Chem.* **2020**, *12*, 412-423.

[95] N. Mizushima, M. Komatsu, *Cell* **2011**, *147*, 728-741.

[96] N. Mizushima, *Genes Dev.* **2007**, *21*, 2861-2873.

[97] D. Glick, S. Barth, K. F. Macleod, *J. Pathol.* **2010**, *221*, 3-12.

[98] U. Anthoni, C. Christophersen, P. H. Nielsen, *Alkaloids: Chemical and Biological Perspectives* **1999**, *13*, 163-236.

[99] A. J. Kochanowska-Karamyan, M. T. Hamann, *Chem. Rev.* **2010**, *110*, 4489-4497.

[100] K. T. Shaw, T. Utsuki, J. Rogers, Q.-S. Yu, K. Sambamurti, A. Brossi, Y.-W. Ge, D. K. Lahiri, N. H. Greig, *Proc. Natl. Acad. Sci. U.S.A.* **2001**, *98*, 7605-7610.

[101] P. Tuntiwachwuttikul, T. Taechowisan, A. Wanbanjob, S. Thadaniti, W. C. Taylor, *Tetrahedron* **2008**, *64*, 7583-7586.

[102] M. Yanagihara, N. Sasaki-Takahashi, T. Sugahara, S. Yamamoto, M. Shinomi, I. Yamashita, M. Hayashida, B. Yamanoha, A. Numata, T. Yamori, *Cancer Sci.* **2005**, *96*, 816-824.

[103] F.-T. Sheng, J.-Y. Wang, W. Tan, Y.-C. Zhang, F. Shi, *Org. Chem. Front.* **2020**, *7*, 3967-3998.

[104] L. M. Repka, J. Ni, S. E. Reisman, *J. Am. Chem. Soc.* **2010**, *132*, 14418-14420.

[105] J. E. Spangler, H. M. Davies, *J. Am. Chem. Soc.* **2013**, *135*, 6802-6805.

[106] W. Ji, L. Yao, X. Liao, *Org. Lett.* **2016**, *18*, 628-630.

[107] S. Gore, S. Baskaran, B. König, *Org. Lett.* **2012**, *14*, 4568-4571.

[108] B. Robinson, *Chem. Rev.* **1969**, *69*, 227-250.

[109] C. S. Jeffrey, K. L. Barnes, J. A. Eickhoff, C. R. Carson, *J. Am. Chem. Soc.* **2011**, *133*, 7688-7691.

[110] A. López-Pérez, J. Adrio, J. C. Carretero, *Angew. Chem. Int. Ed.* **2009**, *121*, 346-349.

[111] A. López-Pérez, J. Adrio, J. C. Carretero, *J. Am. Chem. Soc.* **2008**, *130*, 10084-10085.

[112] C.-J. Wang, G. Liang, Z.-Y. Xue, F. Gao, *J. Am. Chem. Soc.* **2008**, *130*, 17250-17251.

[113] O. Cusso, M. Cianfanelli, X. Ribas, R. J. Klein Gebbink, M. Costas, *J. Am. Chem. Soc.* **2016**, *138*, 2732-2738.

# 8 Appendix

## 8.1 List of abbreviations

| | |
|---|---|
| Ac | acetyl |
| AcOH | acetic acid |
| AgOAc | silver acetate |
| aq. | aqueous |
| Bn | benzyl |
| BIOS | Biology Oriented Synthesis |
| CA | cycloaddition |
| calcd | calculated |
| cat. | catalyst |
| $Cs_2CO_3$ | cesium carbonate |
| COMAS | Compound Management and Screening Center |
| conc. | concentration |
| $CuBF_4$ | $Cu(CH_3CN)_4BF_4$ |
| $CuPF_6$ | $Cu(CH_3CN)_4PF_6$ |
| DBU | 1,8-Diazabicyclo(5.4.0)undec-7-ene |
| DCE | 1,2-dichloroethane |
| DCM | dichloromethane |
| DIPEA | diisopropylethylamine |
| DMF | dimethylformamide |
| DMSO | dimethylsulfoxide |
| d.r. | *diastereomeric ratio* |
| e.e. | *enantiomeric excess* |
| ESI | electrospray ionization |
| Et | ethyl |
| $Et_3N$ | triethylamine |
| $Et_2O$ | diethylether |
| EtOAc | ethylacetate |
| equiv. | equivalent |
| EWG | electron withdrawing group |
| FT-IR | Fourier-Transform Infrared spectroscopy |
| $\Delta G$ | Gibbs-energy |

| | |
|---|---|
| GLUT | Glucosetransporter |
| h | hour |
| Hh | hedgehog |
| HOMO | Highest occupied molecular orbital |
| HPLC | high-performance liquid chromatography |
| HRMS | high resolution mass spectrometry |
| Hz | Hertz |
| $IC_{50}$ | half-maximal inhibitory concentration |
| *i*Pr | iso-propyl |
| *J* | coupling constants |
| LDA | lithium diisopropylamide |
| LUMO | lowest unoccupied molecular orbital |
| *m* | meta |
| Me | methyl |
| MeCN | acetonitrile |
| MLCK1 | Myosin light chain kinase |
| NMR | nuclear magnetic resonance |
| n.d. | not detected |
| NP | Natural product |
| Nu | Nucleophile |
| *o* | ortho |
| OAc | acetate |
| *p* | para |
| $PPh_3$ | triphenylphosphine |
| ppm | parts per million |
| rt | room temperature |
| *p*TsOH | para toluenesulfonic acid |
| $R_f$ | Retention factor |
| SAR | Structure-activity relationship |
| Sat. | saturated |
| SCONP | Structural Classification of Natural Products |
| *t*Bu | *tert*-butyl |
| Temp. | temperature |
| THF | tetrahydrofuran |

| | |
|---|---|
| $t_R$ | retention time |
| Ts | para-tosyl |
| TsCl | Para toluenesulfonyl chloride |
| TS | transitionstate |

## 8.2 Acknowledgement

First and foremost, I am extremely grateful to my supervisor Prof. Dr. Herbert Waldmann and would like to thank him for giving me the opportunity to work on this interesting and challenging project in such an excellent scientific environment and his invaluable advice, continuous support, and patience during my PhD study. His immense knowledge and plentiful experience have encouraged me in all the time of my academic research and daily life. The research will never be achieved without his guidance and supervision.

I would like to express my gratitude to Prof. Dr. Andrey Antonchick for all his help, supportive advice and highly valuable input on this PhD. His immense knowledge in organic chemistry as well as his encouragement contributed a lot for solving all the scientific issues during my PhD study. I am also deeply grateful to him for being my second examiner.

I am truly thankful to Dr. Michael Grigalunas for helping me with the project and for his great support. I would like to thank him for proofreading this thesis.

I would like especially address my appreciation to Dr. Saad Shaaban for his intensive discussions and supportive help through my whole PhD study and for proofreading this thesis.

I would like to thank all analytic departments involved in the characterization of the synthesized compounds emphasizing my gratitude to Jens Warmers and Svetlana Gerdt for the maintenance of the analytical HPLCs, Dr. Petra Janning and Christiane Heitbrink for HRMS measurements as well as Bernhard Griewel and the NMR-Team of the TU Dortmund for all NMR experiments. I am grateful to the COMAS team for the biological compound screening and data analysis. I would like to express my gratitude to Prof. Dr. Carsten Strohmann and Lukas Brieger for carrying out the X-Ray analysis.

I would like to thank the whole department IV for the great working atmosphere that made me enjoy my PhD every day. I want to especially name Vicky, Mahesh, Chun-ngai, Saad Shaaban, Michael Grigalunas, Jie, Caitlin, Mahyar Akbarzadeh, Lin Wang, Sukdev Bag and Adrian.

Finally, my deepest and heartfelt appreciation goes to my family for their continuous support and encouragement.

„*Beşikten mezara kadar ilim tahsil ediniz*‘‘

## 8.3 Curriculum Vitae

### Personal Information


| | |
|---|---|
| Name | Okan Yildirim |
| Date of birth | 20.04.1993 |
| Place of birth | Dortmund, Germany |
| Nationality | German |
| Email | yildirim.okan@gmx.de |


### Academic and School education

Since 03/2018 **PhD in Chemical Biology**

*Max Planck Institute of Molecular Physiology (Dortmund, Germany)*

- Supervision: Prof. Dr. Dr. h.c. Herbert Waldmann
- Project: Design, Synthesis and Biological Evaluation of a pseudo-Natural Product Compound Collection
  - Accomplished interdisciplinary projects in organic chemistry and biology
  - Designed and executed the synthesis of complex organic molecules with multiple stereocenters
  - Asymmetric synthesis and ligand design
  - Biological evaluation of relevant compounds
  - Responsible for trainees, paractical courses, and successful completion of theses for students

10/2015 – 09/2017 **Master of Science in Chemistry**

*Ruhr University Bochum (Bochum, Germany)*

*Overall Grade: 1.3*

- **Master thesis** in organic chemistry with Prof. Dr. Frank Schulz
  - „Synthetic Investigation of the Binding Mode of Action of Ketolides in the Bacterial Ribosome‘‘

10/2012 – 08/2015 **Bachelor of Science in Biochemistry**

*Ruhr University Bochum (Bochum, Germany)*

*Overall Grade: 2.3*

- **Bachelor thesis** in organic chemistry with Prof. Dr. Frank Schulz
  - „Synthesis of novel acetic acid based Clarithromycin-Derivatives‘‘

06/2012 **Abitur**

*Helmholtz-Gymnasium (Dortmund, Germany)*

*Overall Grade: 1.6*

## 8.4 Eidesstattliche Versicherung (Affidativ)

### Eidesstattliche Versicherung (Affidavit)

Yildirim, Okan
Name, Vorname
(Surname, first name)

208189
Matrikel-Nr.
(Enrolment number)

Belehrung:

Wer vorsätzlich gegen eine die Täuschung über Prüfungsleistungen betreffende Regelung einer Hochschulprüfungsordnung verstößt, handelt ordnungswidrig. Die Ordnungswidrigkeit kann mit einer Geldbuße von bis zu 50.000,00 € geahndet werden. Zuständige Verwaltungsbehörde für die Verfolgung und Ahndung von Ordnungswidrigkeiten ist der Kanzler/die Kanzlerin der Technischen Universität Dortmund. Im Falle eines mehrfachen oder sonstigen schwerwiegenden Täuschungsversuches kann der Prüfling zudem exmatrikuliert werden, § 63 Abs. 5 Hochschulgesetz NRW.

Die Abgabe einer falschen Versicherung an Eides statt ist strafbar.

Wer vorsätzlich eine falsche Versicherung an Eides statt abgibt, kann mit einer Freiheitsstrafe bis zu drei Jahren oder mit Geldstrafe bestraft werden, § 156 StGB. Die fahrlässige Abgabe einer falschen Versicherung an Eides statt kann mit einer Freiheitsstrafe bis zu einem Jahr oder Geldstrafe bestraft werden, § 161 StGB.

Die oben stehende Belehrung habe ich zur Kenntnis genommen:

Official notification:

Any person who intentionally breaches any regulation of university examination regulations relating to deception in examination performance is acting improperly. This offence can be punished with a fine of up to EUR 50,000.00. The competent administrative authority for the pursuit and prosecution of offences of this type is the chancellor of the TU Dortmund University. In the case of multiple or other serious attempts at deception, the candidate can also be unenrolled, Section 63, paragraph 5 of the Universities Act of North Rhine-Westphalia.

The submission of a false affidavit is punishable.

Any person who intentionally submits a false affidavit can be punished with a prison sentence of up to three years or a fine, Section 156 of the Criminal Code. The negligent submission of a false affidavit can be punished with a prison sentence of up to one year or a fine, Section 161 of the Criminal Code.

I have taken note of the above official notification.

Dortmund,
Ort, Datum
(Place, date)

Unterschrift
(Signature)

Titel der Dissertation:
(Title of the thesis):

Design, Synthesis and Biological Evaluation of a Pseudo Natural Product Compound Collection

Ich versichere hiermit an Eides statt, dass ich die vorliegende Dissertation mit dem Titel selbstständig und ohne unzulässige fremde Hilfe angefertigt habe. Ich habe keine anderen als die angegebenen Quellen und Hilfsmittel benutzt sowie wörtliche und sinngemäße Zitate kenntlich gemacht.
Die Arbeit hat in gegenwärtiger oder in einer anderen Fassung weder der TU Dortmund noch einer anderen Hochschule im Zusammenhang mit einer staatlichen oder akademischen Prüfung vorgelegen.

I hereby swear that I have completed the present dissertation independently and without inadmissible external support. I have not used any sources or tools other than those indicated and have identified literal and analogous quotations.

The thesis in its current version or another version has not been presented to the TU Dortmund University or another university in connection with a state or academic examination.*

*Please be aware that solely the German version of the affidavit ("Eidesstattliche Versicherung") for the PhD thesis is the official and legally binding version.

Dortmund,
Ort, Datum
(Place, date)

Unterschrift
(Signature)